



The
University
Of
Sheffield.

**Using electronic tagging data to investigate the individual-,
population- and community-level consequences of movement
in free-roaming marine fish**

By:

Christopher A. Griffiths

A thesis submitted in partial fulfilment of the requirements for the degree of

Doctor of Philosophy

The University of Sheffield
Faculty of Science
School of Mathematics and Statistics

Submission Date: **September 2018**

Declaration.

I hereby declare that except where specific reference is made to the work of others, the contents of this thesis are original and have not been submitted in whole or in part for consideration for any other degree or qualification to this, or any other university. Submission is made solely to the University of Sheffield and the University of Tasmania as per a cotutelle agreement. This thesis is my own work and contains nothing which is the outcome of work done in collaboration with others, except as specified in the text and the following acknowledgements.

Christopher A. Griffiths

September 2018.

Acknowledgements.

I would like to thank my supervisors, Professor Paul Blackwell, Dr Julia Blanchard, Dr David Righton and Dr Jon Pitchford, for your expertise, guidance and infinite patience. My time spent with all four of you has been invaluable and without your continued words of wisdom I'm not sure this globe-trotting and often ambitious project would have succeeded. I hope, and fully expect us, to flourish as both friends and colleagues in the future. I would especially like to thank Paul who very kindly stepped in and took on the responsibilities of 'primary supervisor' at a time when this project was in its infancy.

The list of collaborators that have contributed to the development of this project is fairly large. In no particular order, I would like to say a massive thank you to Dr Toby Patterson, Dr Simon Wotherspoon, Dr Christopher Cooney, Dr Alison Parton, Dr Ewan Hunter, Dr Michael Spence, Dr Tom Webb, Miss Hayley Bannister, Dr Serena Wright, Dr Jeroen van der Kooij, Professor Richard Law, Dr Gustav Delius, Miss Stacey McCormack, Miss Emma John, Mr Robert Goodsell and Mr Simon Mills.

Chapter 3 features an extension to the published article Griffiths et al. (2018). Thank you to my co-authors as well as two anonymous reviewers for their useful feedback, getting this paper over the line really was a 'Klopp fist pump' moment for me. A detailed 'author contribution' statement is provided in the published article. Chapter 3 also refers (briefly in the discussion) to a second piece of collaborative work that is currently in review at the Journal of Animal Ecology (Adam et al., in review). The work stemmed from a very interesting conversation at the 6th International Bio-logging Science Symposium held in Constance, Germany and has emerged as a novel application of multi-scale multi-state HMMs to animal movement data. Thank you to my collaborators Mr Timo Adam, Dr Vianey Leos-Barajas, Miss Emily Meese, Dr Chris Lowe and Professor Roland Langrock.

In addition to those I have already acknowledged, I am very grateful to the many staff and students in the APS department and the wider university for their continued help and support. Coffee club, Interval and the S10 gym have all become stable fixtures in my life over the last four years. Specifically, I would like to name the members of E floor office, Olivia Richardson, Yuan Pan, Abi Marshall, Miriam Dobson, Tom Sinclair and Ejok. Thank you for listening to my woes and accepting that I am a very vocal coder who adores sport and 'trashy' TV.

Last but certainly not least I would like to thank my partner in crime, Miss Kathryn Murray you're my rock and without you I wouldn't have finished this PhD. I have also leaned heavily on my family and can never truly pay tribute to how supportive they have all been

throughout my life to date. This is especially true of my mother, Mrs Helen Owen who always picks up the phone and listens to my pointless and quite often endless rants about life.

This PhD was funded by the Natural Environment Research Council via the Adapting to the Challenges of Changing Environment (ACCE) Doctoral Training Programme (Grant code: NE/L002450/1). My studentship was also CASE sponsored by CEFAS and was supported by a 2017 Tasmania graduate research scholarship.

Abstract.

Tagging studies are now commonplace in ecology. Technological advances in telemetry devices have revolutionised our ability to track the movements of individual animals over vast spatial scales. This is especially true in marine ecology, where animals move through a world that is otherwise unobservable. The aim of many tagging studies is that by understanding the movements of the few we might gain some meaningful inference about the movements of the many, with clear consequences for conservation and management. Achieving this aim requires the scaling of inferences from the individual- to the population- and community-levels. Concentrating on the movements of marine fish, this scaling process forms the rationale behind this thesis.

I start at the individual-level by investigating how movement influences stock structure and patterns of space use, with important implications for stock recovery. At the population-level, I introduce a novel method for behavioural classification, which addresses issues surrounding individual variation by assuming that individuals of the same species share two broad behavioural modes. Application of this method to the movements of two commercially important species reveals clear spatio-temporal patterns, as fish switch their horizontal and vertical activity levels on a seasonal basis. I step towards the community-level by first scrutinising the scaling relationship between body size and movement in marine fish before applying the findings to a dynamic size-structured community model. I show how changes to the underlying assumptions surrounding movement have large emergent consequences for community structure, species coexistence and fisheries yield.

Marine tagging studies are currently underutilised by conservation and management, owing to small sample sizes, variations in data quality and a lack of methods for the scaling up of inference. Here I provide a body of work that tackles these issues and more generally demonstrates the importance of movement to our understanding of fish populations and marine communities.

Table of Contents.

List of Figures	IX
List of Tables	XI
Nomenclature	XIII
Chapter 1 – Introduction	1
1.1 Tagging data	3
1.1.1 Mark recapture tags	4
1.1.2 Data storage tags (DSTs)	5
1.1.3 Partial satellite archival tags (PSATs)	6
1.1.4 Tagging effects on fish behaviour, physiology and performance	7
1.2 Hidden Markov models (HMMs)	11
1.3 Size spectrum modelling	12
1.4 Aims of the thesis	13
Chapter 2 – Movement and stock dynamics of Atlantic cod (<i>Gadus morhua</i>) in the Irish Sea and Celtic Sea	17
2.1 Introduction	17
2.2 Methods	19
2.2.1 Study area	19
2.2.2 Data storage tags	19
2.2.3 Tag implementation	20
2.2.4 Estimates of geographic position	21
2.2.5 Horizontal and vertical movement	22
2.2.6 Data analysis	23
2.2.7 Other data sources	25
2.3 Results	26
2.3.1 Long-term movement patterns	26
2.3.2 Foraging period	27
2.3.3 Spawning period	33
2.3.4 Diet	35
2.4 Discussion	35
Chapter 3 – Scaling marine fish movement behaviour from individuals to populations	43
3.1 Introduction	43
3.2 Methods	46
3.2.1 Case study data	46
3.2.2 The model	47
3.2.3 Classifying fish movement	50
3.2.4 Prior sensitivity analysis	51
	VII

3.2.5	Univariate modelling	52
3.2.6	Inferring population patterns	52
3.3	Results	57
3.3.1	Individual fish movement	57
3.3.2	Population patterns	57
3.3.3	Prior sensitivity analysis	60
3.3.4	Distribution of state dwell time	62
3.3.5	Comparison to univariate modelling	62
3.4	Discussion	63
Chapter 4 – Testing movement allometry in free-roaming marine fish		71
4.1	Introduction	71
4.2	Methods	74
4.2.1	Movement data	74
4.2.2	Statistical analysis of movement allometry	85
4.3	Results	88
4.4	Discussion	94
Chapter 5 – Movement allometry in a trait-based size spectrum model		103
5.1	Introduction	103
5.2	Methods	106
5.2.1	Model description	106
5.2.2	Varying q	110
5.2.3	Fishing mortality	111
5.2.4	Interaction matrix	112
5.2.5	Model output	113
5.3	Results	114
5.4	Discussion	123
Chapter 6 – General Discussion		131
6.1	Key findings	131
6.2	Limitations and future work	133
6.3	Broader implications and practical recommendations	137
6.4	Final remarks	139
References		141
Appendices		167

List of Figures.

1.1	Photographic example of a DST on an Atlantic cod	5
1.2	Photographic example of a PSAT on an Atlantic Bluefin tuna	6
1.3	Structure of a hidden Markov model	11
2.1	Release and recapture locations of Atlantic cod in the Irish and Celtic Sea	20
2.2	Stock-level locations and composite home ranges of Atlantic cod	28
2.3	Individual locations and individual home ranges of Atlantic cod	29
2.4	Space use patterns of Atlantic cod during the foraging period	31
2.5	Seabed habitat type occupied by Atlantic cod in the Irish and Celtic Sea	32
2.6	Space use patterns of Atlantic cod during the spawning period	34
2.7	Stomach content data for Atlantic cod in the Irish and Celtic Sea	36
3.1	Release locations of Atlantic cod and European plaice	47
3.2	Estimated state-dependent distributions	53
3.3	Mean bivariate movement rates by state in European plaice	54
3.4	Movement parameter prior's influence on state classification	55
3.5	Influence of movement parameter prior on an exceptionally short time series	56
3.6	Examples of state dependent movement behaviour	58
3.7	Temporal distribution of the resident state	59
3.8	State dependent space use patterns	61
3.9	State dwell time distributions by state in Atlantic cod	63
3.10	State dwell time distributions by state in European plaice	64
4.1	Morphological illustrations of two post-flexion stage larval fish	80
4.2	Sub-sampling of vertical movement through time in larval fish	83
4.3	Sub-sampling of vertical movement through time in adult fish	84
4.4	Scaling of realised movement with body mass in marine fish	90
4.5	Scaling of realised movement with body mass in marine fish	91
4.6	Scaling of realised movement with body mass in marine fish	92
4.7	Scaling of realised movement with body mass in adult and larval fish	93
5.1	Relations between q and its dependent parameters	112
5.2	Community slope as a function of a varying q and f	115
5.3	Community abundance and relative abundance at size ($f = 0$)	116
5.4	Community abundance and relative abundance at size ($f = 0.25$)	117
5.5	Community abundance and relative abundance at size ($f = 0.7$)	118
5.6	Relative total biomass as a function of a varying q and f	119
5.7	Relative total yield as a function of a varying q and f	122
5.8	Species coexistence as a function of a varying q and f	125

List of Tables.

2.1	Tagging details of Atlantic cod in the Irish and Celtic Sea	21
2.2	Movement summary of Atlantic cod tagged in the Irish and Celtic Sea	30
2.3	Site fidelity of Atlantic cod tagged in the Irish and Celtic Sea	39
3.1	State dependent movement rates in Atlantic cod and European Plaice	60
3.2	HMM prior sensitivity results	62
4.1	Realised movement rates of free-roaming marine fish	75
4.2	Length to mass conversion rates	77
4.3	FL to TL conversion factors	78
4.4	Further details of adult tagging data	79
4.5	Vertical movement v. sample time model selection	82
4.6	Realised movement v. body mass model selection	89
4.7	Realised movement v. body mass with added trait values	95
5.1	SS model equations	107
5.2	SS model parameters	109
5.3	SS model output for empirical values of interest (q and f)	120

Nomenclature.

List of Abbreviations

AFBI	Agri-Food and Biosciences Institute
ARGOS	Advanced Research and Global Observation Satellite
CEFAS	Centre for Environment, Fisheries and Aquaculture Science
CPUE	Catch per unit effort
DEFRA	Department for Environment, Food and Rural Affairs
DST	Data storage tag
FAO	Food and Aquaculture Organisation
FL	Fork length
GEBCO	General Bathymetric Chart of the Oceans
GPS	Global positioning system
HMM	Hidden Markov model
hHMM	hierarchical hidden Markov model
ICCAT	International Commission for the Conservation of Atlantic Tunas
ICES	International Council for the Exploration of the Sea
JNCC	Joint Nature Conservation Committee
LOO	Leave-one-out cross validation
MC	Markov chain
MCMC	Markov chain Monte Carlo
MMO	Marine Management Organisation
MPA	Marine protected area
MSY	Maximum sustainable yield
MVN	Multivariate normal
PPMR	Predator-prey mass ratio
PSAT	Partial satellite archival tag
Re	Reynolds number
SS	Size spectrum
SSM	State-space model
TL	Total length
TOPP	Tagging of Pacific Predators
UD	Utilisation distribution

Chapter 1.

Introduction.

'Marine organisms do not care about international boundaries; they move where they will.'

Paul Snelgrove, Oceanographer.

Movement is a fundamental feature of animal life in an ever-changing marine world. It dictates survival and reproduction by allowing individuals to reach resources and mating partners, escape predation, and switch optimally between local habitats or transit great distances between foraging and spawning grounds. By creating and sustaining individual space use patterns (Jetz et al., 2004) and stock structures (Bias et al., 2017; Neat et al., 2014), movement provides a mechanism by which animals can respond to changes in climate (Parmesan and Yohe, 2003) or maintain genetic diversity (Neat et al., 2014; Reiss et al., 2009). Additionally, movement by controlling rates of encounter between a predator and its prey, provides the cornerstone of community and ecosystem dynamics and plays a key role in ecosystem stability (Neutel et al., 2007; Pawar et al., 2012). As a result, a greater understanding of movement in a marine world that is both directly exploited (fishing) and heavily relied upon (ecosystem services) by humans, is essential for its persistence, its management and its conservation (Halpern et al., 2015; Nash et al., 2017; Pauly et al., 2005).

Knowledge of movement in marine animals is a topic of great interest and is often centred around a number of key overarching research questions: Where are marine animals now and where are they going to be in the future? When do marine animals move and do these movements represent a seasonal cycle, a reaction to a resource that varies in space or time, or a long-term response to changes in environmental conditions (e.g. sea temperature)? What are the long-term drivers of movement, is it simply a function of the need to find food or meet potential breeding partners, or a much more enigmatic process, influenced by individual plasticity, learned versus innate behaviours or physical constraints? And finally, how does movement structure population and community dynamics and how can knowledge gained be used to inform conservation and management?

A key advancement in the field surrounds the advent of electronic telemetry devices (commonly referred to as tags), capable of recording the movements of individual animals as they roam freely through their natural habitats. The data they collect is often

difficult to interpret, being a complex, noisy mixture of decisions and responses to a three-dimensional environment we know very little about. Additionally, any data gained will exhibit high temporal and spatial correlations and be cluttered with bouts of non-linearity and apparent randomness (Cagnacci et al., 2010). Despite this, these devices provide a slim window into a world that is otherwise unobservable and have served as the primary driving force behind the heralded 'golden age' of animal movement (Hays et al., 2016; Hussey et al., 2015; Jonsen et al., 2013). Iconic examples include the first ARGOS (Advanced Research and Global Observation Satellite) satellite tracked basking shark off the Scottish west coast (*Cetorhinus maximus*; Priede, 1984), the near 2500km long migration of a single American eel (*Anguilla rostrata*; Béguyer-Pon et al., 2015) and the vertical thermoregulation strategies of the world's largest fish, the whale shark (*Rhincodon typus*; Thums et al., 2012). Used to track the movements of marine animals inhabiting corals reefs (Brodie et al., 2016; Maljković and Côté, 2011) or transiting across entire ocean basins (e.g. Block et al., 2005; Bonfil et al., 2005; Brodie et al., 2018; Harrison et al., 2018; Hays et al., 2006; Hindell et al., 2016; Skomal et al., 2009), it is clear that the deployment of tags has taught us much about the ecology, space use habits and behaviour of species threatened with extinction (e.g. Aarestrup et al., 2009) or of significant commercial importance (e.g. Block et al., 2005; Righton et al., 2001).

Advances in telemetry have been followed by a suite of methodological and quantitative developments which make full use of modern-day computing. Ranging in complexity from mixed-effect (e.g. Bürkner, 2017; Doherty et al., 2017) or generalised additive models (Adlerstein and Welleman, 2000; Costa et al., 2012), to state-space formulations capable of inferring behavioural modes (e.g. hidden Markov models; Jonsen et al., 2013; Michelot et al., 2016) or refining our estimations of geographical location (e.g. particle or Kalman filters; Patterson et al., 2008; Pedersen et al., 2008). Such developments have allowed ecologists to ask increasingly more complex questions of their movement data, evolving far beyond the intrigue of 'discovery science' towards a much more deeper understanding of movement behaviour and the ecology of migration (Costa et al., 2012; McGowan et al., 2017; Ogburn et al., 2017).

Regardless of such advances, tagging studies are not without their critics (e.g. Carter et al., 2016; Hebblewhite and Haydon, 2010; McGowan et al., 2017; Ogburn et al., 2017)). Tags are expensive, liable to malfunction or loss and frequently impact the mortality and reproduction of the animals involved (Cooke et al., 2004; McMahon et al., 2012). These factors impose severe ethical and functional constraints on sample size (in terms of the number of individual animals involved), weaken study design and call into question whether the cost of such studies yield the expected gains (Carter et al., 2016;

Hebblewhite and Haydon, 2010). Justification for use typically homes in on the big research topics of our era: population and community dynamics, spatial and temporal management and species conservation. However, examples where the fine-scale movements of individual animals have been used to infer population and community dynamics are few (but see Fossette et al., 2013; Hindell et al., 2016), as are ‘success stories’ where knowledge gained has directly informed management and conservation (but see Cooke et al., 2012; Scott et al., 2012). For instance, a recent survey into the deployment of satellite tags on sea turtles (Jeffers and Godley, 2016) revealed that 36% of published papers (133 out of 369, between 1982-2014) made direct recommendations for conservation, but participants only knew of few definitive examples where tagging data had been translated from paper to policy (Table 3, Jeffers and Godley, 2016). Additionally, an in-depth review into the use of tags in ecology (Hebblewhite and Haydon, 2010) stated that ‘one of the most difficult problems facing ecologists using tags is how to scale-up to the population consequences of movement’.

There is no doubt that the quantity and quality of animal movement data collected via the deployment of tags has rapidly increased, as have the statistical and analytical ways in which ecologists can analyse these data. Nonetheless tagging studies, often costing millions of dollars (e.g. Block et al., 2011; Harrison et al., 2018), are currently being underutilised when it comes to inferring population and community dynamics or designing conservation strategies (Hays et al., 2016). The current conservation crisis (McGowan et al., 2017), coupled with a reduction in scientific research funding (Ogburn et al., 2017), points towards a clear need for a body of work that not only investigates how individual movement can inform management and conservation, but also develops approaches capable of scaling-up inference from individuals to populations and communities.

In the following sections we will introduce the tag types considered in this thesis and the two main modelling frameworks which we will use to investigate the population and community level consequences of movement, before providing an overview of our aims and objectives.

1.1 Tagging data

Any number of tag types are now being deployed on mobile marine animals, ranging not only in size, cost and complexity but also in their relevance to the underlying ecology of the species of interest. In this thesis we will refer to the following three tag types: (1) simple mark recapture tags, also called conventional tags; (2) archival data storage tags

(DSTs) and (3) partial satellite archival tags (PSATs). Below we provide a brief synopsis of each tag type, including details of the data they record and how that data is retrieved, their size, their cost, their measurement uncertainty (when appropriate) and examples of their use. We will also briefly explore what effect, if any, tags and the tagging procedure itself can have on the behaviour, physiology and performance of marine animals.

From this point onwards, we will shift focus from the movements of all marine animals to the primary focus of this thesis; the movement of fish.

1.1.1 *Mark recapture tags*

Deployed *en masse* on thousands of individual fish, these tags are simple plastic 'name' tags, noting information about the individual's unique identification and the tag's return address. Tags are typically attached externally to musculature of the animal (typically at the base of the first dorsal fin) and will remain in place until the tag either falls off or is removed upon recapture. Information gained consist of three data points: (1) the individual's release location (plus release date), (2) the individual's body size (body length or mass) and (3) the individual's recapture location (plus recapture date). Individual tags are small, cheap and must be physically returned (typically by fishermen) alongside a recapture date and location before inference can be made.

Examples of their use are numerous (e.g. Bendall et al., 2009; Brander, 1975; Connolly and Officer, 2001; Righton et al., 2007) and prior to the turn of the century they were the go to method for investigating the movements of free-roaming marine fish. Typically, fish will be tagged on spatially predictable spawning grounds and their recapture locations will be subsetting by month (e.g. 6 months after release) or season (e.g. summer vs. winter) to provide a broad-scale indication of space use and stock structure (e.g. Brander, 1975). Straight-line distances between release and recapture locations will inform geographical range estimates and areas where recaptures congregate will facilitate the identification of potential foraging and/or spawning grounds (Righton et al., 2007). Such tagging studies can also contribute to stock abundance estimates and our understanding of survival rates (Pine et al., 2003).

In Chapter 2, evidence from mark recapture studies conducted on Atlantic cod (*Gadus morhua*) in the Irish and Celtic Sea (Bendall et al., 2009; Brander, 1975; Connolly and Officer, 2001) will provide a primary information source and will be used to inform our interpretation of individual fish movement.



Figure 1.1. Example of data storage tag (DST) attached externally to the dorsal musculature of an Atlantic cod (*Gadus morhua*). The costs and benefits of external vs. internal tagging are discussed in detail by Righton et al. (2006). Image sourced directly from www.cals.ncsu.edu. Website accessed on 11/09/2018.

1.1.2 Data storage tags (DSTs)

A tag typically deployed on demersal-dwelling fish that spend very little time near the surface of the water but have a high likelihood of capture (Figure 1.1), DSTs are preprogrammed to measure depth (m; measurement accuracy = $\pm 1\%$) and environmental variables such as sea temperature ($^{\circ}\text{C}$; measurement accuracy = $\pm 0.1^{\circ}\text{C}$) at regular time intervals. These time intervals will vary depending on the battery life of the tag or the research question of interest, however a 10-minute sampling interval is commonplace in the published literature (Hobson et al., 2007; Hunter et al., 2004b). Individual tags are relatively small (weighing 1g in water – Cefas Technology Limited), cost around £300 (Cefas Technology Limited) and are either externally attached (as shown in Figure 1.1) or internally implanted into the belly of the fish (see Chapter 2 section 2.2.3 for a brief description). All measurements are archived within the tag's memory and as a result data retrieval requires the physical return of the tag, typically by fishermen in return for some financial reward. Tag return rates vary but recent authors quote values of approximately 15-40% (e.g. Hunter et al., 2003; Neat et al., 2014).

To date, DSTs have been used to investigate the movements of several commercially important species including Atlantic cod (Hobson et al., 2009, 2007; Righton et al., 2001) and European plaice (*Pleuronectes platessa*; Hunter et al., 2004b, 2004a) occupying the

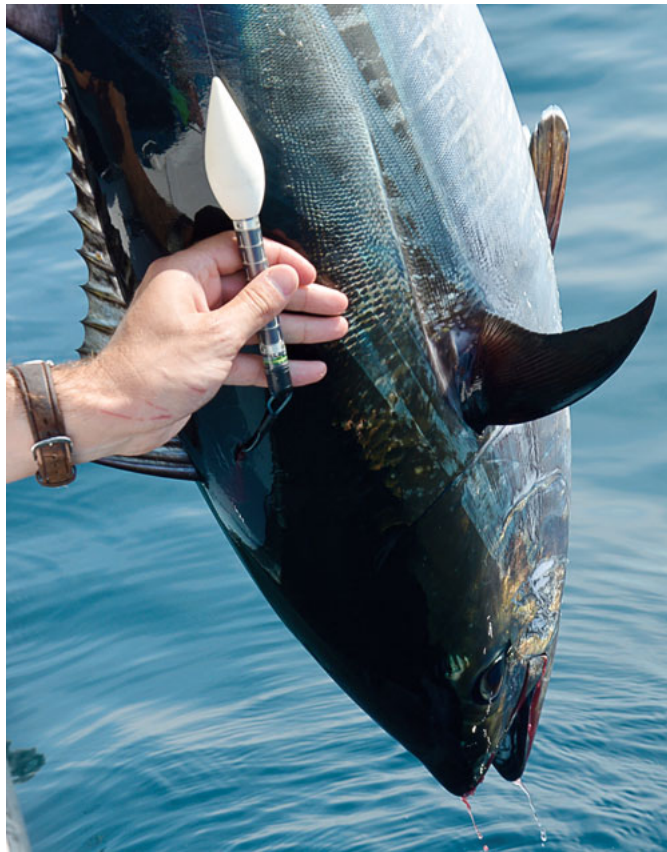


Figure 1.2. Example of a partial satellite archival tag (PSAT) attached externally to the dorsal musculature of an Atlantic Bluefin tuna (*Thunnus thynnus*). Tagging was conducted by ICCAT (International Commission for the Conservation of Atlantic Tunas). Image sourced directly from <https://www.onthewater.com>. Website accessed on 16/09/2018. Photo by Captain Bobby Rice.

shelf-seas of the North Atlantic. Insights gained relate to the location of potential foraging and spawning grounds (Hunter et al., 2006; Neat et al., 2006), seasonal changes in behaviour and distribution (Griffiths et al., 2018) as well as the use of favourable tidal currents during migration (Arnold et al., 1994; Hunter et al., 2004b; Righton et al., 2007). Additionally, DST data collected throughout the waters surrounding the British Isles have shed light on the intricacies of stock structure (Neat et al., 2014).

. In Chapters 2-4 we will analyse the movements of numerous demersal fish which have been tagged with DSTs.

1.1.3 Partial satellite archival tags (PSATs)

Often seen as a technological advancement on DSTs, PSATs (also referred to as pop-up satellite archival tags) are used to record the movements of larger pelagic-dwelling fish (Figure 1.2). The reasons for this are twofold: (1) they are heavier, weighing over 30 grams in water (Microwave Telemetry, Inc.) so ethically must be deployed on larger fish

and (2) they require an infrequent satellite link to be established, which can only occur when the fish is moving close to the surface of the water (Rutz and Hays, 2009).

PSATs are preprogrammed to record depth (m; measurement accuracy = ± 0.5 m) and sea temperature ($^{\circ}$ C; measurement accuracy = ± 0.1 $^{\circ}$ C) at 10 second to 1 minute sampling intervals. Unlike DSTs, where recordings are taken and stored until tag recovery, the observations measured by PSATs are transmitted to the ARGOS system on a pseudo-random schedule. This is to ensure that an equal distribution of data points is transmitted throughout tag deployment, meaning the temporal resolution of the animal's observed time series gradually increases as more data is received. However, this does mean that instances of battery failure or tag malfunction will yield a sparse time series cluttered with missing values and irregular sampling rates. This will also be the case if the fish under investigation does any of the following: surfaces at times when the satellite isn't overhead, moves into equatorial regions where satellite coverage is poor or simply spends less time close to the surface of the water (Carter et al., 2016). To combat this, it is common for researchers to interpolate depth and sea temperature observations to the 10 minute sampling interval (e.g. Strøm et al., 2016).

PSATs are expensive, costing around \$4200 per unit (Microwave Telemetry, Inc.) but do benefit from a much higher return rate (60%; Bias et al., 2017) as they can be pre-programmed to 'pop-off' their harness and float freely to the surface of the water ('pop-off' dates are typically six or twelve months after release). Retrieval is then logistically demanding but relatively straightforward.

To date PSATs have been used to track the return migration patterns of porbeagle sharks (*Lamna nasus*, Bias et al., 2017), map the space use and spawning habits of Atlantic Bluefin tuna (*Thunnus thynnus*; Block et al., 2005) and record the transoceanic movements of great white sharks (*Carcharodon carcharias*; Bonfil et al., 2005). Moreover, PSATs have been the preferred tag type for several major collaborative efforts aimed at monitoring the long-term movements of large pelagic predators, for example TOPP (Tagging of Pacific Predators; Block et al., 2011; Harrison et al., 2018).

In Chapter 4 we consider the movements of several large pelagic predators, including Blue (*Prionace glauca*) and Shortfin mako sharks (*Isurus oxyrinchus*) tagged with PSATs in the North Atlantic (data sourced from Campana et al., 2016)

1.1.4 Tagging effects on fish behaviour, physiology and performance

Many of the following chapters will use tagging data to learn about fish behaviour and by extension population and community dynamics. Key to this process, is the assumption

that the behaviour and movements of tagged animals are analogous to those of the wider untagged population (Bridger and Booth, 2003). Numerous studies have aimed to test this assumption in fish (e.g. Aarestrup et al., 2002; Jepsen et al., 2008; Righton et al., 2006), effectively asking whether the tagging procedure or the physical presence of a tag has any abnormal effects on the behaviour, physiology and performance of fish in the wild. If effects are present, it is essential that they are acknowledged and understood, otherwise researchers may make conclusions based on erroneous data, resulting in poor fisheries and management plans.

In recent reviews, negative effects are noted, however the overall trends remain inconsistent (Cooke et al., 2011; Jepsen et al., 2015). It is noteworthy that the majority of tagging-effect studies have been conducted on freshwater species in laboratory environments, owing to the complexity of monitoring indicators of 'normal' behaviour in the wild (Bridger and Booth, 2003; Cooke et al., 2011; Wargo-Rub et al., 2014). Further, many use radio transmitters or acoustic tags (not utilised in this thesis) with authors noting that further studies that consider archival data loggers and transmitters (e.g. DSTs and PSATs) in wild marine fish are needed (Cooke et al., 2011). Here we briefly review some of these effects and consider how we might limit their implications throughout our research.

Swimming performance. Reduced swimming performance is one of the expected effects of tagging, especially when transmitters are attached externally (as in PSATs), as the tag may exert additional drag or unintentionally alter the streamlined body shape of the fish (Jepsen et al., 2015; Thorstad et al., 2013). Comparing between tagged and untagged controls, flume-based experiments found that external tags reduced the burst swimming speed of Atlantic salmon smolts (*Salmo salar*; McCleave and Stred, 1975; Peake et al., 1997). Externally tagged juvenile white sturgeon (*Acipenser transmontanus*) also exhibited lower burst speeds than control fish (Counihan and Frost, 1999). In comparison, Anglea et al. (2004) showed that swimming speeds were comparable between surgically implanted juvenile Chinook salmon (*Oncorhynchus tshawytscha*) and untagged fish at 1- and 21-days post-surgery. Investigations into endurance instead of speed found no difference between fish tagged with small external tags, large external tags, surgically implanted tags and control fish (Thorstad et al., 2000). Moreover, Koed and Thorstad (2001) noted that adult pikeperch (*Sander lucioperca*) tagged internally for a time period of one year displayed no reductions in swimming performance compared to untagged controls.

Growth. Several studies have demonstrated an initial negative effect of tagging on growth, followed by a compensatory period in which growth rates trend towards those of untagged controls (Baras et al., 2000; Jepsen et al., 2008). Alternatively, some studies find only negative effects (e.g. Deng et al., 2012; Greenstreet and Morgan, 1989; Weimer et al., 2006) whilst other studies observed no negative effect on fish growth and condition (e.g. Anras et al., 1998; Jepsen and Aarestrup, 1999). In a study relevant to our work, adult Atlantic cod were found to experience no differences in growth when tagged with DSTs, either externally or internally, when compared to control fish (Righton et al., 2006). Interestingly, Righton and colleagues (2006) noted that the external attachment of DSTs frequently caused wounds and recommended the use of internal implantation whenever possible in long-term tagging studies.

Feeding. Food consumption rates in wild Atlantic salmon were found to be similar among tagged and untagged conspecifics (Robertson et al., 2003). Moreover, juvenile largemouth bass (*Micropterus salmoides*) tagged with surgically implanted radio transmitters resumed feeding on pellets within 24 hours of surgery (Thompson et al., 2014), suggesting that tagging had a negligible effect on feeding.

Behaviour. Tags that are attached externally have been shown to cause irregular behaviour in certain species (Bridger and Booth, 2003; Cooke et al., 2011). For instance, Collins et al. (2000) observed shortnose sturgeon (*Acipenser brevirostrum*) frequently rubbing themselves against the side of their tanks causing eventual tag loss. In addition, numerous authors note that external tags can be prone to entanglement in certain environments (Bridger and Booth, 2003; Thorstad et al., 2013). In comparison, several studies have demonstrated that surgically implanted fish display the same behaviour as untagged fish (Aarestrup et al., 2002; Jepsen et al., 2008; Thoreau and Baras, 1997). For example, Thoreau and Baras (1997) found that tagged fish resumed diurnal activity patterns throughout the study period, but that individuals seemed sluggish during the first 12-24 hours' post-surgery. In a recent study, Hedger et al. (2017) investigated the effects of different tag types on the behaviour of adult Atlantic salmon. They found that the depth distribution of individuals tagged with PSATs and DSTs were comparable. However, fish tagged with PSATs were shown to dive less frequently and to shallower depths than DST tagged conspecifics (Hedger et al., 2017).

Buoyancy. Reductions in buoyancy at depth can affect the behaviour and survivability of tagged fish (Bridger and Booth, 2003; Cooke et al., 2011). Perry et al. (2001) found that Chinook salmon smolts were quick to recover from the tagging procedure but struggled to deal with changes in depth (as mimicked by a hyperbaric chamber) when compared

to untagged fish. Further, Atlantic cod (Nichol and Chilton, 2006) and tilapia (*Oreochromis aureus*; Thoreau and Baras, 1997) showed a period of re-acclimatisation to their capture depth post-implantation. This post-tagging behaviour is shown to last for 3-7 days in either species (Hobson et al., 2007; Nichol and Chilton, 2006; Thoreau and Baras, 1997).

Predation susceptibility. In some studies, fish tagging has been linked to high rates of predation mortality immediately following release (Jepsen et al., 2006, 1998; Koed et al., 2006), especially when sea temperatures are elevated (e.g. Morris et al., 2000). Conversely, studies that have sought to address this topic directly, investigating metrics of predator avoidance and rates of predation in controlled experiments, indicated that tagged fish are not necessarily easier prey than untagged fish (Anglea et al., 2004; Jepsen et al., 2008). For discussions on how the tagging procedure itself can influence mortality from an animal welfare perspective, we refer the reader to reviews by Cooke et al. (2013) and Wargo-Rub et al. (2014).

Reproduction. Despite the importance of quantifying the effect of tagging on reproduction physiology and spawning behaviour, few studies have been conducted. In those that have been conducted, tagged fish have been shown to develop gonads at comparable rates to untagged conspecifics (Baras et al., 2000; Close et al., 2003). Sexual activity has also been shown to be consistent among tagging treatments in steelhead trout (Berejikian et al., 2007).

To conclude, several studies have demonstrated that tagged fish display the same behaviour, physiology and performance as untagged fish (e.g. Aarestrup et al., 2002; Jepsen et al., 2008). Consequently, we are confident when drawing meaningful conclusions from the long-term movement patterns of DST tagged Atlantic cod and European plaice (in Chapters 2 and 3). From our review of the literature it is clear that tagging effects are highly species dependent and vary based on the tag type being deployed and the tagging method being used. One emergent trend is that tagging effects, for instance on fish growth, behaviour and buoyancy control, often occur in the first few days post-tagging. To account for this we remove the first two weeks from all our movement paths (as in Hobson et al., 2007). We also ensure that all observed movements are checked visually, and any anomalies are investigated. For example, in Chapter 2 we remove extra days from the movement paths of two Atlantic cod following further analysis.

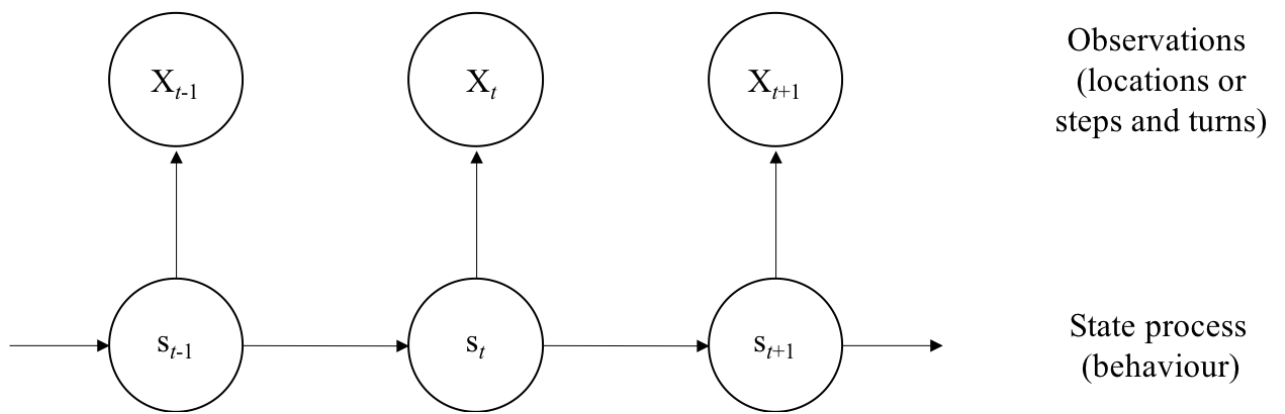


Figure 1.3. General dependence structure of an HMM. Notable is that the HMM approach requires observations to be regularly spaced in time and to be measured with no or negligible error (Patterson et al., 2017).

1.2 Hidden Markov models

Over the last decade, hidden Markov models (HMMs) have emerged as a popular tool for animal movement modelling, where they provide a natural framework capable of inferring behavioural modes from different types of telemetry data (Patterson et al. 2017; Michelot et al. 2016). HMMs comprise of two parts; a series of observations X_t, \dots, X_T , and an underlying state process, S_t, \dots, S_T , adhering to a general dependence structure as shown in Figure 1.3. In practice, the series of observations represents an animal's location, and therefore its steps (horizontal or vertical) and turns (change in direction) as it moves through a dynamic environment. Whereas, the state process consists of a discrete number of states which are typically interpreted as broad proxies for the behavioural mode of the animal. Examples of behavioural modes include, exploratory and encamped in GPS tagged elks (*Cervus elaphus*; Morales et al., 2004) or resident and migrating in PSAT tagged southern Bluefin tuna (*Thunnus maccoyii*; Patterson et al., 2009).

Favoured, in part, because they match our intuitive understanding that movement is governed by a series of unobserved switches in an animal's motivation (Patterson et al., 2017), HMMs have been used to investigate a number of ecologically important questions. For instance, how Manx shearwaters (*Puffinus puffinus*) alternate their behaviour while at sea (Dean et al., 2012) and how behaviour differs between genders in the endangered Florida panther (*Puma concolor*; van de Kerk et al., 2015). They have also been expanded upon to investigate the influence of environmental covariates like wind speed (Leos-Barajas et al., 2017b) or seasonality (McKellar et al., 2015), account

for periodicities such as diurnal variations (Li and Bolker, 2017) and explore the behavioural response of animals to human-induced change (DeRuiter et al., 2017). Moreover, their flexibility, statistical tractability and computational efficiency make HMMs credible candidates when attempting to investigate population dynamics using individual movement (e.g. Jonsen, 2016).

1.3 Size spectrum modelling

A powerful process-based solution to the problem of ecosystem modelling (Pope et al., 2006), size spectrum models (and many other size-based ecosystem models; Blanchard et al., 2017) make full use of the role that body size plays in marine systems (Andersen et al., 2016a, 2016b). Focussing on how individual size governs feeding interactions (Blanchard et al., 2017), trophic niches (Barnes et al., 2008; Jennings et al., 2001) and vital biological rates (e.g. metabolism; Brown et al., 2004), size spectrum models resolve an entire fish community as a continuous size distribution (Andersen and Beyer, 2006; Andersen and Pedersen, 2010), where the currency of interest (biomass, abundance or production) exhibits a characteristic scaling relationship with body size (typically mass or weight). Rooted in 50 years of empirical research and dating back to the observations of Sheldon and colleagues (Sheldon et al., 1972), size spectrum models have undergone a rapid phase of development (Andersen et al., 2016b; Blanchard et al., 2017). This has seen them evolve far beyond the 'community' size spectrum where species identity and differences between populations are ignored (Benôit and Rochet, 2004; Blanchard et al., 2009; Law et al., 2009), towards trait-based (Andersen and Pedersen, 2010; Houle et al., 2013; Jacobsen et al., 2013) and multispecies (Blanchard et al., 2014) extensions of the same core concepts. To date size spectrum models have been used to investigate a number of important ecological phenomena, including the response of marine communities to industrial fishing (Andersen and Pedersen, 2010; Houle et al., 2013), the effects imposed by projected climate change scenarios (Blanchard et al., 2012; Woodworth-Jefcoats et al., 2013) and the vulnerability of coral reef communities to the loss of structural complexity (Rogers et al., 2014). Additionally, the information they provide has contributed to the debate surrounding balanced harvesting (Jacobsen et al., 2013; Law et al., 2016) and has allowed us to gain meaningful insights into the ecological effects of community recovery plans (Andersen and Rice, 2010).

Size spectrum models are perfectly suited to investigate the population and community-level consequences of individual movement for three core reasons. (1) They are built on a foundation of individual-level processes, namely growth, mortality and reproduction, so

provide a clear framework for the inclusion of information about individual movement. (2) Many are spatially implicit (e.g. Blanchard et al., 2014; Scott et al., 2014), allowing interactions between a predator and its prey to vary based on rates of encounter and availability. (3) The fact that size spectrum models are size based, means they can be readily applied to fisheries (Andersen et al., 2016b), as body size provides an excellent descriptor of mesh- and gear-size regulations and is frequently used as a defining feature of catch value (Andersen et al., 2015). Thus, the inclusion of movement can be scrutinised for the effects it has on community structure, species coexistence and estimated yield with fisheries management and conservation in mind. Moreover, despite some advances towards the inclusion of movement in size-based ecosystem models (e.g. Andersen et al., 2017; Castle et al., 2011; Maury, 2010), size spectrum models haven't been advanced or tested with detailed movement data. This highlights a clear avenue for new scientific research.

1.4 Aims of the Thesis

Tagging data provides a wealth of information about the movements of individual animals as they transit through variable habitats, respond to intrinsic and extrinsic pressures and alter their distribution in a bid to feed, reproduce and survive (Hays et al., 2016; Hussey et al., 2015; Rutz and Hays, 2009). Despite this, tagging data is currently being underutilised when it comes to conservation and management (Hays et al., 2016), owing in part to the issues of sample size and the scaling of inference (Carter et al., 2016; Hebblewhite and Haydon, 2010). Through this thesis we aim to analyse the movements of individual fish and provide a viable pathway by which movement observed at the level of the individual can be used to gain meaningful insights into population and community dynamics. Building on the models introduced above, we use a suite of approaches representing both novel methodologies and adaptations to current techniques, which allow us to achieve this aim. We consider the movements of hundreds of fish, varying not only by their taxonomic identity, trophic position and body size but also by the environment in which they inhabit. Moreover, where appropriate, we use our findings to make informed recommendations for fisheries management and conservation.

Sequentially the thesis will step the reader through this scaling process. In Chapter 2 we start at the individual level, using the deployment of DSTs in the Irish and Celtic Sea to learn about the movements of Atlantic cod. Comparable to the 'discovery science' justification provided in Ogburn et al. (2017), this chapter uses the movement of twelve individual fish to describe patterns of space use, spawning and foraging dynamics and

comment on stock structure in an area where species distributions are uncertain. Furthermore, because cod stocks in the Irish and Celtic sea have struggled to recover from historic exploitation, our work provides new information for fisheries management under the caveat of a small sample size.

In Chapter 3, we move towards the population level, applying a two-state bivariate HMM to the horizontal and vertical movements of 46 Atlantic cod and 61 European plaice. Initially we consider a basic model, but encounter large amounts of individual variation, both in terms of state allocation and data quality. These factors impair our ability to use collective individual behaviour to infer population dynamics. To overcome this, we introduce a novel adaptation to hidden Markov modelling. We make the explicit assumption that fish of the same species share two broad-scale behaviour states and allow prior distributions to inform the model about how we expect these states to be numerically distributed. Application of this adapted model ensures that behavioural states remain interpretable across multiple individuals, allowing population-level inference to be gained about how fish movement behaviour varies in space and time throughout the North Sea and the English Channel.

In Chapters 4 and 5, we consider movement at the community-level. First, in Chapter 4, we investigate the scaling relationship between movement and body size in marine fish. Scaling (or allometric) relationships are common throughout ecology (e.g. Brown et al., 2004; Hirt et al., 2017; Jetz et al., 2004) and past studies assume that movement scales with body mass according to a taxon independent exponent of 0.133 (Andersen et al., 2016a; Ware, 1978). Fitting to over 550 individual fish, spanning seven orders of magnitude in body mass, we show that this assumption is inappropriate in general and masks a range of ecologically important phenomena, most notably life stage effects and within species variation. In Chapter 5, we apply Chapter 4's findings to a trait-based size spectrum model, allowing our new knowledge about the scaling of movement to govern rates of encounter between a predator and its prey. We show how changes to a vital search parameter directly influence the individual-level processes of consumption, growth and mortality. Scaled up to the community-level, such changes have large emergent consequences on community size composition, community biomass, fisheries yield and rates of species coexistence. These findings highlight why a more comprehensive understanding of movement is critical to future modelling efforts, especially when these models are used to investigate important ecological problems.

In the final chapter, Chapter 6, we synthesise the work presented in Chapters 2-5 and discuss how they fit into the dual fields of movement ecology and marine ecosystem

modelling. We provide suggestions for future work and draw meaningful conclusions. Finally, we emphasise how, by making the most out of their tagging data, ecologists can achieve the scaling of inference from individuals to populations and communities with clear benefits to conservation and management.

Chapter 2.

Movement and stock dynamics of Atlantic cod (*Gadus morhua*) in the Irish and Celtic Sea.

2.1 Introduction

Atlantic cod (*Gadus morhua*) is a highly important demersal fish species found throughout the waters surrounding the British Isles. As well as playing a crucial ecological role as a tertiary consumer (Essington and Hansson, 2004; Savenkoff et al., 2004), cod is a species of high commercial value (FAO, 2012) and has been subjected to decades of heavy exploitation (Kurlansky, 1998). Despite concerted efforts to conserve and manage the exploitation of cod, many stocks have experienced steep declines in abundance and have, to date, shown minimal signs of recovery (Hilborn and Litzinger, 2009; Kelly et al., 2006; Lilly et al., 2008). Essential to fisheries management is information about when, where and how individuals undertake key life-history events such as foraging, spawning and migration (Hussey et al., 2015). The tagging of cod to gain this information has been ongoing for a number of years and has greatly increased our knowledge of individual behaviour (Hobson et al., 2009, 2007; Righton et al., 2001) and stock structure (Neat et al., 2014).

Two stocks that have struggled to achieve recovery are situated in the Irish and Celtic Seas. Both stocks are small (in terms of mean landings and mean total biomass; Marteinsdottir et al., 2005) and have experienced almost consistent declines in estimated abundance, estimated recruitment and reported landings dating back to the 1980s (Christensen et al., 2003; Cook et al., 1997; ICES, 2017a; Myers and Worm, 2003). Such adverse trends are the reason why both stocks have previously been classified as 'high risk' by ICES (International Council for the Exploration of the Sea) and have been repeatedly benchmarked by ICES working groups (e.g. ICES, 2017b, 2013a). Attempts to aid stock recovery via the implementation of fisheries management strategies have been numerous and multi-faceted. Measures include restrictions on Total Allowable Catch (TACs) and fishing effort, changes to mesh size as well as the establishment of size-based landing thresholds (e.g. no fish with a body length less than 35cm can be landed in British waters; (MMO, 2017)). Additionally, fisheries on both stocks are subject to spatial closures during the spawning period (Anon Commission Regulation, 2000; Defra, 2015). Many of these measures are explicitly designed to maximize the survival of new recruits and juvenile fish, theoretically boosting the annual recruitment of individuals to the stock. Recent evidence points towards success in the Celtic Sea, as

spawning stock biomass is currently estimated to be above safe biological limits (ICES, 2017a). However, despite these efforts, cod in the Irish Sea have shown no sustained signs of recovery (ICES, 2017a).

Such failures to facilitate stock recovery spark concern and beg the question as to what other factors are impairing the survival, growth and productivity of cod in the Irish Sea. Rising sea temperatures will no doubt play a role (Clark et al., 2003; Drinkwater, 2005), as will environmental variability (Brander, 2005; Köster et al., 2005; Rose, 2004). Recent reports have also pointed towards a multi-species argument (Swain and Sinclair, 2000; Trzcinski et al., 2006), where the depletion of cod has allowed other species to prosper and supersede cod in the community's food web. Such changes will have cascading effects on the abundance of cod, as any new species will act as both a competitor for food and a predator on smaller life stages.

Another factor that has emerged is whether or not current stock boundaries appropriately reflect the underlying structure and biological processes of the population (Ciannelli et al., 2013; Kritzer and Sale, 2004; Neat et al., 2014; Reiss et al., 2009). From an assessment and management perspective, cod in the Irish and Celtic Sea are assumed to be discrete units, displaying little or no mixing across stock boundaries. Tagging studies (both via mark recapture methods and telemetry devices) conducted in the area yield clear but contrasting evidence for this assumption. For instance, work conducted by Bendall et al. (2009) and Neat et al. (2014) demonstrate that fish tagged in the Celtic Sea remain exclusively in ICES Divisions VIIf, VIIh and VIIg (see Appendix 2.1) and display no evidence of northward migrations. Conversely, cod tagged in the Irish Sea have been shown to migrate both southwards into the Celtic Sea (Bendall et al., 2009; Neat et al., 2014) and northwards into the waters off the west coast of Scotland (Brander, 1975; Neat et al., 2014). Knowledge of such movement is critical to fisheries management, as fish that cross stock boundaries will be exploited as part of a separate stock (e.g. Block et al., 2005). Conversely, fish that remain in reproductively isolated units will be prone to localised depletion and are less likely to bounce back from historical overexploitation.

Here, we provide an in-depth description of the movement and spatial ecology of Atlantic cod in the Irish and Celtic Sea. Concentrating solely on a handful of very long time series ($n = 12$), produced via the deployment of data storage tags, we investigate the following research questions: (1) Whether or not stock mixing between adjacent ICES Divisions is present? (2) Where does foraging and spawning occur in the Irish and Celtic Sea? (3) How do daily horizontal and vertical movement rates differ between stocks and between

foraging and spawning periods? (4) How does the environment that individual fish inhabit during the foraging and spawning period differ between these stocks in terms of sea temperature, seabed habitat and sea depth, and does it alter the prey that cod consume?

We acknowledge that our analysis explicitly considers some of the same individuals ($n = 4$) as Bendall et al. (2009). However, we are confident that our work extends this study in several important ways. For example, we calculate novel individual and composite utilisations distributions for each stock, we thoroughly investigate daily horizontal and vertical movement rates, and we also elucidate how the movements of individual fish are linked to variances in the underlying properties of the environment they inhabit.

2.2 Methods

2.2.1 Study area

Tagging data were collated from a number of different studies and reflect an ongoing collaboration between CEFAS (Centre for Environment, Fisheries and Aquaculture Sciences), the Marine Institute in Ireland and the Agri-Food and Biosciences Institute (AFBI) in Northern Ireland. Tagging was carried out between 1999 and 2011 and the movements of individual fish span five sea areas (Figure 2.1; Table 2.1): the Scottish west coast (ICES Division VIa); the Irish Sea (ICES Division VIIa); the Celtic Sea (ICES Divisions VIIg and VIIh); the Bristol Channel (ICES Division VIIf) and the western English Channel (VIIe). We allocate each fish to the Irish Sea or Celtic Sea stock based on release location (Figure 2.1). A single fish (CEL_4683) was released within the British Channel but for the sake of simplicity we assume that it is part of the Celtic Sea stock. All tagging was carried out during the spawning period (classed here as from 1st January to 30th April).

2.2.2 Data storage tags

Three different types of data storage tags (DST) were used during this study: (1) the Milli or Centi tags made by Star-Oddi (Star-Oddi Marine Device Manufacturing Ltd, Gardabaer, Iceland); (2) the LTD1200 or LTD1400 tags made by LOTEK (Lotek Marine Technologies Inc., Ontario, Canada); (3) the G5 tag made by CEFAS (Cefas Technology Ltd, Lowestoft, UK). Each DST was programmed to record temperature (°C) and depth (m) at 10-minute intervals for the duration of deployment.

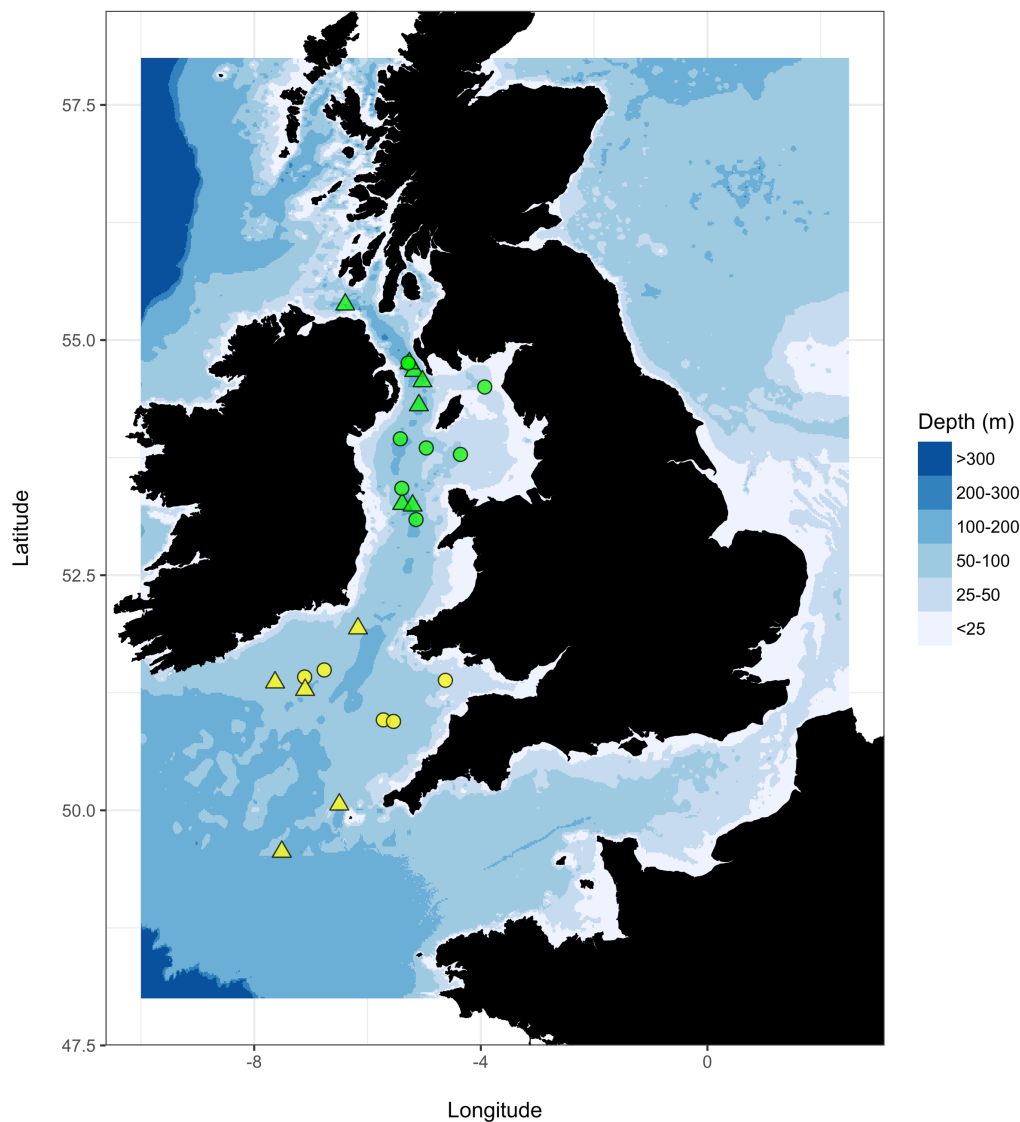


Figure 2.1. Release (circles) and recapture (triangles) locations of Atlantic cod (*Gadus morhua*) tagged in the Irish (green, n = 7) and Celtic Sea (yellow, n = 5).

2.2.3 Tag implantation

For full details of internal tag implantation, we refer the reader to Righton et al. (2006). In brief, individual cod were first captured using a modified commercial trawl or by line in shallow inshore areas. After being brought slowly to the surface (to avoid swimbladder rupture; van der Kooij et al., 2007), individual cod (body length > 45cm) were anaesthetised in a bath of seawater containing phenoxyethanol. Once anaesthetised, a small inclusion was made in the belly of the cod and a sterilised DST was inserted. To ensure the DST remained in place a thin plastic filament, often referred to as a spaghetti tag, was threaded from the DST, through the external wall of the fish and was secured externally. The small incision was then closed and glued. To aid identification, a second conventional mark recapture tag was externally stitched into the musculature at the base of the first dorsal fin. Each cod was then allowed to recover in a tank of seawater before

Table 2.1 Tagging details of cod in the Irish (n = 7) and Celtic Sea (n = 5). All cod were tagged with data storage tags (DSTs).

Fish ID	Body length (cm)	Stock*	Release date	Recapture date	Time at liberty (days)
IRE_1430	61	Irish Sea	17/04/1999	25/06/2000	436
IRE_3183	69	Irish Sea	20/03/2009	29/05/2010	436
IRE_3184	55	Irish Sea	19/03/2009	11/10/2009	207
IRE_5569	63	Irish Sea	23/03/2010	06/03/2011	349
IRE_5595	89	Irish Sea	25/03/2010	05/03/2011	346
IRE_5596	71	Irish Sea	26/03/2010	15/06/2011	447
IRE_5621	71	Irish Sea	25/03/2010	02/03/2011	343
CEL_1477	77	Celtic Sea	20/03/2008	24/09/2009	554
CEL_1527	71	Celtic Sea	19/03/2008	05/03/2009	352
CEL_4683	57	Celtic Sea	31/03/2004	05/10/2004	189
CEL_5613	79	Celtic Sea	08/03/2010	09/01/2011	308
CEL_5616	81	Celtic Sea	09/03/2010	07/03/2011	364

*Stock allocation is based on release location – see Figure 2.1.

being released overboard. Prior to release, each cod's body length (total length; cm) was measured and recorded. A GPS location of the vessel at the point of release was also noted.

Since the physical recovery of DSTs requires the cooperation of fishermen, a financial reward was offered for the return of the tag as well as the return of the fish carcass (see Bendall et al., 2009 for details).

2.2.4 Estimates of geographic position

Once a DST has been recovered and the data retrieved, the following information is available about an individual cod: an estimated body length (cm), a release location (longitude and latitude), a release date (dd/mm/yyyy), a time series of recorded depth (m) and a time series of recorded temperature (°C). Nested within the depth recordings are periods of time when the fish is at rest of the sea floor. These periods of time are not characterised by a flat relationship between depth and time but instead take the form of

sinusoidal cycle (Metcalf and Arnold, 1997). This cycle is indicative of the rise and fall of the tide and can be used to geographically reconstruct (\pm some uncertainty) the movement of an individual cod. This method is formalised as the tidal location method (TLM) and was first proposed by Metcalfe and Arnold in 1997. Here we use a method that couples the TLM with a Bayesian state-space model to estimate, for each day at liberty, the nonparametric probability distribution of each daily geographic position (longitude and latitude; Pedersen et al., 2008). This method assumes diffusion between locations, where the fish's distribution necessarily evolves over time according to a Fokker-Planck equation. Thus, the method is based on fitting a diffusion model to the movement between observations, by solving its Fokker-Planck equation numerically on a discrete spatial grid. The uncertainty associated with each daily geographic position varies as a function of two factors: (1) the quality of the tidal signal detected in the depth data and (2) the geographical proximity to tidal amphidromic nodes (Pedersen et al., 2008).

2.2.5 Horizontal and vertical movement

For each cod, we excluded the first two weeks and the last day from each time series (depth, temperature and geographic position) to remove any erroneous or irregular measurements associated with release and recapture events (as per Hobson et al., 2007). We calculated vertical movement (m day^{-1}) as the summed absolute difference between corresponding depth observations. Horizontal movement (km day^{-1}) was calculated as the straight-line distance between daily geographic positions using the Great Circle equation.

After visually inspecting each cod's movement through time we excluded further days from end of two individual cod's time series': CEL_5613 (74 days) and IRE_5596 (39 days). In IRE_5596 we observe an almost instantaneous drop off in depth, temperature and daily vertical movement (Appendix 2.2) 40 days prior to recapture. Such trends suggest that the tag either fell off or malfunctioned. Interestingly, we suspect that CEL_5613 was eaten by a much larger predator, possibly a surface-dwelling seal, approximately 75 days prior to tag recapture. Our reasons for suspecting this are threefold (Appendix 2.3). First, observed depth and daily vertical movement trend towards values of 0, indicating that the tag was spending prolonged periods of time at the surface with little or no vertical displacement. Second, daily horizontal movement remains fairly consistent suggesting the fish hasn't been landed by a fast-moving commercial fishing vessel. Third, observed temperature peaks, hitting abnormally high values (above 30 °C). We assume that such prolonged temperature peaks demonstrate

instances of consumption and digestion by an endothermic predator (Jorgensen et al., 2015).

2.2.6 Data analysis

Data analysis was conducted in R (R Core Team, 2016). We subset our dataset into three separate analyses. The first considers all of the 4331 daily observations (12 cod) and allows us to describe the longer-term movement and space use habits of Atlantic cod. The second considers observations made in the foraging period (1st June – 31st October; 12 cod). The third considers observations made in the spawning period (1st January – 30th April; 9 cod).

Since each fish was tagged and released with an unknown portion of its spawning season having already elapsed, we constrained analysis three to any observations made during the second spawning period (i.e. approximately ten months after release for the majority of cod considered here). Past studies show that cod have limited space use while spawning (Siceloff and Howell, 2013), show strong site fidelity (Robichaud and Rose, 2001; Skjæraasen et al., 2011; Zemeckis et al., 2014) and will often spend 10-50 days in a single spawning aggregation (Dean et al., 2014). For these reasons we chose to impose a second constraint on analysis three, and only consider daily observations with corresponding horizontal movement rates that are less or equal to 5km. These two constraints reduce the sample size considered in the analysis from twelve fish to nine fish (number of observations = 690). We lose CEL_4683 and IRE_3184 because they lack a second spawning period. We also lose IRE_3183 because its observed horizontal movements throughout the spawning period were greater than 5km. CEL_1477 is an exceptional long time series and as result contributes two separate foraging periods to analysis two. All 12 fish contribute to analysis two (number of observations = 1882).

Patterns of space use in each analysis are described using utilisation distributions (UDs). A UD is essentially a map of the probability of locating a tagged animal over a period of time (Worton, 1987). We calculate both individual varying and composite UD, where a composite UD refers explicitly to the collective space use of multiple cod in a given stock. All UD are calculated via the kernel density estimation (KDE) approach using the `adehabitatHR` package (Calenge, 2015, 2006) in R. Under the KDE approach, a single bivariate normal kernel (K) is placed over each geographical position, such that:

$$K(p) = \frac{1}{2\pi} \exp\left(-\frac{1}{2}p^t p\right), \quad [Eqn. 2.1]$$

where p is a vector containing the 1, ..., n geographical positions and p^t refers to the transpose of that vector. Here we have chosen to use a bivariate normal kernel due to commonality in the animal movement literature (e.g. Calenge, 2015, 2006). We do however note that other kernel functions are available (e.g. the Epanechnikov kernel) and that previous work on the subject demonstrates that the choice of kernel function does not greatly change the model's estimates (Silverman, 1986; Wand and Jones, 1995). The kernel estimation of the UD is therefore obtained by:

$$\hat{f}(p) = 1/(nh^2) \sum_{i=1}^n K\{1/h(p - P_i)\}, \quad [Eqn. 2.2]$$

where n is the number of geographical positions, h is a smoothing parameter and P_i is the i^{th} position of the animal. The smoothing parameter h controls the width of K and has been shown to be highly influential (Calenge, 2015, 2006). For example, a value of h that is too large will result in high levels of oversmoothing and yield a UD that frequently predicts the presence of an animal in areas that are not actually visited. Whereas, when h is too small the UD has a high variance. Usually, h is estimated in one of three ways. One, by the so-called 'reference bandwidth' approach where h is estimated as:

$$h = \sigma \times n^{-1/6} \quad [Eqn. 2.3]$$

where

$$\sigma = 0.5 \times (\sigma_{lon} + \sigma_{lat}) \quad [Eqn. 2.4]$$

and σ_{lon} and σ_{lat} are the standard deviations of the longitude and latitude coordinates of the animal's geographic position. Equation 2.4 is derived from assuming that the true distribution f is a multivariate gaussian, however this is uncommon in animal movement studies where animals will often have multiple modes of attraction. Two, by Least Square Cross Validation (LSCV), where the aim is to estimate an optimum value that minimises the difference between f and the estimated UD (by attempting to minimise the Mean Integrated Square Error; Seaman and Powell, 1996). Although appealing, the LSCV approach failed to converge for our movement data, and as a result (and as advised by Calenge, 2015, 2006) we do not consider it a viable approach during further analysis. The third way, which we apply here, is based on visual inspection, where successive trails are run and a value of h is chosen (as in Silverman, 1986; Wand and Jones, 1995). The range of these trails extend from $h = 0.1$ to $h = 0.45$ in intervals of 0.05 and include the 'reference bandwidth' to aid interpretation (see Appendix 2.4 and Appendix 2.5). Values of h are chosen per stock and applied to all individual and composite UDs. For

cod in the Celtic Sea we use a h value of 0.15. For cod in the Irish Sea we use a h value of 0.20. For a visual comparison between each stock's UD with the chosen h value compared to the h value estimated via the 'reference bandwidth' approach see Appendix 2.6 and Appendix 2.7. As is common in wildlife telemetry studies, we extract out the 95% probability contours and use them to demonstrate an individual's 'home range' or in case of each composite UD, the collective 'home range' of a stock (Downs and Horner, 2008). To aid clarity, we interpret an individual's 'home range' as a visual description of nearly all the areas that a tagged individual might visit during its time at liberty (Dean et al., 2014).

For analysis two and three, we summarise temperature ($^{\circ}\text{C}$) and depth (m) records to give daily means and standard deviations for each fish and for each stock. We also calculate daily means and standard deviations for the horizontal (km) and vertical (m) movement rates of each fish and each stock. We assume that all tagged cod are mature adults as their body lengths (Table 2.1) lie within the upper bounds of Atlantic cod's estimated length at first maturity (31-74cm; Froese and Pauly, 2017).

2.2.7 Other data sources

One of our aims was to investigate whether changes in seabed depth (m), seabed sediment or diet could help explain variances in the movement of individual cod tagged in the Irish and Celtic Sea. We sourced seabed depth (m) from the General Bathymetric Chart of the Oceans online repository (GEBCO, 2017), which is a global topographic dataset with a one-minute (1') spatial resolution (see Appendix 2.8). We sourced seabed sediment data from EMODnet's (The European Marine Observation and Data Network) Seabed Habitats online data portal (EMODnet, 2016), which provides a broad-scale habitat map comprising of the following seabed habitat types: coarse sediment; fine mud; mixed sediment; mud to muddy sand; rock or other hard substrata; sand; sandy mud to muddy sand and seabed (see Appendix 2.9). We sourced diet data from the CEFAS Data Hub which provides a detailed fish stomach record for Atlantic cod running from 1889 to 2011 (Pinnegar, 2014). For the Celtic Sea we used stomach records from ICES Divisions VII_f, VII_g and VII_h. For the Irish Sea we used stomach records from ICES Division VII_a. To more accurately represent our sample, we constrained the fish stomach records to a minimum predator size of 50 cm. We also removed any fish stomach entries where the length of the cod was unknown.

Both seabed depth and seabed habitat datasets were provided as raster objects. Using R, we first cropped each dataset and converted each raster object to a large spatial point data frame. We then extracted attribute values for each estimated daily geographic

position using the *over* method in the *sp* package (Pebesma, 2018) in R. Attribute values of interest were numerical depth estimates (m) and categorical seabed habitat types.

As with daily horizontal and vertical movement rates, we summarise seabed depth estimates to give daily means and standard deviations for each fish, for each stock and for each analysis. We calculated the percentage time spent in each seabed habitat type for each stock during the foraging (1st June – 31st October) and spawning (1st January – 30th April) period. We also calculated the percentage contribution of each prey type to the observed diet of cod in the Irish and Celtic Sea.

All plots were generated using the *ggplot2* (Wickham, 2009) and *ggmap* (Kahle and Wickham, 2013) packages in R.

2.3 Results

In total we consider the movement of 12 individual cod, five that were released in the Celtic Sea and seven that were released in the Irish Sea. The average time spent at liberty was 361 days (\pm 101 days).

2.3.1 Long-term movement patterns

In the Celtic Sea, we observe extensive and complex movement patterns but no clear signs of migration (Figure 2.2, panel A). Three of the five fish (CEL_4683, CEL_5613 and CEL_5616) moved in a southerly direction after their release, spending prolonged periods of time residing in the southern parts of ICES Division VIIg and in the northern parts of ICES Division VIIh (Figure 2.3, panel A; Appendix 2.10). CEL_4683 was recaptured in October. The other two cod (CEL_5613 and CEL_5616) move northwards at the end of year before being recaptured in roughly the same area as their release (Figure 2.3, panel A; Appendix 2.10). In both cases release and recapture occurred during the spawning period (Table 2.1). The other two fish (CEL_1477 and CEL_1527) remained exclusively in the Celtic Sea (ICES Divisions VIIg and VIIh) and despite turning back on themselves numerous times, showed no evidence of migration out the area (Figure 2.3, panel A; Appendix 2.10). No fish tagged in the Celtic Sea moved north into the Irish Sea or moved west into the English Channel (Figure 2.2). All five cod had relatively high rates of daily horizontal movement (Table 2.2), which coupled with an apparent lack of migration into other ICES Divisions, suggests that individual fish were undertaking bouts of extensive localised movement. Despite being released in a number of different locations, home range estimates for individual cod in the Celtic Sea are highly

overlapping (Figure 2.3, panel B; Appendix 2.11) and are collectively distributed within the spatial boundaries of ICES Divisions VIIg and VIIh (Figure 2.2, panel B).

In the Irish Sea we find no evidence of cod moving south into the Celtic Sea (Figure 2.2, pane; A). Individual cod were either tagged and released in the central (n = 5) or eastern (n = 2) Irish Sea (Figure 2.1). Cod in the eastern Irish Sea (IRE_5596 and IRE_5621) remained almost exclusively within the area and spent large periods of time in the shallow inshore waters surrounding the Isle of Man (Figure 2.3, panel A; Appendix 2.10). Both IRE_5596 and IRE_5621 did display some changes in space use, moving north into the North Channel before very quickly returning to the eastern Irish Sea. Within the five fish that were tagged in the central Irish Sea we note two very distinct movement patterns (Figure 2.3, panel A; Appendix 2.10). Two cod (IRE_3184 and IRE_5569) remained exclusively within the central Irish Sea. Both cod displayed some southerly movements however neither individual left the spatial boundaries of ICES Division VIIa. The other three cod (IRE_1430, IRE_3183 and IRE_5595) show extensive movements north up through the North Channel. IRE_5595 and IRE_1430 move as far north as the northern extent of the North Channel whereas IRE_3183 moves all the way out into the much deeper water of the North Atlantic Ocean (max seabed depth experienced = 777 metres). All three cod move out of ICES Division VIIa and move into ICES Division VIa. As in the Celtic Sea, home range estimates for cod in the Irish Sea are highly overlapping (Figure 2.3, panel B; Appendix 2.11). Despite this, it is clear that spatial extent of those home ranges is greater and much more varied within cod tagged in the Irish Sea.

2.3.2 Foraging period

Cod tagged in the Celtic Sea remain exclusively in the ICES Division VIIg and the northern parts of VIIh. Their movements (Figure 2.4, panel B; Appendix 2.12) and home ranges (Figure 2.4, panel A; Appendix 2.12) are highly overlapping, as individuals mix on what we assume is highly productive foraging grounds. Such spatial overlap is not apparent in the Irish Sea. Two cod (IRE_5569 & IRE_3184) remain in the centre of the Irish Sea between the Welsh and Irish coasts (Figure 2.4, panel B; Appendix 2.12). Four cod remain the North Channel (IRE_1430, IRE_5595, IRE_5596 and IRE_5621), whereas one cod (IRE_3183) spends the duration of the foraging period in the very deep waters of North Atlantic Ocean (Figure 2.4, panel B; Appendix 2.12). All five of these cod move from ICES Division VIIa to ICES Division VIa and are likely to come into contact with cod occupying waters off the Scottish west coast.

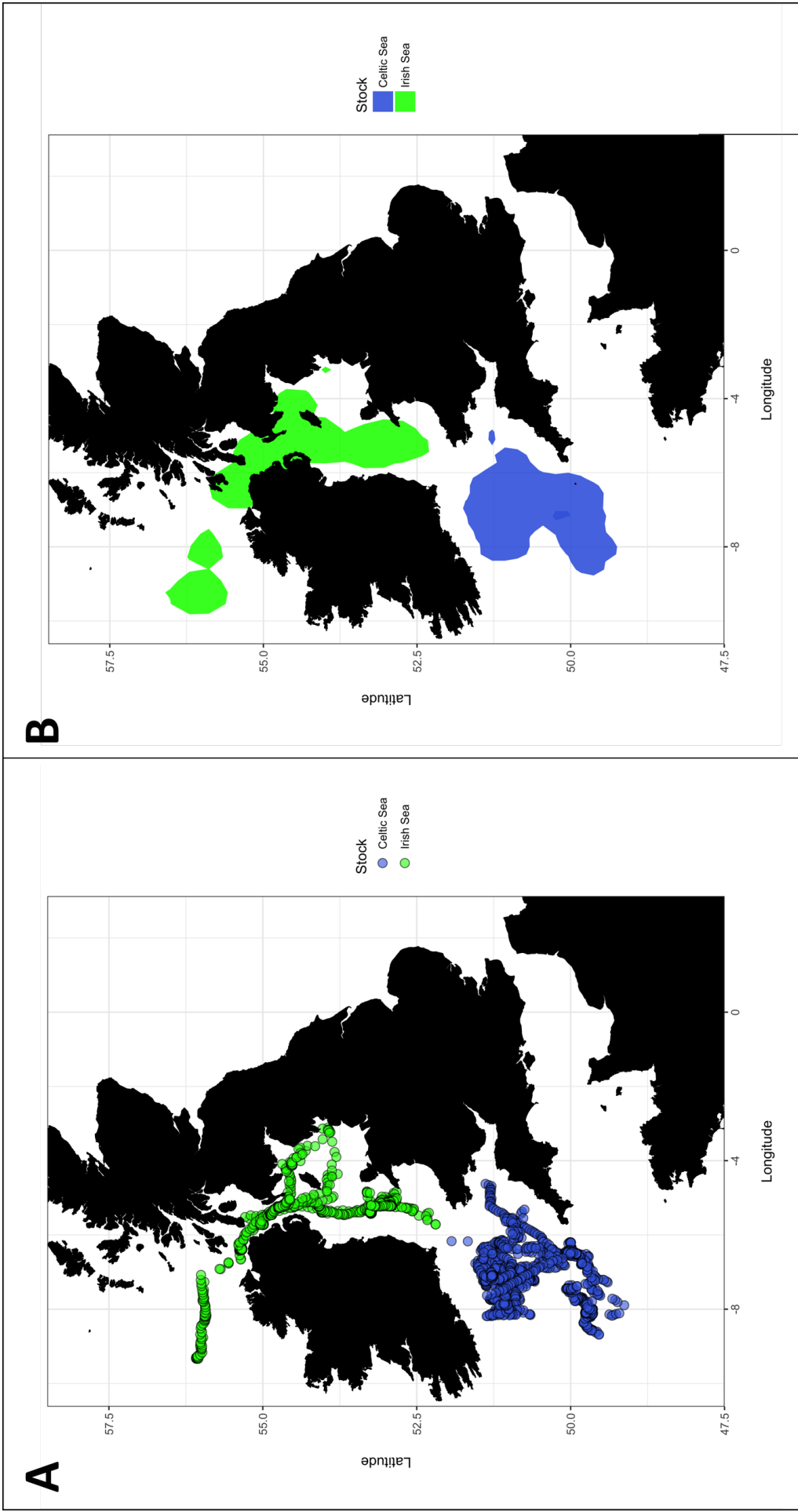


Figure 2.2. Estimated daily geographic positions (A) and estimated composite home ranges (B) of Atlantic cod tagged in the Irish (green, $n = 7$) and Celtic (blue, $n = 5$) Sea.

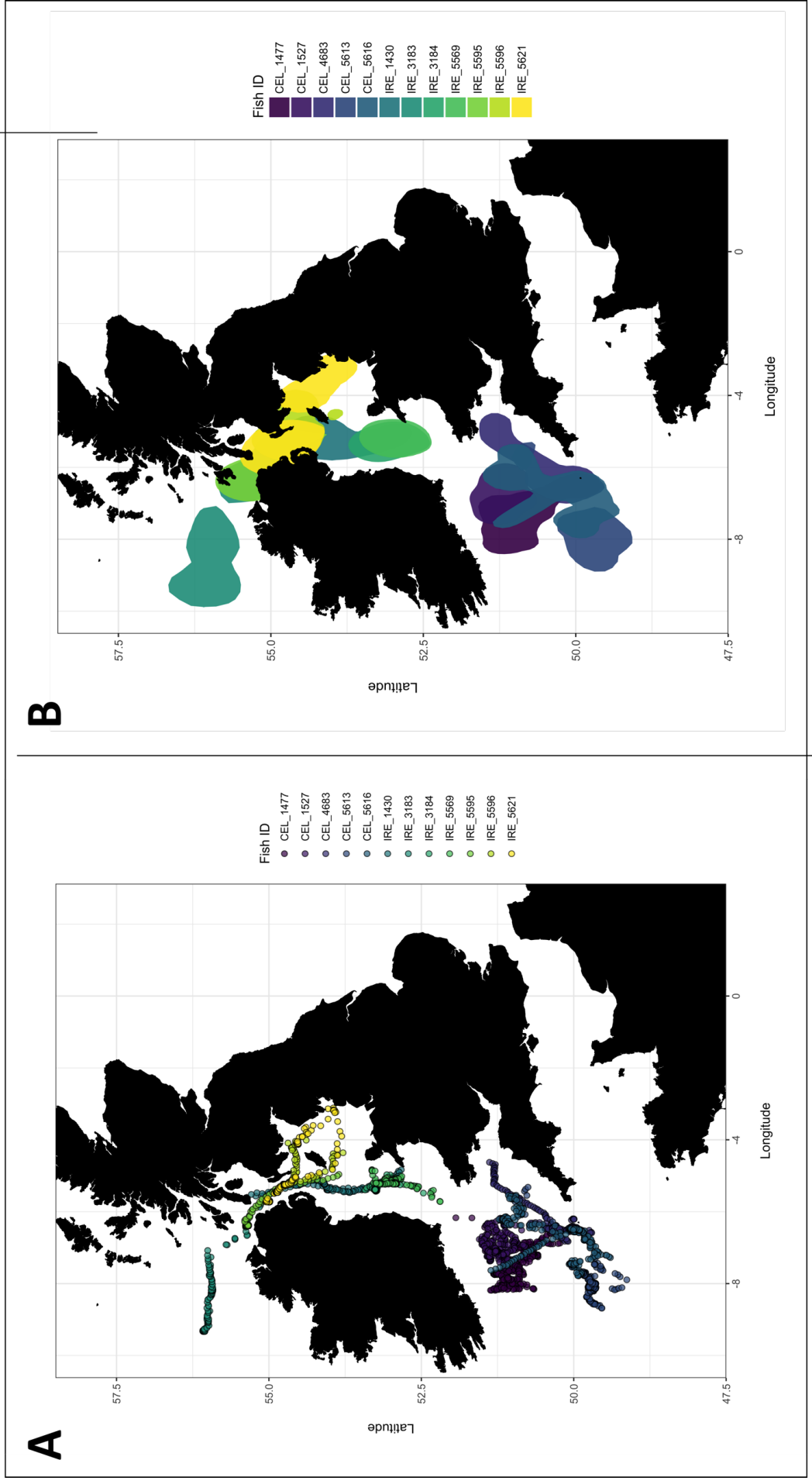


Figure 2.3. (A) Estimated daily geographic positions of individual cod tagged in the Irish and Celtic sea. (B) Estimated home ranges of individual cod tagged in the Irish and Celtic sea. For details on Fish ID we refer the reader to Table 2.1.

Table 2.2 Statistics summarising the movement (horizontal and vertical movement), fish depth, sea depth and temperature experienced by cod in the Irish (n = 7) and Celtic sea (n = 5). All values are averages (\pm 1 standard deviation) calculated at the daily level across all tagged cod in a given area. For individual cod values we refer the reader to Appendix 2.12 and Appendix 2.15.

	Horizontal distance travelled (km)	Vertical distance travelled (m)	Fish depth (m)	Sea depth (m)	Temperature (°C)
Irish Sea (All)	2.5 (\pm 3.2)	369.9 (\pm 208.9)	99.8 (\pm 45.5)	217.8 (\pm 185.0)	10.5 (\pm 2.5)
Celtic sea (All)	4.1 (\pm 4.6)	97.8 (\pm 91.3)	106.3 (\pm 24.5)	115.9 (\pm 30.2)	9.9 (\pm 0.7)
Irish Sea (spawning)	1.8 (\pm 1.0)	317.1 (\pm 158.9)	69.3 (\pm 35.5)	150.1 (\pm 57.9)	7.9 (\pm 1.3)
Celtic sea (spawning)	2.1 (\pm 1.2)	226.6 (\pm 121.0)	95.7 (\pm 16.4)	132.7 (\pm 41.2)	9.1 (\pm 0.5)
Irish Sea (foraging)	1.9 (\pm 2.3)	394.0 (\pm 222.5)	121.0 (\pm 45.6)	253.9 (\pm 215.9)	12.6 (\pm 1.7)
Celtic sea (foraging)	4.0 (\pm 4.1)	60.8 (\pm 41.8)	111.8 (\pm 19.5)	113.4 (\pm 24.2)	10.2 (\pm 0.6)

All, all data points. spawning, 1st January to 30th April. foraging, 1st June – 31st October.

Throughout the foraging period, daily horizontal movement was much larger in cod tagged in the Celtic Sea than cod tagged in the Irish Sea (Welch's t-test: $t = 12.7$, $df = 1225.2$, p value < 0.001 ; Table 2.2 Appendix 2.13). Conversely, daily vertical movement was significantly larger in cod tagged in the Irish Sea than cod tagged in the Celtic Sea (Welch's t-test: $t = 47.5$, $df = 1143.1$. p value < 0.001 ; Table 2.2; Appendix 2.13). Irish Sea cod spent the foraging period at greater depths than cod in the Celtic Sea (Welch's t-test: $t = 5.9$, $df = 1491$. p value < 0.001 ; Table 2.2; Appendix 2.13). Such differences in movement and depth utilisation suggest that cod in either stock are exploiting their environments in very different ways.

From an environment perspective, cod in the Irish Sea continuously occupied much deeper water than cod in the Celtic Sea (Welch's t-test: $t = 20.9$, $df = 1083.4$, p value < 0.001 ; Table 2.2; Appendix 2.13). We find that the temperature experienced by cod in the Irish Sea is significantly warmer than cod in the Celtic Sea (Welch's t-test: $t = 43.8$, $df = 1359.3$, p value < 0.001 ; Table 2.2; Appendix 2.13). We also note that seabed habitat experienced by cod in the Celtic Sea (Figure 2.5, panel A) is different to that experienced by cod in the Irish Sea (Figure 2.5, panel C). For instance, cod in the Celtic Sea appear

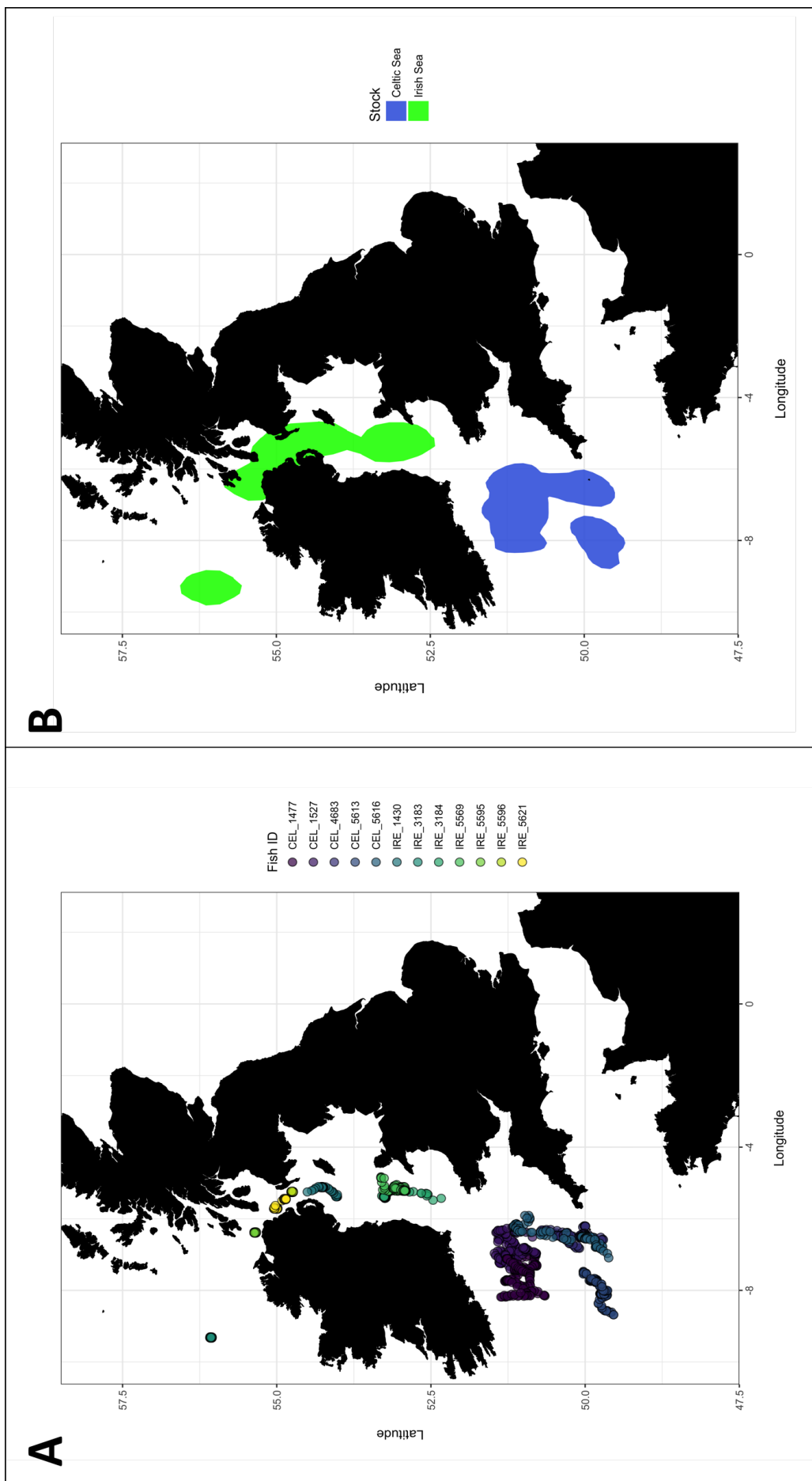


Figure 2.4. (A) Estimated daily geographic positions of individual cod tagged in the Irish and Celtic Sea during the foraging period (1st June – 31st October). (B) Estimated composite home ranges of cod tagged in the Irish (green, n = 5) and Celtic Sea (blue, n = 7) during the foraging period. For details on Fish ID we refer the reader to Table 2.1.

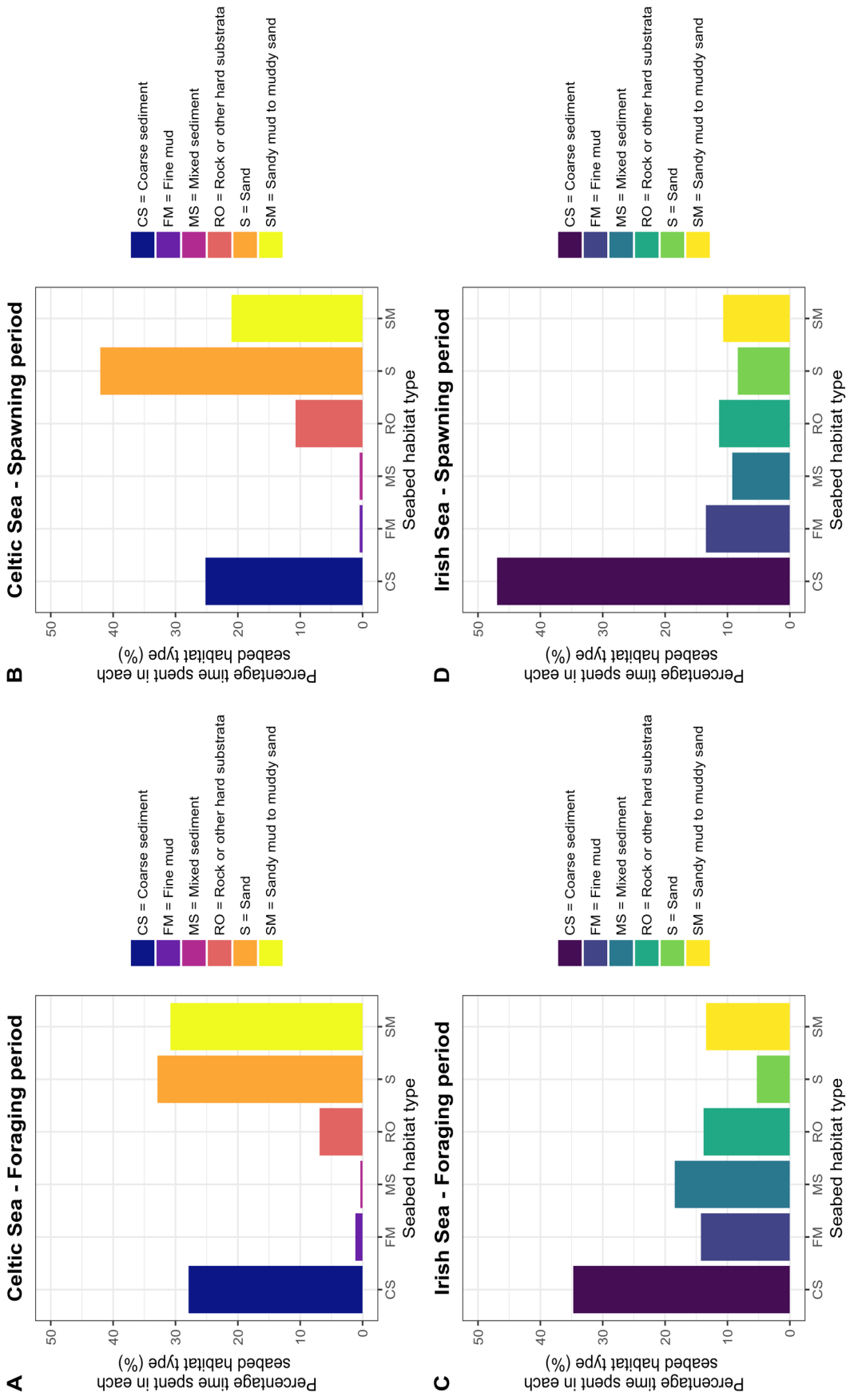


Figure 2.5. Percentage time spent in each seabed habitat type during the foraging (1st June – 31st October, A and C) and spawning (1st January – 30th April, B and D) period in cod tagged in the Irish (C and D) and Celtic Sea (A and B).

to favour seabed habitat types of sand and sandy mud, whereas the seabed habitat profile of cod in the Irish Sea is heavily skewed towards coarse sediment.

2.3.3 Spawning period

During the spawning period, the estimated home ranges of cod in the Celtic and Irish Sea were smaller (Figure 2.6, panel B). Three of the four cod (CEL_1477, CEL_1527 and CEL_5616) tagged in the Celtic Sea remained in ICES Division VIlg (Figure 2.6, panel A; Appendix 2.14). The other cod tagged in the Celtic Sea (CEL_5613) remained in ICES Division VIIh (Figure 2.6, panel A; Appendix 2.14). In all four cases, the spatial use of individual cod during foraging and spawning periods are similar. A similar pattern was present in the Irish Sea. Four cod (IRE_1430, IRE_5595, IRE_5596 & IRE_5621) occupied waters in the North Channel and the north/north-eastern Irish Sea (Figure 2.6, panel A; Appendix 2.14), consistent with their space use during the foraging period (Figure 2.4, panel A; Appendix 2.12). The remaining cod (IRE_5595) stayed in the centre of the Irish Sea (Figure 2.6, panel A; Appendix 2.14), also consistent with observations made during the foraging period (Figure 2.4, panel A; Appendix 2.12).

Daily horizontal movement during the spawning period was significantly greater in cod tagged in the Celtic Sea than those tagged in the Irish Sea (Welch's t-test: $t = 3.2$, $df = 359.2$, p value = 0.002; Table 2.2; Appendix 2.15). Daily vertical movement during the spawning period was also significantly larger in cod tagged in the Irish Sea than those cod tagged in Celtic Sea (Welch's t-test: $t = 7.8$, $df = 533.7$, p value < 0.0001; Table 2.2; Appendix 2.15). In addition to these differences, horizontal movement was significantly greater during the foraging period than during the spawning period (Celtic Sea – Welch's t-test: $t = 3.2$, $df = 566.0$, p value = 0.002; Irish Sea – Welch's t-test: $t = 2.7$, $df = 751.0$, p value = 0.007; Table 2.2; Appendix 2.15). However, for cod tagged in the Celtic Sea, daily vertical movement was significantly greater in the spawning period than in the foraging period (Welch's t-test: $t = 20.9$, $df = 279.0$, p value < 0.0001; Table 2.2; Appendix 2.15). The opposite was true in cod tagged in the Irish Sea, where daily vertical movement was significantly greater in the foraging period than in the spawning period (Welch's t-test: $t = 8.2$, $df = 1101.0$, p value < 0.0001; Table 2.2; Appendix 2.15).

During the spawning period, the average depth of individual fish and the average temperature experienced was significantly lower in the Irish Sea compared to the Celtic Sea (fish depth – Welch's t-test: $t = 12.4$, $df = 592.5$, p value < 0.0001; sea temperature – Welch's t-test: $t = 43.8$, $df = 1359.3$, p value < 0.0001; Table 2.2; Appendix 2.15). These findings are reversed during the foraging period. Sea depth was significantly deeper in

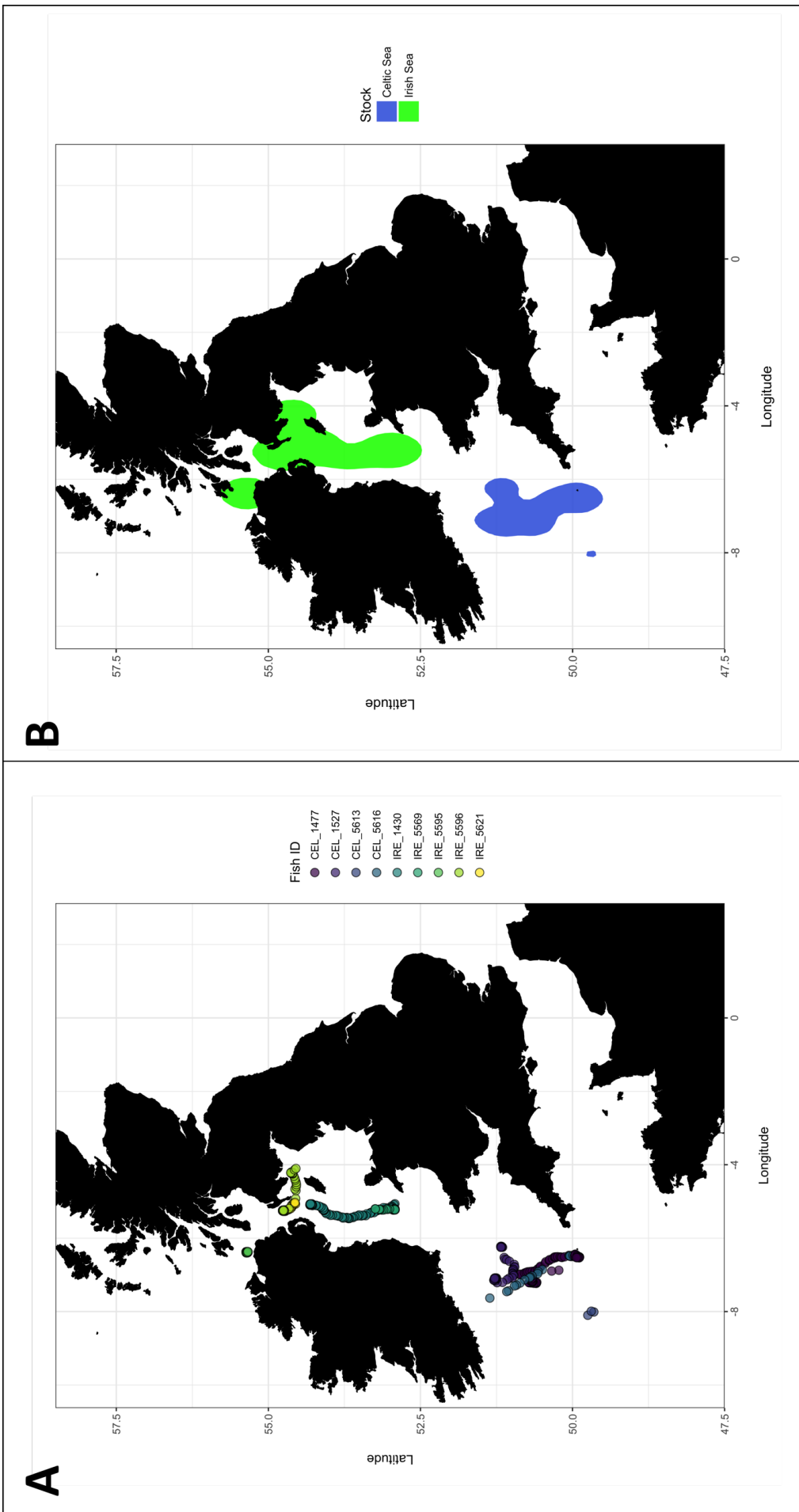


Figure 2.6. (A) Estimated daily geographic positions of individual cod tagged in the Irish and Celtic Sea during the spawning period (1st January – 31st April). (B) Estimated composite home ranges of cod tagged in the Irish (green, n = 5) and Celtic Sea (blue, n = 4) during the spawning period. For details on Fish ID we refer the reader to Table 2.1.

the Irish Sea compared the Celtic Sea (Welch's t-test: $t = 4.3$, $df = 556.8$, $p \text{ value} < 0.0001$) however the difference was much less during the spawning period than during the foraging period (Table 2.2).

The seabed sediment experienced by cod during the spawning period was almost identical to what is experienced during the foraging period (Figure 2.5). The only notable differences were that Celtic Sea cod spent more time in sandy habitats (Figure 2.5, panel B) whereas Irish Sea cod displayed an even greater affinity to coarse sediment (Figure 2.5, panel D).

2.3.4 Diet

Stomach content data revealed marked differences in the prey types of similarly sized cod (fish size listed in Table 2.1). Celtic Sea cod feed, in the majority, on a range of crabs (33%) and crab like crustaceans (22%; Figure 2.7, panel A). Irish Sea cod feed primarily on lobsters (36%; Figure 2.7, panel B). Both Irish and Celtic Sea cod also feed of other smaller (unidentified) fish species (Irish Sea, 35%; Celtic Sea, 26%).

2.4. Discussion

In this study, we shed much needed light on the broad-scale movement and spatial ecology of Atlantic cod in the Irish and Celtic Sea. In doing so we note four main findings. (1) That given our sample size, we find no evidence of stock mixing between the Irish and Celtic Sea. However, we do note that mixing is a prevalent feature between cod in the Irish Sea and cod stocks situated off the west coast of Scotland (ICES Divisions VIa). (2) That despite exhibiting high rates of horizontal movement (4.1 km day^{-1} ; Table 2.2), cod in the Celtic Sea appear to forage and spawn in very similar locations, a finding that is indicative of a resident stock within ICES Divisions VIIf, VIIg and VIIh. Conversely, Irish Sea cod seem to be operating as two semi-discrete sub-populations, one situated almost exclusively in the centre of the Irish Sea and the second moving between foraging grounds in the northern North Channel and spawning grounds in the north/north-eastern Irish Sea. (3) That horizontal and vertical movements play critical but very differing roles in the foraging and spawning strategies of cod in the Irish and Celtic Sea. For instance, we show that horizontal movement is consistently higher in the cod tagged in the Celtic Sea than in cod tagged in the Irish Sea whereas the opposite is true for vertical movement. (4) That despite occupying very different environments and moving through these environments in very different ways, cod in the Irish and Celtic sea feed on very

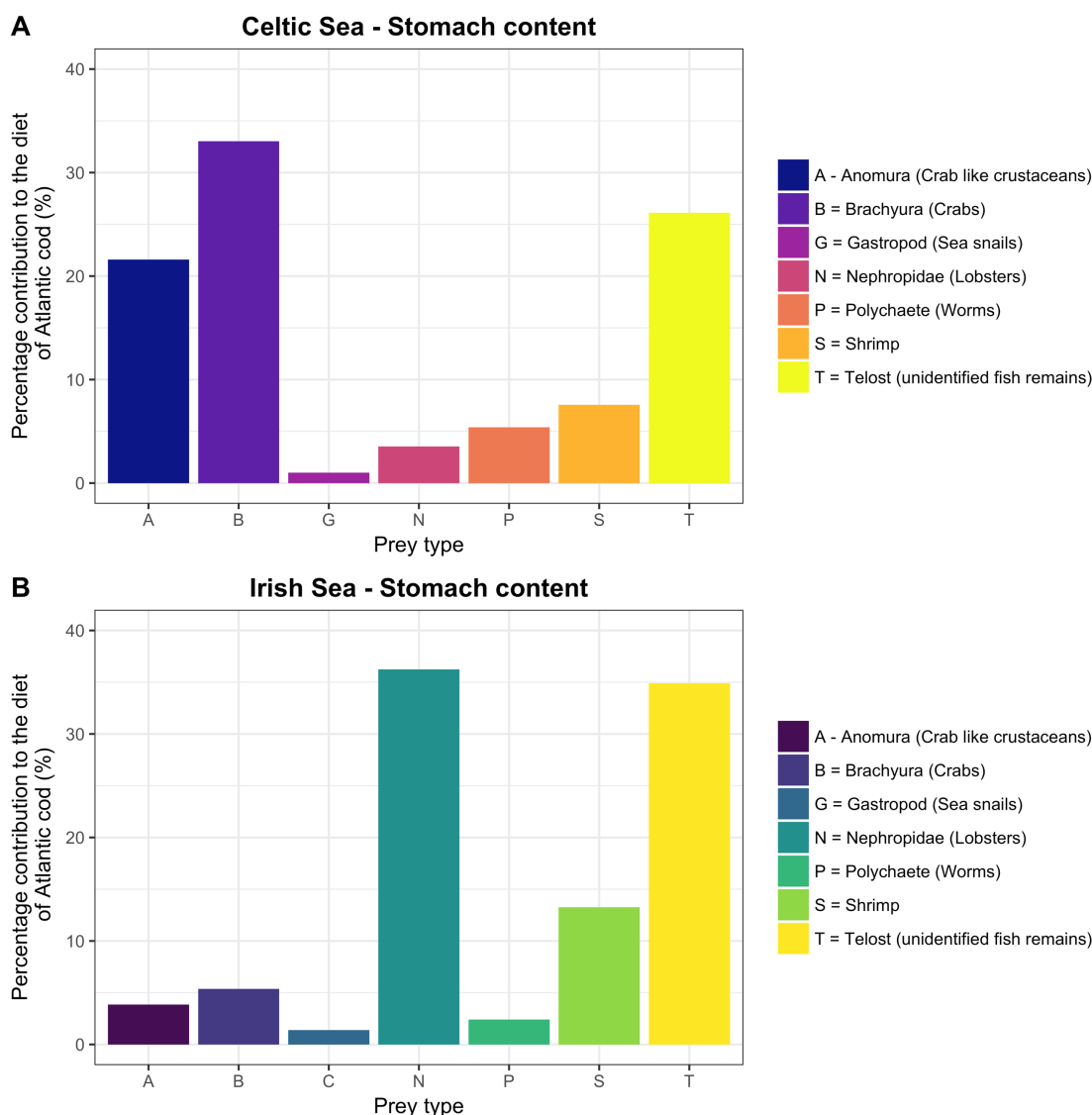


Figure 2.7. Percentage contribution of each prey type to the diet (stomach content) of Atlantic cod in the Celtic (A) and Irish (B) Sea. Only prey types that contributed more than 1% to the stomach content of Atlantic cod in each area were considered.

similar prey items; a mix of benthic dwelling crustaceans and smaller (unidentified) fish. In the following discussion we will interpret these findings and highlight how they can inform the management of these two heavily exploited stocks.

Here, we find no evidence of that cod in the Celtic Sea move north into the Irish Sea or that cod in the Irish Sea move south in the Celtic Sea. This lack of exchange supports current stock assessment model and management strategies where Celtic and Irish Sea cod are treated as discrete units. However, our findings do contradict past studies where mature cod in the Irish Sea have been shown to disperse in a southerly direction towards ICES Division VIIg after spawning (Bendall et al., 2009; Brander, 1975; Connolly and Officer, 2001). Such differences could be a consequence of a limited sample size, highlighting (as discussed in Chapter 1) that any inference gained from the movements

of a select number of individual animals can often overlook or skew our understanding of population dynamics (Hebblewhite and Haydon, 2010; McGowan et al., 2017). However, in this case it is worth noting that all three previously cited studies rely heavily on mark recapture methods, where only the release and recapture locations of individual cod are known (Bolle et al., 2005). We have already shown that cod in the Irish and Celtic sea undergo complex and extensive movement patterns, often turning back on themselves. For example, cod IRE_1430 displays southerly movements after its release, moving down through the centre of Irish Sea before turning back on itself and transiting north towards foraging grounds in the northern Irish Sea (Figure 2.4, panel A; Appendix 2.8; Appendix 2.16). An analogous movement pattern is observed in cod IRE_3184, where dispersion to the south is followed by a return to the deeper waters of the central Irish Sea after approximately 90 days (Appendix 2.8; Appendix 2.16). Such fine scale movements will go unobserved in mark-recapture studies and as result any inference gained from the deployment of DSTs must be viewed as an advancement on our understanding of cod movement in the Irish Sea.

Cod in the Celtic Sea are shown to remain exclusively within ICES Divisions VIIIf, VIIh and VIIg. Despite exhibiting high rates of daily horizontal movement (4.1 km day^{-1} ; Table 2.2), individual (Figure 2.3, panel B) and composite (Figure 2.2, panel B) space use patterns of cod in the Celtic Sea are highly overlapping and show minimal variance between foraging (Figure 2.4, panel B) and spawning periods (Figure 2.6, panel B). Such findings are indicative of a resident stock, who forage and spawn in the same locale. Resident stocks are a prevalent feature of cod ecology (Robichaud and Rose, 2004) and have been shown to occur in the German Bight, a shallow inshore area off the south-west coast of Denmark (Griffiths et al., 2018) and the Scalloway area of the Shetland Isles (Neat et al., 2006). From a management perspective, stocks that reside in same geographical location are notoriously prone to local depletion (Heath et al., 2008; Kritzer and Sale, 2004). This is because resident stocks are inherently spatially predictable and despite the enforcement of catch control measures (e.g. TACs and mesh size restrictions), management at the stock level has minimal control over of spatial distribution of fishing effort (Neat et al., 2006; Rose and Kulka, 1999). Despite this, the spawning stock biomass of cod in Celtic Sea is increasingly slowly and show signs of recovery (ICES, 2017a). We hypothesise that this success may be a direct consequence of two factors: (1) the establishment of marine protected areas (MPAs) and (2) the rising abundance of crab in the Celtic Sea. A network of MPAs or analogous areas of conservation (e.g. Special Area for Conservation or Marine Conservation Zones) have been in place in the Western English Channel and Celtic Sea since 2009 (JNCC, 2017).

Many of these areas were originally designed to reduce the impact of otter gears on vulnerable marine habitats (JNCC, 2017) however because cod remain in the area year-round they will indirectly benefit from reductions in trawl capture. Using landings data as a proxy for abundance, preliminary investigations also suggest that crab (Brown crab, *Cancer pagurus*; Appendix 2.17) have experienced a population boom in the Celtic Sea, with reported landings experiencing a three-fold increase between 2005 and 2013 (ICES, 2013b). We have shown that crab and crab like crustaceans are an important food source for cod in this area (Figure 2.7), therefore individuals will benefit from an increased availability of prey.

Despite providing no evidence for the exchange of cod between the Irish and Celtic Sea, we do observe several instances when cod in the Irish Sea move north into ICES Division VIa. These movements typically occur outside of the spawning period and draw parallels to the tendencies of other marine species (e.g. Atlantic Bluefin tuna, *Thunnus thynnus*; Block et al., 2005) who spawn in relative isolation but mix with other populations during foraging. In this case, movements north will bring cod from the Irish Sea into contact with cod occupying waters off the Scottish west coast and the Firth of Clyde (Neat et al., 2014). Stocks in these areas have also struggled to recover from historic overexploitation and despite an enforced total allowable catch of zero (ICES, 2017c), spawning stock biomass remains low (ICES, 2017c). Current hypotheses for this lack of recovery are centred around two factors. First, a steady increase in the abundance of grey seals since the 1960s which will exert significant predation pressure on cod (Alexander et al., 2015; Cook et al., 2015; Houle et al., 2016). Second, the rising importance of the Nephrops fishery off the west coast of Scotland (ICES, 2013c) which not only targets one the preferred prey items of cod (lobsters e.g. Norway lobster, *Nephrops norvegicus*; Figure 2.7) but also exerts high rates of bycatch on cod and other gadoid species (Catchpole et al., 2007; ICES, 2013c). Current stock assessment and management strategies in the Irish Sea do not consider the exchange of cod northwards into ICES Division VIa (ICES, 2017a). As a result, it is likely that two potentially important sources of mortality are being overlooked, both of which hold significant explanatory power for the impaired recovery of cod in the Irish Sea.

Previous investigations into the movement of cod in the Irish Sea point towards a semi-discrete stock structure, where cod in the eastern/northern Irish Sea remain separated from cod in the western/central Irish Sea for large periods of the annual cycle (Brander, 1975). Here we add evidence to these conclusions but demonstrate a need for further

Table 2.3. Straight-line distance (km) between the release and recapture locations of tagged cod in the western and central Irish Sea. Straight-line distances were calculated using the Great Circle Equation.

Fish ID	Release location (RL1)		Recapture location (RL2)		Distance between RL1 and RL2 (km)
	Latitude	Longitude	Latitude	Longitude	
IRE_1430†	53.95	-5.42	54.31	-5.09	45.05
IRE_3183†	54.76	-5.28	55.38	-6.39	99.08
IRE_3184*	53.42	-5.40	53.26	-5.39	18.50
IRE_5569*	53.09	-5.14	53.24	-5.20	17.01
IRE_5595†	53.85	-4.96	54.67	-5.18	92.15

*, remain in the central Irish Sea. †, move north into North Channel.

work. First, we show that cod released in the eastern Irish Sea (IRE_5596 and IRE_5621) move north into the North Channel but display no signs of east-west or east-south movements. Moreover, cod released in the western/central Irish Sea either remain in the central Irish Sea (IRE_3184 and IRE_5569) or move northwards into the North Channel and beyond (IRE_1430, IRE_3183 and IRE_5595). For those that do remain in the central Irish Sea, site fidelity is shown to be a prevalent feature as the straight-line distance between their release and recapture locations is, on average, only 18 km (Table 2.3). For those cod that do move north (e.g. IRE_1430 and IRE_5595), it is likely that they come into contact with cod from the eastern Irish Sea during the foraging period. Such spatial overlap during the foraging period suggests that the North Channel is an area of significant importance to cod in the Irish Sea, and merits further investigation (in the context of an MPA). Interestingly, if cod in the eastern/northern and western/central Irish Sea exhibited a semi-discrete stock structure and only mixed during the foraging period, we might expect those cod that moved north out of the central Irish Sea (IRE_1430, IRE_3183 and IRE_5595) to display similar evidence of site fidelity (Brander, 1975; Connolly and Officer, 2001; Pawson, 1993). However, this does not appear to be the case (Table 2.3). Theoretically, this lack of movement back down through the North Channel and into the central Irish Sea could be a consequence of tag malfunction or an unobserved error during data manipulation, as only a handful of very deep depth measurements are sufficient to offset the geographically estimation step leading to fairly large uncertainties (David Righton, *pers coms*). We suspect this latter explanation could

be valid in cod IRE_3183 as this would provide the first example of cod in the Irish Sea moving out into the deeper waters (sea depth greater than 700m, Appendix 2.13) of North Atlantic. Alternatively, the lack of return trip could be an ecological phenomenon, marking either a distributional shift in the tendencies of the stock (as predicted in response to widespread warming by Drinkwater, 2005 and Serpetti et al., 2017), or demonstrate a gap in our knowledge about the movement and spawning dynamics of cod in the Irish Sea. Either way, further tagging studies are essential.

In terms of movement rates, we have shown that horizontal and vertical movement play very different roles in the foraging and spawning dynamics of cod in the Celtic and Irish Sea. Daily horizontal movement is shown to be much greater in the Celtic Sea than in Irish Sea. The opposite is true when it comes to vertical movement, as daily vertical movement is much larger in cod tagged in the Irish Sea than cod tagged in the Celtic Sea. Both of these trends are consistent across the spawning and foraging periods. Such differences could simply illustrate how local bathymetry dictates swimming and foraging strategy (an idea proposed by Hobson et al., 2009). For example, Irish Sea cod are moving through a very deep but highly variable environment (as shown by a standard deviation of ± 185.0 , Table 2.2). Therefore, it is likely that individuals are travelling in midwater and using vertical displacements to move up into the water column in search of food. Such behaviour is analogous to the foraging strategies of juvenile Pacific Bluefin tuna (*Thunnus orientalis*; Kitagawa et al., 2007), striped marlin (*Tetrapturus audax*; Sippel et al., 2007) and tiger sharks (*Galeocerdo cuvier*; Heithaus et al., 2002; Holland et al., 1999), where the water column is continually traversed in the search for food. Conversely, Celtic Sea cod are consistently recorded at depths that are comparable to the estimated seabed depth (Table 2.2), suggesting that individuals travelling horizontally along what is shown to be a sandy seabed (Figure 2.5). Such movement will be advantageous in terms of prey encounter, as crustaceans such as crabs and other small fish are also found in close proximity to the seabed (Adlerstein and Welleman, 2000).

We also show that cod in the Celtic Sea significantly increase their vertical movement rates during the spawning period. Vertical displacements have been shown by several authors to a prominent characteristic of spawning in cod, as individuals undertake courtship in close proximity to the seabed (Dean et al., 2014) but move towards the surface during spawning release (Brawn, 1961; Hutchings et al., 1999; Meager et al., 2009). The same increase in vertical activity isn't found in cod tagged in the Irish Sea, however when comparing the movement rates across the two sampled stocks, it is clear that vertical movement is just consistently high in the cod tagged in the Irish Sea.

Furthermore, when the horizontal movement rates of cod in the either stock are compared to the work of others, it is clear that the average movement rates calculated here are much lower than in the North Sea (Griffiths et al., 2018; Righton et al., 2007) and English Channel (Griffiths et al., 2018; Hobson et al., 2009), where cod are shown to move at speeds of 5-50 km day⁻¹. Such findings add support to the contention that movement is highly variable in cod, varying from individual to individual, and stock to stock, consistent with the concept that behaviour in this species is the result of a complex interplay between biological and ecological factors (Hobson et al., 2009; Righton et al., 2001).

Two further findings surround the temperature and seabed habitat type experienced by cod in the Irish Sea during the foraging period. Given their high rates of vertical activity and their preference for benthic-dwelling lobsters (Figure 2.7), our prior expectation was that individuals tagged in the Irish Sea would be inhabiting a rocky seabed. Vertical movement would therefore become a foraging necessity, as individuals were forced to move up and down a variable seabed in their pursuit of prey. Despite such expectations, we found that Irish sea cod inhabited a seabed habitat that is dominated by coarse sediment (Figure 2.5). This finding reinforces our previous comments surrounding midwater movement patterns, as Irish Sea cod are moving vertically into the midwater (as supported by a large average difference between sea and fish depth, Table 2.2), as opposed to moving along a variable seafloor. Additionally, average sea temperature is shown to be very high during the foraging period (12.6 °C, Table 2.2) before dropping off during the spawning period (7.9 °C, Table 2.2). Previous work by Neat et al. (2014) suggests that Irish Sea cod experience strong seasonal cycles in temperature, a feature that is not present in the Celtic Sea, despite its more southerly latitude (Neat et al., 2014). Acclimatisation or adaptation to consistently cooler conditions may limit the movement of Celtic Sea cod north into the warmer and more variable waters of the Irish Sea. Such differences in thermal conditions could help explain why mixing between the two stocks is not observed and why Celtic Sea stocks remain resident in ICES Divisions VIIIf, VIIh and VIIg. Moreover, these findings highlight why studies that aim to investigate blanket climate driven range shifts in temperate marine species (e.g. Dulvy et al., 2008; Rutterford et al., 2015), must do so with care and knowledge of the biology and ecology of the species they are investigating (Heath et al., 2012).

By describing the movements and spatial ecology of Atlantic cod in the Irish and Celtic Sea we have investigated four main research questions and highlighted their importance for management. To summarise, we have shown that limited mixing occurs between cod in the Irish and Celtic Sea, validating current stock assessment and management

strategies. In the Celtic sea we have shown that cod form a resident stock in ICES Divisions VII f, VII h and VII g and despite recent signs of recovery, could be highly susceptible to continued rates of exploitation as well as climate change. In the Irish Sea we have added evidence to past observations that cod form a semi-discrete stock and introduced the idea that the North Channel may be of significant importance during the foraging period. We have also used recorded movement rates and external data sources (temperature and seabed habitat types) to detail how cod move through very different environments in a bid to grow, reproduce and ultimately survive. Finally, we have used stomach content data and previous investigations to support our theories about the recovery of cod in the Irish and Celtic Sea (Alexander et al., 2015; Bendall et al., 2009; Brander, 1975; Catchpole et al., 2007; Connolly and Officer, 2001; Neat et al., 2014). These findings do not answer the overarching research question; why have cod stocks in the Irish and Celtic Sea struggled to recover from historical overexploitation? However, our analysis of tagging data is a step towards informing future studies in the area.

On numerous occasions in this chapter we refer to the need for a greater sample size. More information inherently provides a greater level of certainty and allows inferences gained to take on a much more actionable quality in the eyes of fisheries managers and conservation decision makers. A greater sample size however comes with its own complexities. Here, we have simply described the movements of twelve individual cod, however this approach cannot be simply extended to the movement of hundreds of fish, each of which exhibits its own degree of individual variation. In Chapter 3 we tackle this problem head on by introducing a novel methodology for the analysis of three-dimensional movement in marine fish. By making the explicit assumption that fish of the same species behave in a numerically similar way, we use a hidden Markov model (HMM) framework coupled with Bayesian priors to gain population-level inference from a large dataset of individual movements (Griffiths et al., 2018).

Chapter 3.

Scaling marine fish movement behaviour from individuals to populations.

The following chapter is a slightly extended version of the published article Griffiths et al. (2018). A full authors' contribution statement can be found in the published article. In the discussion of this chapter we also refer to a second piece of collaborative work lead by Timo Adam (University of Bielefeld, Germany) that has recently been accepted for publication in *Methods in Ecology and Evolution* (Adam et al., in review).

3.1 Introduction

The spatial management of the marine world requires in-depth information about how animals move, when they move and where they move to. Key to increasing our understanding of species space use, movement patterns, and how individuals interact with the environment they inhabit, is the rising deployment of small and reliable data loggers and transmitters on free-roaming marine animals (Costa et al., 2012; Hays et al., 2016; Hussey et al., 2015). Capable of recording a range of movement metrics, including horizontal and vertical movement alongside basic environmental information such as water temperature, salinity and ambient daylight, these devices have revolutionized our understanding of fundamental ecology (Hussey et al., 2015), documented ocean-wide dispersal events (Block et al., 2011), highlighted areas that are essential for species survival (Raymond et al., 2015) and even allowed us to test the effectiveness of current conservation policies (Pittman et al., 2014; Scott et al., 2012).

One of the main motivations for animal-borne telemetry studies is that by understanding individual movement behaviour, we might infer the population-, species- and community-level consequences of movement (Block et al., 2011; Hindell et al., 2016; Raymond et al., 2015; Wakefield et al., 2011). This is especially true in marine systems, as individual observations provide our only insight into the otherwise unobservable. As highlighted in Chapter 1 and Chapter 2, the scaling of inference from individual movement patterns to population dynamics requires two important components. The first is an adequate sample size (number of individuals) to address the ecological question of interest (Hebblewhite and Haydon, 2010) and second, a statistical means by which we gain meaningful inference at the individual- and population-level from a finite sample of individuals (e.g. Jonsen, 2016; Langrock et al., 2012; McClintock et al., 2013).

The issue of sample size has been extensively discussed, especially when considering how movement studies can inform marine conservation and spatial management (Hebblewhite and Haydon, 2010; McGowan et al., 2017; Nguyen et al., 2017; Ogburn et al., 2017). Tags can be expensive (McGowan et al., 2017), are liable to occasional failure or loss and often result in individual pathways that are data-poor or have a low number of observations. As a result, meeting the minimum sample size of 20+ individuals when making simple statistical comparisons between populations is uncommon (Hebblewhite and Haydon, 2010), with even greater numbers needed when testing for the effects of age, sex and species identity (Lindberg and Walker, 2007). In the absence of a collaborative effort across multiple institutions (e.g. Block et al., 2011a; Hindell et al., 2016), a significant increase in funding or a community-wide shift to data sharing (e.g. via online data repositories like Movebank - Kranstauber et al., 2011); it would appear that the most viable route towards robust population-level inferences are approaches that make the most of the tagging data we already have.

As the technology underpinning tags continues to advance, so too have the methods used to explore the behavioural structure of animal movement data (Gurarie et al., 2016). Among these methods are autocorrelation functions (e.g. Boyce et al., 2010), clustering algorithms (e.g. van Moorter et al., 2010), changepoint analyses (e.g. Gurarie et al., 2009; Madon and Hingrat, 2014), frequency-based Fourier or wavelet analyses (e.g. Guzmán et al., 2017; Shepard et al., 2006), first passage time approaches (e.g. Benhamou, 2004) and multistate random walks (e.g. Forester et al., 2007; Morales et al., 2004), many of which have been applied to ecological questions. For instance, fast Fourier transforms have been used to identify periodicities in the vertical movements of basking sharks (*Cetorhinus maximus*; Shepard et al., 2006), whereas multiple change point algorithms have been used to investigate behavioural changes in the daily movements of Macqueen's Bustards (*Chlamydotis macqueenii*; Madon and Hingrat, 2014). Despite such methodological proliferation, hidden Markov models (HMMs) and hidden semi-Markov models have taken centre stage in recent years, especially when observational error is negligible and behavioural classification is the desired outcome (e.g. McClintock et al., 2012; Patterson et al., 2008). Favoured because they match our intuitive understanding that movement is given by switches in an animal's motivation (Patterson et al., 2017), HMMs provide a mechanistic, computationally efficient and statistically robust means of objectively classifying movements into discrete states with different statistical properties (Langrock et al., 2012). Moreover, the flexibility of the HMM approach means they are capable of dealing with missing observations (Parton 2018) as well as varying amounts of temporal non-independence (Langrock et

al., 2012). HMMs have also been extended to account for periodicities by linking the model's underlying state process to behavioural patterns that are heterogenous in time, such as diurnal variations (e.g. Leos-Barajas et al., 2017b; Towner et al., 2016).

HMMs have been fitted to multiple individual pathways simultaneously in both the frequentist (e.g. Langrock et al., 2012; McKellar et al., 2015) and Bayesian statistical paradigms (Jonsen, 2016; McClintock et al., 2013). However, these approaches are typically implemented by specialist statisticians and require the coupling of HMM and hierarchical structures, producing a hierarchical Hidden Markov model (hHMM). The alternative is the use of HMMs or other state-space approaches that fit on an individual by individual basis (e.g. Jonsen et al., 2007; Michelot et al., 2017). This latter, more frequently used approach has its advantages, the most notable being an ease of use for statisticians and biologists alike. Fitting per individual also has its disadvantages. The first is that it requires individual movement paths that are suitably data-rich to achieve model convergence, imposing even stricter restrictions on sample size. The second is a distinct lack of any formal process by which state one in animal A is ensured consistency with state one in animal B. This lack of consistency means that estimated parameters can readily inform individual-level movement studies but will result in tricky interspecific and intraspecific comparisons, limiting a researcher's ability to ask *post-hoc* population-level questions of their data.

Our objective is to introduce an alternative framework that uses HMMs to overcome the described limitations of individually fitted HMMs whilst maintaining their heralded ease of use advantages. Our approach combines an N -state HMM and several hierarchical structures but bypasses the need to integrate over the random effects (as in hHMMs; Langrock et al., 2012) by using information we gain from our data-rich pathways as *a priori* approximations of each states movement parameters. Doing so not only allows us to achieve coherent individual- and population-level state classification, but also ensures that we maximise our sample size by gaining meaningful inference from our data-poor and data-rich movement paths.

To illustrate our approach, we apply it to a real ecological problem – quantifying seasonal space use patterns in Atlantic cod (*Gadus morhua*) and European plaice (*Pleuronectes platessa*) in the North Sea and English Channel. Both Atlantic cod and European plaice have significant commercial and conservation value and as a result have been the subject of several long-term tagging programs (e.g. Hobson et al., 2009, 2007; Hunter et al., 2004b, 2004a; Righton et al., 2001). Drawing on this, the rest of this chapter considers a case study of 107 individual bivariate movement paths, many of which

(n=73) have limited observations and/or lack clear biological signals. Our findings demonstrate clear spatio-temporal patterns in the movement behaviour of either species that are consistent with individual-level studies (Hobson et al., 2007, 2009; Hunter et al., 2004b, 2004a; Neat et al., 2014). Furthermore, by analysing a relatively large dataset, we provide a unique insight into how differing sub-stocks of cod and plaice shift their behaviour on a seasonal basis, with clear consequences for fisheries management and conservation.

3.2 Methods

3.2.1 Case study data

Movement paths were taken directly from the deployment of data storage tags (DSTs) on free-roaming fish in the North Sea or English Channel. The dataset includes 107 individuals from two species of European demersal fish: Atlantic cod (n=46) and European plaice (n=61). All fish were tagged and released between December 1996 and June 2011. Fish were broadly separated into sub-stocks based on release location (see Figure 3.1) and displayed considerable variation in movement path duration (Appendix 3.1).

Each DST was programmed to record depth (m) at 10-minute intervals for the duration of deployment. The first two weeks and the last day of every time series were excluded to remove any erroneous or irregular measurements associated with release and recapture events as per Hobson et al. (2007). For details of tag type, fish catchment, tag implantation and measurement accuracy see Righton et al. (2010; *Gadus morhua*) or Hunter et al. (2004b; *Pleuronectes platessa*). Each movement path is a bivariate time series of horizontal and vertical movement per day. Net vertical movement (m day^{-1}) of each fish was taken directly from the raw DST data by calculating the absolute difference between corresponding 10-minute depth measurements and summing the values for each day at liberty. Horizontal movement (m day^{-1}), in comparison, was inferred indirectly from the depth data in a two-step approach. First, daily geolocation estimates were produced via a Fokker-Planck-based method that combines Metcalfe and Arnold's (1997) tidal location method and a Bayesian state-space model (see Pedersen et al., 2008 for model details). The straight-line distance between daily geographic estimates (commonly referred to as 'step-length') was then calculated using the Great Circle equation. Both vertical (v) and horizontal (h) movement metrics were log (natural log) transformed prior to model implementation. Only time series that were longer than 40+

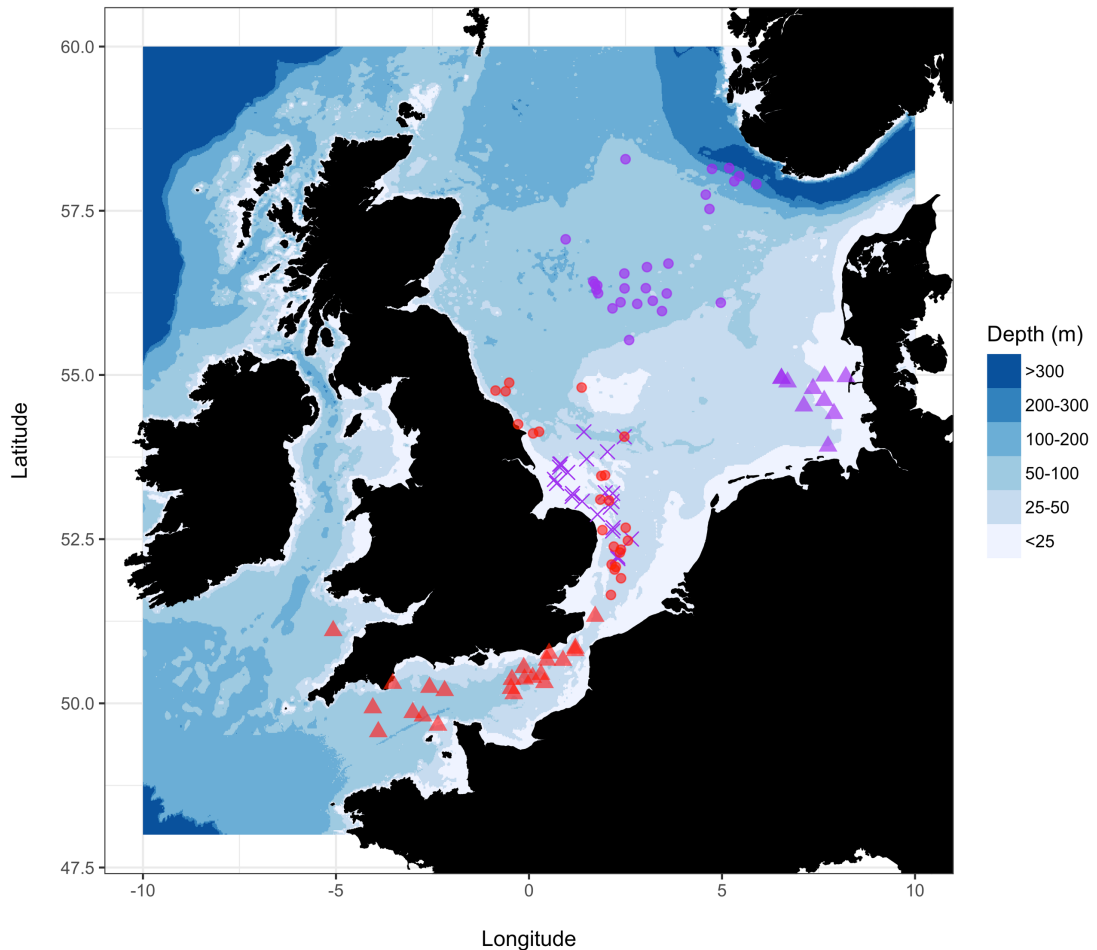


Figure 3.1. Release locations of all tagged fish. Atlantic cod ($n=46$) are shown in red, fish are grouped into the English Channel sub-stock (triangles, $n=23$) or the Southern North Sea sub-stock (circles, $n=23$) based on release location. European plaice ($n=61$) are shown in purple, fish are grouped into three sub-stocks based on release location: Central North Sea (circles, $n=27$), German Bight (triangles, $n=10$) or Southern North Sea (crosses, $n=24$).

Days and had complete depth recordings were used in this study. For descriptions of horizontal and vertical movement in Atlantic cod and European plaice see Hobson et al. (2009, 2007) and Hunter et al. (2004b, 2004a).

All geolocation estimates (latitude and longitude), date stamps and daily horizontal and vertical movement rates, along with estimated state sequences (product of the model described in sections 3.2.2 and 3.2.3) are freely available on the CEFAS Data Hub (<https://doi.org/10.14466/cefasedatahub.54>).

3.2.2 The model

Previous individual-level studies demonstrate that Atlantic cod and European plaice display periods of high activity while in the water column punctuated by periods of

relatively low activity while on the seabed (Hunter et al., 2003; Righton et al., 2010). Thus, we consider a discrete 2-state HMM. We label state one as ‘resident’ (R), representing periods of time with low movement rates. We label state two as ‘migrating’ (M), representing a much more active phase where movement rates in the horizontal and vertical dimension are greatly increased. As in all attempts to infer behaviour from movement observations, state labels must be interpreted with care as they provide simplified proxies of unobserved behavioural modes, not direct equivalents (Patterson et al., 2017).

For a movement path of length T , it is assumed that an underlying, non-observed state sequence S_1, \dots, S_T , taking values in $\{R, M\}$ describes the persistence within and stochastic switching between states. The time varying evolution of this state process takes the form of a (first-order) Markov chain, with transition probability matrix Γ

$$\Gamma = \begin{pmatrix} \gamma_{R \rightarrow R} & \gamma_{R \rightarrow M} \\ \gamma_{M \rightarrow R} & \gamma_{M \rightarrow M} \end{pmatrix} \quad [Eqn. 3.1]$$

and

$$\gamma_{j \rightarrow k} = \Pr(S_{t+1} = k | S_t = j) \quad [Eqn. 3.2]$$

for any j, k in $\{R, M\}$. Given a state j at time t the observation x_t is assumed to be drawn from a multivariate normal distribution (MVN):

$$x_t \sim MVN(\mu_j, \Sigma_j) \quad [Eqn. 3.3]$$

with

$$\mu_j = \begin{pmatrix} \mu_{jH} \\ \mu_{jV} \end{pmatrix} \quad [Eqn. 3.4]$$

and

$$\Sigma_j = \begin{pmatrix} \sigma_{jH}^2 & \rho_j \sigma_{jH} \sigma_{jV} \\ \rho_j \sigma_{jH} \sigma_{jV} & \sigma_{jV}^2 \end{pmatrix} \quad [Eqn. 3.5]$$

and H and V represent movements made in the horizontal and vertical dimension, respectively. Thus, the complete-data likelihood given a state sequence S_1, \dots, S_T is

$$\omega_{S_1} \phi_{S_1}(x_1) \gamma_{S_1 \rightarrow S_2} \phi_{S_2}(x_2) \dots \gamma_{S_{T-1} \rightarrow S_T} \phi_{S_T}(x_T) \quad [Eqn. 3.6]$$

where the row vector ω is the Markov chain initial state probability (which we assume to be uniform at $t=1$) and ϕ_j refers to the multivariate normal density stated in equation 3.3.

We allow distinct parameters for each fish, indexed by $i = 1, \dots, 107$, and write these as Γ^i , μ_j^i and Σ_j^i .

In practice, standard HMM algorithms allow us to calculate the actual likelihood, when the states are unobserved, very efficiently by integrating over all possible state sequences using the forward algorithm (Zucchini et al., 2016). Framing the model in this way enables us to conduct parameter estimation using a Bayesian approach, by numerically maximising the posterior density. The classification probability of each state at t is then determined using the backward smoothing algorithm (Zucchini et al., 2016). More details for how the efficient HMM machinery can be used to conduct statistical inference are given in Zucchini et al. (2016), for the particular case of animal movement modelling see Patterson et al. (2017). For our case study, we used the R optimisation routine *optim* to numerically maximize the log posterior density. State allocation is carried out by selecting the most likely state at each time point separately.

Two limitations of the HMM approach to behavioural classification are mentionable. First, the discrete-time approach is only suited to regularly timed observations. This isn't a problem here however when analysing movements recorded via PSATs, where irregular sampling is common (see Chapter 1 section 1.1.3), the assumption that state transition probabilities and state-dependent distributions are homogeneous will often be improper (Langrock et al., 2012). In these cases, a continuous-time HMM, where an observation is treated as a sample of an underlying continuous movement model, may be more appropriate (Parton, 2018). Such models are scale-invariant and as a result do not require regularly spaced observations to infer behaviour (Langrock et al., 2012). The second limitation is that observations, be it movement rates or locations in space and time, must be observed with no or negligible error. Here we estimate location, and by association horizontal displacements, using an adapted tidal geolocation model (Pedersen et al. 2008). The original tidal location method of Metcalfe and Arnold (1997) certainly has the potential for fairly large uncertainties (in the range of 10-40km; Hunter et al., 2004) as locations are estimated one point at a time. In comparison, when the fish's locations are modelled as a sequence, the iterative build-up of information greatly reduces this uncertainty (as in Pedersen et al., 2008). Consequently, we are confident that the uncertainty surrounding each fish's movement path is within the scale of the observations (David Righton, *pers coms*) and can be considered negligible (a condition advised by Patterson et al., 2017). For example, the standard deviation across one thousand possible sample paths in cod 1186 (illustrated in Appendix 3.2) is on average 8.0 km day⁻¹ (range 0 – 16km day⁻¹), a value that is comparable to those reported in

Hobson et al. (2009). Put into context, this uncertainty is comparable to locations estimated by the ARGOS system (Hays et al., 2001) and is an order of magnitude better than light-based geolocation estimators (Teo et al., 2004). When error is much larger or is likely to inform the analysis, Bayesian state-space formulations of the behavioural classification problem are often the preferred approach (e.g. Breed et al., 2012; Jonsen et al., 2013).

Periods of relative inactivity (low h and v movement rates) can persist for 3-5 months in either species (Metcalfe et al., 2006; Righton et al., 2010). To accommodate this persistence within state, we have imposed a prior penalty term on the transition probabilities, such that

$$\gamma_{11} \sim \text{beta}(\alpha, \beta) \quad [\text{Eqn. 3.7}]$$

and

$$\gamma_{22} \sim \text{beta}(\alpha, \beta) \quad [\text{Eqn. 3.8}]$$

where $\alpha = 99$ and $\beta = 1$. This prior, termed here after as the transition probability prior, is designed to ensure that states R and M correspond to strong seasonal shifts in movement behaviour and not day-to-day fluctuations.

3.2.3 Classifying fish movement

We apply the model described in section 3.2.2 to all 107 individual movement paths, such that each fish gets its own parameter set. Each parameter set consists of 12 estimated parameters, two transition probabilities and 2 sets of 5 parameters describing the mean (μ_j) and covariance (Σ_j) of each state. A total number of 24,624 days (Atlantic cod = 9290 days; European plaice = 15,334 days) were considered. As expected, the resulting state sequences are predominately made up of two clearly defined behavioural modes – one more active and one less active (see Appendix 3.3 and 3.4 for example output). However, the parameters describing the numerical structure of these modes showed great variation among fish, with no clear consistency. Moreover, a handful of movement paths failed to achieve model convergence, as an upper threshold of observations is needed for robust parameter estimation (Patterson et al., 2009).

To avoid the wasteful removal of valuable data or a tedious *post-hoc* description of the individual variation that exists in the HMMs output, we adopted an alternative approach. Based on the selection criteria outlined in Appendix 3.5, we select model output from 34 fish (Atlantic cod, $n=11$; European plaice, $n=23$) spread evenly across the five sub-stocks (Appendix 3.6). We then calculate summary statistics (means m and variances δ) that

describe the numerical structure of the two states (Appendix 3.7). These summary statistics are used to construct Gaussian distributions (Figure 3.2), $N(m, \delta)$ where m and δ are dimension (h or v) d , state j and species specific given the selected sample. These informative distributions (4 per species), termed here after as priors on the model's movement parameters, are then introduced directly into the HMMs likelihood function, such that equation 3.6 is multiplied by

$$\prod_j \prod_d \phi(\mu_{jd} | m_{jd}, \delta_{jd}) \quad [Eqn. 3.9]$$

where $\phi(\cdot | m, \delta)$ is the Gaussian density with mean m and variance δ . Thus, our informative priors act to constrain the mean parameters of each state during the classification process.

This adapted approach is applied to the classification of the remaining 73 individual pathways (Atlantic cod, $n=35$; European plaice, $n=38$), outputting state sequences that comprise comparable states (Figure 3.3). This enables *post-hoc* comparisons to be made at the individual- and population-level with relative ease.

In order to illustrate how prior inclusion influences the state classification process, we have run a single European plaice's movement through both versions of the model (Figure 3.4). Most notable is the reclassification of data points from a migratory state in the HMM to a resident state in the adapted HMM. Additionally, because one of our stated objectives was to effectively use the information gained from our data rich pathways to inform the classification of data poor pathways, we feel it necessary to provide an example (see Figure 3.5).

All HMMs were coded and implemented in R (R Core Team, 2016; example code can be downloaded from GitHub: https://github.com/cagriffiths1/Fish_HMM). All plots were generated using the *ggplot2* (Wickham, 2009) and *ggmap* (Kahle and Wickham, 2013) packages in R. Bathymetric data was sampled from the General Bathymetric Chart of the Oceans online repository (GEBCO, 2017), which is a global topographic dataset with a one-minute (1') spatial resolution.

3.2.4 Prior sensitivity analysis

When imposing prior distributions in statistical models it is always important to test what influence those priors have on the models' predictions, in our case the model's estimated state sequences. To test the sensitivity of our model to changes in the transition probability prior we varied the α and β values that characterise the priors' beta distribution and re-ran the HMM for all 34 'selected' fish. In test 1 ($\alpha = 49.5$, $\beta = 0.5$) we

still expect a behavioural switch to occur at an order of every 100 days. However, we approximately double our prior's variance. In test 2 ($\alpha = 49$, $\beta = 1$) the expected rate of switching is halved.

To test the model's sensitivity to changes in the movement parameter priors, we varied the variances (δ 's) that describe the spread of each state and re-ran the adapted HMM for 10 randomly selected fish from each species. In test A, we increased all δ values by 10%, reflecting a prior expectation of greater variability between the parameters of individual fish, and in test B we decreased all δ values by 10%, reflecting an expectation of reduced variability. During all re-runs of the adapted HMM (Test A and Test B) the state transition prior is kept constant, therefore ensuring that any change in state is a direct consequence of the changes to the model's movement parameter prior.

3.2.5 Univariate modelling

To assess the advantages of using bivariate responses, we also carried out an analysis using a univariate observation model, considering only movements made in the horizontal dimension. The same model for transition probabilities is used as described above. We apply this approach to the 34 fish (Atlantic cod, $n=11$; European plaice, $n=23$) previously characterized as data-rich movement paths. Reported comparisons reflect the percentage change, if any, in the resultant state sequences for each individual fish.

3.2.6 Inferring population patterns

Since population dynamics emerge as the sum of the individuals that comprise the population we used individual movement behaviours to explore spatiotemporal patterns. Annual temporal patterns of movement behaviour were calculated for each species in two ways. First, the daily individual probabilities of each fish being in each state were averaged across all individuals and over each week of the year. Secondly, the proportion of fish classified to each state was calculated by averaging the daily number of fish in each state and smoothing it, again to the weekly time step. Week refers to weeks of the year, starting on the 1st January and ending on the 31st December and is independent of year.

Patterns of space use while in either state were visualised using utilization distributions (Kie et al., 2010; Womble and Gende, 2013; Worton, 1989). For each species and sub-stock, utilization distributions were calculated by pooling all daily horizontal geolocations for specified time periods and spatially binning them into 5km² grid cells (Maxwell et al., 2011; Womble and Gende, 2013). Specified time periods were state dependent and based on a weekly averaged probability of observing a given state across all individuals

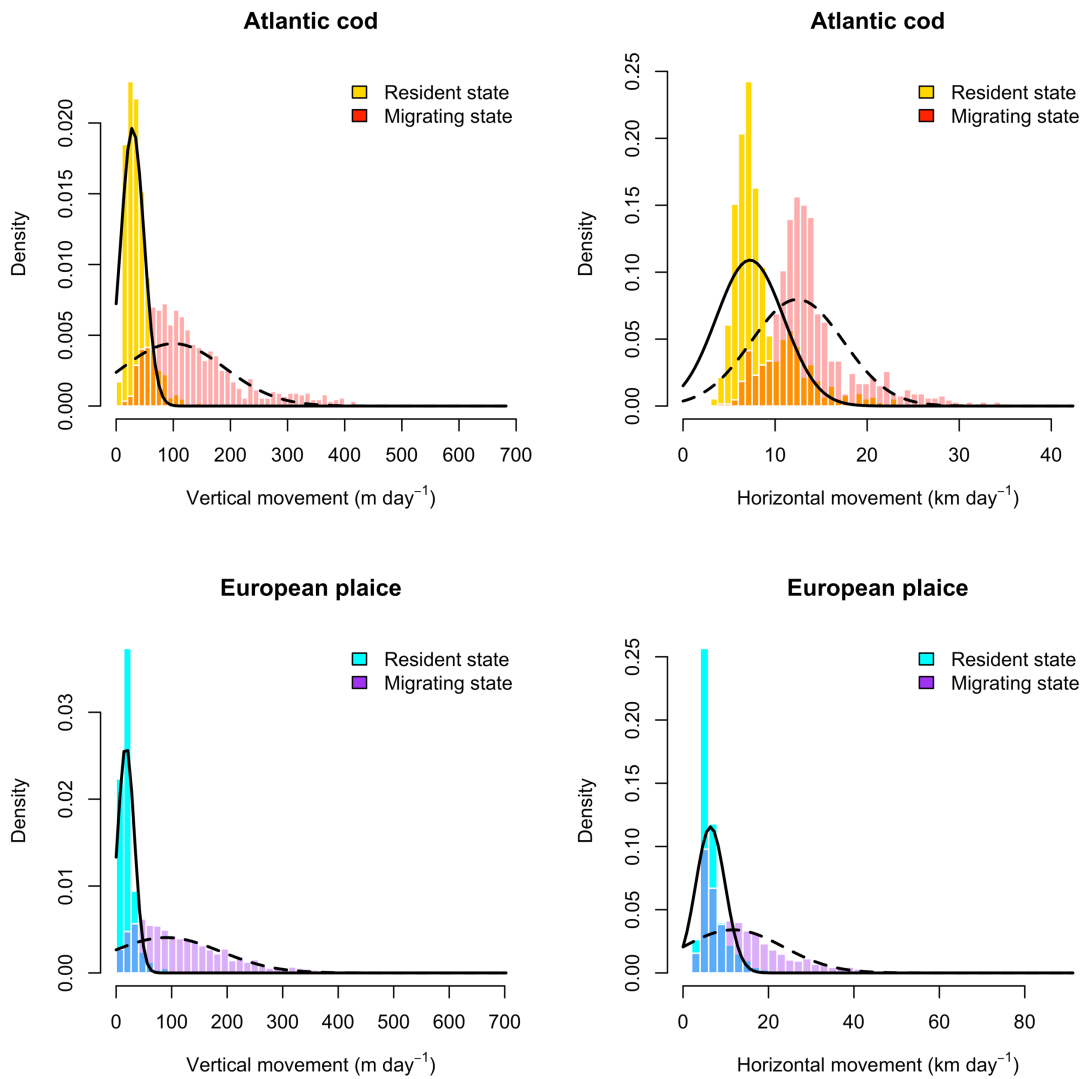


Figure 3.2. Estimated state-dependent distributions (bars) for vertical (left) and horizontal (right) movements of all 34-selected fish. Black lines illustrate the movement parameter prior distributions $N(m, \delta)$ that were constructed based on collective model output. Prior distributions are state (resident, solid line; migratory, dashed line), species (Atlantic cod, top; European plaice, bottom) and dimension (horizontal or vertical) specific.

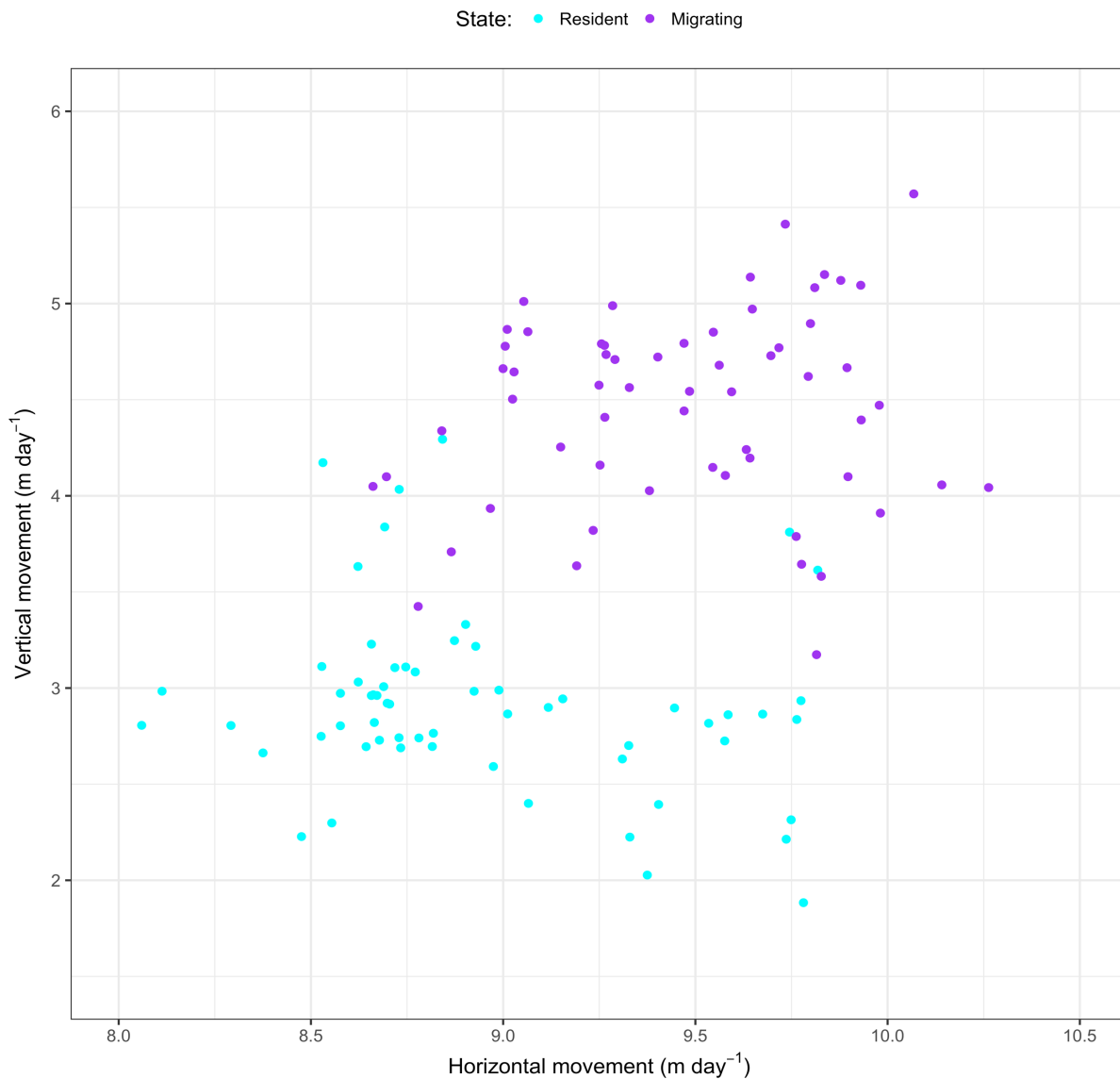


Figure 3.3. Mean bivariate movement rates by state in all 61 European plaice. All horizontal and vertical movement rates have been log (natural log) transformed.

exceeding 0.5. Successive weeks classified to the same behavioural state were then grouped. In Atlantic cod this meant locations that were classified to a resident state between June – October and locations classified to a migrating state between November – May were used. In European plaice locations classified to a resident state between April – September and locations classified to a migrating state between October – March were used.

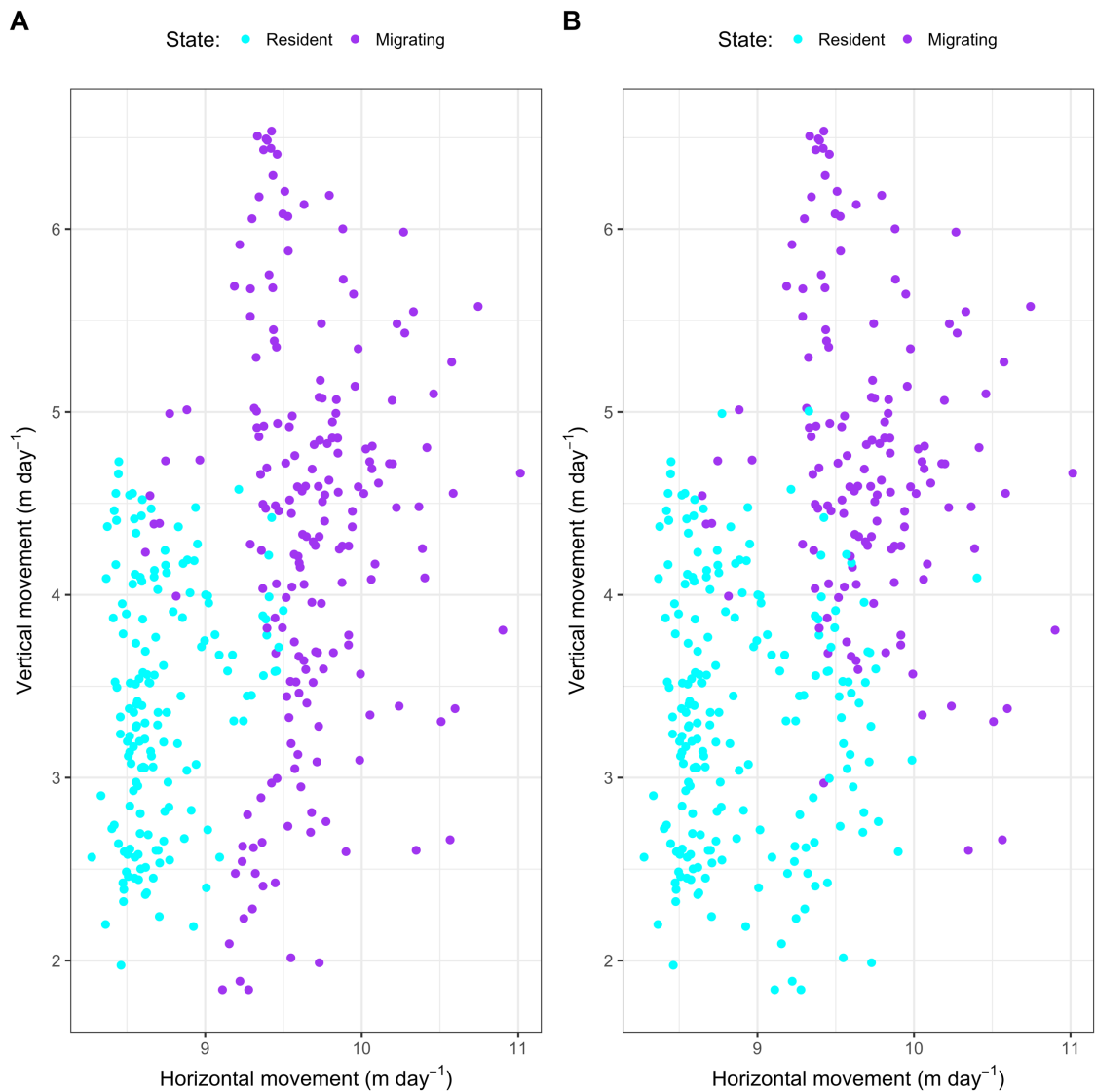


Figure 3.4. Movement parameter prior's influence on state classification. Shown are the results of running the same movement path through the HMM (A) and the adapted HMM (B). Each point is a bivariate movement observation coloured by estimated state. Most notable is the re-classification of data points from a migratory state in the HMM to a resident state in the adapted HMM. The fish in question is a European plaice from the Southern North Sea, tagged on the 3rd November 2004 (path duration = 349 days). All horizontal and vertical movement rates have been log (natural log) transformed.

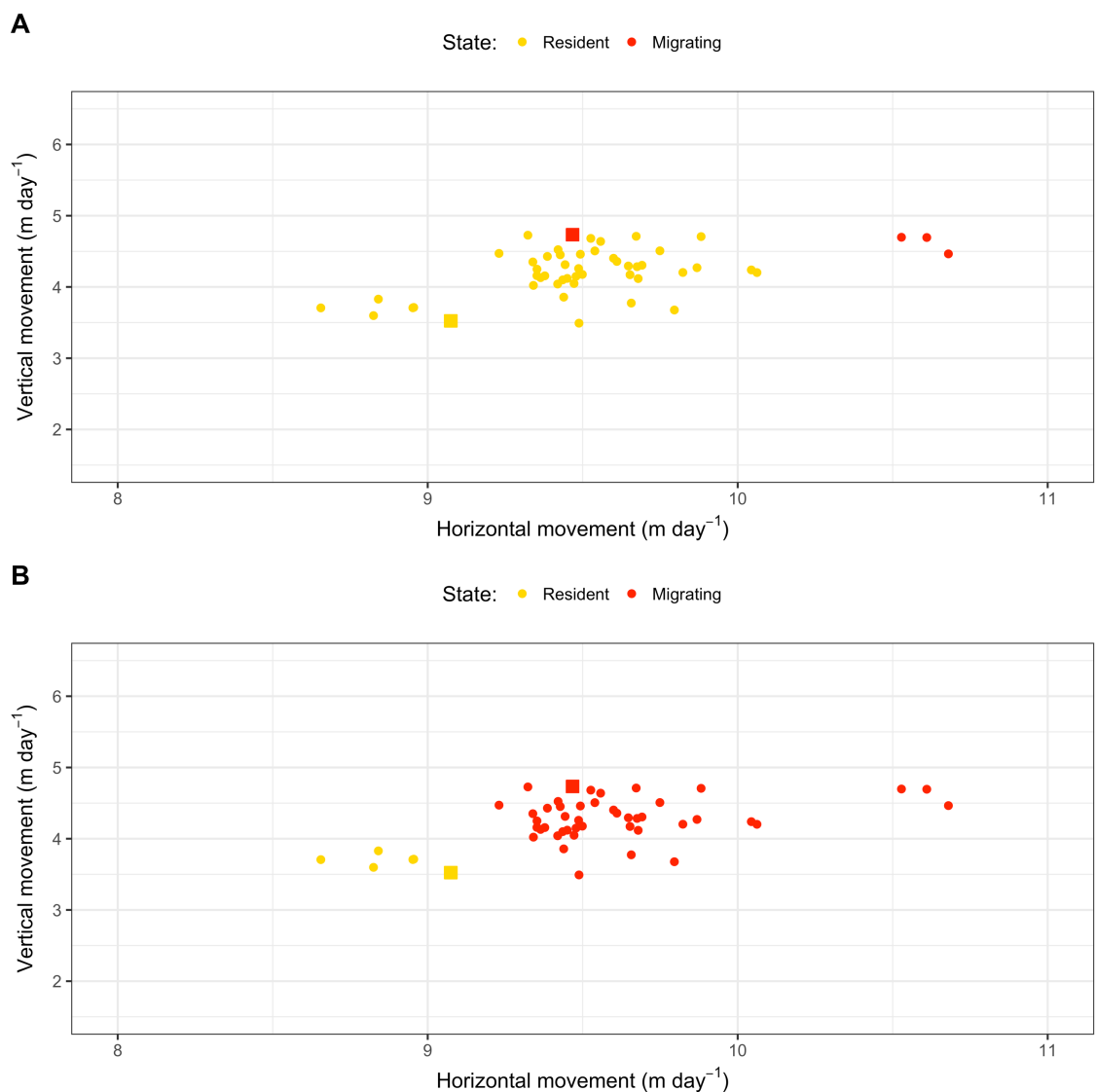


Figure 3.5. Influence of movement parameter prior on state classification process. Shown are the results of running the same exceptionally data-poor movement path (Atlantic cod, path duration = 46 days) through the HMM (A) and the adapted HMM (B). The sub-stock's (English Channel, number of fish = 23) mean movement rate in each state is demonstrated by coloured squares.

3.3 Results

3.3.1 Individual fish movement

Mapping the posterior probability of being in a particular state indicated that individual fish from either species switch between periods of highly directed movement when in a migratory state and periods of random and highly localized movements when in the less active resident state (Figure 3.6). Time spent in either state and the transitions between states were shown to vary in space and time and can be linked to certain habitats. For example, cod 1186 spent 197 days (June - November) consecutively in the resident state within the deeper waters of the Celtic Sea and only shifted into a migratory state when transiting through the English Channel. In comparison, plaice 1084 undertook long-distance directed movements after its release in the German Bight, spending 54 days consecutively in the migrating state before switching to the resident state in the shallow waters of the Central North Sea.

The majority of individual time series had observations that shifted between resident and migratory states ($n=41$ Atlantic cod, $n=60$ European plaice). However, a small number of individuals ($n=6$) persisted in a single state for the duration of their time series: one European plaice and four Atlantic cod remained in a resident state throughout, whereas the movements of one Atlantic cod were consistently classified to the migratory state. All 6 single state movement paths had short duration times (average movement path duration = 56 ± 21 days) and were released throughout the year (November – May).

3.3.2 Population patterns

The mean probability of observing a resident state and the proportion of observations classified to a resident state varied throughout the year (Figure 3.7). In both species, migratory behaviour dominated throughout the winter and into spring, with the onset of summer signifying a shift in movement behaviour to the resident state. This shift in state occurred earlier in European plaice than in Atlantic cod, with movements of plaice having a higher probability of classification to the slower, less active resident state between late April and September, compared to June through to November in cod.

The model predicted large variation in average movement rates within each state (Table 3.1). Horizontal movement rates of plaice tagged and released in the Southern North Sea and German Bight were significantly lower than those tagged in the Central North Sea (resident, Welch's t-test, $p < 0.001$; migrating, Welch's t-test, $p < 0.001$). In the resident state, plaice from the Southern North Sea and German Bight moved on average 6.5 km day^{-1} horizontally and between $20.0\text{-}26.1 \text{ m day}^{-1}$ vertically compared to 13.9 km

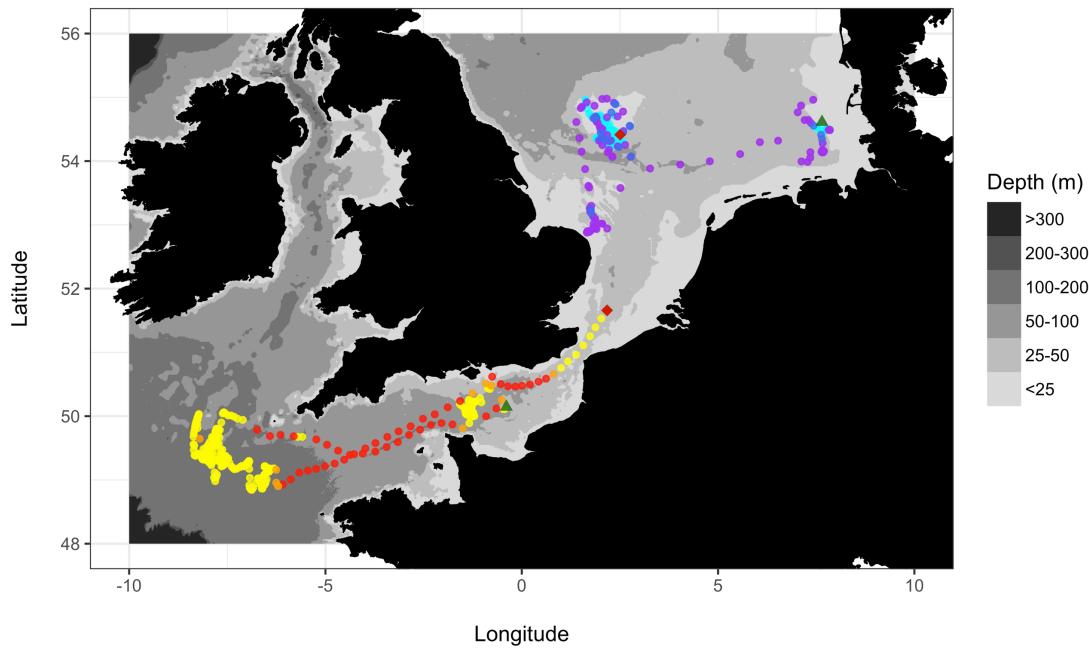


Figure 3.6. State dependent movement behaviour of two individual fish. Shown in a colour scale from red to yellow is the movement behaviour of one Atlantic cod tagged on the 25th March 2005 (duration = 300 days). Red points represent a migrating state, yellow a resident state and those points shown in orange illustrate times when the model was uncertain of state classification (i.e. the daily probability of state classification was less than 0.85). Shown in a scale from purple to cyan is the movement behaviour of one European plaice tagged on the 14th November 1997 (duration = 253 days). Purple points represent a migrating state, cyan a resident state and those points shown in royal blue illustrate times when the model was uncertain of state classification. The start and end point of each individual’s movement path are shown as a green triangle and a red diamond, respectively.

day⁻¹ horizontally and between 15.6-125.8 m day⁻¹ vertically in the migratory state. In comparison, plaice tagged in the Central North Sea exhibited much higher horizontal movement rates, moving on average 12.9 km day⁻¹ and 19.5 km day⁻¹ in the resident and migratory states, respectively.

Predicted spatial utilization distributions showed that migration occurred throughout the spatial domain, with no clear concentration of migratory activity in either species (Figure 3.8; Appendix 3.8 and 3.9). In comparison, periods of time spent in a resident state produced clear geographical patches of space use while in certain habitats. These habitats varied with species (Figure 3.8) and sub-stock (Appendix 3.8 and 3.9), however

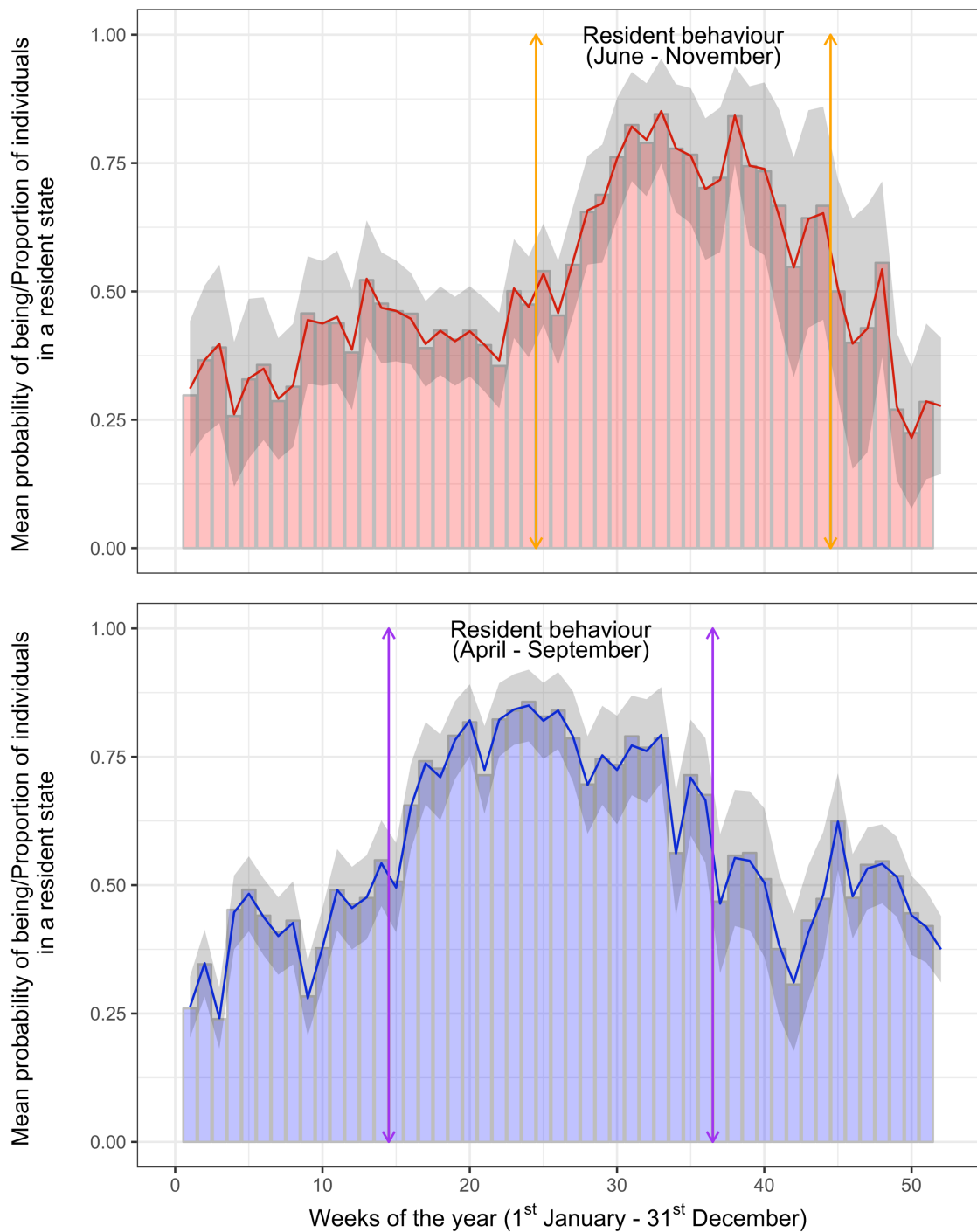


Figure 3.7. Annual temporal distributions of the resident state in Atlantic cod (red) and European plaice (blue). The plotted line in either graph illustrates the mean probability of observing a resident state (± 1 SE – grey shading). The underlying barplots demonstrate the proportion of individual fish that are in a resident state during each week. Periods of time when the mean probability of observing a resident state is continually >0.5 are illustrated in either species.

Table 3.1. State dependent movement rates (horizontal: km day⁻¹, vertical: m day⁻¹) by sub-stock in Atlantic cod and European plaice. All values are taken from collated model output and are averaged across all fish.

Species	Sub-stock	Resident state		Migrating state	
		Horizontal movement (km)	Vertical movement (m)	Horizontal movement (km)	Vertical movement (m)
Atlantic cod	SNS	9.2	31.5	13.9	158.3
	EC	9.6	53.5	13.4	125.4
European plaice	SNS	6.4	20.0	12.9	115.6
	GB	6.6	26.1	14.9	125.8
	CNS	12.9	26.2	19.5	121.0

SNS, Southern North Sea. EC, English Channel. GB, German Bight. CNS, Central North Sea.

Southern North Sea cod and plaice both aggregated in the coastal waters off the English mainland. Cod in the English Channel shift to a resident state when in the western mouth of the Channel. In the German Bight, 90% of plaice spent most of their time at liberty within the area, displaying little or no dispersal. Of those plaice tagged in the Central North Sea, 48% were estimated to be in the resident state within the Northern North Sea whilst a further 11 fish undertook southern migrations before shifting to a resident mode in the shallow waters of the Central North Sea.

3.3.3 *Prior sensitivity analysis*

Minimal change in the classification of states was found during prior sensitivity analysis (Table 3.2). Re-running the HMM with changes to the transition probability prior revealed an average percentage change in state across all individuals of 1.5% in cod and 1.8% in plaice. In comparison, re-running the adapted HMM with changes to the movement parameters priors resulted in a percentage change in state that was on average <1% in cod and 2.3% in plaice. Such findings demonstrate that the precise details of these priors are not crucial, with state classifications and biologically-important results being robust to fairly large changes in prior parameters.

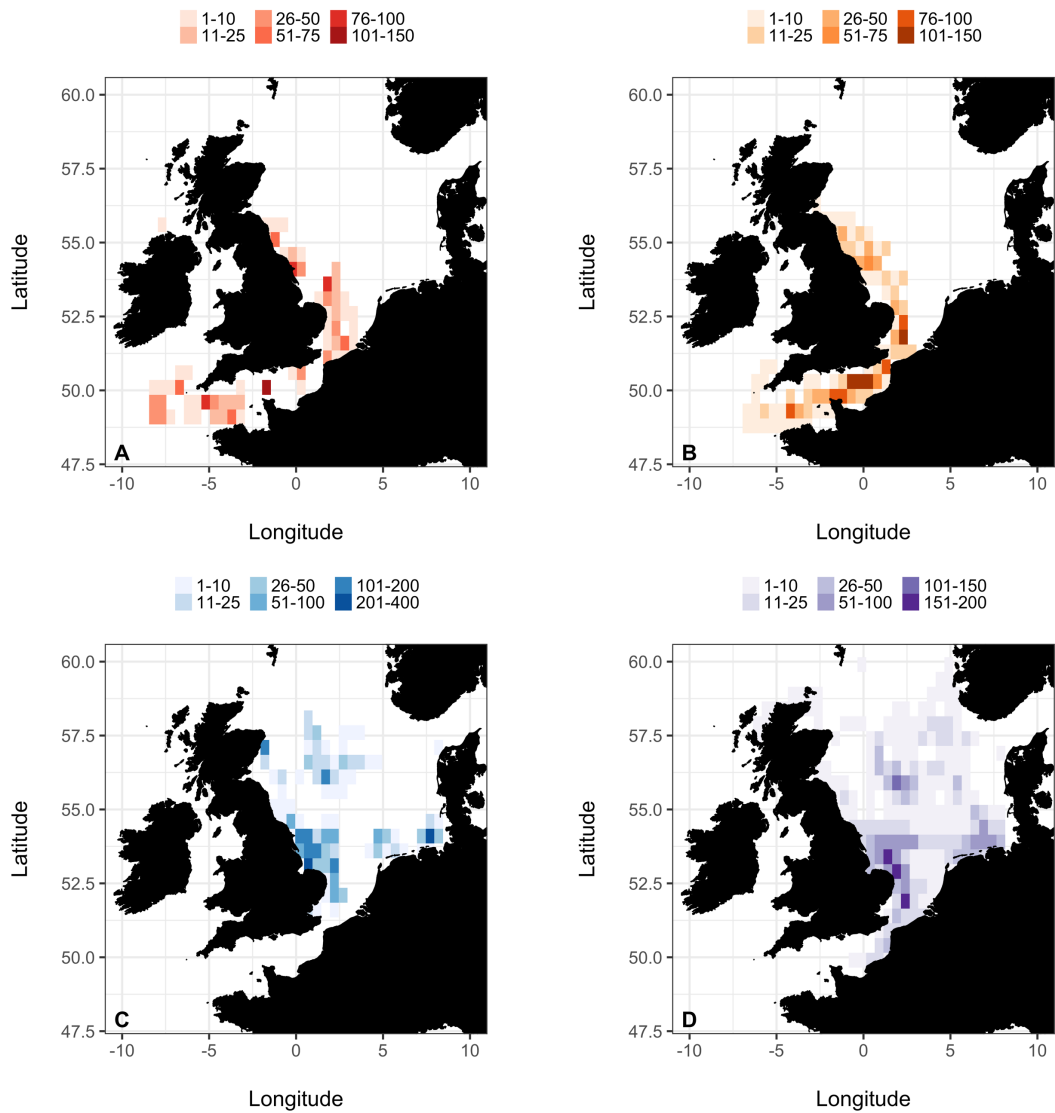


Figure 3.8. Annual state dependent space use patterns of Atlantic cod (A and B) and European plaice (C and D) in the North Sea and English Channel. Plots are split into periods of resident dominant (A and C) and migrating dominant (B and D), where dominance is defined by a mean probability of observing a given state at a given time that exceeds 0.5. All grid cells (5km²) are illustrated in a colour gradient so as to illustrate the sum total number of days spent in a certain state in a given grid cell within a specified time period.

3.3.4 Distribution of state dwell time

In an HMM, the length of time that an individual spends in one state before switching to the other necessarily follows a geometric distribution. Pooling across individuals, we find that these distributions are indeed geometric (see Figure 3.9 and Figure 3.10), and so the dynamics of the fitted changes in state are consistent with the Markov nature of the model. Further model assessment is provided by residual plots in Appendix 3.10 and 3.11.

3.3.5 Comparison to univariate modelling

State allocation was found to be different across the two tested observation models. The bivariate model resulted in state sequences that differed from the univariate model in 8.0% and 23.3% of cases in Atlantic cod and European plaice, respectively. This result confirms the need for the bivariate analysis.

Table 3.2. Prior sensitivity results on HMM and adapted HMM state classification process.

Species	Prior	Sensitivity test	Mean (%)*	Maximum (%)
Atlantic cod (<i>Gadus morhua</i>)	Transition probability	1	1.83 (± 2.61)	9.17
		2	1.27 (± 2.52)	8.33
	Movement parameter	A	0.55 (± 1.06)	3.23
		B	0.55 (± 1.06)	3.37
European plaice (<i>Pleuronectes platessa</i>)	Transition probability	1	1.86 (± 2.88)	13.59
		2	1.72 (± 1.70)	5.63
	Movement parameter	A	2.27 (± 2.23)	7.79
		B	2.45 (± 2.49)	8.44

*Values (± 1 standard deviation) are reported as mean percentage change and maximum percentage change in state across all tested movement paths.

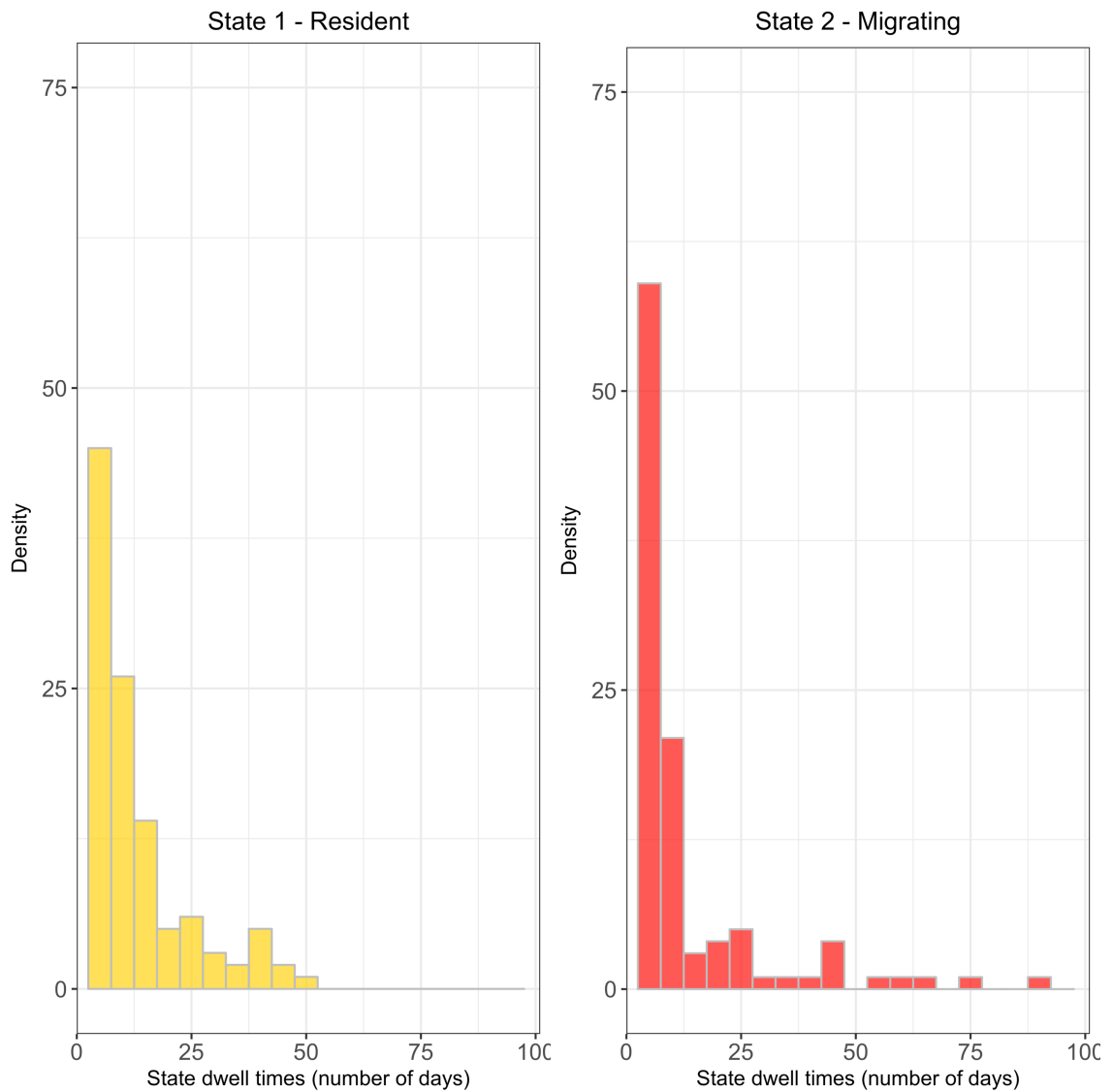


Figure 3.9. State dwell time distributions by state in Atlantic cod. The first and last period of time spent in a given state has been omitted.

3.4 Discussion

One of the main objectives of animal movement studies is the scaling of inference about movement behaviours from individuals to populations (Block et al., 2011; Hays et al., 2016; Raymond et al., 2015; Wakefield et al., 2011). HMMs (McKellar et al., 2015; Michelot et al., 2016; Patterson et al., 2009) or their Bayesian equivalents (Jonsen et al., 2013; McClintock et al., 2013) provide a powerful way of achieving this objective but only when movement behaviours are identified consistently across multiple individuals. Here we have achieved this consistency by ‘borrowing’ information from a finite sample of individuals and using it to provide our model with data-driven approximations of each state. Using this novel extension to HMM methodology, we investigated spatial and

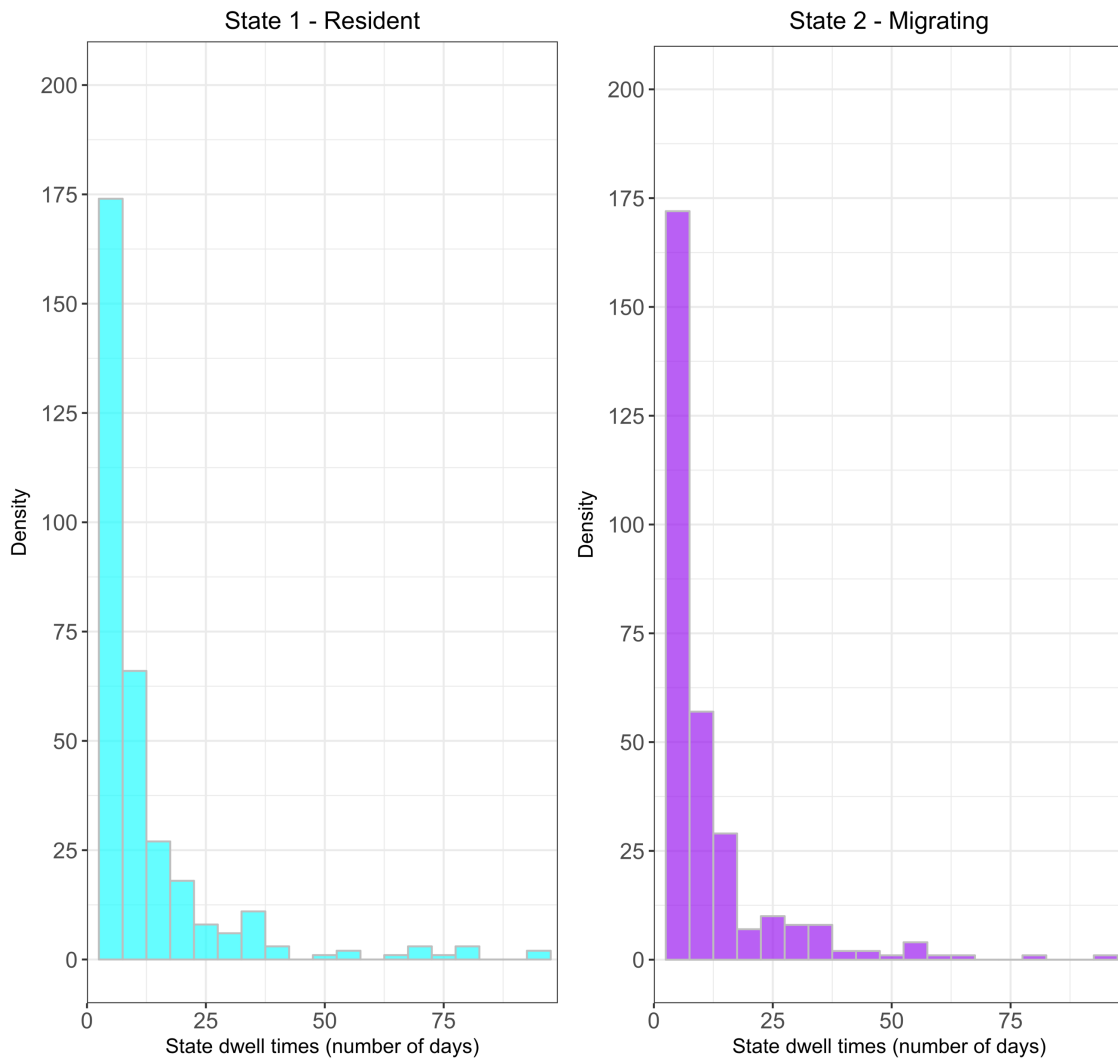


Figure 3.10. State dwell time distributions by state in European plaice. The first and last period of time spent in a given state has been omitted.

temporal shifts in movement behaviour from a large sample size of bivariate movement pathways. We demonstrated where and when shifts between two ecologically meaningful states are most likely to occur and add further confidence to observations of seasonal dependence in the movements of commercially important demersal fish. Our biological findings complement and advance current understanding and highlight how our approach has significant utility in the fields of movement ecology and conservation.

Our approach to behaviour classification has two major advantages. First, it enabled us to gain meaningful inference from 73 (68% of the dataset) additional movement pathways, many of which are data-poor and would otherwise be subject to *post-hoc* removal. This retention of all individual-level information is favourable because it maximised our sample size and lends more information to our analysis. Second, our approach ensures that state labels are allocated consistently across multiple individuals, without resorting to large increases in model complexity. As a direct consequence of

these two advantages, we were able to ask population-level *post-hoc* questions of our movement data and provide answers that are meaningful for conservation and spatial management.

Studies that classify behaviour based on horizontal and vertical movements are rare (but see Bestley et al., 2015; Breed et al., 2013; DeRuiter et al., 2017). Here, we have assumed that h_t and v_t are conditionally dependent given latent states, which is a novel addition to the movement ecology literature. Our reasons for doing so are linked to *a priori* information about how the species of interest alter their activity levels within an annual cycle (e.g. Hobson et al., 2009). However, we intuitively expect other species occupying three-dimensional environments to exhibit similar degrees of coupling. For example, Bestley et al. (2015) reveal that the directed horizontal movements in multiple Antarctic pinniped species are associated with longer dive durations, whereas an inverted relationship is noted in blue whales (*Balaenoptera musculus*) with perceived shallow foraging behaviours being characterised by shallow dives and short horizontal movements (DeRuiter et al., 2017). Future studies may find similar observation models a powerful tool for investigating the dependences of horizontal and vertical movement rates (Carter et al., 2016).

Our estimates of average movement rates are consistent with previous work. In cod, horizontal movement rates whilst in the migratory state are shown to be approximately 13.5km day^{-1} which is comparable to past observations (Hobson et al., 2009) and laboratory studies (Bainbridge, 1957; Videler and Wardle, 1991). In plaice, previous research reports that seven tagged individuals swam on average $255 \pm 60.2\text{km}$ during pre-spawning migrations (Hunter et al., 2003). Assuming an average migration time of 2-4 weeks (as noted in Hunter et al., 2003), our estimates of horizontal movement rates between $13\text{-}20\text{km day}^{-1}$ seem reasonable. Therefore, we are confident that our choice of state labels is biologically meaningful for the species in question.

Much work has considered the horizontal and vertical movements of Atlantic cod (Hobson et al., 2009, 2007) and European plaice (Hunter et al., 2004b, 2004a), noting strong seasonal dependence in the movement patterns of individual fish. Here we add confidence to these findings by providing a mechanistic view of how fish switch between two movement modes during their annual cycle. Specifically, we show that cod and plaice are more likely to occupy a resident state during the summer months (April – September in plaice; June – November in cod). These periods are dominated by low horizontal and vertical movement rates, therefore our findings support the hypothesis that both species spend their summer in a sedentary state with minimal activity levels

(Metcalf et al., 2006; Righton et al., 2010). Past studies show that these summer months are spent in close proximity to the seabed (Hunter et al., 2004b; Righton et al., 2010), however we note that localised foraging, analogous to the area restricted search behaviours (classified by short step lengths and high turning angles) described in striped marlin (Sippel et al., 2011), leatherback turtles (*Dermochelys coriacea*; Jonsen et al., 2007) and basking sharks (*Cetorhinus maximus*; Sims et al., 2006) are expected to occur. This is especially true in the Atlantic cod who have been shown to ramp up vertical excursions, a trend indicative of localised foraging, in weeks prior to pre-spawning migration (Righton et al., 2001). Activity levels are greatly increased during the winter and early spring (October – March in plaice; December – May in cod), resulting in a collective shift in state. As in previous studies (Hobson et al., 2009; Hunter et al., 2004a), we interpret this shift to be reflective of pre-spawning migrations, the onset of spawning and subsequent post-spawning migrations. One limitation of the two-state model considered here is that we cannot directly infer foraging or spawning behaviour. Foraging and spawning events are likely to represent an intermediate activity level, with both behaviours involving notable vertical displacement to and from the water column (Hobson et al., 2009). The inclusion of a third intermediate state would be a relatively straightforward extension to the model structure (see Michelot et al., 2017; Peel and Good, 2011; Vermard et al., 2010 for examples of HMMs that consider more than 2 states). However, it is unlikely that the scale of these vertical excursions is large enough to allow classification at the daily time step. Further, the task of model selection, in particular the choice of the number of behavioural states, is non-trivial and cannot be assumed to be analogous to conventional model selection steps. For instance, both Li and Bolker (2017) and Pohle et al. (2017) show that information criterion techniques repeatedly support models with a higher than expected number of states. Therefore, we side with past reviews (e.g. Langrock et al., 2012; Patterson et al., 2017) which advise pragmatism and attribute our choice of a two-state model over three or four-state alternatives to our prior knowledge of the species, the temporal resolution of the data and the research question of interest. If the aim of the study was to identify fine scale behavioural processes (e.g. instances of foraging), one solution would be to deploy a more sophisticated tag, for example an accelerometer capable of recording acceleration rates, where bursts in speed are assumed to represent prey pursuit (see Leos-Barajas et al., 2017b) for an example of HMM application to accelerometer data). Alternatively, given the current data, we could move towards a more complex modelling approach (e.g. Leos-Barajas et al., 2017a). Here we have considered horizontal and vertical movement at the daily level, however in reality vertical movement is sampled at a much finer temporal resolution (every 10 minutes). Past studies have shown us that vertical

observations made at the 10-minute scale are sufficiently resolved to infer bouts of localised foraging (Hobson et al., 2007) and the rises and falls often associated with spawning (Dean et al., 2014). These fine scale patterns of movement will only be observed in the vertical dimension, due to sampling and tag type, however their biological interpretation will be somewhat conditional on the broad behavioural state of the fish (i.e. foraging will predominantly occur during the broad resident state). As a collaborative effort with colleagues at the University of Bielefeld, we have built a hHMM that can jointly infer behavioural states across multiple temporal scales and applied it to the movement of a single Atlantic cod (Adam et al., in review). Specifically, the model employs a coarse-scale HMM that classifies daily horizontal movements into the broad states of residency and migration; this part of the model is analogous to the univariate model considered above. However, nested within each day is a fine-scale HMM which classifies 10-minute vertical movement observations to fine-scale behavioural states conditional on the current coarse-scale state of the fish. Doing so has three clear benefits. One, it provides a more nuanced depiction of animal movement, as behaviour can be inferred at the time scale of observation. Two, it permits the classification of fine scale movements (like spawning) that are of significant interest to fisheries scientists and management decision makers. Three, it provides another example of how the application of robust statistical techniques can maximise the inference gained from tagging data.

Over the last 70 years, landings data for the North Sea and English Channel demonstrate that catch per unit effort (CPUE) for demersal species is higher during the summer months (Righton et al., 2009). Such increases in CPUE are undoubtedly linked to changes in the populations' underlying movement behaviour, as time spent on the seabed results in an increased vulnerability to commercial exploitation (Righton et al., 2009). By assuming that time spent in a resident state is linked to sea-bottom dwelling, we show that cod and plaice aggregate in certain habitat types. For example, cod in the English Channel have greatest density in the deeper waters at the western mouth of the English Channel. In contrast, cod and plaice in the Southern North Sea aggregate in coastal waters off the English mainland. We also demonstrate that plaice in the German Bight remain exclusively within this region, suggesting the presence of a sedentary resident population in which fish spawn and forage in the same locality (previously noted in plaice by Hunter et al., 2004a and in cod by Neat et al., 2006). Such spatial information is essential for defining multi-species management measures, as strategies typically involve gear restrictions (Moustakas et al., 2006) aimed at limiting the exploitation of certain species/life stages and spatial fisheries closures aimed at protecting areas of

particular importance for species survival e.g. foraging and spawning grounds (Hunter et al., 2004b; Righton et al., 2007).

One limitation of our method is the way in which we deal with individual variation. Currently we assume that by analysing the movements of a finite sample of data-rich pathways ($n=34$) we gain sufficient information about how the mean movement of each state is distributed throughout the population. We then expect the movements of all other individuals to be drawn from one of these distributions and make no attempt to explain any deviance away from this 'expected' process. One way to improve our approach and make it more generic would be the inclusion of covariate information (e.g. Phillips et al., 2015). For example, four Atlantic cod were unexpectedly classified solely to a resident state even through their movements occurred throughout the winter (November – April). *Post-hoc* investigations reveal an average body length of ~56cm which lies within the predicted range of length at first maturity (31-74cm; Froese and Pauly, 2017). It is likely that immature fish act differently to their mature conspecifics (Sippel et al., 2015) and that tagging programmes like the one considered here include fish of differing sex and age (Carter et al., 2016). Consideration of these factors would be a logical next step. However, we believe that the inclusion of body length (see Towner et al., 2016 for an ecological example) or other individual covariates within the HMM's likelihood function would provide a fruitful avenue for future research.

Technological advancements in telemetry devices have led to huge efforts to track the movements of free-roaming marine animals (Hays et al., 2016; Hussey et al., 2015). Tagging data is now seen as a valuable information source for stock assessment models (Sippel et al., 2015), monitoring the effectiveness of conservation efforts (McGowan et al., 2017; Raymond et al., 2015) and understanding population dynamics across vast spatial scales (Block et al., 2011; Hindell et al., 2016). However, there is no avoiding the fact that tags are expensive (McGowan et al., 2017), liable to occasional failure and often produce individual pathways that are of limited use (data-poor or a low number of observations). Here we illustrate how the adoption of our approach can make tagging studies more cost-effective, as inference can still be gained from data-poor movement paths without resorting to redeployment or a renewed effort to secure further funding. Moreover, we have introduced a methodology that makes the process of scaling up inference about movement behaviours from individuals to population more readily achievable. In Chapter 4 we will take this scaling of individual-level movement data one step further by moving away from behaviour and thinking about how movement propagates through a whole marine community. Specifically, we analyse the scaling

relationship between movement and body size and theorise how changes the slope of this relationship will have emerging community-level consequences.

Chapter 4.

Testing movement allometry in free-roaming marine fish.

4.1 Introduction

An animal's ability to encounter prey, escape predation and ultimately survive in an ever-changing environment is all a function of movement (Hirt et al., 2017). Mobile organisms often transit vast distances on an annual basis to feed and reproduce (Block et al., 2011). This ability to re-distribute across varying habitat patches and thermal niches also profoundly influences an individual's ability to cope with changes in climate (Parmesan and Yohe, 2003). In Chapters 2 and 3 we discuss how movement observations made via the deployment of DSTs greatly increase our understanding of fish movement and provide insight into how movement may drive stock dynamics. However, we cannot simply tag all fish. Thus, gaining meaningful inference about how movement influences species interactions (e.g. predation events) at the community-level requires us to consider fish movement in a much broader sense.

Power law functions where body size (usually body mass; m) is used to characterise the scaling of a physiological rate (p) across major taxa based on an intercept α and a slope β , are common throughout ecology, and can be written as

$$p \approx \alpha m^{\beta} \quad [\text{Eqn. 4.1}].$$

To date power law functions have been used to describe metabolism (Barneche et al., 2014), visual range (Andersen et al., 2016a), predator: prey size ratios (Rall et al., 2012) and maximum uptakes rates (Edwards et al., 2012; Marañón et al., 2013). Movement (M), be it velocity (e.g. maximum speed; Hirt et al., 2017) or displacement per unit time (e.g. daily distance travelled; Carbone et al., 2005), behaves similarly and our current understanding of how movement scales with body mass in marine fish is based on a taxa independent power law function where:

$$M \approx \alpha m^{0.13} \quad [\text{Eqn. 4.2}].$$

This scaling relationship is derived from the work of Ware (1978) who, using Brett's work (1973, 1965, 1964, 1963) on the energetics of sockeye salmon (*Oncorhynchus nerka*), estimated that optimal cruising speed (the rate of movement that maximises the distance travelled per unit energy expenditure) and optimal foraging speed (the rate of movement that maximises the flow of surplus energy) in pelagic fish scaled with body length (l) according to:

$$M_s \approx \alpha l^{0.4} \quad [\text{Eqn. 4.3}]$$

where M_s represents both optimal cruising and optimal foraging speed. To expand, Ware's (1978) work allows an optimal cruising speed at size to emerge as the product of a trade-off between the cost of movement (both in terms of the power needed to overcome drag and the cost of standard metabolism) and the displacement achieved per unit time. Whereas, optimal foraging speed at size (in a pelagic predator that relies solely on sight to locate its' prey) is a trade-off between the cost of movement and the net food intake per unit time (F), where F is dependent on the density of prey items, a size-based handling time relationship (the time it takes to pursue and consume prey) and visual acuity at size (introduced in Chapter 5). In both cases, equation 4.3 is shown to be consistent, with validation occurring by comparing estimated rates at size to those observed by Brett (1973, 1965, 1964, 1963). Given the generality and size-based nature of Ware's (1978) work it currently has widespread applications in a range of size-based marine population and community models (e.g. Hartvig et al., 2011), where it is used to quantify how often a predator of size j encounters its prey of size i per unit time. These size-based models have greatly increased our knowledge about how size-structured populations and/or communities will respond to current and future environmental perturbations (Dueri et al., 2014), as well as acting as useful tools in fisheries management (Blanchard et al., 2009; Jacobsen et al., 2017, 2013). Despite this, the use of the theoretical exponent of 0.13 has never been validated using empirical observations.

Several studies have considered the question of how movement scales with body size in fish. For instance, maximum speed (Hirt et al., 2017), home range (Nash et al., 2015; Tamburello et al., 2015) and maximum migration distance (Hein et al., 2012; Watanabe et al., 2015) have all previously been shown to be body size dependent in swimming animals. Furthermore, physical and environmental traits such as thermoregulation (Watanabe et al., 2015), phylogenetic class (Tamburello et al., 2015) and habitat dimensionality (Pawar et al., 2012) have all been used to explain deviances from a singular, all-encompassing power law relationship. Despite widespread effort to collect, analyse and better understand movement in fish, investigations like those of Watanabe et al. (2015) typically rely on species average estimates (i.e. one data point per species) and are often forced to simplify the recorded movement process into a very specific type of movement (such as maximum speed) to find common ground among varying data sources. In doing so these studies ignore intraspecific variation. Moreover, the inference

gained from these studies (e.g. Hirt et al., 2017) often lacks relevance to a population or community model which needs its assumptions surrounding fish movement to be consistent and relevant across a prolonged observations window (e.g. months and years).

Here we expand on previous work in three ways. First, we analyse observations of individuals within and across species, a novel addition to the power law literature which has previously focussed on mean values per species. Second, we are the first to consider movement in both larval and adult fish. Third, by relying on movement observations made *in situ* over a prolonged observation window, we aim to calculate a movement rate that is both more representative of movement in the field and more relevant to size-based population and community models. This final point is important if we hope to validate or invalidate current assumptions.

Drawing on the rising quality and quantity of marine telemetry devices (Hays et al., 2016; Hussey et al., 2015), and the *in situ* work of some of our collaborators (Jeffrey Leis – Adjunct Professor, University of Tasmania), we constructed a dataset of movement from over 550 free-roaming marine fish. Our dataset includes 18 species spanning 7 orders of magnitude in body mass and includes movement from both adult and larval fish. Using movement in the horizontal and vertical dimension, we calculate a new movement metric which we term realised movement (M_{real}). We define M_{real} as a mean displacement rate (m day^{-1}) per individual averaged over a prolonged observation window (10 minutes in larval fish; >40 days in adult fish), during which movement is recorded at regular time intervals.

We use this extensive dataset to investigate the following four questions in a sequential manner: (Q1) Does M_{real} scale with body mass in marine fish according to a taxa independent exponent of 0.13? (Q2) Are our taxa-independent findings replicated by models that account for within- and across-species variance? (Q3) Does the scaling of movement with body mass change based on life stage? (Q4) In adult fish (body length > 30cm) do factors such as: habitat type (demersal-dwelling vs. pelagic-dwelling), thermoregulatory strategy (ectothermic vs. endothermic) or phylogenetic class (Actinopterygii vs. Chondrichthyes), help explain the variance we observe in individual fish movement? For each of the above questions (Q1-4) we pay particular attention to the exponent governing the slope of the relationship between movement and body mass however we do report estimated intercepts for transparency.

4.2 Methods

4.2.1. Movement data

Horizontal and vertical movement rates of marine fish were compiled from the literature or from unpublished data sources (n = 583; Table 4.1). Individual fish were either tagged using data loggers/transmitters (n = 428) or observed swimming *in situ* in the wild (n = 155). All tagged fish were assumed to be mature adults and have a species specific minimum size that is dictated by the ethical limits of tag deployment (i.e. tag weight should not exceed 2% of the body weight of the subject fish, regardless of attachment method; Winter, 1996). All fish observed *in situ* were reared pre-settlement stage pelagic larvae of demersal fish. The maximum size of larvae is simply a limitation of these *in situ* procedures, as larger fish move too fast for scuba divers to follow. Thus, our dataset can be viewed as two data clusters, one larval and one adult, separated by a body mass range of approximately 200 grams (largest larvae = 0.24 g; smallest adult = 199.86 g). All body masses were either reported in the literature or calculated from total body lengths (cm) using estimated length-mass ratios (Table 4.2). For certain species, only fork lengths (FLs) were available. FLs were converted to total lengths (TLs) using published conversion factors (Table 4.3).

In the following sub-sections, we detail the two different types of movement data that contribute to our analysis, demonstrate how the sub-sampling of vertical movement has informed the scaling of larval movement to the daily level and ultimately calculate a realised movement rate for each individual fish.

Table 4.1.1. Realised movement rates of free-roaming marine fish.

Group	Species	Number of individuals	Mean body length (TL; cm)	Mean body mass (g)	Mean movement rates (m day ⁻¹)	Observation method	2D vs. 3D	Source
Bony fish	Atlantic cod (<i>Gadus morhua</i>)	109	60.7 (± 1.1)	2588.9 (± 155.0)	11450.5 (± 179.2)	Tag	3D	Hobson et al., 2009; Neat et al., 2014; Righton et al., 2010
	European plaice (<i>Pleuronectes platessa</i>)	128	38.2 (± 0.5)	609.6 (± 24.1)	13020.9 (± 420.5)	Tag	3D	Hunter et al., 2004b, 2004a
	Atlantic salmon (<i>Salmo salar</i>)	18	81.9 (± 2.0)	6808.9 (± 504.5)	31003.8 (± 901.2)	Tag	3D	*Unpublished
	Atlantic Bluefin tuna (<i>Thunnus thynnus</i>)	39	128.7 (± 9.1)	31599.4 (± 6898.2)	20207.1 (± 2260.6)	Tag	2D	*Unpublished
	Orange-spotted grouper (<i>Epinephelus coioides</i>)	18	1.8 (± 0.03)	0.09 (± 0.005)	929.7 (± 109.7)	In situ	3D	Leis et al., 2009a
	Brown-marbled grouper (<i>Epinephelus fuscoguttatus</i>)	11	1.8 (± 0.05)	0.08 (± 0.005)	849.1 (± 128.0)	In situ	3D	Leis et al., 2009a
	Four-finger threadfin (<i>Eleutheronema tetradactylum</i>)	25	1.4 (± 0.09)	0.01 (± 0.002)	419.9 (± 47.0)	In situ	3D	Leis et al., 2009b
	Common ponyfish (<i>Leiognathus equulus</i>)	9	1.0 (± 0.07)	0.02 (± 0.004)	355.4 (± 85.2)	In situ	3D	Leis et al., 2009b
	Saddletail snapper (<i>Lutjanus malabaricus</i>)	27	1.7 (± 0.06)	0.10 (± 0.01)	644.9 (± 52.5)	In situ	3D	Leis et al., 2009a
	Longfin battfish (<i>Platax teira</i>)	6	0.8 (± 0.05)	0.02 (± 0.03)	562.7 (± 198.8)	In situ	3D	Leis et al., 2009a
	Australasian snapper (<i>Pagrus auratus</i>)	9	0.9 (± 0.02)	0.02 (± 0.001)	164.8 (± 23.6)	In situ	3D	Leis et al., 2006
	Surf bream (<i>Acanthopagrus australis</i>)	33	1.0 (± 0.01)	0.01 (± 0.001)	388.3 (± 28.7)	In situ	3D	Leis et al., 2006

Table 4.1. Realised movement rates of free-roaming marine fish. Continued.

Group	Species	Number of individuals	Mean body length (TL; cm)	Mean body mass (g)	Mean movement rates (m day ⁻¹)	Observation method	2D vs. 3D	Source
Bony fish	Mulloway (<i>Argyrosomus japonicus</i>)	17	1.0 (± 0.04)	0.03 (± 0.004)	226.0 (± 25.2)	In situ	3D	Leis et al., 2006
Shark	Porbeagle shark (<i>Lamna nasus</i>)	22	172.9 (± 7.4)	85913.5 (± 10500.6)	33546.1 (± 1278.1)	Tag	2D (7 fish) 3D (15 fish)	Campana, 2016; Campana et al., 2016
	Blue shark (<i>Prionace glauca</i>)	15	149.8 (± 4.8)	54243.8 (± 5895.5)	25773 (± 2116.0)	Tag	2D	Campana, 2016; Campana et al., 2016
	Shortfin mako shark (<i>Isurus oxyrinchus</i>)	13	140.8 (± 10.7)	33959.3 (± 8162.3)	31651.9 (± 2473.2)	Tag	2D	Campana, 2016; Campana et al., 2016
	Spiny dogfish (<i>Squalus acanthias</i>)	8	96.3 (± 5.1)	3820.2 (± 552.3)	17123.5 (± 572.7)	Tag	3D	* Unpublished
Rays	Thornback ray (<i>Raja clavate</i>)	76	69.1 (± 1.1)	1899.8 (± 99.2)	11041.1 (± 113.6)	Tag	3D	Hunter et al., 2006

TL, total length. 3D, horizontal and vertical movement. 2D, horizontal movement. Numerical values are reported (± 1 standard error).

Table 4.2. Length (cm) to mass (g) conversion ratios.

Species	log ¹⁰ (intercept)	slope
Atlantic cod (<i>Gadus morhua</i>)	0.0071	3.08
European plaice (<i>Pleuronectes platessa</i>)	0.0093	3.02
Atlantic salmon (<i>Salmo salar</i>)	0.0120	3.00
Atlantic Bluefin tuna (<i>Thunnus thynnus</i>)	0.0135	2.92
Orange-spotted grouper (<i>Epinephelus coioides</i>)	0.0141	3.07
Brown-marbled grouper (<i>Epinephelus fuscoguttatus</i>)	0.0138	3.04
Four-finger threadfin (<i>Eleutheronema tetradactylum</i>)	0.0068	3.04
Common ponyfish (<i>Leiognathus equulus</i>)	0.0151	3.15
Saddletail snapper (<i>Lutjanus malabaricus</i>)	0.0209	2.93
Longfin batfish (<i>Platax teira</i>)	0.0245†	2.96†
Australasian snapper (<i>Pagrus auratus</i>)	0.0269	2.94
Surf bream (<i>Acanthopagrus australis</i>)	0.0128†	3.03†
Mulloway (<i>Argyrosomus japonicus</i>)	0.0288	2.80
Porbeagle shark (<i>Lamna nasus</i>)	0.0204	2.94
Blue shark (<i>Prionace glauca</i>)	0.0046	3.24
Shortfin mako shark (<i>Isurus oxyrinchus</i>)	0.0054	3.12
Spiny dogfish (<i>Squalus acanthias</i>)	0.0028	3.08
Thornback Ray (<i>Raja clavata</i>)	0.0025	3.18

All intercept and slope values are sourced from FishBase observations (Froese and Pauly, 2017). † Not observed, sourced from a Bayesian estimation approach (Froese et al., 2014).

Table 4.3. Fork length to total body length conversion factors.

Species	FL to TL conversion factor	Reference
Porbeagle shark (<i>Lamna nasus</i>)	1.12	Campana et al., 2013
Blue shark (<i>Prionace glauca</i>)	1.17	Campana et al., 2005
Shortfin mako shark (<i>Isurus oxyrinchus</i>)	1.08	Pratt Jr. and Casey, 1983

FL, Fork length (cm). TL, Total length (cm).

4.2.1.1. Adult movement

All adult fish were tagged with archival data storage tags (DSTs; $n = 321$) or partial satellite archival tags (PSATS; $n = 107$). DSTs and PSATs were both pre-programmed to record depth (m) and sea temperature ($^{\circ}\text{C}$) at regular time intervals (typically every 10 minutes) for the duration of tag deployment. In our dataset, DSTs were generally used to record the movement of smaller demersal species (body mass range: 0.19 – 9.1kg), whereas PSATs are deployed on larger more pelagic roaming species (body mass range: 2.0 – 200.0kg). Adult species include 4 bony fish, 4 sharks and 1 ray (Table 4.1).

Horizontal and vertical time series were obtained for the majority of adult fish. As in Chapter 3, vertical movement (m day^{-1}) was calculated as the absolute difference between corresponding depth observations summed to the daily level. Horizontal movement (m day^{-1}) was then calculated in a two-stage process. First, a daily geolocation (latitude and longitude) was estimated from the recorded depth and temperature measurements using a path reconstruction method. Second, Euclidean distances between successive geolocations were calculated using the Great Circle equation and assumed to represent horizontal movement per day (h). The choice of reconstruction method varied by study and tag type (see Table 4.4 and references therein), however all methods rely on a state-space formulation of the tracking problem. Furthermore, all reconstruction models serve the same purpose: the estimation of one geolocation per day that best explains the daily variance in recorded depth and sea temperature. Thus, we are confident when comparing across light- and tidal-based reconstruction methods.

To minimise the presence of erroneous or irregular measurements associated with release and recapture events, we removed the first two weeks and the last day from each time series (as in Griffiths et al., 2018; Hobson et al., 2007). To ensure daily movement rates were consistent through time, only tagged fish with time series of at

Table 4.4. Further details of adult tagging data.

Species	Tag type	Habitat	Thermoregulation strategy	Phylogenetic class	Reconstruction method	Reconstruction reference
Atlantic cod (<i>Gadus morhua</i>)	DST	Demersal	Ectothermic	Actinopterygii	Tidal-based	Pedersen et al., 2008
European plaice (<i>Pleuronectes platessa</i>)	DST	Demersal	Ectothermic	Actinopterygii	Tidal-based	Pedersen et al., 2008
Atlantic salmon† (<i>Salmo salar</i>)	PSAT	Pelagic*	Ectothermic	Actinopterygii	Tidal-based	Pedersen et al., 2008
Atlantic Bluefin tuna† (<i>Thunnus thynnus</i>)	PSAT	Pelagic	Endothermic	Actinopterygii	Light-based	Nielsen and Sibert, 2007
Porbeagle shark (<i>Lamna nasus</i>)	PSAT	Pelagic	Endothermic	Chondrichthyes	Tidal-based (15 fish) †	Pedersen et al., 2008
					Light-based (7 fish)	Nielsen and Sibert, 2007
Blue shark (<i>Prionace glauca</i>)	PSAT	Pelagic	Ectothermic	Chondrichthyes	Light-based	Nielsen and Sibert, 2007
Shortfin mako shark (<i>Isurus oxyrinchus</i>)	PSAT	Pelagic	Endothermic	Chondrichthyes	Light-based	Nielsen and Sibert, 2007
Spiny dogfish† (<i>Squalus acanthias</i>)	DST	Demersal	Ectothermic	Chondrichthyes	Tidal-based	Pedersen et al., 2008
Thornback Ray (<i>Raja clavata</i>)	DST	Demersal	Ectothermic	Chondrichthyes	Tidal-based	Pedersen et al., 2008

DST, data storage tags. PSAT, pop-up satellite tags. Information on habitat, thermoregulation strategy and phylogenetic class were all sourced from FishBase (Froese and Pauly, 2017). *Despite being an anadromous species we classify Atlantic salmon as pelagic as individuals were only tracked during their time at sea. †Unpublished tagging data. Atlantic salmon and porbeagle were tagged with PSATs (Microwave Telemetry X-Tags, Microwave Telemetry Inc) following the tagging procedure detailed in Strøm et al. (2016) and Bias et al. (2017), respectively. Spiny dogfish were tagged with G5 DSTs (CEFAS Technologies) following the same tagging procedure detailed for Atlantic cod in Hobson et al. (2009, 2007). Atlantic Bluefin tuna were tagged with PSATs (Microwave Telemetry X-Tags, Microwave Telemetry Inc).

least 40 days were used. Vertical movement (v) was not available for all species ($n = 75$; see Table 4.1). In these four species, horizontal movement (h) is assumed to equal M_{real} .

4.2.1.2. Larvae movement

All larvae were post-flexion stage (see Figure 4.1 for a morphological illustration) meaning individuals were morphologically well developed with good swimming abilities, control of their vertical distribution and capable of orientating their horizontal movements (Leis, 2006; Leis et al., 2006; Leis and Carson-Ewart, 2003). Larval species include three warm temperate and six tropical perciform fish (Table 4.1). For full details of fish rearing, transportation and release we refer the reader to Leis et al. (2009a, 2009b, 2006).

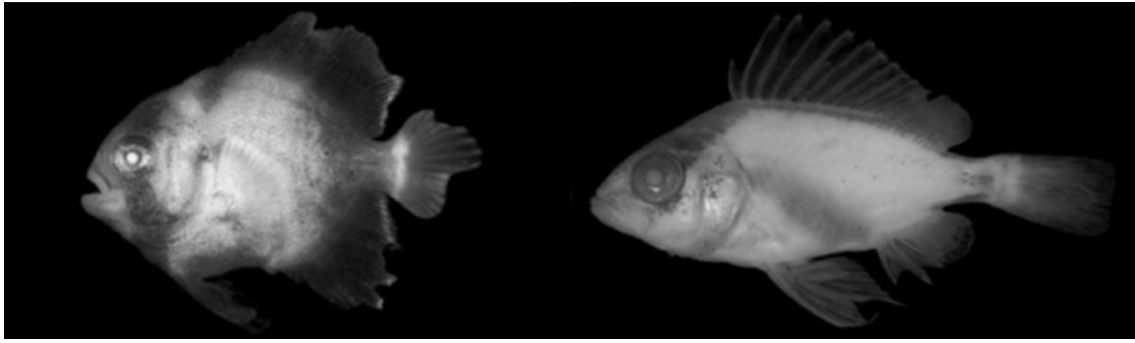


Figure 4.1. Morphological illustrations of two post-flexion stage larval fish. Each individual has been preserved in ethanol prior to imagery. Shown on the left is a Longfin batfish (*Platax teira*; body length = 1.10 cm) and on the right a Saddletail snapper (*Lutjanus malabaricus*; body length = 1.85 cm). Images are taken directly from Leis et al. (2009a) and were originally taken by M. M. Lockett and A. C. Hay. Images are not to scale.

Upon release, larval movement was observed following standard *in situ* procedures (Leis and Carson-Ewart, 1998, 1997). Briefly, two scuba divers descended to a depth of five metres where the observer (diver one) released an individual fish from a small container. Once the larva chose its initial trajectory, both divers followed. Diver one's sole responsibility was to follow the larvae whilst the second recorded the data. The influence a following diver has on larvae movement has been heavily discussed within the published literature (Leis and Carson-Ewart, 2003, 2002, 2000).

Each fish was followed for a maximum of 10 minutes. Swimming depth (m) and direction of travel, recorded as degrees relative to magnetic north (3° west of true north in the study area), were recorded at 30 second intervals with a dive computer and compass, respectively. Speed (cm s⁻¹) was also calculated from distance travelled as measured by a calibrated flowmeter at 5-minute intervals. Only movement paths containing complete depth recordings (21 data points) and two speed recordings over a full 10-minute observation period were considered.

One issue we faced when integrating larval movement into our dataset was whether each fish was moving through a viscous or inertial hydrodynamic regime. Adult movement will undoubtedly be occurring in an inertial regime so movement through a viscous regime should be considered incomparable. To overcome this, we calculated Reynolds numbers (Re; Nachtigall, 2001)

$$Re = \frac{u \cdot l}{\nu} \quad [Eqn. 4.4]$$

where u is the mean swimming speed (cm s^{-1}) of each larva, l is body length (cm) and ν is the kinematic viscosity of sea water ($\text{cm}^2 \text{s}^{-1}$). ν is calculated as a function of water temperature (t) and salinity (s ; El-Dessouky and Ettouney, 2002). As larva were observed in two main locations, one in Taiwan ($t = 27.5^\circ\text{C}$, $s = 34.5$ parts per trillion (ppt; Leis et al., 2009a, 2009b); and one in New South Wales, Australia ($t = 21.5^\circ\text{C}$, $s = 34.5$ ppt; Leis et al., 2006) we calculated separate site-specific ν values (Taiwan = $0.00887 \text{ cm}^2 \text{ s}^{-1}$, NSW = $0.01012 \text{ cm}^2 \text{ s}^{-1}$). As in Leis et al. (2009a), we assume that Re values less than 300 are indicative of a viscous hydrodynamic regime, whereas Re values greater than 1000 are indicative of movement in an inertial regime. Reynolds numbers between 300 and 1000 are thought to reflect an intermediate hydrodynamic regime where both inertial and viscous forces are influential. As such only larvae with estimated Re values > 300 were considered. This cut off is likely to be a little conservative however it ensures that all recorded movements occur in an intermediate or inertial hydrodynamic regime and allows us to maintain a large majority of our data set.

As in adult movement, the absolute differences between corresponding depth measurements were summed to produce a vertical movement rate (m per 10 minutes; v_{10}). Recorded speeds were converted to horizontal movement (m per 10 minutes; h_{10}) in a two-stage process. First, each speed recording was scaled to a metric of horizontal movement per five minutes (h_5 ; m) according to:

$$h_5 = \tau \sqrt{\left(\sum_{i=1}^n \sin \beta_i\right)^2 + \left(\sum_{i=1}^n \cos \beta_i\right)^2} \quad [\text{Eqn. 4.5}]$$

where τ is the recorded speed multiplied by 30 (scales speed from cm per second to cm per 30 seconds) and β is the direction of travel ($^\circ$) during each 30 second time interval. Second, since each fish has two speed recordings, h_5 is calculated twice and an average (mean) of the two values is taken. This average value is then doubled to produce h_{10} .

4.2.1.3. *Scaling of vertical movement*

Scaling h_{10} and v_{10} up to the daily level requires knowledge about the underlying processes that drive movement through time. To gain this knowledge, vertical movements (recorded at 30 second intervals) were sub-sampled at regular intervals (30 second, 1 minute, 2 minute, 5 minute and 10 minute). For each fish, we calculate the 30 second, 1 minute, 2 minute, 5 minute and 10 minute series by taking the absolute differences between observations lagged at intervals of 1, 2, 4, 10 and 20, respectively. A mean is then taken for each sub-sampled series of absolute differences. Thus, each

Table 4.5. Relationship between vertical movement rate and sampling time in larval and adult marine fish. Model selection conducted using AIC.

Life stage	Model	df	AIC	Δ AIC
Larvae	VM ~ sampling time + (1 species)	4	1561.36	0
	VM ~ 1 + (1 species)	3	1946.83	385.47
Adult	VM ~ sampling time + (1 species)	4	3159.32	0
	VM ~ 1 + (1 species)	3	4539.38	1380.06

df, degrees of freedom. VM, vertical movement rate. The best models are shown in bold.

larval fish has an average vertical movement rate at the 30 second, 1 minute, 2 minute, 5 minute and 10 minute interval. The relationship between these average vertical movement rates and sampling time is then analysed using linear mixed effect models (lme4 package; Bates et al., 2015) in R (R Core Team, 2016). Both explanatory (sampling time) and response variables (average vertical movement rate) were log transformed, and we include species as a categorical random effect on the model's intercept. Our information (number of data points) about each average vertical movement rate scales negatively with sampling interval. For example, at the 30 second interval 20 data points contribute, whereas only 2 data points contribute to the average vertical movement rate at the 5 minute interval. To account for this, we also include a vector of prior weights on the models fitting process, allowing values at the 30 second interval to have a greater contribution to the model's log-likelihood.

Model selection via the Akaike Information Criterion (AIC) favours the more complex model (Table 4.5), demonstrating a positive relationship between averaged vertical movement and sampling time in larval fish (Figure 4.2). The scaling of this relationship is described by an estimated exponent of 0.54 (± 0.023) which suggests that vertical movement through time follows a somewhat diffusive process. A perfectly diffusive process would have an exponent of exactly 0.5. As per these findings, we scale v_{10} and h_{10} to the daily level by multiplying each value by $144^{0.54}$. Thus, we gain a h ($m \text{ day}^{-1}$) and v ($m \text{ day}^{-1}$) estimate for each larval fish that is comparable to the previously estimated h and v values for adult fish.

To add further validation to this approach we carried out a similar sub-sampling experiment in adult fish. Again, we sub-sampled vertical movement (recorded every 10 minutes) at regular time intervals (10 minute, 20 minute, 1 hour, 2 hour and 4 hour) and calculate an average vertical movement rate at each sampling interval.

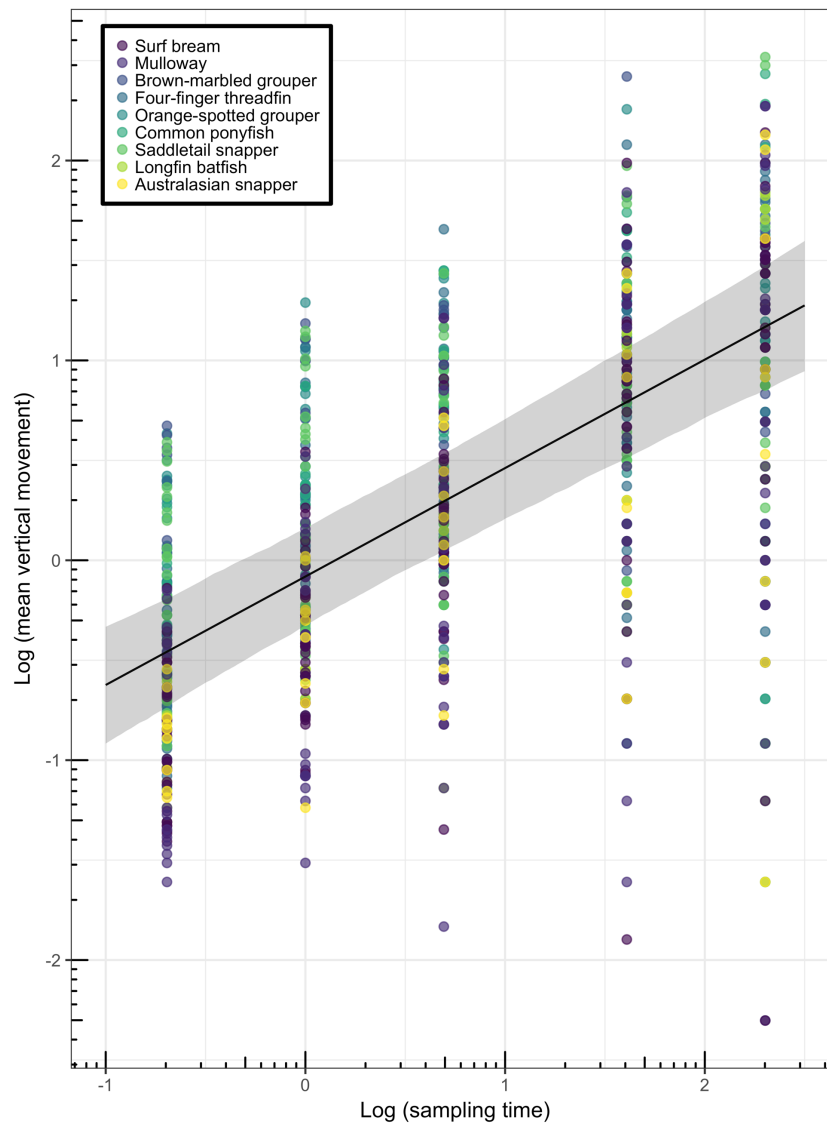


Figure 4.2. Sub-sampling of vertical movement (m) through time (30 second, 1 minute, 2 minute, 5 minute and 10 minute sampling intervals) in larval fish. The best fitting model (Table 4.5, exponent = 0.54 ± 0.023) is illustrated (solid black line). Model uncertainty (95% confidence intervals, grey shading) is calculated using parametric bootstrapping (using the bootMer function in the lme4 package). Both x and y values have been log (natural log) transformed.

In this case, absolute differences between depth observations are lagged at intervals of 1, 2, 6, 12 and 24. Only depth recordings between the hours of 10am and 2pm were used as all larval movement observations occurred during day light hours. Moreover, fish are known to display strong diurnal patterns in vertical activity (e.g. Righton et al., 2001), therefore by truncating our dataset we attempt to ensure consistency across varying observation methods and expected differences in fish behaviour.

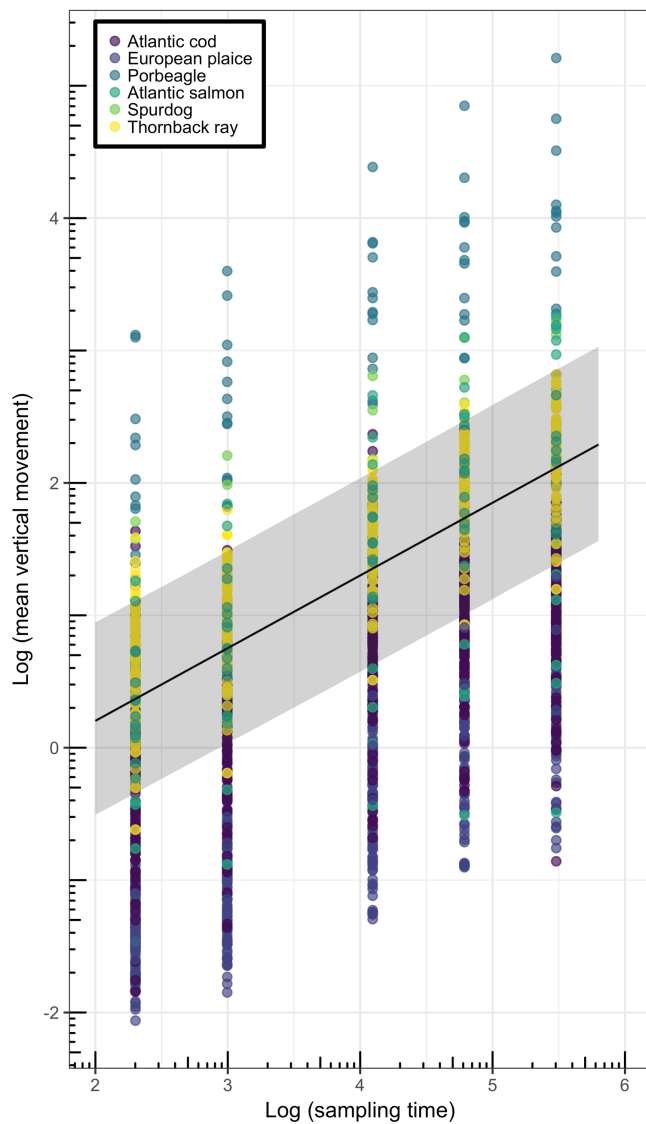


Figure 4.3. Sub-sampling of vertical movement (m) through time (10 minute, 20 minute, 1 hour, 2 hour and 4 hour sampling intervals) in adult fish. The best fitting model (Table 4.5, exponent = 0.55 ± 0.01) is illustrated (solid black line). Model uncertainty (95% confidence intervals, grey shading) is calculated using parametric bootstrapping (using the bootMer function in the lme4 package). Both x and y values have been log (natural log) transformed.

Again, the relationship between average vertical movement rate and sampling time is analysed using linear mixed effect models. The same model formulation as described above is considered. However, prior weights are omitted from the models fitting process as the number of data points contributing to each average vertical movement rate in adults is suitably large. As in larval fish, model selection via AIC (Table 4.5) favoured the more complicated model demonstrating a positive relationship between averaged vertical movement and sampling time in adult fish (Figure 4.3). The scaling of this relationship is described by an estimated exponent of $0.55 (\pm 0.01)$, demonstrating that vertical movement in adult fish also follows a somewhat diffusive process. An exponent

of 0.55 (adult fish) is indistinguishable from an exponent of 0.54 (larval fish) adding further justification to our scaling of h_{10} and v_{10} to the daily level.

Vertical movement as opposed to horizontal movement was used in sub-sampling of movement through time for two reasons. First, data availability in larval fish, as sub-sampling from 21 vertical observations is more robust than sub-sampling from two horizontal observations. Second, temporal comparability exists in the vertical dimension, as both adults and larvae were observed at the 10 minute time resolution. This comparability was not available in the horizontal dimension.

4.2.1.4. Calculating realised movement

Daily h and v values are then combined to produce an average three-dimensional movement rate (M_{real}) as per:

$$M_{real} = \sqrt{h^2 + v^2} \quad [Eqn. 4.6].$$

Thus, 508 M_{real} values are produced based on movement in both the horizontal and vertical dimension. For those 75 adult fish for whom only horizontal movement is available we assumed h equals M_{real} .

4.2.2. Statistical analysis of movement allometry

We apply the following three linear models to our dataset of fish movement. First,

$$\ln Y = \ln \alpha + \beta \ln X + \ln \varepsilon \quad [Eqn. 4.7]$$

where $\ln Y$ is a vector of natural log-transformed M_{real} values (response variable), $\ln \alpha$ is a fixed effect intercept, β is a fixed effect slope, $\ln X$ is a vector of natural log-transformed body mass values (predictor variable) and $\ln \varepsilon$ is the model's unexplained residual variation. Second,

$$\ln Y = (\ln \alpha + \ln \gamma_{species} + \ln \gamma_{phylo}) + \beta \ln X + \ln \varepsilon \quad [Eqn. 4.8]$$

where the additional vectors, $\ln \gamma_{species}$ and $\ln \gamma_{phylo}$ represent random effect coefficients on the model's intercept. $\ln \gamma_{species}$ accounts for the residual intercept deviations attributable to species uniqueness. $\ln \gamma_{phylo}$ accounts for the residual intercept deviations attributable to patterns of phylogenetic relatedness among species. Third,

$$\ln Y = (\ln \alpha + \ln \gamma_{species} + \ln \gamma_{phylo}) + (\beta \ln X + \ln \lambda_{species}) + \ln \varepsilon \quad [Eqn. 4.9]$$

where the additional vector $\ln \lambda_{species}$ accounts for the residual slope deviations attributable to species uniqueness.

Each model (simple model: Eqn. 4.7; species as a random intercept: Eqn. 4.8; species as a random intercept and slope: Eqn. 4.9) is designed to answer a specific research question as outlined in the chapter's introduction. In Q1, we consider the simple model, as our aim is to test the taxa independent relationship between movement and mass. Thus, we assume that each data point is independent. In Q2, we account for species uniqueness as well as patterns of phylogenetic relatedness by considering phylogenetically informed random intercept and random intercept and slope models. In Q3, we apply all three models to larvae and adult data clusters separately (six models in total). Thus, the vectors $\ln Y$ and $\ln X$ become life-stage specific. In Q4, we add a second fixed effect predictor variable to the random intercept and slope model, such that Eqn. 4.9 becomes:

$$\ln Y = (\ln \alpha + \ln \gamma_{species} + \ln \gamma_{phylo}) + (\beta \ln X + \ln \lambda_{species}) + \sigma + \ln \epsilon \quad [Eqn. 4.10]$$

where σ is a categorical variable taking the form of one of the following traits: thermoregulation (ectothermic v. endothermic), habitat type (demersal-dwelling v. pelagic-dwelling) or phylogenetic class (Actinopterygii vs. Chondrichthyes). In total we fit six models, three where each categorical trait is inputted without an interaction term so is acting solely as a fixed effect on the models intercept and three where each categorical trait is inputted with an interaction term. Trait classification of each adult species can be found in Table 4.4. We chose to only fit a random intercept and slope model throughout Q4 as it was most supported by model selection in Q3.

Phylogenetic relatedness is thought to influence broad-scale variation in life-history traits (Lynch, 1991). Closely related species will likely share some ancestral state, therefore variation in physiological rates (such as movement) might be expected to be a function of that shared evolutionary history. To account for phylogenetic relatedness, we created a tree containing all 18 fish species. The tree was constructed using the *ape* (Paradis et al., 2004), *geiger* (Harmon et al., 2008) and *phylotools* (Revell, 2012) packages in R and was viewed using FigTree v1.4.3 (Rambaut, 2009). A dendrogram is provided in Appendix 4.2. Our tree is effectively ultrametric as nodes are the same length to approximately 0.1 million years. Phylogenetic relationships among species are sourced from the published literature (Aschliman et al., 2012; Froese and Pauly, 2017; Rabosky et al., 2013; Vélez-Zuazo and Agnarsson, 2011). Two species were missing from the aforementioned references – Thornback ray (*Raja Clavata*) and Mulloway (*Argyrosomus japonicus*). Thornback ray are part of the superorder of cartilaginous fishes (*Batoidea*) but are in a basal group which split from all other sharks approximately 215 million years ago (mya; Aschliman et al., 2012); we added Thornback ray accordingly. Less

information is available about Mulloway however their family (*Sciaenidae* – groupers) is closely related to the snapper family (*Lutjanidae*) which contains one of our other species, Saddletail snapper (*Lutjanus malabaricus*). Consequently, we insert Mulloway next to Saddletail snapper and assume a divergence date of 47 mya.

Species may also present unique variations in physiological rates that are independent of phylogeny (Barneche et al., 2018). To account for this uniqueness, we have added multiple species uniqueness terms. The name species uniqueness is somewhat arbitrary however it is best thought of as a description of the intraspecific variation that exists within each species' sample. As species uniqueness terms are introduced alongside a phylogenetic correlation matrix, their estimates contribute to the model's species-level effects but are independent of phylogeny. We expect both species uniqueness and phylogenetic relatedness to contribute to the variance we observe in the relationship between movement and body mass.

All models are fitted in a Bayesian framework using the *brms* package (Bürkner, 2017) in R. We estimated intercept and slope parameters for each model by taking the mean of their posterior. All posterior distributions were estimated using Markov chain Monte Carlo (MCMC) methods. Parameter uncertainty is reported as upper (u-95%) and lower (l-95%) 95% credible intervals. We include weakly informative priors on each model's intercept and slope. These are Gaussian distributed with a mean of zero and standard deviations of 50 (intercept) and 10 (slope), respectively. When appropriate we used a Student t prior for each random effect (degrees of freedom = 3, scale = 10). All models consider four Markov chains. Each chain runs for 5000 iterations, with 1000 iterations removed as a burn-in and a thinning rate of 10. Convergence is assessed using estimated Rhat values, where a Rhat value of 1.00 indicates convergence (Bürkner, 2017). Phylogenetic information is inputted as a covariance matrix, *A*. *A* is calculated in a three-stage process: first the tree is pruned to retain all focal species, second the tree object is inverted using the *inverseA* function in the *MCMCglmm* package (Hadfield, 2010) and third the inverted matrix is solved using the *solve* function. Providing a covariance matrix and not its inverse is a unique feature of the *brms* package (Bürkner, 2017).

Previous power law relationships have been tested using species averages (one observation per species, e.g. Watanabe et al., 2015). Our sample size at the species level is relatively small (18 species), so model convergence is problematic, and any inference gained is limited. Despite this we do see the merits of this approach. Fitting a species averaged model can be seen as an intermediate stage between a taxa

independent model (simple model) where each data point is assumed to be independent and a more complex model that accounts for the dual factors of species uniqueness and phylogenetic relatedness. To this end, we fitted three additional models, one in Q1 and two in Q3, where species-specific mean body masses ($\ln Y_\pi$) were fitted against mean M_{real} values ($\ln X_\pi$) using a phylogenetic regression:

$$\ln Y_\pi = (\ln \alpha + \ln \gamma_{phylo}) + \beta \ln X_\pi + \ln \varepsilon \quad [Eqn. 4.11].$$

We use these additional models as validation tools for the taxa independent approach and find that in all three cases estimated intercepts and slopes are highly comparable (Appendix 4.1).

Model comparison uses approximate leave-one-out cross validation (LOO information criterion) via the *loo* package (Bürkner, 2017; Vehtari et al., 2016). LOO is a fully Bayesian model selection procedure for estimating pointwise out-of-sample prediction accuracy (Hooten and Hobbs, 2015; Vehtari et al., 2016). We assume a smaller LOO indicates a better model fit (Bürkner, 2017). All plots are generated using the *ggplot2* library (Wickham, 2009) in R and make full use of the *viridis* colour palette (Rudis et al., 2018).

We do not consider models with species as a fixed effect as our aim is to identify a universal relationship between body mass and movement in marine fish. We do however plot the species-level effects of each random factor (in Q2) to highlight how these relationships influence the overall model fit. In the species as a random intercept model our use of the term ‘species-level effects’ refers to the marginal effects of $\ln \gamma_{phylo}$ and $\ln \gamma_{species}$. In the species as a random intercept and slope model, ‘species-level effects’ refers to the marginal effects of $\ln \gamma_{phylo}$, $\ln \gamma_{species}$ and $\ln \lambda_{species}$.

In Q4, we chose not to fit a global model (including all three covariates in a single model) as there is a strong association among traits. Instead we aim to identify which trait, if any, explains the most deviance in the relationship between body mass and movement in adult fish.

4.3 Results

Using our data set of fish movement, we demonstrate clear empirical patterns in the scaling of body mass (g) with realised movement (m day⁻¹) in marine fish (Table 4.6). In Q1 we observe a taxa independent relationship that follows an exponent of 0.30 (Figure 4.4).

Table 4.6. Relationship between log realised movement ($m \text{ day}^{-1}$) and log body mass (g) in marine fish. Model selection is conducted using LOO information criterion.

Data	Model	Log(intercept)	Slope	LOO	Δ LOO
All	$M_{real} \sim \text{body mass}$ [1]	7.14 (l=7.09, u=7.2)	0.30 (l=0.3, u=0.31)	873.99 (SE=45.96)	266.10
	$M_{real} \sim \text{body mass} + (1 \text{phylo}) + (1 \text{species})$ [2]	8.06 (l=6.29, u=10.11)	0.16 (l=0.10, u=0.22)	639.98 (SE=51.05)	32.09
	$M_{real} \sim \text{body mass} + (1 \text{phylo}) + (\text{body mass} \text{species})$ [2]	8.51 (l=5.99, u=11.50)	0.10 (l=-0.02, u=0.21)	607.89 (SE=53.78)	0
Larvae only	$M_{real} \sim \text{body mass}$ [3]	6.94 (l=6.56, u=7.33)	0.27 (l=0.17, u=0.37)	333.20 (SE=19.90)	38.55
	$M_{real} \sim \text{body mass} + (1 \text{phylo}) + (1 \text{species})$ [3]	6.34 (l=5.36, u=7.12)	0.11 (l=-0.06, u=0.27)	294.65 (SE=19.71)	0
	$M_{real} \sim \text{body mass} + (1 \text{phylo}) + (\text{body mass} \text{species})$ [3]	6.33 (l=5.37, u=7.27)	0.11 (l=-0.11, u=0.32)	296.25 (SE=19.69)	1.60
Adult only	$M_{real} \sim \text{body mass}$ [3]	8.09 (l=7.91, u=8.27)	0.19 (l=0.16, u=0.21)	381.00 (SE=25.11)	222.83
	$M_{real} \sim \text{body mass} + (1 \text{phylo}) + (1 \text{species})$ [3]	8.84 (l=8.15, u=9.63)	0.11 (l=0.06, u=0.16)	228.87 (SE=37.74)	70.70
	$M_{real} \sim \text{body mass} + (1 \text{phylo}) + (\text{body mass} \text{species})$ [3]	9.58 (l=7.68, u=11.51)	0.02 (l=-0.13, u=0.18)	158.17 (SE=37.10)	0

l, lower 95% credible interval. u, upper 95% credible interval. SE, standard error on LOO estimate. phylo, patterns of phylogenetic relatedness among species. species, species uniqueness. Best models are shown in bold. The investigation each model is specific to is identified within [...]. When a random intercept and slope model is supported by LOO information criterion we have documented the estimated marginal effects (log(intercept) and slope) of each species (see Appendix 4.3 and 4.4).

This estimate is markedly steeper than the currently accepted taxa independent exponent of 0.13. Additionally, we show that this finding is consistent with estimates derived from a phylogenetic regression fitted to species averaged observations (Appendix 4.1).

In Q2 we have fitted two separate models in an attempt to validate our taxa independent findings (Figures 4.5 and 4.6; Table 4.6). In the first of these models (varying intercepts), we estimate a population-level exponent of 0.16 which is markedly shallower than in the taxa independent case. Observationally, the estimated species-level effects do a reasonable job in both the adult and larval data clusters (Figure 4.5), adding support to the assumption of a single power law relationship between movement and body mass in fish. Moreover, the estimated species-level intercepts are fairly consistent among data clusters (Appendix 4.3). Despite this, the population-level relationship does completely miss the larval data cluster suggesting a poor overall model fit.

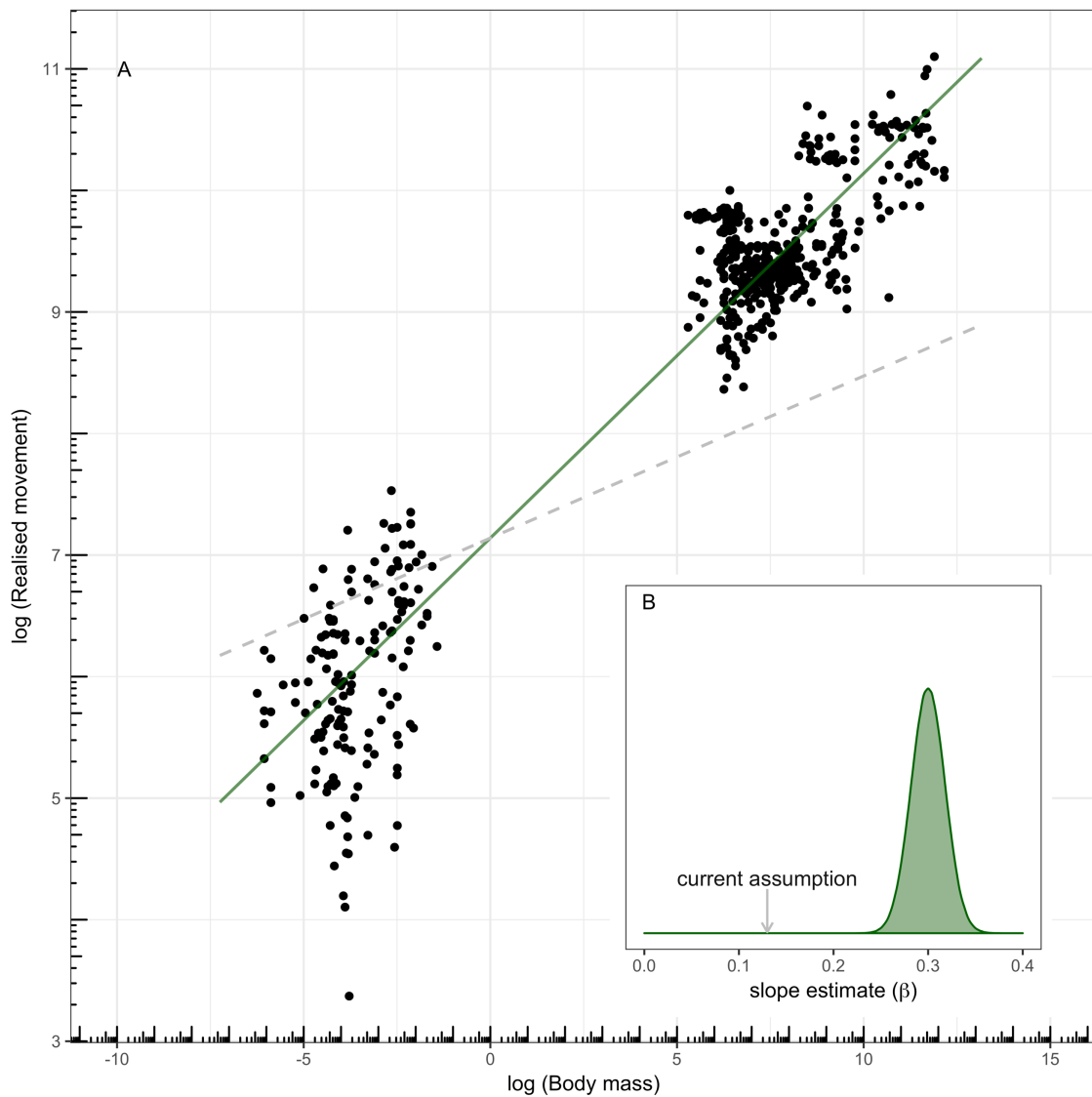


Figure 4.4. Scaling of realised movement (m day^{-1}) with body mass (g) in marine fish (A). The best fitting taxon independent relationship (Table 4.6, exponent = 0.30) is plotted (green solid line) alongside the widely accepted 0.13 relationship (grey dotted line). Both x and y values have been log (natural log) transformed. The posterior distribution of the models estimated slope (β) is also shown (B).

This is likely a consequence of variable sample sizes, as the model's likelihood will be skewed heavily towards the species with larger sample sizes e.g. Atlantic cod (*Gadus morhua*; $n=109$) and Thornback ray ($n=76$).

In the second model, we add complexity by allowing multiple species-level effects (varying intercepts and slopes; Figure 4.6). We estimate an even shallower relationship between body mass and realised movement, with a population mean exponent of 0.10, varying between species with a standard deviation of 0.13.

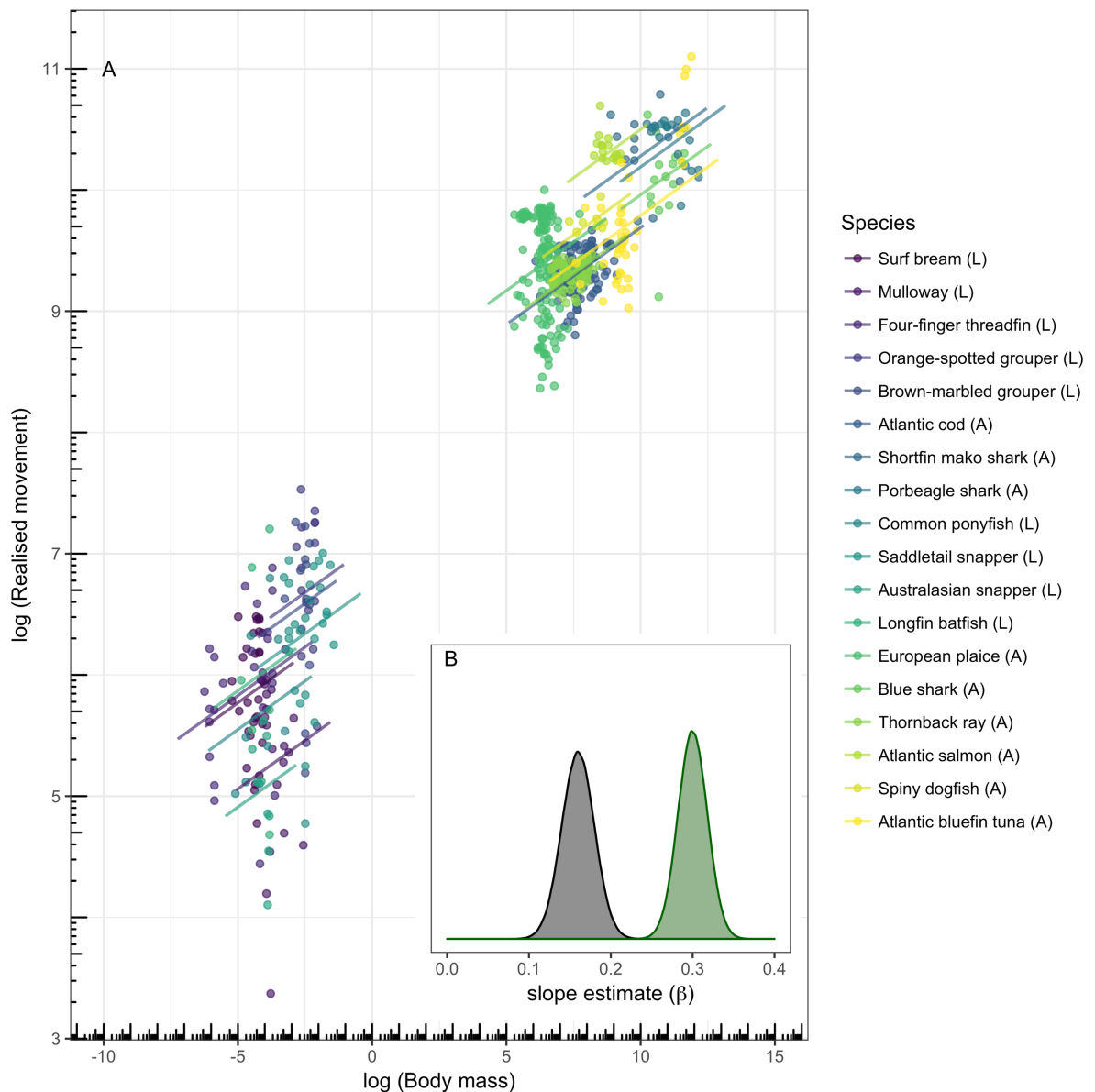


Figure 4.5. Scaling of realised movement ($m \text{ day}^{-1}$) with body mass (g) in marine fish (A). Plotted is a random intercept model fitted to log (natural log) transformed x and y values. Population-level estimates (black line) and marginal species-level effects (varying intercepts but constant slopes) are illustrated. The posterior distribution of the estimated population-level slope (B, black) is added to the taxa independent case (green) from Figure 4.4. Within the list of species the letters ‘L’ and ‘A’ denote larval and adult.

Again, the overall population-level relationship misses the larval data cluster suggesting a skewed result. Model selection favours the more complicated model by some margin ($\Delta\text{LOO} = 32.09$; Table 4.6). Examining the species-level effects (Figure 4.6 and Appendix 4.4), it is clear that larval species all share a positive exponent between 0.08 and 0.18. This consistency is lost in adult fish, where the estimated slopes range from being very positive in Atlantic bluefin tuna (*Thunnus thynnus*; 0.32) to fairly negative in European

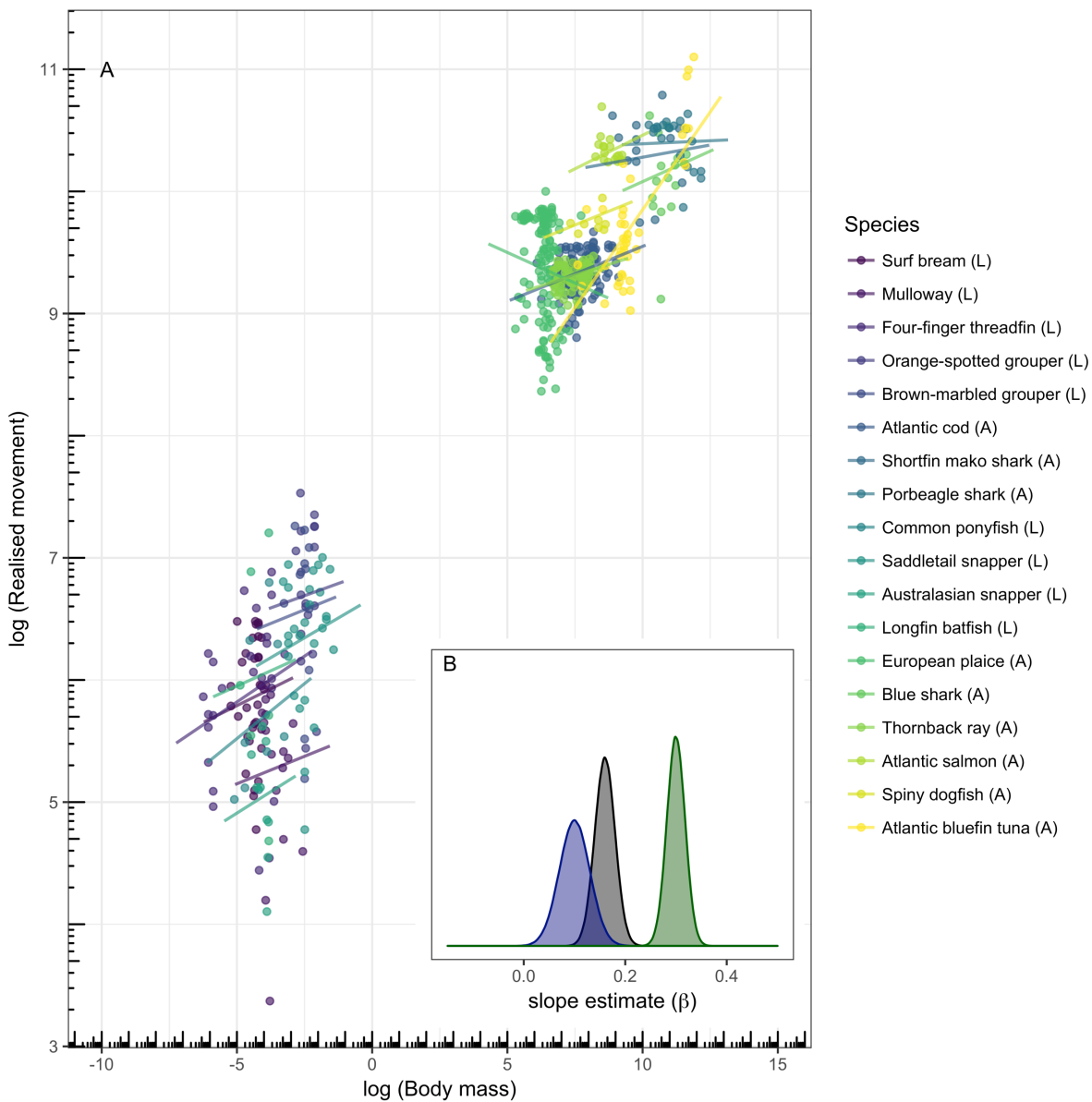


Figure 4.6. Scaling of realised movement ($m \text{ day}^{-1}$) with body mass (g) in marine fish (A). Plotted is a random intercept and slope model fitted to log (natural log) transformed x and y values. Population-level estimates (dark blue line) and marginal species-level effects (varying intercepts and varying slopes) are illustrated. The posterior distribution of the estimated population-level slope (B, dark blue) is added to the taxa independent case (green) from Figure 4.4 and the intercept varying case (black) from Figure 4.5. Within the list of species the letters ‘L’ and ‘A’ denote larval and adult.

plaice (*Pleuronectes platessa*; -0.10). It is worth noting that larval fish are phylogenetically highly related, therefore correlating species-level intercepts and slopes are to be expected to some extent. However, the model’s underlying phylogenetic correlation structure is unlikely to explain the variance we observe in adults.

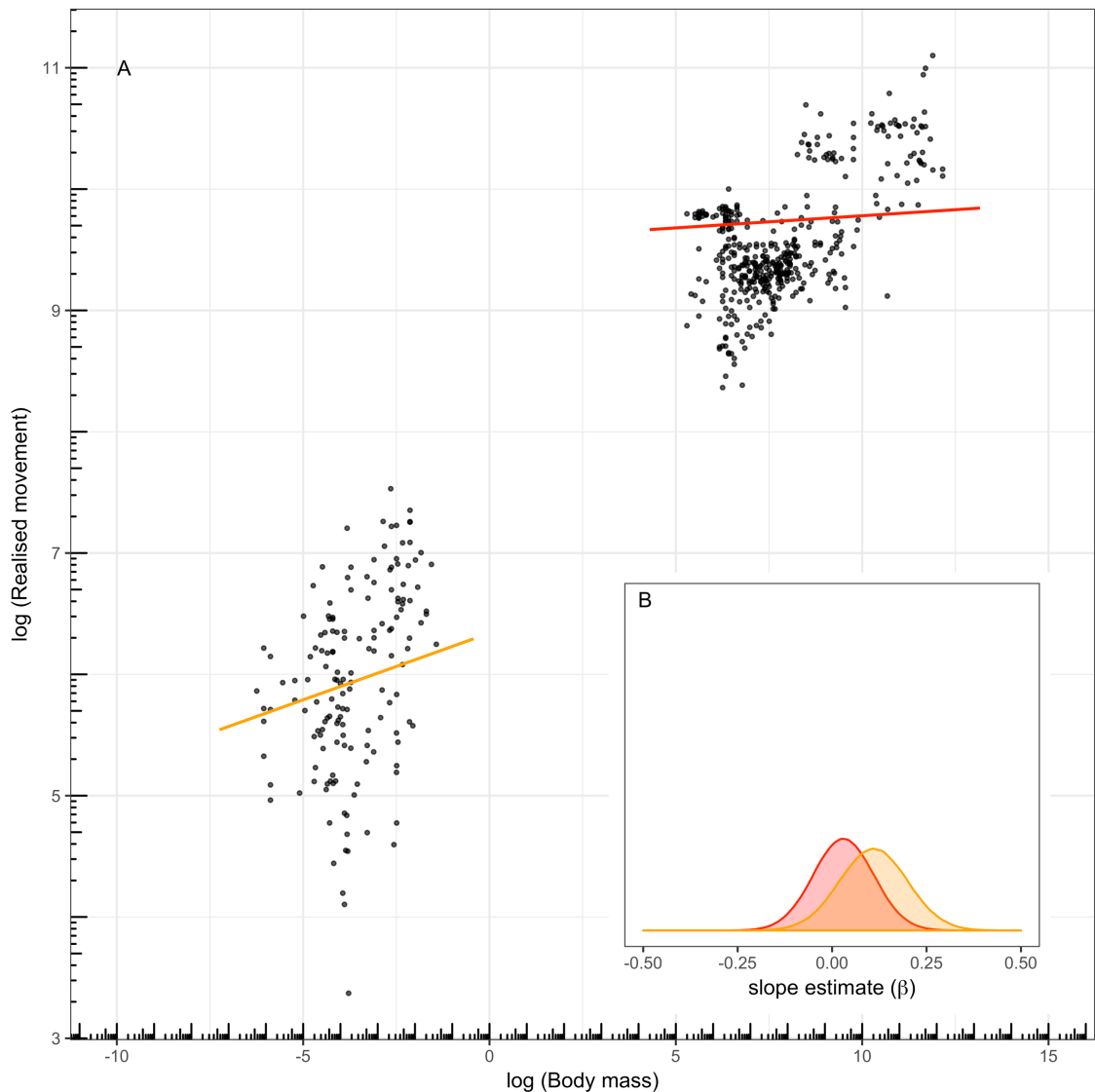


Figure 4.7. Scaling of realised movement (m day^{-1}) with body mass (g) in adult (red) and larval (orange) fish (A). Plotted is a random intercept and slope model fitted to log (natural log) transformed adult x and y values (red). Also plotted is a random intercept model fitted to log (natural log) transformed larvae x and y values (orange). Note, the red line is only fitted to the adult data and the orange line is only fitted to the larval data. Thus, larvae and adults are treated separately. Both models are supported by model selection (see Table 4.6). The posterior distribution of each model's estimated population-level slope (B) is shown in red (adults) and orange (larvae).

In Q3 we investigated whether the exponent governing the relationship between body mass and realised movement differed between life stages (Figure 4.7). Confirming our observations in Q2, model selection slightly favours the varying intercept model in larvae, indicating a shared species-level exponent, whereas a varying intercept and slope model is clearly favoured in adults (Table 4.6). In larvae, a population-level slope of 0.11 is estimated. In adults, a population-level slope of 0.02 is estimated, which is much

shallower than the exponent estimated for the larval data cluster. One thing to note is the apparent lack of any consistency among the estimated species-level effects in adults (Appendix 4.5). One might expect species with shared covariate information (e.g. habitat type, thermoregulatory strategy or phylogenetic class) to exhibit similar scaling relationships (intercepts and slopes), however at first glance this does not seem to be the case.

In Q4 we investigated whether or not shared covariate information among adult fish explains the species-level deviance we observe in Q3. Despite prior evidence supporting all three traits (thermoregulatory strategy, habitat type and phylogenetic class), model selection supports the simplest model without the addition of these traits (Table 4.7). There is a very small decrease in LOO associated with the inclusion of thermoregulation (varying intercept) and phylogenetic class (varying intercept; varying intercept and slope) however the difference cannot be considered credible ($\Delta\text{LOO} < 2.00$).

4.4 Discussion

Movement is one of life's fundamental processes. Plotting realised movement against body mass in marine fish we observe a positive scaling relationship on the log scale. This scaling relationship has previously been assumed to be governed by an exponent of 0.133 based on the theoretical work of Ware (1978). Here we show that this assumption is inappropriate in general and masks a range of ecologically important phenomena, a finding with wide ranging consequences for basic ecological theory, our understanding of predator-prey interactions as well as efforts to model the marine world using size-structured population and/or community models. Despite the significance of this finding, a more detailed statistical approach that appropriately accounts for the nuances of our data set yields differing results and adds complexity to our understanding of movement allometry in marine fish. Additionally, we show that life stage is a crucial factor when explaining underlying trends in the scaling of movement. However, for the present dataset, we find no evidence to support previous work where traits such as thermoregulation (Watanabe et al., 2015), habitat type (Pawar et al., 2012) and/or phylogenetic class (Tamburello et al., 2015) have been used to describe systematic variation in movement allometry in adults.

In our simple taxon invariant model (Equation 4.7), we estimate an exponent of 0.30 which is steeper than current assumptions. A steeper scaling relationship means that

Table 4.7. Relationship between log realised movement ($m \text{ day}^{-1}$) and log body mass (g) in adult marine fish. Covariates include thermoregulatory strategy (ectothermic vs. endothermic), habitat (demersal-dwelling vs. pelagic-dwelling) and phylogenetic class (Actinopterygii vs. Chondrichthyes). All covariates are inputted as categorical values. Model selection is conducted using LOO information criterion.

Model	Covariate	Log(intercept)	Slope	LOO	Δ LOO
$M_{real} \sim \text{body mass} + (1 \text{phylo}) + (\text{body mass} \text{species})$	-	9.58 (l=7.68, u=11.51)	0.02 (l=-0.13, u=0.18)	158.17 (SE=37.10)	0
$M_{real} \sim \text{body mass} + \text{thermoregulation} + (1 \text{phylo}) + (\text{body mass} \text{species})$	Ectothermic	9.45 (l=7.51, u=11.40)	0.02 (l=-0.14, u=0.18)	156.64 (SE=37.07)	1.53
	Endothermic	9.95 (l=7.62, u=12.13)	-		
$M_{real} \sim \text{body mass} * \text{thermoregulation} + (1 \text{phylo}) + (\text{body mass} \text{species})$	Ectothermic	9.84 (l=7.39, u=12.25)	-0.02 (l=-0.23, u=0.19)	158.11 (SE=37.12)	0.06
	Endothermic	9.37 (l=6.57, u=12.51)	0.08 (l=-0.19, u=0.33)		
$M_{real} \sim \text{body mass} + \text{habitat} + (1 \text{phylo}) + (\text{body mass} \text{species})$	Demersal	9.24 (l=7.28, u=11.13)	0.01 (l=-0.16, u=0.17)	158.49 (SE=37.20)	-0.32
	Pelagic	10.01 (l=8.21, u=11.80)	-		
$M_{real} \sim \text{body mass} * \text{habitat} + (1 \text{phylo}) + (\text{body mass} \text{species})$	Demersal	9.57 (l=7.08, u=11.90)	-0.02 (l=-0.26, u=0.21)	158.12 (SE=37.15)	0.05
	Pelagic	9.70 (l=7.35, u=12.06)	0.05 (l=-0.17, u=0.25)		
$M_{real} \sim \text{body mass} + \text{class} + (1 \text{phylo}) + (\text{body mass} \text{species})$	Actinopterygii	9.35 (l=6.78, u=11.94)	0.02 (l=-0.14, u=0.18)	158.13 (SE=37.2)	0.04
	Chondrichthyes	9.77 (l=7.24, u=12.32)	-		
$M_{real} \sim \text{body mass} * \text{class} + (1 \text{phylo}) + (\text{body mass} \text{species})$	Actinopterygii	9.15 (l=6.23, u=12.39)	0.05 (l=-0.22, u=0.28)	157.64 (SE=37.12)	0.53
	Chondrichthyes	10.05 (l=6.71, u=12.91)	-0.01 (l=-0.25, u=0.23)		

l, lower 95% credible interval. u, upper 95% credible interval. SE, standard error on LOO estimate. phylo, patterns of phylogenetic relatedness among species. species, species uniqueness. The best model is shown in bold. All models relate to investigation 4.

small increases in body mass are partnered by a proportionally greater increase in realised movement. In adult fish this change will result in a marked increase in estimated movement. For instance, under an exponent of 0.133 a fish weighing in at 20kg (average mass of an Atlantic bluefin tuna in our data set) would be expected to move at an average

distance of 4.7km each day. At the same weight and assuming a common intercept, this value increases substantially to approximately 24km each day under our estimated exponent of 0.30. Moving further each day will incur greater metabolic costs (Brown et al., 2004), however any increase in energy requirement would presumably be met by a notable increase in prey encounter rate. Moreover, a greater prey encounter rate will theoretically increase foraging efficiency and reproductive output, since the increase in potential food intake rates may permit energy surplus. Greater levels of movement could also aid the processes of migration, dispersal and bridging habitat patches, however in the context of foraging efficiency it is important to note that food intake rate per unit time will trend towards saturation, either due to increases in prey encounter rates (Barraquand and Murrell, 2013) or increases in prey density (Ware, 1972). Therefore, there is a finite region within which greater movement rates are beneficial before food intake rates plateau (as characterised by a consumer's function response; e.g. Holling, 1966) and the time taken to handle prey items becomes limiting (Ware, 1978).

The reverse is true in larvae, with estimated movement rates being less under an exponent of 0.30 when compared to current assumptions. For example, based on a logged intercept value of 4.17 (Table 4.6), a fish weighing in at 0.05g (average mass of our larval data cluster) would be expected to move at average daily distances of 512.4m and 845.2m under scaling exponents of 0.30 and 0.133, respectively. A reduction in movement at small sizes may increase the likelihood of mortality, both via starvation and predation, as processes of pursuit and escape are functions of an individual's movement potential. Furthermore, because any change in exponent is influential across multiple orders of magnitude in body mass, the potential consequences to predator-prey interactions, biomass fluxes and community wide stability will be numerous. In the absence of fishing, we hypothesise that our proposed change to movement allometry in fish would cause biomass peaks at high size classes as consumption rates rise to meet metabolic demands. Increases in large fish abundance would have cascading predation-driven trophic effects (as shown in response to fishing in Andersen and Pedersen, 2010), resulting in a systemic shift in community structure. This new community would, in theory, be subject to top-down regulation and would in turn would become inherently unstable, as consumer-resource dynamics become frequently more boom-or-bust. These predictions are hypothetical however they are consistent with the three-dimensional predictions of Pawar et al. (2012) and the observed cross-system differences in stability made by Rip and Mccann (2011). We consider these broad-scale consequences and how they interact with fishing in much more detail in Chapter 5.

A steeper scaling exponent in fish is not without precedent. Maximum speed (cm s^{-1} , Hirt et al., 2017), cruising speed (cm s^{-1} , Acuña et al., 2011; m s^{-1} , Watanabe et al., 2015) and maximum migration distance (km, Hein et al., 2012) have all been shown to scale with body mass according to exponents between 0.20 and 0.36. Daily displacement (km), probably the most parsimonious movement metric to the one considered here in terms of temporal scale, has also been shown to scale with body mass according to an exponent of 0.25 in terrestrial mammals (Carbone et al., 2005). Moreover, our taxa-independent findings (exponent = 0.30; Table 4.6) are captured by our species average model (exponent = 0.31; Appendix 4.1). Despite such support, we feel it necessary to highlight the limitations of the taxa independent and species average approach. In the taxa independent case we have allowed the model to assume statistical independence among data points. Our reasons for doing so are simple, to achieve a taxon independent fit. However, given that our data set contains multiple species and multiple observations within each species, the assumption of independence is almost certainly violated. Furthermore, although patterns of phylogenetic relatedness are built into the species average model we are tentative about drawing meaningful conclusions from a model fitted to so few observations ($n = 18$). Despite being an over-simplification, it is clear from Figure 4.4 that a taxon independent fit to our data would not adhere to an exponent of 0.133 and as a result our steeper finding is likely to hold utility to taxa independent modellers that strive to estimate trends of abundance or biomass across wide body mass ranges, e.g. the community size spectrum (see Benoit and Rochet, 2004; Blanchard et al., 2009; Law et al., 2009).

To address these statistical imperfections, we have fitted two more detailed models to our data set of fish movement. The first, the intercept varying model, estimates a scaling exponent of 0.16 which is comparable to the work of others (e.g. Acuña et al., 2011). The second, the intercept and slope varying model, estimates an average scaling exponent of 0.10. Both of these estimates, 0.16 and 0.10, have 95% credible intervals that incorporate Ware's (1978) theoretical scaling exponent but not our taxa-independent findings. Thus, we show that an exponent of 0.133 (Ware, 1978) can be seen as a reasonable approximation of an average relationship between body mass and movement in marine fish, however it can only be obtained by allowing for the estimation of species level effects.

Model selection favours these more complicated multi-level models by some margin (Table 4.6). By fitting them we have formally accounted for the dual factors of species uniqueness and phylogenetic relatedness. However, because our data set is highly variable, any output must be interpreted with care and any inference gained must be

weighed against the structure of the model used. For instance, all of the larval species considered are very closely related, and we therefore expect them to share very similar parameter estimates. The same is not true in adults as the time since divergence between a cartilaginous shark species (e.g. Shortfin mako shark, *Isurus oxyrinchus*) and a bony fish species (e.g. Atlantic cod) is suitably large. A similar pattern exists in morphology, where the larval species considered (all pre-settlement stage pelagic larvae of demersal fish) share similar body shapes, being deep-bodied and compressed (as described in Leis et al., 2009b, 2009a). In comparison, the body shape of adults varies vastly from the elongated, streamline *thunniform* shape of an Atlantic Bluefin tuna to a flat, cross-sectionally compressed European plaice. These morphological differences partially coincide with phylogeny however it is interesting that the body shape of the larvae species considered is much more comparable to that of *batoids* (e.g. Thornback ray) than for example *gadoids* (e.g. Atlantic cod). It is not totally clear what effect these differences will have on the model's population-level parameters. However, it is clear to see that the variance in species-level effects is much greater in adults compared to larvae (Appendix 4.4).

One thing that is important to note, especially when comparing our estimations to the work of others (e.g. Carbone et al., 2005; Hirt et al., 2017; Ware, 1978), is the temporal resolution at which movement is observed (as discussed in section 4.2.1.3). Here, we are explicitly considering displacement at the daily level due to the structure of our data, however in the work of others this temporal resolution is often different (e.g. Hein et al., 2012). Such differences could yield different scaling exponents and therefore it is important to acknowledge that the relationship between speed and displacement will vary with temporal scale.

To conclude our discussion in regard to Q1 and Q2, it is clear that there is a positive scaling relationship between movement and body mass in marine fish. However, the scaling exponent governing this relationship remains uncertain. Our findings, ranging from 0.10 to 0.31, mirror the spread that exists in the published literature. To our knowledge, we are first study to analyse movement across 7 orders of magnitude in body mass and are first to consider a data set with multiple intraspecific observations. Consequently, we can be confident that our work contributes to the field and adds understanding to how movement scales with body mass in marine fish.

Further work will be essential to advancing our efforts. Tagging data sets are becoming increasingly open access via online depositories (e.g. MoveBank; Kranstauber et al., 2011) or more readily shared via large collaborative efforts (e.g. Hindell et al., 2016). As

they do, we hope to add to our data set and provide a more comprehensive analysis of movement scaling in fish. Moreover, as telemetry devices and their technology evolve, the likelihood of plugging the gap between larval and adult data clusters will hopefully become more likely. One area of particular interest is how the species-variation we observe in our estimated species-level effects propagate through a larger sample. For example, our findings suggest that movement in European plaice scales negatively with body mass. It would be interesting to find out whether this is purely a species or sample effect, or whether this outlier is a prevalent trend in flatfish. Species like European plaice spend prolonged periods of time on the seabed (Ewan Hunter et al., 2004b) and predominantly feed on sessile benthic invertebrates (Amara et al., 2001), therefore the need to actively pursue mobile prey is reduced (as shown in Holmes and Gibson, 1983). Along these lines, Domenici (2003) and Langerhans and Reznick (2010) both used meta-analyses to show that swimming performance exhibits clear relations with body shape and environment under laboratory conditions. For instance, they find that fish occurring in structurally complex environments (e.g. benthic habitats) have evolved differing morphologies (characterised by lower caudal fin aspect ratios) and favour short bursts of speed (characterised by high acceleration rates and high turning angles) compared to their more streamlined open-water counterparts who generally exhibit lower drag coefficients and higher endurance (for an empirical example see Blake et al., 2005). If flatfish or other species that have evolved to function in complex habitat types really do share an altogether different movement allometry than other fish types (e.g. roaming pelagic predators), then this would spark interesting debate surrounding movement and foraging efficiency and how they are influenced by body shape and habitat type. Alternatively, if our species-level variance only increased throughout a larger interspecific sample it would call into question the validity of a single all-encompassing power law relationship.

We also showed that movement scaling is different between life stages. This additional step was certainly opportunistic but made the most out of the data set and poses some very interesting questions. For instance, we show that movement scaling is steeper in larvae than it is in adults. Larval fish are subject to very high mortality rates in the wild and other aspects of larval biology have frequently shown that only the best performers survive (e.g. fastest growers; Vigliola and Meekan, 2002). A steeper scaling exponent could therefore be a direct consequence of this evolutionary pressure, as individuals attempt to maximise their growth rates through prey encounters as well as their ability to evade predators. In theory both of these aspects would boost their likelihood of survival and in turn would be favoured by evolution. From an evolutionary perspective, adult fish

find themselves in a completely different situation. As adults they have successfully overcome the high predation pressure of their larval and juvenile life stages, so theoretically the need to move at, or near to, their maximum at all times is diminished. Instead they must carefully balance continued survival with the need to reproduce. Consequently, movement is allowed to become a much more targeted process as individuals migrate and pursue prey but also prioritise the conservation of energy through shifts in movement behaviour (as shown in Chapter 3). This build-up of energy may then be used during annual spawning events allowing individuals to contribute to the next generation. It therefore seems reasonable that a reduction in movement allometry could be an indicator of this evolutionary process, especially considering that larger adult fish have been shown to contribute disproportionately to reproduction (Barneche et al., 2018). Additionally, being older and bigger will presumably afford individuals the luxury of optimising their movements instead of moving simply to survive. An alternative explanation for our findings may be linked to growth. Larvae do not grow isometrically and change their shape considerably during development (Fuiman, 1983; Webb and Weihs, 1986). As body size increases larvae progressively become more elongated (their length increases disproportionately to their mass) and their body shape becomes increasingly more streamlined, which reduces the power needed to overcome drag (Langerhans and Reznick, 2010). Such changes in morphology will, in theory, boost swimming performance (both in terms of speed and displacement) as Reynolds numbers increase (the fish passes from a viscous to an inertial flow regime) and swimming at high speeds becomes energetically less costly (Muller and Videler, 1996; Voosenek et al., 2018). As a result, it is difficult to disentangle whether the observed differences in scaling at small body sizes, both within- and across-species, is driven by the need to survive or simply a consequence of morphological development. Future work will certainly help unravel this issue and we propose that further analyses consider individual body shape as well as individual body mass when attempting to explain the scaling of realised movement rates in marine fish. This is especially true in analyses that consider larval fish.

In adults, it is also noteworthy that we find that differences in thermoregulation, habitat type and phylogenetic class provide no additional explanatory power to our analysis. Our prior belief certainly expected one of these factors to be a significant explanatory variable, especially given that all three factors feature in a number of recent high impact publications (e.g. Pawar et al., 2012; Tamburello et al., 2015; Watanabe et al., 2015). This lack of evidence could simply be a consequence of sample size, as despite including near 600 observations, our interspecific sample size of 18 is relatively small when

compared to work of Watanabe et al. (2015) or Tamburello et al. (2015). Linking back to the previous chapter, a finding that supported the inclusion of habitat type would have been of most interest, as differences in movement behaviour, search space and prey density provide a compelling theory as to why movement scaling might vary between a pelagic and a demersal environment (as discussed in Pawar et al., 2012). Further work on a much larger sample will again shed light on this and would undoubtedly provide a fruitful avenue for future research.

In conclusion, the aims of this chapter were straightforward: to collect, analyse and gain meaningful inference about how movement scales with body size in marine fish. In doing so we have added knowledge to an emergent research field. Three take home messages stand out. First, that realised movement (a movement metric calculated as displacement at the daily level from *in situ* movement observations) scales with body mass in a similar way to cruising and maximum speed in marine fish. Second, that by accounting for the dual factors of phylogenetic relatedness and species uniqueness our findings changed significantly. As a result, we advise that future meta-analyses on fish movement take care when choosing the most appropriate statistical model for their data set. If we had solely relied on the simple or species average model, then our findings and the wider scale conclusions drawn from them at the community level, would be significantly different. Third, that life stage is an important evolutionary driver of movement allometry in marine fish.

Movement is a principle component of animal physiology. In roaming visual predators, it dictates the volume of water that can be searched per unit time and in turn influences the processes of energy acquisition, mortality and growth. In this chapter's Introduction we made explicit reference to how Ware's (1978) theoretical work has widespread use in a range of size-structured population and community models. Previous and ongoing work has shown that q , the parameter that controls search volume scaling, is one of the most influential parameters in these models (Bannister et al. in prep.; Law et al., 2009; Plank and Law, 2012). For instance, Bannister et al. (in prep) have shown that even a 10% shift in q results in large deviations in critical community indicators such as total biomass, species coexistence and community size spectrum. In the following chapter (Chapter 5) we take our empirical findings surrounding movement allometry in marine fish and apply them to one of these models.

Chapter 5.

Movement allometry in a trait-based size spectrum model.

5.1 Introduction

Marine systems are highly size-structured. Fish grow several orders of magnitude in body mass during their lifetime, starting life as very small larvae (approximately 1 milligram) and growing to sizes at maturation ranging from 10 grams to 50 kilograms (Werner and Gilliam, 1984). Throughout this development, individuals will feed on prey that are a fraction of their own size, gaining the energy needed for somatic growth, movement and reproduction, whilst inflicting mortality on their prey (Kerr and Dickie, 2001; Law et al., 2009). This size-structuring of fundamental individual-level processes is part of the reason why many consider body size to be a 'master trait' in marine ecology (Andersen et al., 2016a, 2016b; Blanchard et al., 2017). It is also the reason why size, as opposed to taxonomic identity, is considered by many to be a more indicative of trophic position in marine food webs (Jennings et al., 2001).

Marine systems are undergoing phases of rapid change, as the size composition of marine communities across the globe respond to the direct and indirect effects of climate change (e.g. Blanchard et al., 2012; Maury et al., 2007b, 2007a; Woodworth-Jefcoats et al., 2013) and fishing (e.g. Andersen and Pedersen, 2010; Andersen and Rice, 2010; Worm et al., 2009). Motivated by the need to preserve ecosystem services (Rogers et al., 2014), attempts to model the emergent properties of a marine community have become a frequent feature of the published literature. One such attempt leans heavily on the importance of body size in marine systems and allows community dynamics to emerge as a function of many individual-level processes. These models are commonly referred to as size spectrum models as they resolve an entire fish community as a size distribution, where changes in abundance among discrete size classes are a direct consequence of fluxes in growth and mortality (Andersen et al., 2016b; Blanchard et al., 2017). These fluxes give rise to a community-level power law relationship between log mass and log abundance (commonly called a size spectrum; Edwards et al., 2017), where the slope of the relationship (community slope) reveals the size composition of the community (Andersen and Beyer, 2006).

The theory behind size spectrum models dates back to observations of equal biomass of plankton in logarithmically binned body mass classes (Sheldon et al., 1972). This observation lead to two principle conjectures: (1) that the abundance of individuals in marine systems scales negatively with size and (2) that the biomass of smaller prey is

consistently equal to the biomass of larger predators. Since Sheldon's hypothesis, observed size spectra have shown remarkable regularity, spanning not only different communities (e.g. Hua et al., 2013; Kelly-Gerreyn et al., 2014; Rodriguez et al., 2001; San Martin et al., 2006) but also a number of different ecosystems (Sprules et al., 2016). Consequently, size spectrum models have emerged as key tools in any marine ecosystem modeller's toolbox. To date, size spectrum models have been used to investigate how fishing drives trophic cascades (Andersen and Pedersen, 2010), to quantify the concept of balanced harvesting (Jacobsen et al., 2013; Law et al., 2016), to simulate the impact of rising temperatures (Maury et al., 2007b, 2007a) and to explore the potential impacts of a changing climate on fish production (Blanchard et al., 2012; Woodworth-Jefcoats et al., 2013). Additionally, they have even been used to contrast processes of early and late density dependence (Andersen et al., 2017) and show how structural habitat complexity is a critical feature on coral reefs (Rogers et al., 2014).

The advantages of size spectrum models are numerous (see Andersen et al., 2016b or Blanchard et al., 2017 for reviews). They are flexible, provide a middle ground between a simple Lotka-Volterra predator-prey equation and an end-to-end whole ecosystem model (Fulton et al., 2011) in terms of model complexity and can be used with relative ease via the *mizer* package (Scott et al., 2014) in R (R Core Team, 2016). Moreover, because their internal dynamics are all built around individual-level processes, they are mechanistic by design, reliant on a relatively small number of parameters (approximately 18 in the version considered here) and have low computational requirements (Andersen et al., 2016b). Modellers have increasingly used this approach to either capture multispecies communities by incorporating species-specific parameter values (e.g. Blanchard et al., 2014; Zhang et al., 2016) or have used fixed parameters across species applied to multiple systems (e.g. Jacobsen et al., 2017). However, there are large uncertainties surrounding the parameters that describe those fundamental individual-level process and species-specific differences that could substantially affect model predictions.

In Chapter 4, we show that the scaling of movement (measured as daily displacement) with body mass in marine fish is an area of relatively large uncertainty. Size spectrum models currently assume that the rate at which an individual encounters viable prey items per unit time is a function of three processes: (1) the availability of prey, (2) the size suitability of prey and (3) the individual's search volume. The availability of prey at any given time will vary based on the size composition of the community and size of the predator. The size suitability of prey will be some function of an individual's preferred predator-prey mass ratio (PPMR), a topic that has received significant attention in the

literature (see Barnes et al., 2010; Jennings et al., 2001; Ursin, 1973). On the other hand, an individual's search volume (V) can be thought of an individual moving at velocity (v) and having a search area that is assumed to be a circle with radius L^s , the maximum sighting range. Search volume is typically modelled as a power law relationship:

$$V(m) = \gamma m^q \quad (\text{Eqn 5.1})$$

where γ ($\text{g}^{-1} \text{yr}^{-1}$) is the search volume factor (see Methods section 5.2.2), m represents the individual's body mass and q is the exponent of search volume. Search volume with represent to L is

$$V(L) \propto (L^s)^2 \times L^{d_l} = L^{2s+d_l}, \quad (\text{Eqn 5.2})$$

where d_l dictates the scaling of movement with length in marine fish. Assuming an allometric relation between length and mass with exponent b ,

$$V(m) \propto m^{2s/b + d_l/b}, \quad (\text{Eqn 5.3})$$

therefore, with $s = 1.0$ (Andersen and Beyer, 2006) and $d_l = 0.4$, a value that stems from optimal foraging theory and dictates the scaling of movement (optimal cruising and optimal foraging speed; Ware, 1978), and $b = 3.0$ (Andersen and Beyer, 2006),

$$q = 2/3 + d_l/3 \approx 0.8. \quad (\text{Eqn 5.4})$$

Based on tagging observations, we hypothesise that d_m , the scaling of movement with mass i.e. $d_m = d_l/b$, could actually vary anywhere between 0.10 and 0.31, plus or minus some fairly large uncertainty (see Chapter 4). Further, we also expect s to be inherently uncertain as the distance at which a predator of size j can distinguish a prey of size i will vary based on ambient light levels, water turbidity and because prey tend to be inconspicuous (Andersen et al., 2016a; Ware, 1978). For further discussion on this topic we refer the reader to Andersen et al. (2016a). Note, Ware's (1978) theoretical work is based on swimming speed (cm s^{-1}) whereas our work (in Chapter 4) explicitly considers movement as daily displacement (m day^{-1}). As the relationship between speed and displacement will likely vary with time, such differences require acknowledgment and could lead to subtle differences in the value of d_m in marine fish.

Prey encounter is a critical component of any size spectrum model, as it contributes to the amount of food that can be consumed per unit time and subsequently impacts rates of growth, mortality and reproduction. Thus, q can be thought of as a principal model parameter which, when changed, could have large consequences. This is especially true when it is considered that a sensitivity analysis run on multiple versions of the size

spectrum repeatably found q to be one of the model's most influential parameters (Bannister et al., in prep). A need for further work is made even more compelling by two facts. First, that the sensitivity analysis in question only considered a range of q between 0.72 and 0.88 ($0.8 \pm 10\%$), whereas our empirical work suggests a much wider q range from ~ 0.64 to ~ 0.98 . Second, that q is also used to calculate lambda (λ), the exponent of the model's resource spectrum (details can be found in Methods section 5.2.2), which has also been shown to be a highly influential model parameter in terms of species biomasses and size-based indicators such as the slope of the community size spectrum (Bannister et al., in prep). Consequently, a thorough sensitivity analysis into how changes in q propagate through a size spectrum model would appear to be a logical next step with interest to marine ecosystem modellers and fisheries scientists, as well as management decision makers.

Focusing on the trait-based version of the size spectrum model (see Andersen et al., 2016b for a review), we show that a varying q value has large effects on the size composition of our theoretical community. Changes in q are shown to directly impact estimated community slopes as well as the ability of the community to retain its largest species but appear to have minimal effects on relative total biomass. Importantly, by imposing a range of fishing efforts, we show that the scaling of fish movement, via higher or lower q values, alters the resilience of marine communities to harvesting.

5.2 Methods

In the following sections we provide a brief description of the trait-based size spectrum model that is used throughout this analysis and detail how our experimental design allows us to test the interacting community-level consequences of a varying q and a varying fishing effort.

5.2.1 Model description

Much of the following description is adapted from of the work of Andersen and Pedersen (2010), Hartvig et al. (2011) and Jacobsen et al. (2013). All models are implemented using the *mizer* package (version 0.2) in R (R Core Team 2016, version 3.4.0, 'You Stupid Darkness').

Originally developed by Andersen and Beyer (2006), the trait-based version of the size-spectrum model (as is the case in all size-spectrum models) is based on the individual-level processes of encounter, growth, mortality and reproduction. All parameters are related to individual size (m), and in most cases are either estimated directly from the physiology of individual fish or derived from scaling relationships like the one considered

in Chapter 4. The equations governing the model are given in Table 5.1 and all model parameters are stated in Table 5.2. We place our chosen parameter set in the context of the published literature in Appendix 5.1.

The model's framework is built around two central assumptions: (1) that fish eat other organisms across a range of sizes expressed as a fraction of their own size, thus feeding is independent of species identity and (2) that the most important traits of a species are its asymptotic (maximum) size and maturation size, which are assumed to be strongly correlated (Beverton and Holt, 1959; Prince et al., 2015). The model resolves a fish community as a continuum of 'species' with increasing asymptotic body sizes (Andersen et al., 2016b; Andersen and Beyer, 2006). During implementation, the continuum is represented as a discrete number of asymptotic size classes, which are referred to as 'species' for the sake of simplicity. Each species i is characterised by its asymptotic size M and its population by its size distribution $N_i(m)$. Species are typically spread evenly over a chosen asymptotic size range and the number of species used is not important so long as it is greater or equal to ten (Jacobsen et al., 2013). Here, we

Table 5.1. Model equations.

Community size spectrum	$N_c(m) = \sum_i N_i$	(E1)
Size selection of food items	$\varphi(m_{prey}/m) = \exp[-(\ln(\beta m_{prey}/m))^2/(2\sigma^2)]$	(E2)
Encountered food	$E(m) = V(m) \int m_{prey} N_c(m_{prey}) \varphi(m_{prey}/m) dm_{prey}$	(E3)
Feeding level	$f(m) = E(m)/(E(m) + C_{max})$	(E4)
Maximum consumption	$C_{max} = hm^n$	(E5)
Allocation to reproduction	$\psi(m, M) = \left[1 + \left(\frac{m}{\eta M}\right)^{-10}\right]^{-1} \left(\frac{m}{M}\right)^{1-n}$	(E6)
Somatic growth	$g(m) = (1 - \psi(m))(\alpha f(m)C_{max} - k_s m^p)$	(E7)
Predation mortality	$\mu_p(m_{prey}) = \int (1 - f(m))V(m)N_c(m) \varphi(m_{prey}/m) dm$	(E8)
Background mortality	$\mu_b(M) = \mu_0 M^{n-1}$	(E9)
Resource spectrum	$\frac{\delta N_r}{\delta t} = r_0 m^{n-1}(\kappa_r - N_r) - \mu_p N_r$	(E10)
Resource carrying capacity	$\kappa_r(m) = \kappa m^\lambda$	(E11)

*m, individual mass. M, asymptotic (maximum) size. c, community. p, predation. b, background. r, resource.

use 10 species with M values ranging from 10 to 200,000 g. Thus, our chosen size range (0.001 g – 220 kg) covers the empirical size range (0.002 g – 200 kg) considered in Chapter 4.

Each individual fish is described by its individual body mass (m) and by its asymptotic size M . Relying on mechanistic based submodels of growth, mortality and reproduction, the model calculates $N_i(m)$ in units of numbers per volume per mass. The dynamics of the model's continuum are governed by the conservation equation (McKendrick, 1926; von Foerster, 1959):

$$\frac{\delta N_i}{\delta t} + \frac{\delta g_i(m)N_i}{\delta m} = -\mu_i(m)N_i \quad (\text{Eqn 5.5})$$

where the individual-level processes of growth $g_i(m)$ and mortality $\mu_i(m)$ dictate the rate at which an individual fish either gains somatic mass via the consumption of prey or is removed from the community via predation. Scaling from individual- to the community-level, equation 5.5 therefore controls changes in number of fish and biomass in any given size class.

To grow, an individual must encounter and ingest food. Food items are selected from the whole community size spectrum (E1) according to a log-normal size selection function (E2). The key component of this size selection function is a fixed PPMR β (Jennings et al., 2001; Ursin, 1973). The rate at which a predator encounters food items (E3) is a product of available food and a size dependent search volume. Search volume is detailed in equations 5.1 - 5.4. The amount of encountered food that is consumed per unit time is then modelled as a Holling type II functional response (E4), thus a size dependent upper limit is imposed on consumption rate.

Consumed food items are assimilated with a fixed efficiency of α and are used initially to meet metabolism demand $k_s m^p$. Any remaining energy is allocated to somatic growth (E7) and reproduction (E6), the latter of which only becomes active when an individual's size approaches its maturation size. When an individual is fully mature all of this remaining energy is allocated to reproduction over somatic growth. This formulation (E7 and E6) means that growth and reproduction are linked within the model and are both food dependent. Furthermore, the use of E6 means that under a regime where consumption rate is equal to maximum consumption, a von Bertalanffy-like growth curve is produced (Hartvig et al., 2011).

Table 5.2. Model parameters.

Parameter	Value	Definition	Reference
physiology			
α	0.6	Assimilation efficiency*	Kitchell and Stewart, 1977
n	2/3	Exponent of maximum intake	Andersen and Pedersen, 2010
h	$30 g^{1-n} yr^{-1}$	Factor for maximum intake	Andersen and Pedersen, 2010
p	0.75	Exponent of standard metabolism*	West et al., 1997
k_s	$4 g^{1-p} yr^{-1}$	Factor metabolism coefficient*	Winberg, 1956
μ_0	$0.6 g^{1-n} yr^{-1}$	Background mortality factor*	Andersen and Pedersen, 2010
η	0.25	Size at 50% maturation relative to M_i	Beverton, 1992
ε	0.1	Reproductive efficiency	Jacobsen et al., 2017
k_0	50	Recruitment multiplier*	Scott et al., 2014
foraging			
β	100	Preferred predator-prey weight ratio*	Jennings et al., 2001; Ursin, 1973
σ	1.3	Width of selection function*	Andersen and Pedersen, 2010
γ	free $g^{-1} yr^{-1}$	Search volume factor	-
q	free	Search volume exponent	-
f_0	0.5	Expected average feeding level*	Scott et al., 2014
resource (primary production)			
κ_r	$0.005 g^{\lambda-1} m^{-3}$	Resource spectrum carrying capacity*	Andersen and Pedersen, 2010
r_0	$4^{1-p} yr^{-1}$	Growth rate of resource spectrum*	Savage et al., 2004
λ	free	Exponent of the resource spectrum	Scott et al., 2014
fishing			
m_F	0.1	Minimum size selectivity of the fishery, relative to M_i	Jacobsen et al., 2017
ξ	0.5	Selectively of the fishery	Jacobsen et al., 2017
g, grams. yr, years. m, mass. M, asymptotic (maximum) size. i, species. *, default values within the <i>mizer</i> package. free, parameters that vary as a function of q (see Figure 5.1).			

Once mature, an individual uses the energy that has been allocated to reproduction to produce eggs. Eggs hatch to become larvae and their introduction at the smallest size class is regulated by a Beverton-Holt (Beverton and Holt, 1957) like stock-recruitment relationship. Maximum recruitment is calculated using equilibrium theory (Andersen and Pedersen, 2010) and a multiplier, k_0 . As in Jacobsen et al. (2017), we also chose to impose an additional restraint on larval survival, this is imposed via the reproductive

efficiency parameter ε . Reproductive efficiency is designed to represent losses due to egg mortality and spawning effort (Andersen et al., 2016b).

Mortality is modelled as a direct function of two processes. The first is predation mortality which is the consequence of prey encounter and subsequent consumption (E8). The second is background mortality which is included to limit the build-up of excessively large individuals in the absence of fishing (E9). A third mortality rate, starvation mortality, is common throughout the literature (e.g. Hartvig and Andersen, 2013; Jacobsen et al., 2013) but is not currently built into the *mizer* package.

As in Andersen and Pedersen (2010), we also include a background resource spectrum which acts as a food source for smallest of size classes. As is default in the *mizer* package the dynamics of the resource spectrum are modelled as a semi-chemostat growth function with allometric scaling of regeneration (E10) and a carrying capacity given by the theoretical equilibrium spectrum (E11). The background resource spectrum has a continuous size range, ranging from 10^{-10} to 1 g.

All model runs make full use of the *set_trait_model* wrapper function provided by the *mizer* package. The community spectrum is discretised with 100 size bins. We use a time step of 0.1 years and run each model for a total of 500 years. After approximately 100 years the model's solution achieves convergence, trending towards a stable estimation of abundance at size and a dynamic steady state.

5.2.2 Varying q

Based on the empirical findings of Chapter 4, we constructed a sequence of 34 possible d_m (scaling exponent between movement and mass) values where the first value of d_m is -0.02 and thirty fourth value of d_m is 0.31. Values increase incrementally by 0.01. This range is non-random and is designed to include the empirical estimates made in Chapter 4 and their associated uncertainties (see Table 4.6). To ensure consistency, we also manually added a 35th value, where $d_m = 0.1\dot{3}$. This ensures that the theoretical value proposed by Ware (1978) is explicitly considered. Thus, our sequence of possible d_m values increases from 34 to 35.

We convert our 35 possible d_m values to a sequence of 35 possible q values using equation 5.4. Further, to account for the unknown levels of uncertainty surrounding the scaling of maximum sighting range (L^s) in marine fish, we have expanded the range of q considered by $\pm 20\%$. Thus, we add 7 values the top and bottom of the current range, such that q_1 equals $0.057\dot{6}$ and q_{49} equals $1.046\dot{6}$. This sequence of possible q values is

then sequentially inputted into the described model, meaning the model is projected 49 different times, producing 49 different theoretical fish communities.

Varying q in this way will directly alter encounter rates across the whole size range of the community spectrum (see Appendix 5.2). Some species will benefit, allowing processes of consumption, growth and reproduction to be maximised whilst other species will lose out. Alongside its role on equation 5.1, q has two other roles within the internal dynamics of the model. First, it is used to calculate the exponent of the resource spectrum (λ)

$$\lambda = 2 + q - n \quad (\text{Eqn 5.6})$$

where n is the exponent of maximum intake. Second, because λ varies as a function of q , and λ is used to calculate γ , the factor for search volume ($\text{g}^{-1} \text{year}^{-1}$),

$$\gamma_i(f_o) = \frac{f_o h_i \beta_i^{2-\lambda} \exp\left(-(\lambda - \frac{2}{2})^2 \frac{\sigma_i^2}{2}\right)}{(1 - f_o) \sqrt{2\pi} \kappa_r \sigma_i} \quad (\text{Eqn 5.7})$$

γ also varies as a function of q (see Figure 5.1). Thus, between model runs we allow λ and γ to vary as a function of a changing q . It is, however, important to acknowledge that equations 5.5, 5.6 and 5.7 consider a marine community that is in perfect equilibrium (often referred to as the scale-invariant model) where the total abundance of all species of all sizes (including those in the background resource spectrum) follows a perfect power law relationship (i.e. the process of growth and natural mortality are in balance). Consequently, any change in the value of q has the potential to shift the slope of that power law relationship and furthermore the introduction of fishing mortality will act to spoil that equilibrium. This caveat will become significant when drawing meaningful conclusions.

5.2.3 Fishing mortality

One of the principal uses of size spectrum models is to gain a more in-depth understanding of the consequences of fishing (e.g. Andersen and Pedersen, 2010). Fishing typically removes intermediate to large individuals from the community, resulting in top-down trophic cascades (Andersen and Pedersen, 2010). These cascades are driven by rises and falls in predation pressure and food availability, both of which are linked in some way to an individual's encounter rate. As a result, the inclusion of fishing mortality is a logical next step in our analysis.

Fishing mortality is imposed using a standard 'trawl-type' selectivity function, where individuals of each species i , become instantaneously 'available' to the fishery at size $0.1M_i$. Once individuals are 'available' they are caught at a constant catchability rate of

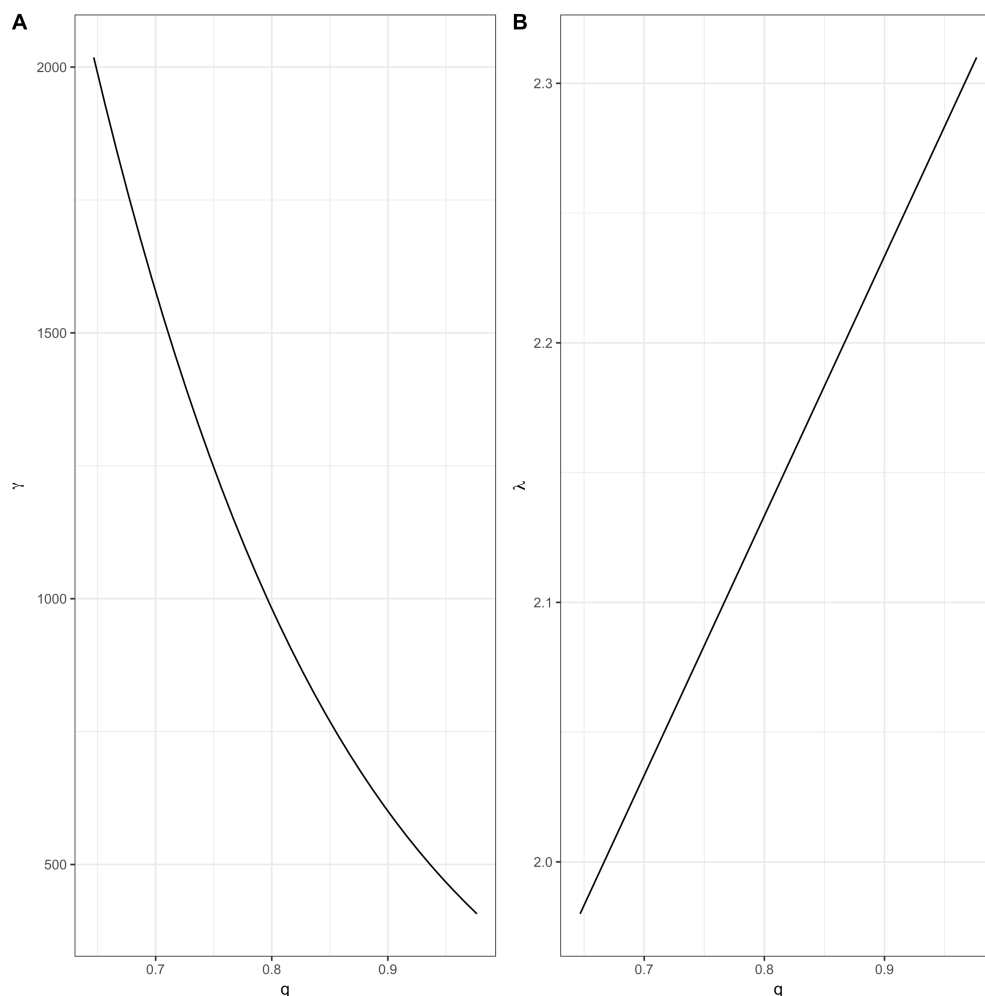


Figure 5.1. Relations between q and its dependent parameters: gamma (factor of search volume; A) and lambda (exponent of the resource spectrum; B). Gamma ($g^{-1} \text{ year}^{-1}$) is shown to decrease as a function of q whilst lambda increases linearly with q .

50% (ξ ; Jacobsen et al., 2017). We allow fishing effort (f ; year^{-1}), a measure of fishing intensity, to vary according to a sequence from 0 to 1 in increments of 0.05 (21 possible f values). The chosen exploitation pattern is comparable to the selective fishing pattern used in Jacobsen et al. (2013), where juveniles are protected and individuals are recruited to the fishery as they approach some fraction of their asymptotic size. It allows us to test the interacting consequences of a varying q and a varying f and explore species-specific rates of coexistence and extinction. Thus, we run the model a total of 1029 times (21 multiplied by 49), where each projected community is characterised by its own unique combination of q and f parameters.

5.2.4 Interaction matrix

One additional parameter that seems open to discussion in the published literature is the rate at which cannibalism is allowed to occur in the model (Andersen et al., 2016b; Canales et al., 2016). As prey selection is size based, cannibalism is an intrinsic model feature and is controlled by the model's interaction matrix φ . The interaction matrix

describes the likelihood with which each pair of species will interact (in terms of encounter) and takes the form of a 10 by 10 matrix. Here, we set all φ values to be 1 (as is default in *mizer*), meaning that prey selection is entirely size based and that all species are viable food items to all species, including conspecifics. Further, to test how sensitive our findings are to the chosen interaction matrix, we re-ran the analysis with all φ values fixed at 0.5. In this second analysis, prey selection remained entirely size based, and all species were still able to feed from all other species however their rates of interaction were halved. We assign the initial analysis (all φ values fixed at 1) to the notation φ_1 and the second analysis (all φ values fixed at 0.5) to the notation $\varphi_{0.5}$.

The model's interaction matrix is used in E3 to scale encounter rates and subsequent predation mortality.

5.2.5 Model output

From each model we output four commonly used ecological indicators: (1) community slope, (2) total biomass (g m^3), (3) total yield of the fishery (g m^3) and (4) species coexistence. The first three indicators are relatively common in the published literature, while the fourth serves as a useful measure of community composition.

Community slope was derived as the slope of a linear regression fitted to each model's estimated log abundance and log mass and was calculated using the `getCommunityslope` *mizer* function. Total biomass of the fish community was calculated as an aggregate biomass of all 10 species using the `getBiomass` *mizer* function. Total yield of the fishery was calculated as an aggregate yield from all 10 species using the `getYield` *mizer* function. Each of the above calculations was made sequentially at the 0.1-year increment (5000 calculations), we then calculated a mean value from the final 500 increments. An averaged value was used to ensure that cyclic solutions were handled appropriately. Each calculation considered the whole community size spectrum, from 1 – 220,000 grams but did not consider the background resource spectrum. Preliminary investigations revealed that the trait-based model produced absolute total biomass and absolute total yield estimates that were unrealistically small, for example under a q value of 0.8 and an f value of 0.15 we estimated a total biomass of 0.0646 g m^3 and a total yield of 0.0005 g m^3 . Consequently, we opted to interpret these indicators in relative terms to a null model, where the null model is the community projected under a q value of 0.8 and f values of 0 and 0.05 for total biomass and total yield, respectively.

Species coexistence is a derived metric and describes the number of species that are able to coexist in the community, without collapsing, under a given q and f parameter

set. As in Worm et al. (2009), we used 10% of unfished biomass as a definition for collapse. The biomass of each species through time was, again, extracted from the model using the `getBiomass mizer` function. We then calculated collapse and subsequent coexistence from averaged values taken from the final 500 increments.

Gaining meaningful inference across a grid of 1029 possible values is no easy task, as a result we have chosen a number of empirical derived values and use them to refine our interpretation. In the q dimension, we select the following values based on the findings of Chapter 4:

- a. $q = 0.66$, where $d_m = 0$ (no relationship between body size and d)
- b. $q = 0.76$, where $d_m = 0.10$ (varying intercept and slope model – Chapter 4)
- c. $q = 0.8$, where $d_m = 0.13$ (Ware 1978)
- d. $q = 0.826$, where $d_m = 0.16$ (varying intercept model – Chapter 4)
- e. $q = 0.96$, where $d_m = 0.30$ (simple model – Chapter 4).

In the f dimension, we select fishing efforts of 0, 0.25 and 0.7 based on the work of Andersen and Rice (2010). These f values are designed to reflect the following exploitation regimes: no fishing ($f=0$), fishing at sustainable levels ($f=0.25$) and heavy exploitation ($f=0.7$). The latter regime ($f=0.7$) has previously been used to mimic the state of fishing in the North Sea (Andersen and Rice, 2010; Pope et al., 2006).

All plots are generated using the `ggplot2` library (Wickham, 2009) in R and make full use of the *viridis* colour palette (Rudis et al., 2018).

5.3 Results

Projecting over a large matrix of possible q and f values, we observe large changes in community slope and rates of species coexistence, as well as variation in total yield compared to the null model. We also found that the total biomass of community was reasonably consistent and only exhibited large relative differences at low values of q .

In terms of community slope (Figure 5.2), smaller q values (below 0.75) result in a community that is highly sensitive to small changes in f . Under fishing efforts between 0 and 0.05, community slopes are between -3 and -5. However, it is worth noting that, even in the absence of fishing, a q value of 0.66 results in a highly variable community spectrum (Figure 5.3), characterised by steep declines in abundance (at sizes greater than 150 g) compared to the null model ($q = 0.8$). Once f surpasses a critical threshold value of approximately 0.15, community slopes very quickly crash to values below -10.

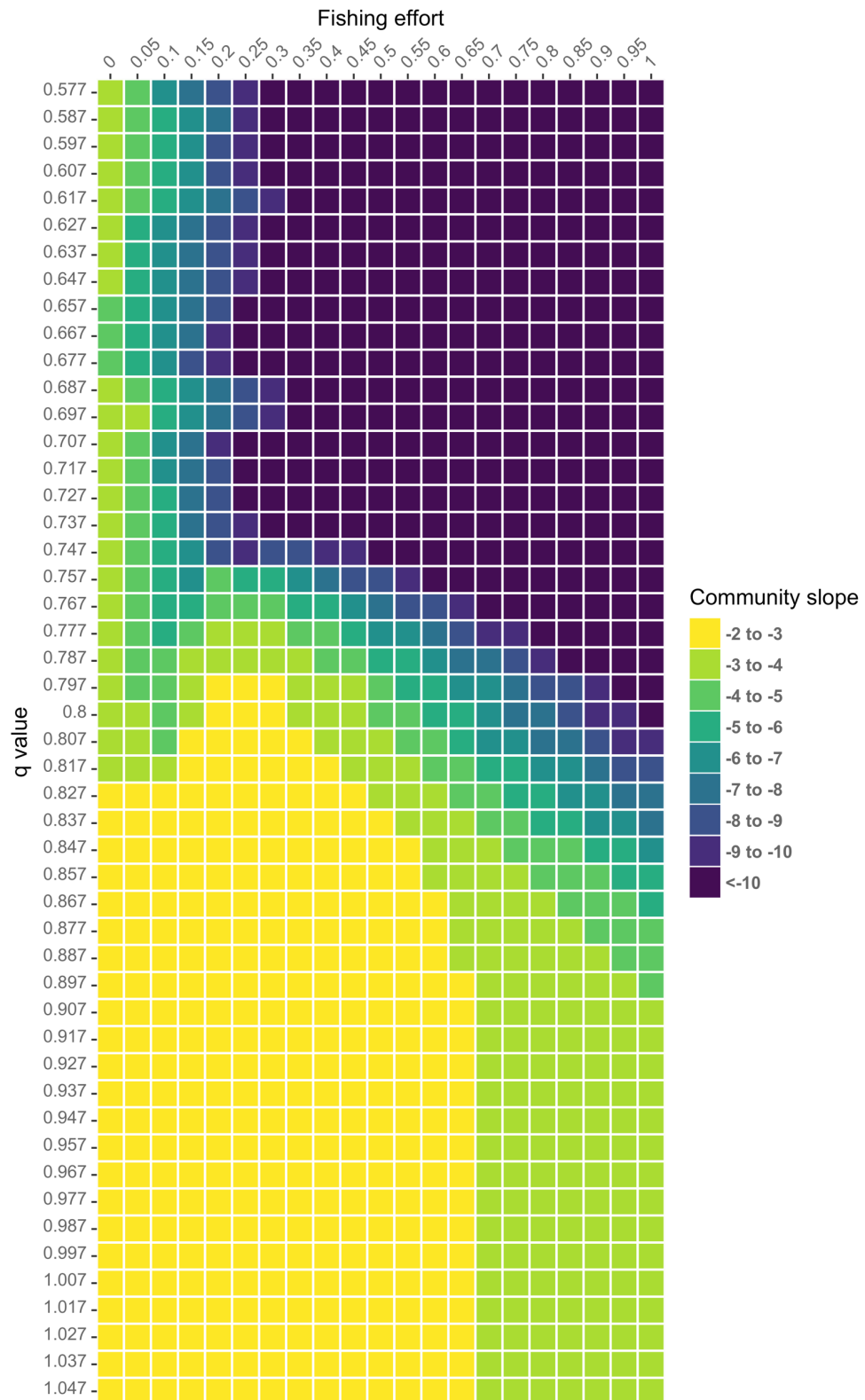


Figure 5.2. Community slope as a function of a varying q (rounded to 3 decimal places) and a varying f . All slope estimates have been discretised to aid visual interpretation. All φ values are fixed at 1.0. A lower threshold of -10 has been imposed because values beyond this point are indicative of a truncated size spectrum where abundance at large size class has been completely lost.

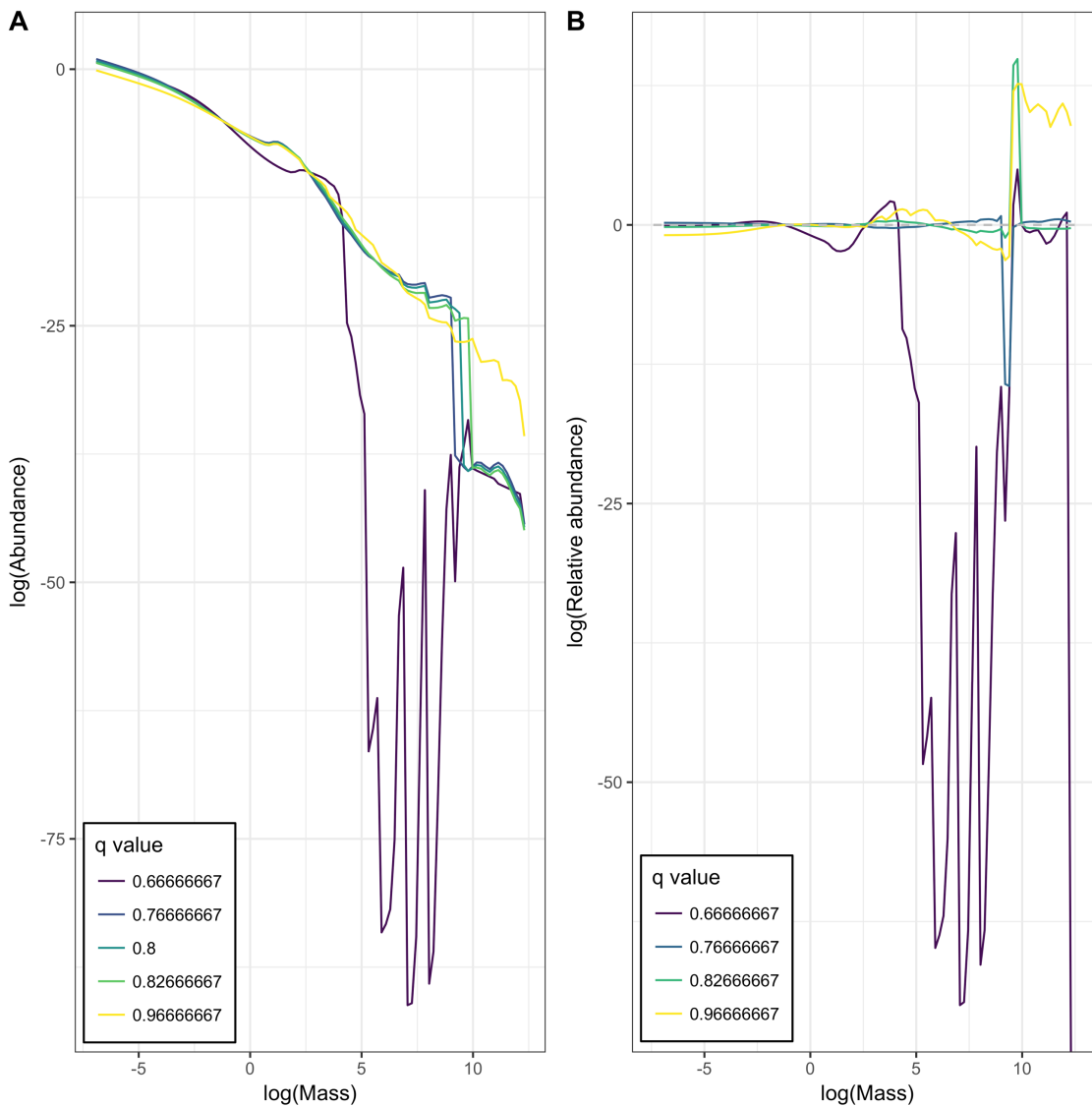


Figure 5.3. Abundance at size (A), and relative abundance at size (B) for each of our empirically derived q values. Abundance was calculated as the sum total of all ten species, where the abundance of a single species represents an averaged estimate taken from the last 500 model time steps. Relative abundance at size was calculated relative to the null model ($q = 0.8$). In B, the null model is plotted as a grey dashed line at $y = 0$. Abundance and mass were log (natural log) transformed to aid visual interpretation. In all cases fishing effort (f) is fixed at $f = 0$. All φ values are fixed at 1.0.

Thus, the community very quickly loses its largest individuals and becomes dominated by biomass at small size classes. This pattern is clearly illustrated by plots of abundance against mass, where abundance at larger size classes (greater than 1500 g) very quickly diminishes towards nominally low values under fishing efforts of 0.25 (Figure 5.4) and 0.7 (Figure 5.5). At q values of approximately 0.8 or higher, fishing efforts between 0 and 0.45 result in community slopes between -2 and -4. However, as f increases, we see a

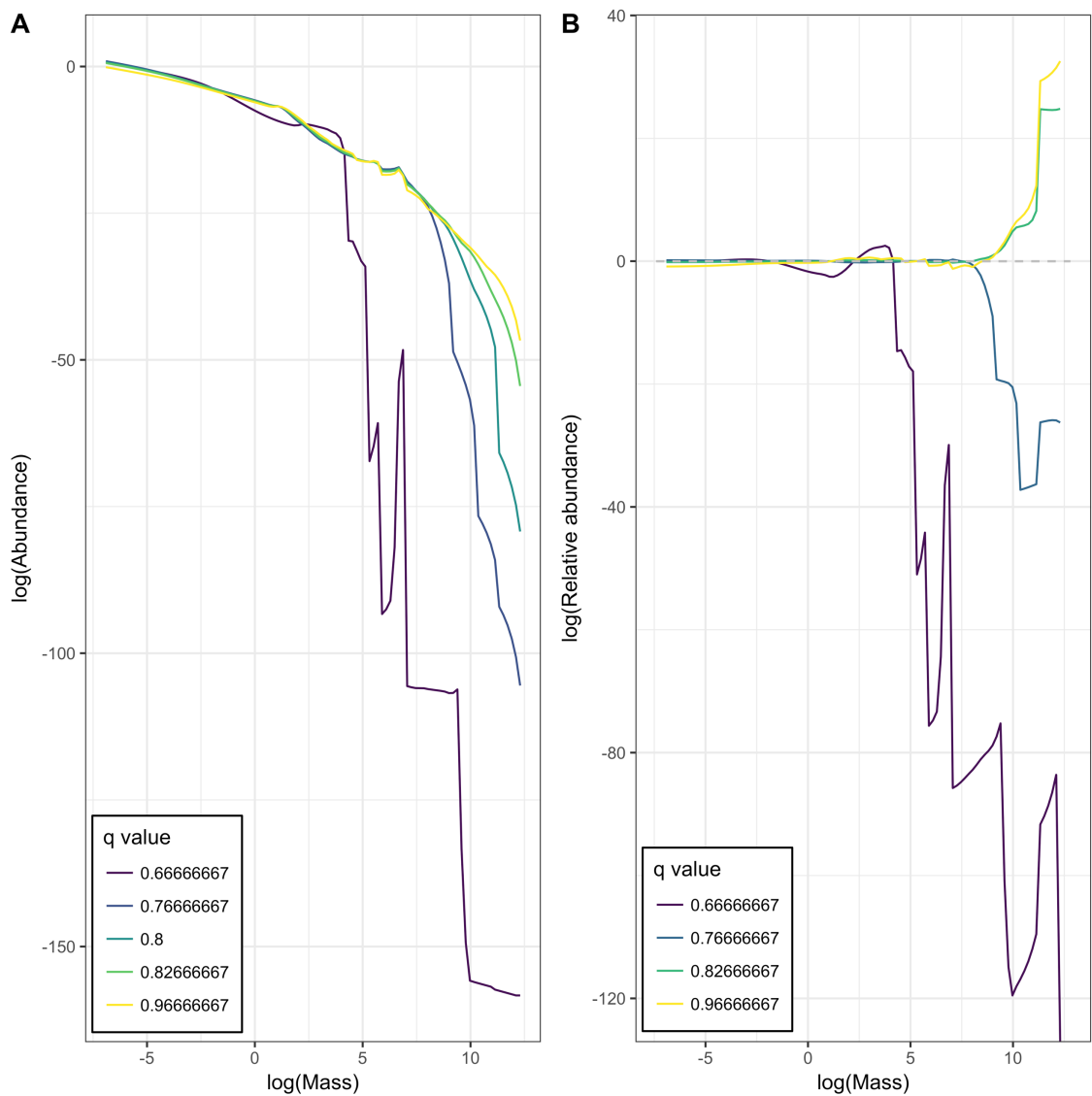


Figure 5.4. Abundance at size (A), and relative abundance at size (B) for each of our empirically derived q values. Abundance was calculated as the sum total of all ten species, where the abundance of a single species represents an averaged estimate taken from the last 500 model time steps. Relative abundance at size was calculated relative to the null model ($q = 0.8$). In B, the null model is plotted as a grey dashed line at $y = 0$. Abundance and mass were \log (natural \log) transformed to aid visual interpretation. In all cases fishing effort (f) was fixed at $f = 0.25$. All ϕ values are fixed at 1.0.

clear and gradual response. Communities characterised by higher q values are able to maintain a shallower community slope for longer, despite increases in fishing. In fact, at q values of 0.9 and above community slopes are maintained at values between -2 and -4 independent of the fishing effort being imposed. This resilience to increases in f is illustrated further in Table 3, as communities projected with q values of 0.8, 0.826 and 0.96 share very similar community slopes under f values of 0 and 0.25. This then changes

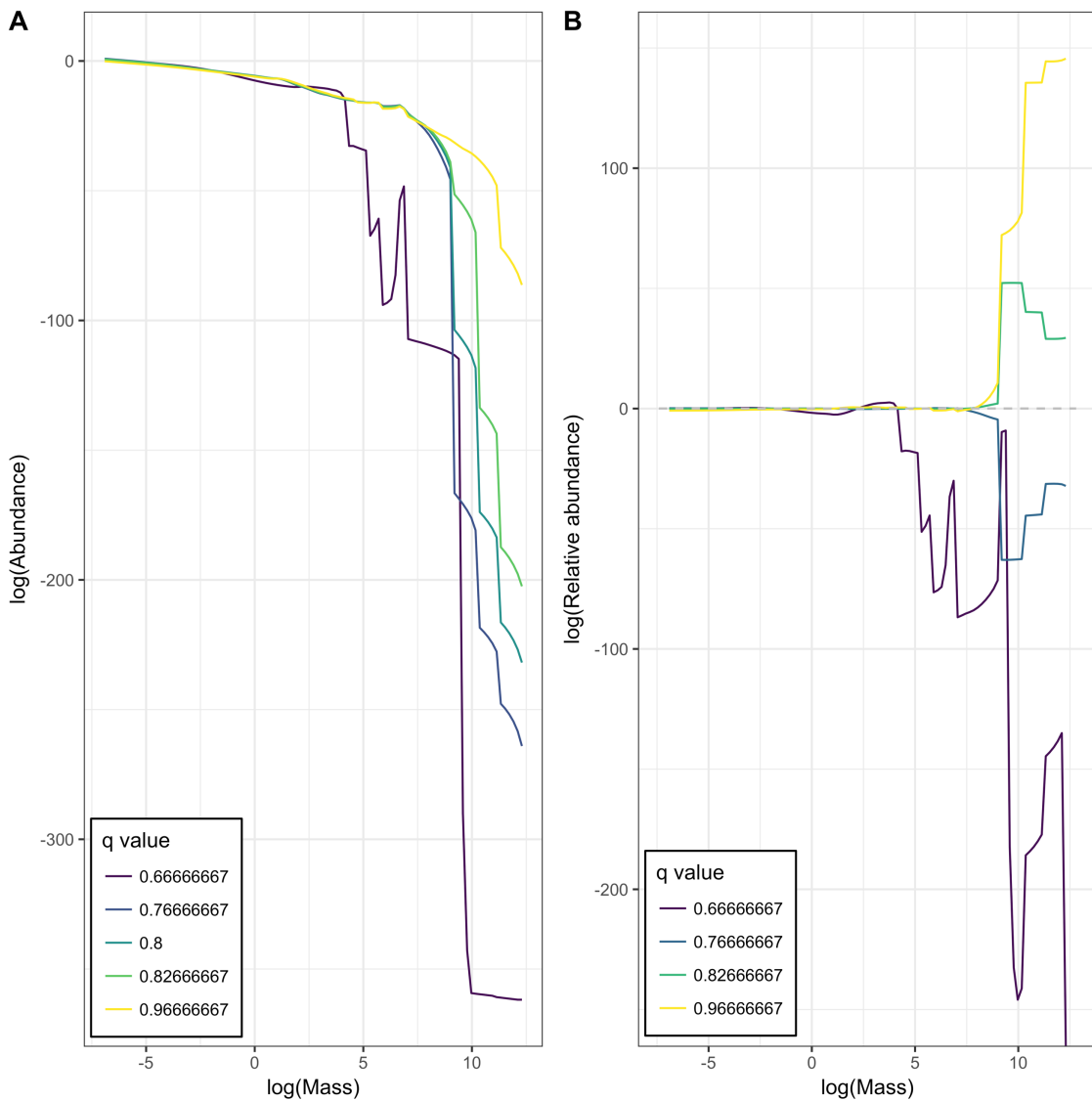


Figure 5.5. Abundance at size (A), and relative abundance at size (B) for each of our empirically derived q values. Abundance was calculated as the sum total of all ten species, where the abundance of a single species represents an averaged estimate taken from the last 500 model time steps. Relative abundance at size was calculated relative to the null model ($q = 0.8$). In B, the null model is plotted as a grey dashed line at $y = 0$. Abundance and mass were log (natural log) transformed to aid visual interpretation. In all cases fishing effort (f) was fixed at $f = 0.7$. All φ values are fixed at 1.0.

at higher fishing efforts, as the difference in community slope between $q=0.8$ and $q=0.96$ raises from 0.19 to 3.50 under f values of 0.25 and 0.7, respectively.

Relative total biomass remains fairly consistent across a large range of q (0.70 – 1.046) and f values (0 – 1) indicating minimal variation from the null model (Figure 5.6). Relative differences peak when the community is projected under a q value of 1.046 and an f value of 0.05. However, it is notable that even in this extreme case total biomass has

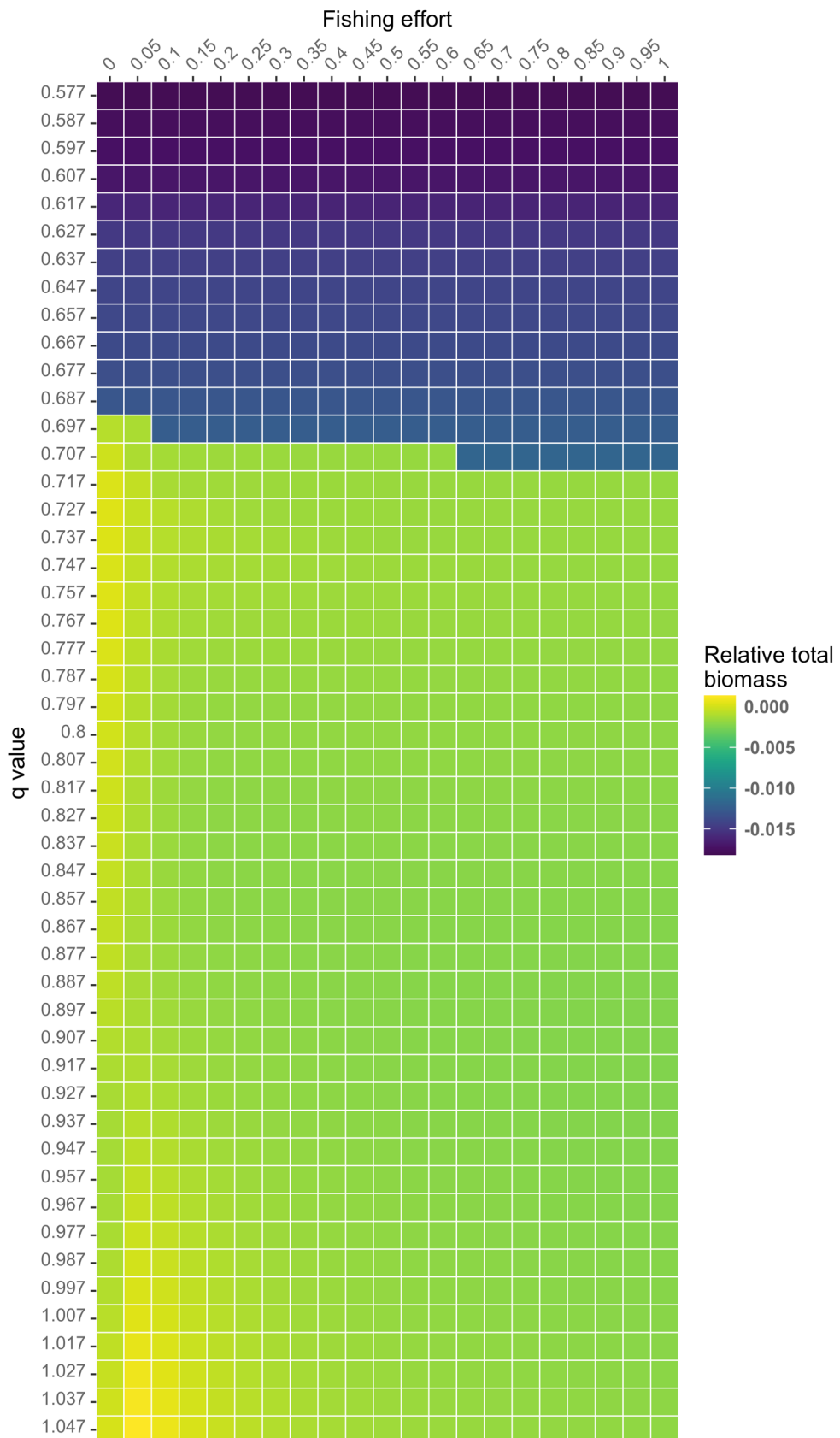


Figure 5.6. Relative total biomass as a function of a varying q (rounded to 3 decimal places) and a varying f . All values are relative to the null model ($q = 0.8$ and $f = 0$). All φ values are fixed at 1.0.

Table 5.3. Size spectrum model out for q and f values of empirical interest.

f	d_m	q	γ	λ	slope	Δ slope	Δ biomass	$\Delta\%$ biomass	Δ yield	$\Delta\%$ yield	species coexistence	Δ species coexistence
0	0	2/3	1841.3	2.00	-4.14	-1.08	-0.0138	-29.63	-	-	-	-
	0.10	0.766	1151.9	2.10	-3.12	-0.07	0.0003	0.71	-	-	-	-
	0.133	0.80	981.6	2.13	-3.05	-	-	-	-	-	-	-
	0.16	0.826	862.4	2.16	-2.96	0.09	-0.0002	-0.51	-	-	-	-
	0.30	0.966	428.6	2.30	-2.24	0.81	-0.0012	-2.66	-	-	-	-
	0	2/3	1841.3	2.00	-10.30	-7.56	-0.0119	-26.74	-0.00069	-100.00	-4	-
0.25	0.10	0.766	1151.9	2.10	-4.26	-1.51	0.0004	0.83	-0.00001	2.54	8	-2
	0.133	0.80	981.6	2.13	-2.75	-	-	-	-	-	10	-
	0.16	0.826	862.4	2.16	-2.61	0.13	-0.0002	-0.36	-0.00008	-11.18	10	0
	0.30	0.966	428.6	2.30	-2.56	0.19	0.0004	0.94	-0.00039	-56.57	9	-1
	0	2/3	1841.3	2.00	-19.50	-12.99	-0.0012	-26.66	-0.00061	-100.00	6	-1
	0.10	0.766	1151.9	2.10	-10.46	-3.96	0.0002	0.44	0.00003	4.74	7	0
0.7	0.133	0.80	981.6	2.13	-6.50	-	-	-	-	-	7	-
	0.16	0.826	862.4	2.16	-4.64	1.86	-0.0001	-0.33	-0.00005	-7.47	7	0
	0.30	0.966	428.6	2.30	-3.01	3.50	-0.0002	-0.52	-0.00033	-54.00	7	0

Δ , change relative to q = 0.8. $\Delta\%$, percentage change relative to q = 0.8. slope, community slope. biomass, total biomass (g m³). yield, total yield (g m³). species coexistence, number of species coexisting in the community. For definitions of community slope, total biomass, total yield and species coexistence we refer the reader to main text (section 5.2 – Methods).

only increased by 2.8% compared to the null model. Below a q value of approximately 0.7, we do observe some reductions in relative total biomass. For instance, at a q value of 0.576 the total biomass of the community is 39.1% smaller than under the null model. These remain consistent despite increases in fishing effort. Focusing in on our empirical values of interest, some difference is observed (Table 5.3). This is especially true when comparing estimates made under a $q = 0.8$ and a $q = 0.66$ parameter set, but overall neither varying q nor varying f seems to have much effect on the community's projected biomass.

Plotting relative total yield across our range of possible q and f values produces clear yield curves (Figure 5.7). The yield of the trawl-type selectivity function reaches its maximum at intermediate q values ($q = 0.776$ to 0.8) and f values between 0.2 and 0.35. From these maximum values yield drops off substantially, resonating away in a wave-like fashion as both q and f increase. Using our empirically chosen values as an example (Table 5.3), total yield is shown to be larger when q equals 0.776 compared to the null model, whereas q values larger than 0.8 lead to reductions in total yield. This pattern is found to consistent under both sustainable ($f = 0.25$) and heavy ($f = 0.7$) fishing pressure. In fact, increasing q from 0.8 to 0.96 results in nearly a 50% reduction in yield. Additionally, we find that relative total yield completely drops off below a q value of approximately 0.7, irrespective of the fishing effort imposed on the community. For example, a community projected under a q value of 0.66 has a total yield that is 100% smaller than under a q value of 0.8. This suggests that the community comprises of very small fish, where the likelihood of growing past the $0.1M_i$ availability threshold is heavily constrained by reductions in encounter rates at larger size classes.

Species coexistence is maximised at high q and low f values, where higher encounter rates per unit time allow larger individuals to thrive (Figure 5.8). As in community slope and total yield, values drop off at low values of q ($q < 0.716$), irrespective of fishing effort, further illustrating that a critical threshold exists in the q dimension. Below this threshold encounter rate scaling, and hence food intake, is found to be insufficient to sustain the 5 largest species in our theoretical community. Between q values of 0.726 and 0.766 we again observe a clear and gradual response to an increasing q and f , where small increases in q allows the community to retain its 7th largest species despite increases in fishing effort. At q values greater and equal to 0.776, the community is much more resilient to increases in fishing. At low fishing efforts (f less than 0.60), the community consists of 9 or more species. This then drops off to 8 species at larger fishing efforts. This pattern clearly demonstrates that large search volume exponents are essential to

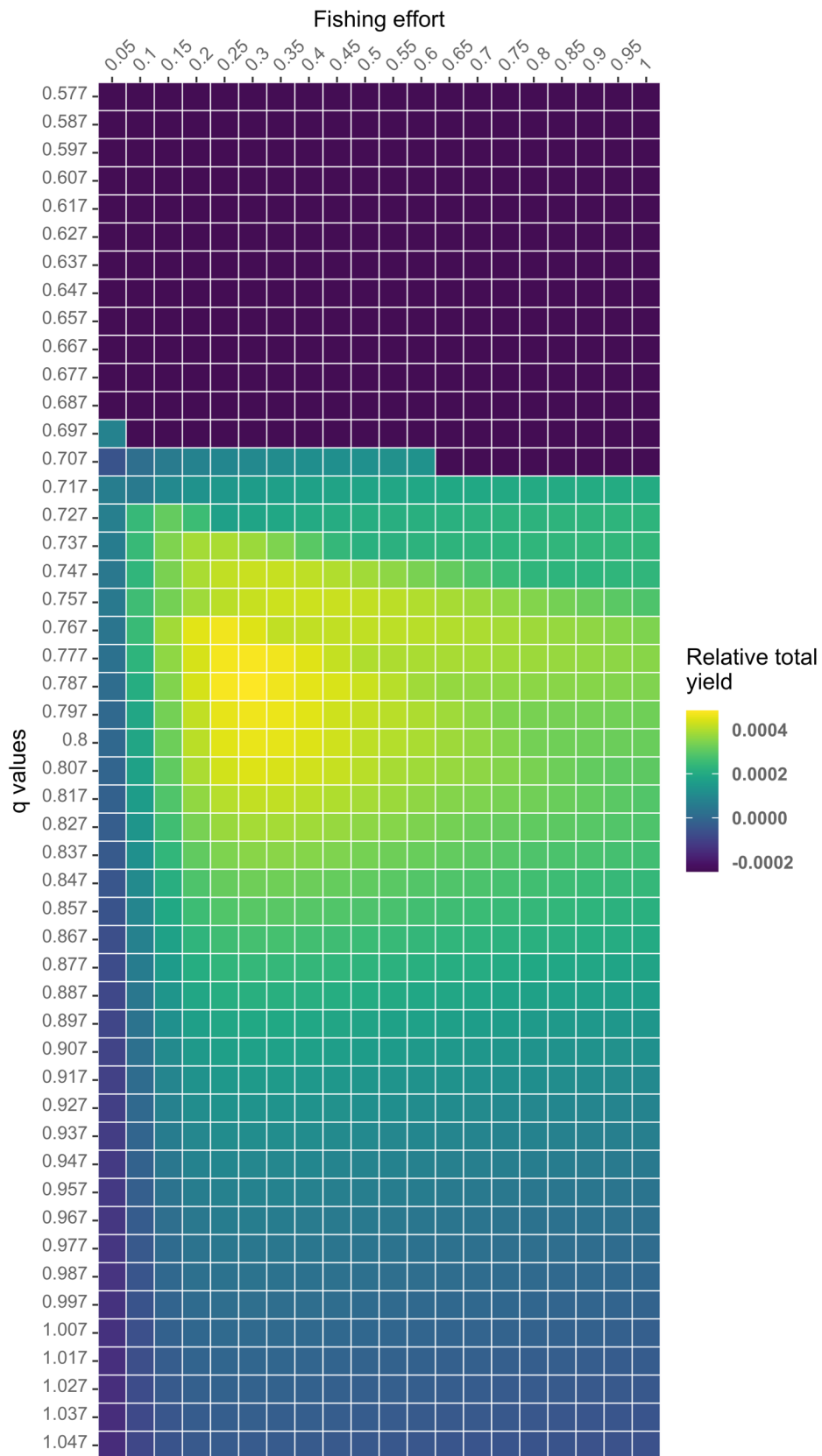


Figure 5.7. Relative total yield as a function of a varying q (rounded to 3 decimal places) and a varying f . All values are relative to the null model ($q = 0.8$ and $f = 0.5$). All φ values are fixed at 1.0.

avoid collapse in larger species, especially when the community is exposed to heavy levels of exploitation.

When the analysis is re-run with a different interaction matrix, we do observe some differences, especially in terms of community slope and species coexistence. For example, we find that q values of 0.876 and above are needed to maintain a community slope between -2 and -4 (Appendix 5.3). This threshold in the q dimension is markedly higher than during the initial analysis (when all φ values are fixed at 1.0). Further, we find that the number of communities with a community slope value below -10 increases, extending from 0.576 to 0.846 in the q dimension and from 0.3 to 1.0 in the f dimension. A similar response is present within species coexistence, with all ten species again coexisting at high q and low f values, however the range is markedly reduced (Appendix 5.4). In comparison, we find that the trends observed in terms of relative total biomass (Appendix 5.5) and relative total yield (Appendix 5.6) are consistent across the two interaction matrices considered. For example, we find that the change in total biomass relative to the null model is minimal across a wide range of q (0.70 – 1.046) and f (0 – 1) values. Whereas total yield again produces clear yield curves and peaks at intermediate q (0.776 to 0.8) and f values (0.35 – 0.5).

5.4 Discussion

Here, we expose a trait-based size spectrum model to an empirically informed range of q values. In doing so, we note four key findings. (1) That the value of q greatly influences the size composition of the estimated community but has no clear effect on the community's total biomass. (2) That high q values, akin to those estimated by our simple model in Chapter 4, result in a community that is much more resilient to increases in fishing pressure. (3) That a minimum critical threshold is present in the q dimension, below which any reasonable increase in f results in a rapid collapse of species abundance at intermediate to large size classes. (4) That our general findings are robust to changes in the model's interaction matrix (φ). In the following discussion we will outline the mechanisms behind these findings with particular focus on the individual-level processes of prey encounter, consumption and growth. We will also relate any observed trends to the published literature and highlight some take-home messages that will be of interest to marine modellers, fisheries scientists as well as management decision makers.

Most size spectrum models implement a fixed q value of 0.8 (e.g. Hartvig et al., 2011; Jacobsen et al., 2013). Setting q at 0.8 and f at 0, our trait-based model resolves a

community of 10 coexisting species which is characterised by a normalised abundance community slope of approximately -3.05, which is equivalent to a normalised biomass slope of -2.05. This slope estimate is a little steeper than those reported for normalised biomass in fish and epifaunal predator communities in the North Sea (-1.2 to -2.25; Bianchi et al., 2000; Blanchard et al., 2009). However, given its relatively close proximity to past findings (Bianchi et al., 2000; Blanchard et al., 2009) and the model's convergence towards a smooth community size spectrum (Appendix 5.7), we are confident that the null model ($q = 0.8$) provides a stable platform from which comparisons can be made.

Regardless of the fishing pressure being imposed, a community projected with a low q value (between $0.57\dot{6}$ and $0.74\dot{6}$ in φ_1 and between $0.57\dot{6}$ and $0.79\dot{6}$ in $\varphi_{0.5}$) is characterised by two components. First, a marked decrease in the abundance of large-bodied fish. Second, a superabundance of small-bodied fish. When q is low, large-bodied fish have relatively lower search volumes per unit time than under null conditions (i.e. when q is set at 0.8). Lower search volumes reduce will reduce rate at which an individual encounters prey and imposes severe constraints on food consumption. As somatic growth only occurs once metabolic demands are met, any reductions in food consumption will limit the rate of which individuals can grow through the size classes. Once scaled up to the community-level, our findings support the conjecture that a reduction in search volume will greatly reduce the abundance of large-bodied fish resulting in a truncated size spectrum and a much steeper community slope. As shown in many studies, this truncation of the size spectrum will only be exacerbated by fishing (Andersen and Pedersen, 2010; Houle et al., 2013; Zhang et al., 2016), as any individual who does emerge at high size classes will have high likelihood of fisheries induced mortality. Even when fishing is absent, a q value of $0.6\dot{6}$ is unable to support community abundance above a size threshold of approximately 60 grams (Figure 5.3). Beyond this size threshold (~ 60 grams) abundance at size suffers a complete collapse and the community size spectrum veers away from an expected smooth relationship towards patterns of extreme volatility (Figure 5.3). These observations lead us to hypothesise that a critical threshold must exist in the q dimension, below which large-bodied fish are not viable parts of the community. By plotting abundance at size for each species across a range of q values (Appendix 5.8) we demonstrate that a q value above 0.76 is needed before the two largest species (species 9 and 10) are able to persist. This threshold value will be highly model dependent and is unique to our chosen parameter set. However, this provides a useful example of how small changes in the scaling of movement with

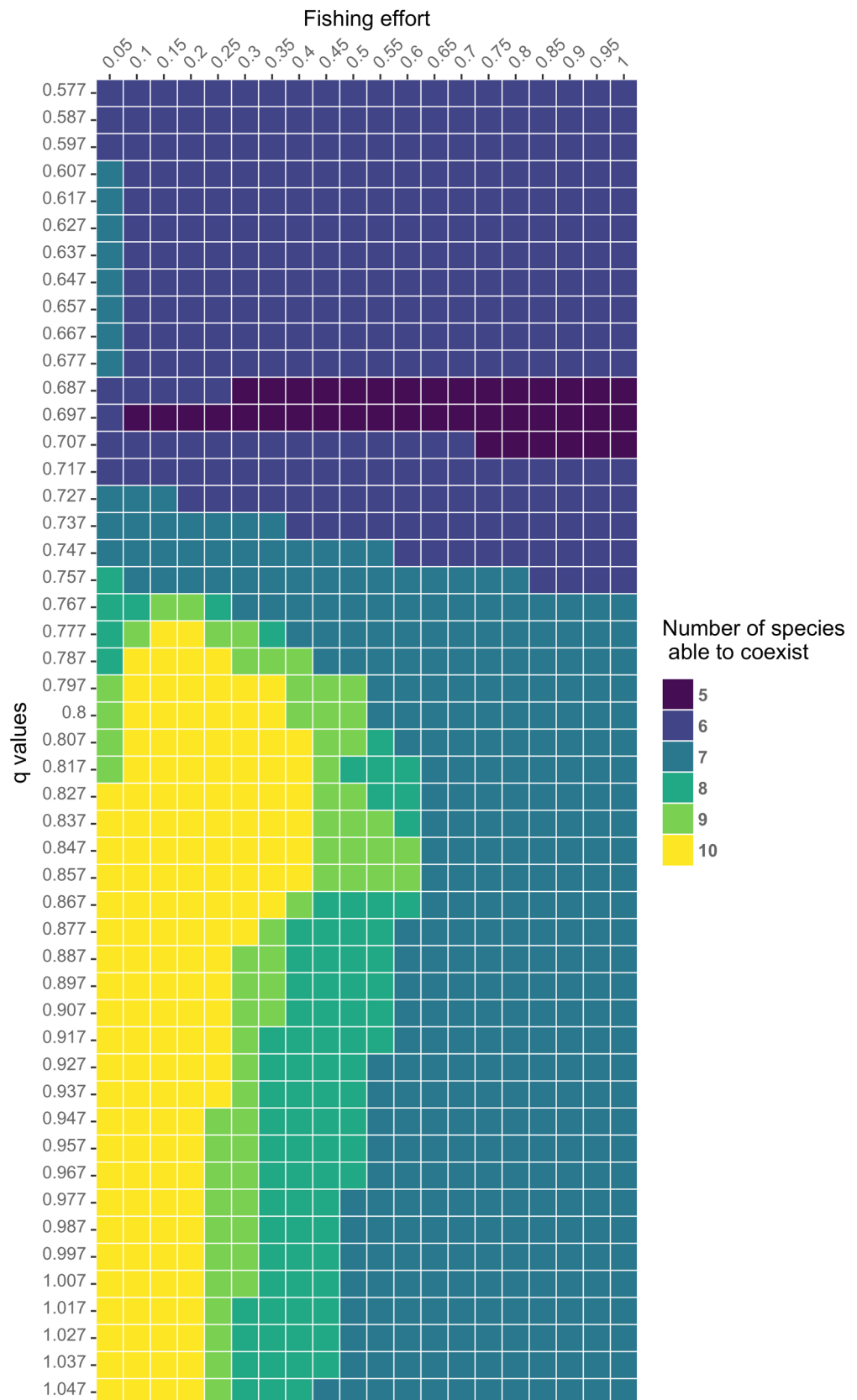


Figure 5.8. Species coexistence as a function of a varying q (rounded to 3 decimal places) and a varying f . All φ values are fixed at 1.0.

mass can have large emerging consequences on the size composition of fish communities.

A superabundance of small-bodied fish when q is fixed at low values is not surprising. By constraining the abundance of large-bodied fish a lower q value suppresses the predation mortality being exerted on smaller individuals. Additionally, small-bodied fish benefit directly from an increased search volume per unit time relative to the null case (when $q = 0.8$). Both of these factors allow smaller fish to prosper, as processes of consumption and growth can be maximised whilst the likelihood of mortality is reduced. This results in a community size composition that is dominated by biomass at small size classes. Interestingly we observe a clear 'hump' in the size spectrum when q is set at a value of 0.66 (Figure 5.3). This non-linearity is consistently present when fishing is imposed on the community (Figure 5.4 and Figure 5.5) and occurs at body masses of approximately 20-80 grams. We theorise that this 'hump', where abundance at size is disproportionately greater than expected is indicative of a growth induced bottle neck. Before this point conditions for growth are optimal allowing individuals, especially the juveniles of larger-bodied species who are not subject to fishing mortality, to grow quickly through the size classes. However, at some theoretical point the shallower scaling of search volume with mass will act to constrain encounter rates, limiting consumption and growth. These lower rates will again limit the energy that can be allocated to somatic growth causing a 'pile up' of individuals at size. This trend is analogous to the findings of Andersen and Pedersen (2010) who note a similar 'pile up' of individuals as a cascading response to fishing and adds further evidence to our theory of a critical q threshold in size-structured communities.

Compared to the null model, communities projected with a higher q value are characterised by a shallower community slope. These changes in size composition are a direct consequence of a change in q , as intermediate- and large-bodied fish are permitted to search a larger volume of water per unit time, boosting rates of prey encounter, consumption and growth. Larger consumption rates allow individuals to grow through the size classes more quickly and as theorised in the discussion of Chapter 4 this leads to an accumulation of individuals at large size classes. In the absence of fishing, this accumulation is another example of a growth induced 'pile up' in the size spectrum. However, in this scenario, the extent of the 'pile up' is restricted by the model's internal background mortality rate (μ_0) and further constrained by top-down predation. For example, although intermediate-bodied fish may benefit from an increased search volume, its likelihood of successfully growing through the size classes is reduced by the high predation pressure being exerted on its size range by an increased abundance of

large-bodied fish. This results in an abundance size spectrum that is almost identical in shape to the null model but has a large peak at the uppermost extent of the size range (Figure 5.3). Once fishing is introduced into the model, large fish are removed from the community which releases the intermediate-bodied fish from that predation pressure. This release allows those intermediate fish that have not been fished out of the system to grow through the size classes and assume the position of top predator. These fluxes in growth and abundance will occur throughout the size spectrum, as fishing first removes individuals, which displaces predation mortality and ultimately allows other individuals to grow into the gaps. This fishing induced trophic cascade is identical in principle to what we observe in the null model and mirrors the findings of Andersen and Pedersen (2010). However, because q is higher, the individual-level processes of prey encounter, consumption and growth will happen at much higher rates. Higher individual-level growth rates mean that the community's abundance at size will be regenerated quickly, allowing larger-bodied species to persist in a community despite increases in fishing mortality. Such emergent community-level features highlight how small changes to an individual-level process can have a large effect on community dynamics.

Interestingly when q is fixed at lower values (between 0.576 and 0.746 in φ_1 and between 0.576 and 0.796 in $\varphi_{0.5}$), we observe clear winners and losers. Small fish benefit from higher search volumes allowing them to become superabundant whilst large fish struggle to consume enough to food to sustain life. This is not the case when q is high, with plots of relative abundance (panel B in Figures 5.3 – 5.5) illustrating minimal difference in abundance at small size classes compared to the null model. Our prior expectation was that under higher q values (> 0.9), small-bodied fish would become much less abundant, as their search volumes per unit time are reduced in relative terms. This would have reverberating consequences, as any size-structured food web will be inherently sensitive to changes in the abundance of small prey. The absence of this phenomenon in the modelled communities' merits further investigation, especially when it is considered that the predation mortality on smaller-bodied species will only be increased by peaks in the abundance of large fish. We initially had two theories to explain this. Theory one surrounds the assumption of cannibalism. In the both analyses (φ_1 and $\varphi_{0.5}$) we assume that cannibalistic feeding interactions occur at the same order as all other interspecific feeding interactions. Cannibalism is known to be widespread among fish (Andersen et al., 2016b; Canales et al., 2016; Persson et al., 2000; Smith and Reay, 1991), however by allowing fish to feed on their conspecifics we have provided an alternative feeding pathway. Thus, in a scenario of high growth rates but low prey abundance, large fish could, in theory, be relying heavily on the consumption of their conspecifics. If this was

true, it would provide another example of how cannibalism prompts species coexistence in size-structured fish communities (as shown in Hartvig and Andersen, 2013). Theory two is by no means independent of theory one and involves the process of reproduction. Because large-bodied fish are encountering more prey per unit time they will presumably be able to allocate more energy to reproduction. More stored reproductive energy means more eggs can be produced per unit time. More eggs mean more larvae and a much greater influx of individuals at small size classes. These larvae stages will act to replace the abundance at size of small-bodied fish and will in turn act as a food source for larger predators. Some of these larger predators will be conspecifics thus processes of cannibalism and reproduction can be considered to be interacting responses of the community to increases in q . Plotting species abundance at size in the absence of fishing (Appendix 5.9), we are able to demonstrate that it is not that smaller species are not losing out, their abundance at size is lower, albeit marginally, when q is high ($q = 0.966$). However, it is clear that under higher q values the larger species within the community (e.g. species 10), are exhibiting elevated abundances at size across their entire size range. Such increases will bolster the community's abundance at small-size classes and will presumably supplement the diet of larger fish. We show that the spawning stock biomass is greater in larger species (species 9 and 10) when q is high ($q = 0.966$; Appendix 5.10) providing direct evidence for theory two. However, we currently unable to separate rates of cannibalistic predation mortality from other forms of predation mortality within *mizer* and recommend that future work replicates our analysis under varying levels of cannibalism. Past studies have shown that cannibalism can remove up to 40% of a cohort in Atlantic cod (Neuenfeldt and Köster, 2000), therefore it is clear that a better understanding of cannibalism is needed (Andersen et al., 2017).

Past studies show us that size spectrum models are particularly useful when attempting to examine the community- and ecosystem-level impacts of fishing (Andersen et al., 2016b; Blanchard et al., 2017; Edwards et al., 2017). Here we have introduced a selective community-wide exploitation pattern where individuals from all 10 species are removed according to a standard trawl-type selectivity function. In doing so we predict that relative total yields are high at intermediate q (between 0.776 and 0.8 in both φ_1 and $\varphi_{0.5}$) and f values (between 0.2 and 0.5 in both φ_1 and $\varphi_{0.5}$). In the f dimension, an association between high yields and immediate fishing efforts is somewhat intuitive and has been shown to occur in Hake (*Merluccius merluccius*; ICES, 2018) and several other commercial fish stocks in the waters surrounding the British Isles (e.g. Haddock (*Melanogrammus aeglefinus*; ICES, 2017d) and Herring (*Clupea harengus*; ICES, 2016)). By continuously fishing at sustainable levels, the rate of removal will be proportional to

rate of productivity (Francis, 1974; Jacobsen et al., 2013; Zhou et al., 2012), thus exploitation can be sustained at some optimal rate for a longer period time. Such optimality is analogous to the original theory behind Maximum Sustainable Yields (MSY; as detailed in Beverton and Holt, 1957; Graham, 1935; Schaefer, 1957, 1954) however whether or not this optimality is achievable in a complex and dynamic multi-species world is subject to large debate (e.g. Hilborn and Ovando, 2014; Ulrich et al., 2017; Worm, 2016). In q dimension, communities projected with intermediate q values (between 0.776 and 0.8) contain many small-bodied fish as well as some larger-bodied fish. This size composition, given our chosen exploitation pattern, will produce higher yields when compared to either a truncated size spectrum (e.g. when $q = 0.66$) or a community that is dominated by abundance at high size classes (e.g. when $q = 0.96$). This might not necessarily be the case when an alternative exploitation pattern is considered. For example, an unselective balanced harvesting scenario, like the one used in Jacobsen et al. (2013), may produce higher relative yields when q is set at low values. This is because the idea behind balanced harvesting is that exploitation should be in accordance with the productivity of the individual or species (Jacobsen et al., 2013; Law et al., 2012), and a small-fish dominated community will be inherently highly productive (Andersen et al., 2009). Conversely, an industrial fishing gear that solely targets larger, more valuable fish (as used in Andersen and Pedersen, 2010) will theoretically achieve maximal yields when q is high.

It is clear that the potential avenues for future work in this project are numerous. We have already highlighted how changes to the rate of cannibalism will allow us to further explore the community-level consequences of a changing q with a particular focus on species coexistence rates. Additionally, by considering alternative exploitation patterns we can investigate how q induced changes in size composition may alter estimated yields and the likelihood of achieving fisheries management goals such as MSY, optimal yield or 'pretty good yield' (Hilborn, 2010; Houle et al., 2013). However, as in any modelling study, it is critical that any inference gained is examined with regard to the model's assumptions and the limitations of the approach. One such limitation surrounds the value of λ (exponent of the resource spectrum). Past observations and theory dictate that the size spectrum of primary production scales with an exponent that is close to 2 (Boudreau and Dickie, 1992; Rinaldo et al., 2002; Sheldon and Parsons, 1967). Here, we have allowed the value of λ to explicitly vary as q changes. For instance, when q is set at 0.976, λ is assumed to be 2.31. This parameter value is much higher than in a number of published applications of the trait-based model, where λ typically takes the value of 2.05 (Andersen and Beyer, 2006; Hartvig et al., 2011). These differences will

have two reverberating consequences. First, they directly alter the shape of the background resource spectrum and will change the food available to small size classes (in the fish size spectrum). Second, because equations 5.5 – 5.7 consider a marine community that is in perfect equilibrium (where the total abundance of all species of all sizes follows a perfect power law relationship), theory dictates that any change in q will consequently produce a λ that maintains this equilibrium. Both of these consequences merit further investigation aimed at disentangling the relationship between q and λ .

In Chapter 4 of this thesis we learn that the scaling of movement (measured as daily displacement) in marine fish is an area of relatively large uncertainty. Motivated by the need to explore how this uncertainty manifests itself the community level, we have exposed a widely-used trait-based size spectrum model to an empirically informed range of q values. In doing so we note three take-home messages. (1) That by changing rates of prey encounter, q directly influences the individual-level processes of consumption, growth and mortality. (2) Scaling up to the community-level, variation in q causes large emergent effects on community size composition both in terms of community slope and species coexistence, as well as altering how a community responds to fishing. (3) That the future application of size spectrum models to ecologically important questions must consider the inherent uncertainty surrounding q and the possible effects that a change in q can have on a model's output.

Chapter 6.

General Discussion.

The rising quality and quantity of movement data, coupled with methodological advancements, have led to a 'golden age' in animal movement (Hays et al., 2016; Hussey et al., 2015; Jonsen et al., 2013). However, authors still query the level of inference that can be gained by deploying tags on individual animals, when the ultimate aim is to inform conservation and management (Carter et al., 2016; Hebblewhite and Haydon, 2010; McGowan et al., 2017; Ogburn et al., 2017). The aim of this thesis was to address these queries, taking what we have observed at the level of the individual and analysing it in such a way as to infer the individual-, population- and community-level consequences of movement.

In the following sections we will summarise our key findings, comment on several emergent research themes and provide direction for future work.

6.1 Key findings

Throughout this thesis we present a sequential guide for the analysis of individual tagging data, which effectively steps through the complexities of the scaling-up process. We start at the individual level by investigating how tag deployment on individual fish informs our understanding of stock structure (Chapter 2), and end with how changes to the scaling of movement governs species coexistence and community structure (Chapter 5). Our key findings maintain this sequential approach:

- (1) At the individual-level, tagging studies inform our understanding of stock structure and allow us to uncover how individual fish alter their distributions on a seasonal basis. In Chapter 2, we observe minimal signs of stock mixing between cod in the Irish and Celtic seas, supporting current stock assessment and management strategies (ICES, 2017a). However, we do show that cod in the Irish sea move north, coming into contact with cod off the west coast of Scotland. This finding, coupled with distinct patterns of seasonal space-use and stock-specific movement characteristics, yields important insights for conservation and management. Potential management implications include the positioning of marine protected areas (MPAs) or no-take zones and the adaptation of stock boundaries to better reflect the fish they aim to protect.

- (2) Hidden Markov models (HMMs) provide a flexible framework via which collective individual movement behaviour can be used to explore population-level spatio-temporal trends. In Chapter 3, we introduce a novel bivariate HMM, which uses prior distributions to address key obstacles faced by ecologists when using individual movement to ask population-level questions of their data. The most notable of these obstacles being large variations in data quality. Application of our approach to a relatively large sample size, consisting of over one hundred demersal fish, facilitated the coherent classification of daily horizontal and vertical movements into two broad behavioural modes (resident and migrating; Griffiths et al., 2018). In the resident state, individual fish are more vulnerable to capture by trawl-based fishing methods (Righton et al., 2009). Consequently, knowing when and where this state occurs has important ramifications for fisheries management and species conservation.

- (3) Movement follows a power law relationship with body mass in marine fish. In Chapter 4, we sought to investigate whether simple rules govern seemingly complex movement patterns. Tested across 583 individuals taken from 18 species and spanning 7 orders of magnitude in body mass, we demonstrate that current assumptions surrounding the scaling of movement with body mass (e.g. Ware, 1978) are valid but mask important ecological phenomenon, notably within-species variations and life-stage effects. Crucially, we show the importance of considering phylogenetic and species-level effects when approximating taxon-independent relationships.

- (4) Size-based ecosystem models are highly influenced by small changes to the scaling of movement. In Chapter 5 we apply our findings from Chapter 4 to a trait-based size spectrum model (Scott et al., 2014). We show that empirically informed changes to a single parameter (q) has large emergent consequences for community size composition and rates of species coexistence. Additionally, by considering a range of fishing efforts, we demonstrate how the scaling of movement has the potential to alter estimated fisheries yields and the resilience of marine communities to fishing. Our findings have important consequences for size-based ecosystem models which are frequently used to ask key ecological questions, e.g. how marine systems have or will respond to fishing (Andersen and Pedersen, 2010; Andersen and Rice, 2010; Blanchard et al., 2017; Houle et al., 2013).

6.2 Limitations and future work

Throughout this thesis, we have discussed numerous avenues for future work and made a conscious effort to highlight the limitations of our work and acknowledge any caveats. In the following text we summarise these caveats by chapter and then discuss areas of limitation that require further work.

- (1) In Chapter 2 we have described the movement patterns of cod in the Irish and Celtic Seas and gained information about stock structure and stock mixing based on the movement paths of twelve individuals. This small sample size may not adequately reflect that of the whole population, however we, like the majority of tagging studies, have assumed that it does (Carter et al., 2016; Hebblewhite and Haydon, 2010; McGowan et al., 2017; Ogburn et al., 2017). As discussed previously, small sample sizes are often a consequence of financial limitations, tag loss or failure, or low numbers of individual observations (McGowan et al., 2017). However, in the case of cod in the Irish Sea an altogether different factor is contributing to our low sample size; since the early 2000s, ICES has been advising zero total allowable catch (TAC) for cod, which results in a reduction in tag return rates as less cod are being landed. (ICES, 2017e, 2016b, David Righton, *pers coms*). This provides an interesting example of how science has influenced fisheries management (by recommending reductions in TAC) and in doing so has temporarily reduced the amount of data gained from the deployment of data storage tags. A second caveat that requires acknowledgment surrounds the use of diet data, which is sourced from the stomachs of dead fish (Pinnegar, 2014). Here, we used diet data to further our understanding of feeding interactions and ultimately how any differences in prey type may underpin differences in the rate of stock recovery. However, it is important to note that stomach content analysis only provides a snapshot in time, informing us about what has recently been consumed and not an individual's historical feeding habits (Baker et al., 2014). These trends may not always represent an individual's preferential prey and consequently may skew any inferences made.

- (2) In Chapter 3 we have used a two-state bivariate HMM to learn about spatial-temporal behavioural patterns in two species of demersal fish (Griffiths et al., 2018). In doing so, we have assumed that two behavioural states are sufficient to describe the underlying movement process and that these states are shared by multiple individuals. Moreover, we assume that we gain enough information at the daily level, in both the vertical and horizontal dimensions, to ascertain

biologically relevant switches between those behavioural states. All of these are simplifying assumptions and have the potential to affect the outcomes of our research. A more detailed discussion of these topics in the context of limitations and future work can be found below, as well as examples of how these assumptions might differ in other species.

- (3) In Chapter 4 we use tagging data to explore the relationship between movement and mass in marine fish. One of the main aims was to evaluate whether the theoretical work of Ware (1978) was supported by empirical observations. We have shown that it is, but only when species-level effects are considered. However, it is important to acknowledge that the movement rate used in our work, being a daily displacement rate, does differ from that of Ware (1978) and other investigations (e.g. Hirt et al., 2017), where speed is often considered the response variable. The relationship between speed and displacement will likely vary temporally and as a result our findings must be interpreted accordingly. Two additional caveats surround our finding that life stage is a significant explanatory variable (i.e. that the relationship between movement and mass differs between adults and larvae). First, that we have not considered the morphological differences that exist between larvae and adults, which could also explain the variance observed, as larvae do not grow isometrically (Fuiman, 1983; Webb and Weihs, 1986). Second, we currently lack data pertaining to intermediately-sized fish (body mass range: 0.5 – 200 grams), highlighting another gap in our current investigation that requires more research.

- (4) Finally, in Chapter 5 we explore the community level consequences of a changing relationship between movement and mass using a trait-based size spectrum model. In doing so, we manipulate the scaling of search volume by varying the parameter q . This has the knock-on effect of changing the parameters λ and γ , as detailed in equations 5.5 – 5.7. A caveat of this process is that these equations consider a marine community that is in a state of equilibrium, where the total abundance of all species follows a perfect power law relationship (Gustav Delius, *pers coms*). The nature of this equilibrium will therefore change with any change in q and will become invalid when fishing mortality is introduced. Any future work must consider this caveat whilst also acknowledging that the model's other parameters are also expected to be uncertain and merit a more global sensitivity analysis (e.g. Bannister et al., in prep). Additionally, we have made fairly broad conclusions about what effect a change in q can have on fisheries yields relative

to a null model. These conclusions must be interpreted with care as only one type of fishing has been considered. Our results may change when other exploitation patterns, e.g. balanced harvesting (Jacobsen et al., 2013; Law et al., 2012), are introduced.

Alongside the aforementioned caveats, three points stand out and merit further mention. The first revolves around the generality of our approach to other marine animals. Throughout Chapters 2 and 3 we have leaned heavily on our prior knowledge about demersal fish, especially the fact they spent prolonged periods of time residing on or in close proximity to the seafloor (Hobson et al., 2007; Ewan Hunter et al., 2004b; Righton et al., 2001). Due to this prior knowledge we have utilised a range of data sources when explaining the movements of individual fish. For instance, we have used seabed habitat type (EMODnet, 2016) to describe changes to the environment that individuals inhabit and drawn meaningful conclusions about foraging by coupling stomach content data (Pinnegar, 2014) with prey species abundance estimates. Further to this, by knowing that demersal fish behave in this way, we have been able to make explicit assumptions about the movement patterns of fish (e.g. by exploiting the dependence between horizontal and vertical movement) and infer the population-level consequences of movement. For example, in Chapter 3 we have used periods of relative inactivity (low horizontal and vertical movement), observed across multiple individuals, to highlight when and where two commercially important species might be more vulnerable to capture by trawling (Righton et al., 2009). Such prior knowledge has provided a foundation for the scaling-up of individual movement and improved our ability to make recommendations for conservation and management. However, application of this approach to other marine species will require careful thought. For instance, pelagic fish move through an environment that is completely different to their demersal counterparts. Often described as a vast expanse, the pelagic realm is a three-dimensional world, devoid of structural complexity, where there is no hiding from predators and prey pursuit is a highly active process (Pawar et al., 2012). Such differences in habitat will have large effects on the movement patterns of individuals and mean that alternative data sources will have to be utilised and differing assumptions will need to be made. For example, past studies show that large pelagic predators track thermal fronts (e.g. Kitagawa et al., 2007), therefore sea temperature may provide a much more informative descriptor of individual movement. Moreover, work conducted by DeRuiter et al. (2017), noted that foraging behaviour in blue whales (*Balaenoptera musculus*) is characterised by large vertical displacements and small horizontal steps, whereas directed bouts of travel are characterised by moderate vertical displacements and large horizontal steps. This

contradicts our assumptions about the dependence structure between horizontal and vertical movement in demersal fish and would require further model adaptation.

The second stems directly from our work on HMMs. In Chapter 3 we have sought to scale the movement of individuals to the level of the population. To achieve this, we have made a number of simplifying assumptions, for example, that movement is described by only two broad-scale behavioural states and that these states are shared but multiple individuals. We have also summarised observations made in the vertical dimension (every 10 minutes) to the daily level, leading to an overall loss of information. These steps have allowed us to analyse the movements of over 100 fish in a matter of minutes (Griffiths et al., 2018), however our ecological inferences are constrained to broad-scale spatio-temporal trends. On the other hand, we have demonstrated, via a collaborative project (Adam et al., *in review*), that a multi-scale multi-state hierarchical HMM can provide a much more comprehensive understanding of fish movement, pinpointing not only diurnal foraging patterns but also the use of selective tidal stream transport in Atlantic cod (*Gadus morhua*). Despite such fine-scale inference, increases to model complexity come at the cost of high computational demands and limited scope for application to a large sample size. These two projects highlight both the flexibility and adaptability of HMMs in analysing animal movement but come with the caveat that researchers must think carefully when matching a model type with a chosen research question.

The third involves the development of size-spectrum models so they explicitly incorporate movement through space and time and its' effects on the individual-level processes of encounter, growth and mortality. Past size-based models have explicitly considered the spatial domain, for example Castle et al. (2011) introduce simple rules based on optimal foraging theory to allow individuals to either actively move towards areas of high prey density or move away from areas of high predator density. These 'prey-seeking' and 'predator-avoiding' behaviours are relatively simplistic reflections of complex movement patterns however they predict systemic changes to community abundance and community slope. Concentrating on tuna, Maury (2010) breaks his sized-based model into three ecosystems: epipelagic, mesopelagic and migratory communities. Movement in the both the horizontal and vertical dimension are then incorporated via environmentally forced sub-models, dictating the vulnerability of individuals to predation. Additionally, in a recent study, Andersen et al. (2017) allow the dynamics of sized-based fish population to vary in space based on a simple argument; that the area occupied by a size group follows a power law relationship with body size, expanding at a fixed rate as individuals grow. This inclusion gives rise to emergent

patterns of density dependence and is used to explain that why the process of density-dependent regulation is different in small (e.g. lakes) vs. large habitats (e.g. marine systems). The inclusion of movement, shown by these three examples, is not trivial but marks an important advancement in the development of marine ecosystem models (Andersen et al., 2017; Law et al., 2016). Based on our findings in Chapter 4, we see three clear avenues for model extension. First, the inclusion of life-stage specific movement parameters. In Chapter 4, we show that movement scales differently with body mass in larvae compared to adults, therefore its inclusion would provide an interesting first step. Second, we note that species-level effects are significant, and it is highly possible that each unique fish species exhibits its own scaling relationship between movement and body mass. This could be explored using a multi-species version of the size-spectrum, for example the North Sea model (Blanchard et al., 2014; Scott et al., 2014), by allowing q to vary by species. The third, is more of a model development than an extension. Currently the individual-level processes of metabolism and movement are controlled by the independent scaling exponents, p and q , respectively (Andersen and Pedersen, 2010; Hartvig et al., 2011; Scott et al., 2014; Gustav Delius *pers coms*). In Chapter 5, when we increase the value of q , encounter rates respond, allowing the processes of feeding and growth to be maximised at large size classes. However, in reality we would expect this increase in movement to come at the cost of higher metabolic rates (Barneche et al., 2014; Brown et al., 2004; Pawar et al., 2012). Such a dependence would offset some of benefits of higher encounter rates, as a greater proportion of assimilated energy would be allocated to meet metabolic demands. This would undoubtedly alter our estimated ecological indicators, and have unknown consequences on community structure, fisheries yield and size composition. As a result, we recommend that future implementations of the trait-based size spectrum consider this disconnect when making ecological inferences.

6.3 Broader implications and practical recommendations

Throughout this thesis we have sought to analyse the movements of marine fish in a way that not only highlights how tagging data could be used to infer population and community dynamics, but also provides information that can inform conservation policy and management. In Chapter one, we have described the stock structure of cod in the Irish and Celtic Seas. For centuries Atlantic cod have been a popular target for the European fishing industry and its management in EU waters is discussed each year within the EU Fisheries Council. The movement data presented here has the potential to inform EU stock management policy, both in supporting and adding confidence to existing stock boundaries. Tracking data from cod in the North Sea is currently utilised

in this way (Hays et al., 2019; D. Righton et al., 2007). On the other hand, unexpected results, such as the dispersal of cod north into the much deeper waters of the North Channel, can help guide future management decisions and update current stock assessment models. For example, we recommend that next year's stock assessment for cod in the Irish Sea accounts for the possible loss of cod north and any additional mortality that could arise as cod interact with a highly valuable *Nephrops* fishery.

Behaviour in demersal fish can also provide tangible evidence for conservation policy and spatial management. Any switch from migration to prolonged residency can be used to identify essential fish habitats that are necessary for spawning, breeding, feeding and growth (Griffiths et al., 2018). Such habitats, for instance the Herds Deep in the eastern English Channel, might provide ideal candidates for spatial management measures where the aim is not only protecting the species of interest but also the preservation of the habitat it needs to prosper. Further, information gained about the different tendencies of stocks that often share very similar waters can also help shape conservation best practice. For example, in Chapter 3 we show that cod in the German Bight are restrictive in their movement patterns, retaining a localised distribution throughout the year. Such residency behaviour and a lack of adult dispersal means that a conservation network of small MPAs might prove sufficient when it comes to stock recovery actions (similar suggestions have been made in coral reef fish e.g. Lee et al., 2015). In comparison, fish that migrate across stock boundaries (e.g. cod and plaice in the Southern North Sea), will require a much more dynamic management strategy capable of rapid change in both space and time (e.g. Maxwell et al. 2015). Moreover, movement behaviour can be linked to indices of catchability and vulnerability (Righton et al., 2009). For instance, time spent near the seabed will increase the vulnerability of demersal fish to capture by bottom trawl. Such information could inform fisheries management, aid the minimisation of bycatch and can help tailor gear and mesh size restrictions.

In Chapters 4 and 5 we shift focus, stepping away from the distributions and movement patterns of fish, to the assumptions that underpin some of our best attempts to theoretically model the marine world and its response to change. The management implications of this work are less clear than those in Chapters 2 and 3 but what it is clear is that these types of size-based models have the potential to inform the ecosystem approach to fisheries management (Hyder et al., 2015; Thorpe et al., 2015). Several of these size-based models have been used to assess the impact of fishing on community and ecosystem dynamics and have greatly improved our understanding of fisheries interactions (Blanchard et al., 2014; Plagányi, 2007; Thorpe et al., 2015). However, relatively few size-based models are currently used in management and policy decisions.

This restricted uptake is often linked to the assumption that model outputs are highly uncertain, owing to both structural and parameter uncertainty (Bannister et al., in prep.; De Oliveira and Thorpe, 2019; Spence et al., 2018). Here we attempt to validate one such parameter with empirical observations, and then explore how sensitive a size-based model is to changes in that parameter. In doing so, we contribute to the development of these models and provide a step towards their wider utilisation.

6.4 Final remarks

It is clear from this thesis and the work of others (e.g. Block et al., 2011; Castle et al., 2011; Jonsen, 2016) that our knowledge of animal movement and its consequences for population and community dynamics is still evolving. It is also clear that the deployment of tags, despite costing large amounts, provides a wealth of information that is currently an untapped resource (Hays et al., 2016; Hussey et al., 2015; Ogburn et al., 2017). Here we don't necessarily provide a complete solution to the problems faced by ecologists when attempting to use tagging data to inform conservation and management. For example, there is no easy solution to a lack of sample size (Hebblewhite and Haydon, 2010), and issues will always arise when attempts to describe complex movement patterns don't appropriately communicate their associated uncertainties (Ogburn et al., 2017).

We do, however, provide a guide for how movement observations made at the level of the individual can be used to investigate the consequences of movement at the individual-, population- and community-level. Such scaling-up of ecological inference provides a direct pathway via which tagging data can become a tangible information source for conservation and management. Thus, our final remark is a call for collaboration. Here we have been afforded the luxury of a relatively large sample size, however this will not always be the case. For example, in Chapter 4 a greater propensity for data sharing would have increased our certainty surrounding the scaling of movement with body mass in marine fish. By sharing data, movement ecology as a research field can combat declines to scientific funding, step towards inferences at much larger geographical scales (e.g. Harrison et al., 2018; Hindell et al., 2016) and become more influential to the decision-making process (Ogburn et al., 2017).

References

- Aarestrup, K., Nielsen, C., Koed, A., 2002. Net ground speed of downstream migrating radio-tagged Atlantic salmon (*Salmo salar* L.) and brown trout (*Salmo trutta* L.) smolts in relation to environmental factors. *Hydrobiologia* 483, 95–102. <https://doi.org/10.1023/A>
- Aarestrup, K., Okland, F., Hansen, M.M., Righton, D., Gargan, P., Castonguay, M., Bernatchez, L., Howey, P., Sparholt, H., Pedersen, M.I., McKinley, R.S., 2009. Oceanic Spawning Migration of the European Eel (*Anguilla anguilla*). *Science* (80). 325, 1660–1660.
- Acuña, J.L., López-Urrutia, Á., Colin, S., 2011. Faking giants: The evolution of high prey clearance rates in jellyfishes. *Science* (80). 333, 1627–1629. <https://doi.org/10.1126/science.1205134>
- Adam, T., Griffiths, C.A., Leos-Barajas, V., Meese, E., Lowe, C., Righton, D.A., Blackwell, P.G., Langrock, R. Joint modelling of multi-scale animal movement data using hierarchical hidden Markov models. In review.
- Adlerstein, S. A, Welleman, H.C., 2000. Diel variation of stomach contents of North Sea cod (*Gadus morhua*) during a 24-h fishing survey: an analysis using generalized additive models. *Can. J. Fish. Aquat. Sci.* 57, 2363–2367. <https://doi.org/10.1139/f00-249>
- Alexander, K.A., Heymans, J.J., Magill, S., Tomczak, M.T., Holmes, S.J., Wilding, T.A., 2015. Investigating the recent decline in gadoid stocks in the west of Scotland shelf ecosystem using a foodweb model. *ICES J. Mar. Sci.* 72, 436–449.
- Amara, R., Laffargue, P., Dewarumez, J.M., Maryniak, C., Lagardère, F., Luzac, C., 2001. Feeding ecology and growth of O-group flatfish (sole, dab and plaice) on a nursery ground (Southern Bight of the North Sea). *J. Fish Biol.* 58, 788–803. <https://doi.org/10.1111/j.1095-8649.2001.tb00531.x>
- Andersen, K.H., Berge, T., Gonçalves, R.J., Hartvig, M., Heuschele, J., Hylander, S., Jacobsen, N.S., Lindemann, C., Martens, E.A., Neuheimer, A.B., Olsson, K., Palacz, A., Prowe, A.E.F., Sainmont, J., Traving, S.J., Visser, A.W., Wadhwa, N., Kiørboe, T., 2016a. Characteristic Sizes of Life in the Oceans, from Bacteria to Whales. *Ann. Rev. Mar. Sci.* 8, 217–241. <https://doi.org/10.1146/annurev-marine-122414-034144>
- Andersen, K.H., Jacobsen, N.S., Farnsworth, K.D., 2016b. The theoretical foundations for size spectrum models of fish communities. *Can. J. Fish. Aquat. Sci.* 73, 575–588. <https://doi.org/10.1139/cjfas-2015-0230>
- Andersen, K.H., Beyer, J.E., 2006. Asymptotic Size Determines Species Abundance in the Marine Size Spectrum. *Am. Nat.* 168, 54–61. <https://doi.org/10.1086/662677>
- Andersen, K.H., Brander, K., Ravn-Jensen, L., 2015. Trade-offs between objectives for ecosystem management of fisheries. *Ecol. Appl.* 25, 1390–1396. <https://doi.org/10.1890/14-1209.1>
- Andersen, K.H., Farnsworth, K.D., Pedersen, M., Gislason, H., Beyer, J.E., 2009. How community ecology links natural mortality, growth, and production of fish populations. *ICES J. Mar. Sci.* 66, 1978–1984.
- Andersen, K.H., Jacobsen, N.S., Jansen, T., Beyer, J.E., 2017. When in life does density dependence occur in fish populations? *Fish Fish.* 18, 656–667. <https://doi.org/10.1111/faf.12195>

- Andersen, K.H., Pedersen, M., 2010. Damped trophic cascades driven by fishing in model marine ecosystems. *Proc. R. Soc. B Biol. Sci.* 277, 795–802. <https://doi.org/10.1098/rspb.2009.1512>
- Andersen, K.H., Rice, J.C., 2010. Direct and indirect community effects of rebuilding plans. *ICES J. Mar. Sci.* 67, 1980–1988. <https://doi.org/10.1093/icesjms/fsq035>
- Anglea, S.M., Geist, D.R., Brown, R.S., Deters, K.A., McDonald, R.D., 2004. Effects of Acoustic Transmitters on Swimming Performance and Predator Avoidance of Juvenile Chinook Salmon. *North Am. J. Fish. Manag.* 24, 162–170. <https://doi.org/10.1577/M03-065>
- Anon Commission Regulation (EC), 2000. No. 304/2000 of 9 February 2000 establishing measures for the recovery of the stock of cod in the Irish sea (ICES Division VIIA). *Off. J. Eur. Communities* L35, 10–11.
- Anras, M.L.B., Bodaly, R.A., McNicol, R., 1998. Use of an Acoustic Beam Actograph to Assess the Effects of External Tagging Procedure on Lake Whitefish Swimming Activity. *Trans. Am. Fish. Soc.* 127, 329–335.
- Arnold, G.P., Greer Walker, M., Emerson, L.S., Holford, B.H., 1994. Movements of cod (*Gadus morhua* L.) in relation to the tidal streams in the southern North Sea. *ICES J. Mar. Sci.* <https://doi.org/10.1006/jmsc.1994.1021>
- Aschliman, N.C., Nishida, M., Miya, M., Inoue, J.G., Rosana, K.M., Naylor, G.J.P., 2012. Body plan convergence in the evolution of skates and rays (*Chondrichthyes: Batoidea*). *Mol. Phylogenet. Evol.* 63, 28–42. <https://doi.org/10.1016/j.ympev.2011.12.012>
- Bainbridge, B.Y.R., 1957. The speed of swimming of fish as related to size and the frequency and amplitude of the tail beat. *J. Exp. Biol.* 35, 109–133. <https://doi.org/10.1098/rspb.1971.0085>
- Baker, R., Buckland, A., Sheaves, M., 2014. Fish gut content analysis: robust measures of diet composition. *Fish Fish.* 15, 170–177. <https://doi.org/10.1111/faf.12026>
- Bannister, H., Spence, M.A., Blackwell, P.G., Hyder, K., Blanchard, J.L., Webb, T.J. Derivative-based global sensitivity analysis of a multispecies size spectrum fisheries model. In prep.
- Baras, E., Malbrouck, C., Houbart, M., Kestemont, P., Mélard, C., 2000. The effect of PIT tags on growth and physiology of age-0 cultured Eurasian perch *Perca fluviatilis* of variable size. *Aquaculture* 185, 159–173. [https://doi.org/https://doi.org/10.1016/S0044-8486\(99\)00346-4](https://doi.org/https://doi.org/10.1016/S0044-8486(99)00346-4)
- Barneche, D.R., Kulbicki, M., Floeter, S.R., Friedlander, A.M., Maina, J., Allen, A.P., 2014. Scaling metabolism from individuals to reef-fish communities at broad spatial scales. *Ecol. Lett.* 17, 1067–1076. <https://doi.org/10.1111/ele.12309>
- Barneche, D.R., Robertson, D.R., White, C.R., Marshall, D.J., 2018. Fish reproductive-energy output increases disproportionately with body size. *Science* (80). 360, 642–645.
- Barnes, C., Bethea, D., Brodeur, R., Spitz, J., Ridoux, V., Pusineri, C., Chase, B., Hunsicker, M.E., Juanes, F., Kellermann, A., Lancaster, J., Menard, F., Bard, F., Munk, P., Pinnegar, J.K., Scharf, F., Rountree, R., Stergiou, K., Sassa, C., Sabates, A., Jennings, S., 2008. Predator and prey body sizes in marine food webs. *Ecology* 89, 881. <https://doi.org/10.1890/07-1551.1>
- Barnes, C., Maxwell, D., Reuman, D.C., Jennings, S., Barnes, C., Maxwell, D., Reuman, D.C., Jennings, S., 2010. Global patterns in predator — prey size relationships reveal size dependency of trophic transfer efficiency. *Ecology* 91, 222–232.
- Barraquand, F., Murrell, D.J., 2013. Scaling up predator — prey dynamics using spatial moment equations. *Methods Ecol. Evol.* 4, 276–289. <https://doi.org/10.1111/2041-210X.12014>

- Bates, D., Mächler, M., Bolker, B.M., Walker, S.C., 2015. Fitting Linear Mixed-Effects Models Using lme4. *J. Stat. Softw.* 67. <https://doi.org/10.18637/jss.v067.i01>
- Béguier-Pon, M., Castonguay, M., Shan, S., Benchetrit, J., Dodson, J.J., 2015. Direct observations of American eels migrating across the continental shelf to the Sargasso Sea. *Nat. Commun.* 6, 1–9. <https://doi.org/10.1038/ncomms9705>
- Bendall, V., Cuaig, M.O., Schön, P.-J., Hetherington, S., Armstrong, M., Graham, N., Righton, D., 2009. Spatio-temporal dynamics of Atlantic cod (*Gadus morhua*) in the Irish and Celtic Sea: results from a collaborative tagging programme, ICES CM 2009/J:06.
- Benhamou, S., 2004. How to reliably estimate the tortuosity of an animal's path: straightness, sinuosity, or fractal dimension? *J. Theor. Biol.* 229, 209–220.
- Benôit, E., Rochet, M.-J., 2004. A continuous model of biomass size spectra governed by predation and the effects of fishing on them. *J. Theor. Biol.* 226, 9–21. [https://doi.org/10.1016/S0022-5193\(03\)00290-X](https://doi.org/10.1016/S0022-5193(03)00290-X)
- Berejikian, B.A., Brown, R.S., Tatara, C.P., Cooke, S.J., 2007. Effects of Telemetry Transmitter Placement on Egg Retention in Naturally Spawning, Captively Reared Steelhead. *North Am. J. Fish. Manag.* 27, 659–664. <https://doi.org/10.1577/M06-142.1>
- Bestley, S., Jonsen, I.D., Hindell, M.A., Harcourt, R.G., Gales, N.J., 2015. Taking animal tracking to new depths: synthesizing horizontal-vertical movement relationships for four marine predators. *Ecology* 96, 417–427.
- Beverton, R.J., 1992. Patterns of reproductive strategy parameters in some marine teleost fishes. *J. Fish. Res. Board Canada* 41, 137–160.
- Beverton, R.J., Holt, S., 1959. A review of the lifespans and mortality of fish in nature and the relation to growth and other physiological characteristics, in: *Ciba Foundation Colloquium on Ageing (Volume 5)*. pp. 142–177.
- Beverton, R.J., Holt, S., 1957. On the dynamics of exploited fish populations, *Fishery Investigations Series II, Vol. XIX*, Ministry of Agriculture. *Fish. Food* 1, 957.
- Bianchi, G., Gislason, H., Graham, K., Hill, L., Jin, X., Koranteng, K., Manickchand-Heileman, S., Payá, I., Sainsbury, K., Sanchez, F., Zwanenburg, K., 2000. Impact of fishing on size composition and diversity of demersal fish communities. *ICES J. Mar. Sci.* 57, 558–571. <https://doi.org/10.1006/jmsc.2000.0727>
- Bias, G., Coupeau, Y., Seret, B., Calmettes, B., Lopez, R., Hetherington, S., Righton, D., 2017. Return migration patterns of porbeagle shark (*Lamna nasus*) in the Northeast Atlantic: implications for stock range and structure. *ICES J. Mar. Sci.* 74, 1268–1276. <https://doi.org/10.1093/icesjms/fsw233>
- Blake, R.W., Law, T.C., Chan, K.H.S., Li, J.F.Z., 2005. Comparison of the prolonged swimming performances of closely related, morphologically distinct three-spined sticklebacks *Gasterosteus* spp. *J. Fish Biol.* 67, 834–848. <https://doi.org/10.1111/j.0022-1112.2005.00788.x>
- Blanchard, J.L., Andersen, K.H., Scott, F., Hintzen, N.T., Piet, G., Jennings, S., 2014. Evaluating targets and trade-offs among fisheries and conservation objectives using a multispecies size spectrum model. *J. Appl. Ecol.* 51, 612–622.

- Blanchard, J.L., Heneghan, R.F., Everett, J.D., Trebilco, R., Richardson, A.J., 2017. From Bacteria to Whales: Using Functional Size Spectra to Model Marine Ecosystems. *Trends Ecol. Evol.* 32, 174–186. <https://doi.org/10.1016/j.tree.2016.12.003>
- Blanchard, J.L., Jennings, S., Holmes, R., Harle, J., Merino, G., Allen, J.I., Holt, J., Dulvy, N.K., Barange, M., 2012. Potential consequences of climate change for primary production and fish production in large marine ecosystems. *Philos. Trans. R. Soc. B Biol. Sci.* 367, 2979–2989. <https://doi.org/10.1098/rstb.2012.0231>
- Blanchard, J.L., Jennings, S., Law, R., Castle, M.D., McClooghrie, P., Rochet, M.-J., Benoît, E., 2009. How does abundance scale with body size in coupled size-structured food webs? *J. Anim. Ecol.* 78, 270–80. <https://doi.org/10.1111/j.1365-2656.2008.01466.x>
- Block, B.A., Jonsen, I.D., Jorgensen, S.J., Winship, A.J., Shaffer, S.A., Bograd, S.J., Hazen, E.L., Foley, D.G., Breed, G.A., Harrison, A.L., Ganong, J.E., Swithenbank, A., Castleton, M., Dewar, H., Mate, B.R., Shillinger, G.L., Schaefer, K.M., Benson, S.R., Weise, M.J., Henry, R.W., Costa, D.P., Harrison, A., Ganong, J.E., Swithenbank, A., Castleton, M., Dewar, H., Mate, B.R., Shillinger, G.L., Schaefer, K.M., Benson, S.R., Weise, M.J., Henry, R.W., Costa, D.P., 2011. Tracking apex marine predator movements in a dynamic ocean. *Nature* 475, 86–90. <https://doi.org/10.1038/nature10082>
- Block, B.A., Teo, S.L.H., Walli, A., Boustany, A., Stokesbury, M.J.W., Farwell, C.J., Weng, K.C., Dewar, H., Williams, T.D., 2005. Electronic tagging and population structure of Atlantic bluefin tuna. *Nature* 434, 1121–1127. <https://doi.org/10.1029/2002PA000862>
- Bolle, L.J., Hunter, E., Rijnsdorp, A.D., Pastoors, M.A., Metcalfe, J.D., Reynolds, J.D., 2005. Do tagging experiments tell the truth? Using electronic tags to evaluate conventional tagging data. *ICES J. Mar. Sci.* 62, 236–246. <https://doi.org/10.1016/j.icesjms.2004.11.010>
- Bonfil, R., Meyer, M., Scholl, M.C., Johnson, R., O'Brien, S., Oosthuizen, H., Swanson, S., Kotze, D., Paterson, M., 2005. Transoceanic Migration, Spatial Dynamics, and Population Linkages of White Sharks. *Science* (80). 310, 100–103. <https://doi.org/10.1126/science.1114898>
- Boudreau, P.R., Dickie, L.M., 1992. Biomass Spectra of Aquatic Ecosystems in Relation to Fisheries Yield. *Can. J. Fish. Aquat. Sci.* 49, 1528–1538. <https://doi.org/10.1139/f92-169>
- Boyce, M.S., Pitt, J., Northrup, J.M., Morehouse, A.T., Knopff, K.H., Cristescu, B., Stenhouse, G.B., 2010. Temporal autocorrelation functions for movement rates from global positioning system radiotelemetry data. *Philos. Trans. R. Soc. B Biol. Sci.* 365, 2213–2219. <https://doi.org/10.1098/rstb.2010.0080>
- Brander, K.M., 2005. Cod recruitment is strongly affected by climate when stock biomass is low. *ICES J. Mar. Sci.* 62, 339–343. <https://doi.org/10.1016/j.icesjms.2004.07.029>
- Brander, K.M., 1975. The population dynamics and biology of cod (*Gadus morhua* L.) in the Irish Sea.
- Brawn, V., 1961. Reproductive Behaviour of the Cod (*Gadus callarias* L.). *Behaviour* 3, 177–198.
- Breed, G.A., Bowen, W.D., Leonard, M.L., 2013. Behavioural signature of intraspecific competition and density dependence in colony-breeding marine predators. *Ecol. Evol.* 3, 3838–3854. <https://doi.org/10.1002/ece3.754>
- Breed, G.A., Costa, D.P., Jonsen, I.D., Robinson, P.W., Mills-Flemming, J., 2012. State-space methods for more completely capturing behavioural dynamics from animal tracks. *Ecol. Modell.* 235–236, 49–58. <https://doi.org/10.1016/j.ecolmodel.2012.03.021>

- Brett, J.R., 1973. Energy expenditure of sockeye salmon (*Oncorhynchus nerka*) during sustained performance. J. Fish. Res. Board Canada 30, 379–387.
- Brett, J.R., 1965. The relation of size to rate of oxygen consumption and sustained swimming speed of sockeye salmon (*Oncorhynchus nerka*). J. Fish. Res. Board Canada 22, 1491–1501.
- Brett, J.R., 1964. The respiratory metabolism and swimming performance of young sockeye salmon. J. Fish. Res. Board Canada 21, 1183–1226.
- Brett, J.R., 1963. The energy required for swimming by young sockeye salmon with a comparison of the drag force on a dead fish. Proc. Trans. R. Soc. Canada 1, 441–457.
- Bridger, C.J., Booth, R.K., 2003. The Effects of Biotelemetry Transmitter Presence and Attachment Procedures on Fish Physiology and Behaviour. Rev. Fish. Sci. 11, 13–34.
- Brodie, S., Lédée, E.J.I., Heupel, M.R., Babcock, R.C., Campbell, H.A., Gledhill, D.C., Hoenner, X., Huveneers, C., Jaïne, F.R.A., Simpfendorfer, C.A., Taylor, M.D., Udyawer, V., Harcourt, R.G., 2018. Continental-scale animal tracking reveals functional movement classes across marine taxa. Sci. Rep. 8, 1–9. <https://doi.org/10.1038/s41598-018-21988-5>
- Brodie, S., Taylor, M.D., Smith, J.A., Suthers, I.M., Gray, C.A., Payne, N.L., 2016. Improving consumption rate estimates by incorporating wild activity into a bioenergetics model. Ecol. Evol. 6, 2262–2274. <https://doi.org/10.1002/ece3.2027>
- Brown, J.H., Gillooly, J.F., Allen, A.P., Savage, V.M., West, G.B., 2004. Toward a metabolic theory of ecology. Ecology 85, 1771–1789. <https://doi.org/10.1890/03-9000>
- Bürkner, P.-C., 2017. brms: An R Package for Bayesian Multilevel Models Using Stan. J. Stat. Softw. 80. <https://doi.org/10.18637/jss.v080.i01>
- Cagnacci, F., Boitani, L., Powell, R.A., Boyce, M.S., 2010. Animal ecology meets GPS-based radiotelemetry: A perfect storm of opportunities and challenges. Philos. Trans. R. Soc. B Biol. Sci. 365, 2157–2162. <https://doi.org/10.1098/rstb.2010.0107>
- Calenge, C., 2015. Home Range Estimation in R: the adehabitatHR Package, R Vignettes. <https://doi.org/10.1111/j.1365-2656.2006.01186.x>
- Calenge, C., 2006. The package ‘adehabitat’ for the R software: A tool for the analysis of space and habitat use by animals. Ecol. Modell. 197, 516–519. <https://doi.org/10.1016/j.ecolmodel.2006.03.017>
- Campana, S.E., Fowler, M., Dorey, A., Joyce, W., 2013. Population dynamics of Northwest Atlantic porbeagle (*Lamna nasus*), with an assessment of status and projections for recovery. Can. Sci. Advis. Secr. 3848.
- Campana, S.E., Joyce, W., Fowler, M., M, S., 2016. Discards, hooking, and post-release mortality of porbeagle (*Lamna nasus*), shortfin mako (*Isurus oxyrinchus*), and blue shark (*Prionace glauca*) in the Canadian pelagic longline fishery. ICES J. Mar. Sci. 73, 520–528. <https://doi.org/10.1093/icesjms/fst034>
- Campana, S.E., Marks, L., Joyce, W., Kohler, N., 2005. Catch, By-Catch and Indices of Population Status of Blue Shark (*Prionace Glauca*) in the Canadian Atlantic. ICCAT Col.Vol. Sci. Pap. 58, 891–934.
- Canales, T.M., Law, R., Blanchard, J.L., Baum, J., 2016. Shifts in plankton size spectra modulate growth and coexistence of anchovy and sardine in upwelling systems 1. Can. J. Fish. Aquat. Sci. 73, 611–621. <https://doi.org/10.1139/cjfas-2015-0181>

- Carbone, C., Cowlshaw, G., Isaac, N.J.B., Rowcliffe, J.M., 2005. How Far Do Animals Go? Determinants of Day Range in Mammals. *Am. Nat.* 165, 290–297.
- Carter, M.I.D., Bennett, K.A., Embling, C.B., Hosegood, P.J., Russell, D.J.F., 2016. Navigating uncertain waters: a critical review of inferring foraging behaviour from location and dive data in pinnipeds. *Mov. Ecol.* 4–25. <https://doi.org/10.1186/s40462-016-0090-9>
- Castle, M.D., Blanchard, J.L., Jennings, S., 2011. Predicted Effects of Behavioural Movement and Passive Transport on Individual Growth and Community Size Structure in Marine Ecosystems. *Adv. Ecol. Res.* 45, 41–66.
- Catchpole, T.L., Tidd, A.N., Kell, L.T., Revill, A.S., Dunlin, G., 2007. The potential for new *Nephrops* trawl designs to positively effect North Sea stocks of cod, haddock and whiting. *Fish. Res.* 86, 262–267. <https://doi.org/10.1016/j.fishres.2007.06.023>
- Christensen, V., Guénette, S., Heymans, J.J., Walters, C.J., Watson, R., Zeller, D., Pauly, D., 2003. Hundred-year decline of North Atlantic predator fishes. *Fish Fish.* 4, 1–24.
- Ciannelli, L., Fisher, J.A.D., Skern-Mauritzen, M., Hunsicker, M.E., Hidalgo, M., Frank, K.T., Bailey, K.M., 2013. Theory, consequences and evidence of eroding population spatial structure in harvested marine fishes: A review. *Mar. Ecol. Prog. Ser.* 480, 227–243. <https://doi.org/10.3354/meps10067>
- Clark, R.A., Fox, C.J., Viner, D., Livermore, M., 2003. North Sea cod and climate change – modelling the effects of temperature on population dynamics. *Glob. Chang. Biol.* 9, 1669–1680. <https://doi.org/10.1046/j.1529-8817.2003.00685.x>
- Close, D.A., Fitzpatrick, M.S., Lorion, C.M., Li, H.W., Schreck, C.B., 2003. Effects of Intraperitoneally Implanted Radio Transmitters on the Swimming Performance and Physiology of Pacific Lamprey. *North Am. J. Fish. Manag.* 23, 1184–1192. <https://doi.org/10.1577/MO2-057>
- Collins, M., Cooke, D., Smith, T., 2000. Telemetry of shortnose and Atlantic sturgeons in the south-eastern USA, in: *Biotelemetry 15: Proceeding of the 15th International Symposium on Biotelemetry*. Janean, Alaska, USA, pp. 17–23.
- Connolly, P., Officer, R., 2001. The use of tagging data in the formulation of the Irish Sea cod recovery plan. ICES CM 2001/O:05.
- Cook, R.M., Holmes, S.J., Fryer, R.J., 2015. Grey seal predation impairs recovery of an over-exploited fish stock. *J. Appl. Ecol.* 52, 969–979. <https://doi.org/10.1111/1365-2664.12439>
- Cook, R.M., Sinclair, A., Stefánsson, G., 1997. Potential collapse of North Sea cod stocks. *Nature*. <https://doi.org/10.1038/385521a0>
- Cooke, S.J., Hinch, S.G., Donaldson, M.R., Clark, T.D., Eliason, E.J., Crossin, G.T., Raby, G.D., Jeffries, K.M., Lapointe, M., Miller, K., Patterson, D.A., Farrell, A.P., 2012. Conservation physiology in practice: How physiological knowledge has improved our ability to sustainably manage Pacific salmon during up-river migration. *Philos. Trans. R. Soc. B Biol. Sci.* 367, 1757–1769. <https://doi.org/10.1098/rstb.2012.0022>
- Cooke, S.J., Hinch, S.G., Wikelski, M., Andrews, R.D., Kuchel, L.J., Wolcott, T.G., Butler, P.J., 2004. Biotelemetry: A mechanistic approach to ecology. *Trends Ecol. Evol.* 19, 334–343. <https://doi.org/10.1016/j.tree.2004.04.003>
- Cooke, S.J., Nguyen, V.M., Murchie, K.J., Thiem, J.D., Donaldson, M.R., Hinch, S.G., Brown, R.S., Fisk, A., 2013. To Tag or not to Tag: Animal Welfare, Conservation, and Stakeholder

- Considerations in Fish Tracking Studies That Use Electronic Tags AU - Cooke, Steven J. J. Int. Wildl. Law Policy 16, 352–374. <https://doi.org/10.1080/13880292.2013.805075>
- Cooke, S.J., Woodley, C., Eppard, M.B., Brown, R.S., Nielsen, J., 2011. Advancing the surgical implantation of electronic tags in fish: a gap analysis and research agenda based on a review of trends in intracoelomic tagging effects studies. *Rev. Fish Biol. Fish.* 21, 127–151.
- Costa, D.P., Breed, G.A., Robinson, P.W., 2012. New Insights into Pelagic Migrations: Implications for Ecology and Conservation. *Annu. Rev. Ecol. Evol. Syst.* 43, 73–96. <https://doi.org/10.1146/annurev-ecolsys-102710-145045>
- Counihan, T.D., Frost, C.N., 1999. Influence of externally attached transmitters on the swimming performance of juvenile white sturgeon. *Trans. Am. Fish. Soc.* 128, 965–970.
- De Oliveira, J.A.A., Thorpe, R.B., 2019. Comparing conceptual frameworks for a fish community MSY (FCMSY) using management strategy evaluation—an example from the North Sea. *ICES J. Mar. Sci.* fsz015. <https://doi.org/10.1093/icesjms/fsz015>
- Dean, B., Freeman, R., Kirk, H., Leonard, K., Phillips, R.A., Perrins, C.M., Guilford, T., 2012. Behavioural mapping of a pelagic seabird: combining multiple sensors and a hidden Markov model reveals the distribution of at-sea behaviour. *J. R. Society Interface* 10, 20120570. <https://doi.org/10.1098/rsif.2012.0570>
- Dean, M., Hoffman, W., Zemeckis, D., Armstrong, M., 2014. Fine-scale diel and gender-based patterns in behaviour of Atlantic cod (*Gadus morhua*) on a spawning ground in the Western Gulf of Maine. *ICES J. Mar. Sci.* 71, 1474–1489. <https://doi.org/10.1093/icesjms/fsw066>
- Defra, 2015. Marine Strategy Part Three: UK programme of measures.
- Deng, Z.D., Martinez, J.J., Colotelo, A.H., Abel, T.K., LeBarge, A.P., Brown, R.S., Pflugrath, B.D., Mueller, R.P., Carlson, T.J., Seaburg, A.G., Johnson, R.L., Ahmann, M.L., 2012. Development of external and neutrally buoyant acoustic transmitters for juvenile salmon turbine passage evaluation. *Fish. Res.* 113, 94–105. <https://doi.org/https://doi.org/10.1016/j.fishres.2011.08.018>
- DeRuiter, S.L., Langrock, R., Skirbutas, T., Goldbogen, J.A., Calambokidis, J., Friedlaender, A.S., Southall, B.L., 2017. A multivariate mixed hidden Markov model for blue whale behaviour and responses to sound exposure. *Ann. Appl. Stat.* 11, 362–392. <https://doi.org/10.1214/16-AOAS1008>
- Doherty, P.D., Baxter, J.M., Gell, F.R., Godley, B.J., Graham, R.T., Hall, G., Hall, J., Hawkes, L.A., Henderson, S.M., Johnson, L., Speedie, C., Witt, M.J., 2017. Long-term satellite tracking reveals variable seasonal migration strategies of basking sharks in the north-east Atlantic. *Sci. Rep.* 7, 1–10. <https://doi.org/10.1038/srep42837>
- Domenici, P., 2003. Habitat, body design and the swimming performance of fish, in: *Vertebrate Biomechanics and Evolution*. BIOS Scientific Publishers Ltd, Oxford, pp. 137–160.
- Downs, J.A., Horner, M.W., 2008. Effects of Point Pattern Shape on Home-Range Estimates. *J. Wildl. Manage.* 72, 1813–1818. <https://doi.org/10.2193/2007-454>
- Drinkwater, K.F., 2005. The response of Atlantic cod (*Gadus morhua*) to future climate change. *ICES J. Mar. Sci.* 62, 1327–1337. <https://doi.org/10.1016/j.icesjms.2005.05.015>
- Dueri, S., Bopp, L., Maury, O., 2014. Projecting the impacts of climate change on skipjack tuna abundance and spatial distribution. *Glob. Chang. Biol.* 20, 742–53. <https://doi.org/10.1111/gcb.12460>

- Dulvy, N.K., Rogers, S.I., Jennings, S., Stelzenmüller, V., Dye, S.R., Skjoldal, H.R., 2008. Climate change and deepening of the North Sea fish assemblage: A biotic indicator of warming seas. *J. Appl. Ecol.* 45, 1029–1039. <https://doi.org/10.1111/j.1365-2664.2008.01488.x>
- Edwards, A.M., Robinson, J.P.W., Plank, M.J., Baum, J.K., Blanchard, J.L., 2017. Testing and recommending methods for fitting size spectra to data. *Methods Ecol. Evol.* 8, 57–67. <https://doi.org/10.1111/2041-210X.12641>
- Edwards, K.F., Thomas, M.K., Klausmeier, C.A., Litchman, E., 2012. Allometric scaling and taxonomic variation in nutrient utilization traits and maximum growth rate of phytoplankton. *Limnol. Oceanogr.* 57, 554–566. <https://doi.org/10.4319/lo.2012.57.2.0554>
- El-Dessouky, H., Ettouney, H., 2002. *Fundamentals of Salt Water Desalination*, 1st ed.
- EMODnet, 2016. European Marine Observation Data Network (EMODnet) Seabed Habitats project.
- Essington, T.E., Hansson, S., 2004. Predator-dependent functional responses and interaction strengths in a natural food web. *Can. J. Fish. Aquat. Sci.* 61, 2215–2226. <https://doi.org/10.1139/f04-146>
- Food and Aquaculture Organisation of the United Nations (FOA), 2012. *The State of World Fisheries and Aquaculture 2012*. Food and Aquaculture Organisation of the United Nations, Rome. 209 pp.
- Forester, J.D., Ives, A.R., Turner, M.G., Anderson, D.P., Fortin, D., Beyer, H.L., Smith, D.W., Boyce, M.S., 2007. State-space models link elk movement patterns to landscape characteristics in Yellowstone National Park. *Ecol. Monogr.* 77, 285–299. <https://doi.org/10.1890/06-0534>
- Fossette, S., Witt, M.J., Miller, P., Nalovic, M.A., Albareda, D., Almedia, A., Broderick, A.C., Chacón-Chaverri, D., Coyne, M.S., Domingo, A., Eckert, S., Evans, D., Fallabrino, A., Ferraroli, S., Formia, A., Giffoni, B., Hays, G.C., Hughes, G., Kelle, L., Leslie, A., Lopez-Mendilaharsu, M., Luschi, P., Prosdoci, L., Rodriguez-Heredia, S., Turny, A., Verhage, S., Godley, B.J., 2013. Pan-Atlantic analysis of the overlap of a highly migratory species, the leatherback turtle, with pelagic longline fisheries. *Proc. R. Soc. B* 281, 20133065.
- Francis, R.C., 1974. Relationship of Fishing Mortality to Natural Mortality at the Level of Maximum Sustainable Yield Under the Logistic Stock Production Model. *J. Fish. Res. Board Canada* 31, 1539–1542. <https://doi.org/10.1139/f74-189>
- Froese, R., Pauly, D., 2017. FishBase. World Wide Web electronic publication. URL www.fishbase.org, version (10/2017)
- Froese, R., Thorson, J.T., Reyes, R.B., 2014. A Bayesian approach for estimating length-weight relationships in fishes. *J. Appl. Ichthyol.* 30, 78–85. <https://doi.org/10.1111/jai.12299>
- Fuiman, L.A., 1983. Growth gradients in fish larvae. *J. Fish Biol.* 23, 117–123. <https://doi.org/10.1111/j.1095-8649.1983.tb02886.x>
- Fulton, E. A, Link, J.S., Kaplan, I.C., Savina-Rolland, M., Johnson, P., Ainsworth, C., Horne, P., Gorton, R., Gamble, R.J., Smith, A.D.M., Smith, D.C., 2011. Lessons in modelling and management of marine ecosystems: the Atlantis experience. *Fish Fish.* 12, 171–188. <https://doi.org/10.1111/j.1467-2979.2011.00412.x>
- GEBCO, 2017. General Bathymetric Chart of the Oceans. URL http://www.bodc.ac.uk/projects/international/gebco/gebco_digital_atlas (accessed 11.17.16).

- Graham, M., 1935. Modern Theory of Exploiting a Fishery, and Application to North Sea Trawling. *ICES J. Mar. Sci.* 10, 264–274. <https://doi.org/10.1093/icesjms/10.3.264>
- Greenstreet, S.P.R., Morgan, R.I.G., 1989. The effect of ultrasonic tags on the growth rates of Atlantic salmon, *Salmo salar* L., *parr* of varying size just prior to smolting. *J. Fish Biol.* 35, 301–309. <https://doi.org/10.1111/j.1095-8649.1989.tb02979.x>
- Griffiths, C.A., Righton, D.A., Patterson, T.A., Blanchard, J.L., Wright, S.R., Pitchford, J.W., Blackwell, P.G., 2018. Scaling marine fish movement behaviour from individuals to populations. *Ecol. Evol.* 1–14. <https://doi.org/10.1002/ece3.4223>
- Gurarie, E., Andrews, R.D., Laidre, K.L., 2009. A novel method for identifying behavioural changes in animal movement data. *Ecol. Lett.* 12, 395–408. <https://doi.org/10.1111/j.1461-0248.2009.01293.x>
- Gurarie, E., Bracis, C., Delgado, M., Meckley, T.D., Kojola, I., Wagner, C.M., 2016. What is the animal doing? Tools for exploring behavioural structure in animal movements. *J. Anim. Ecol.* 85, 69–84. <https://doi.org/10.1111/1365-2656.12379>
- Guzmán, D.A., Flesia, A.G., Aon, M.A., Pellegrini, S., Marin, R.H., Kembro, J.M., 2017. The fractal organization of ultradian rhythms in avian behaviour. *Sci. Rep.* 1–13. <https://doi.org/10.1038/s41598-017-00743-2>
- Hadfield, J.D., 2010. MCMC methods for multi-response generalized linear mixed models: the MCMCglmm R package. *J. Stat. Softw.* 33, 1–22. <https://doi.org/10.1002/ana.22635>
- Halpern, B.S., Frazier, M., Potapenko, J., Casey, K.S., Koenig, K., Longo, C., Lowndes, J.S., Rockwood, R.C., Selig, E.R., Selkoe, K.A., Walbridge, S., 2015. Spatial and temporal changes in cumulative human impacts on the world's ocean. *Nat. Commun.* 6, 1–7. <https://doi.org/10.1038/ncomms8615>
- Harmon, L.J., Weir, J.T., Brock, C.D., Glor, R.E., Challenger, W., 2008. GEIGER: Investigating evolutionary radiations. *Bioinformatics* 24, 129–131. <https://doi.org/10.1093/bioinformatics/btm538>
- Harrison, A.-L., Costa, D.P., Winship, A.J., Benson, S.R., Bograd, S.J., Antolos, M., Carlisle, A.B., Dewar, H., Dutton, P.H., Jorgensen, S.J., Kohin, S., Mate, B.R., Robinson, P.W., Schaefer, K.M., Shaffer, S.A., Shillinger, G.L., Simmons, S.E., Weng, K.C., Gjerde, K.M., Block, B.A., 2018. The political biogeography of migratory marine predators. *Nat. Ecol. Evol.* <https://doi.org/10.1038/s41559-018-0646-8> <https://doi.org/10.1038/s41559-018-0646-8>
- Hartvig, M., Andersen, K.H., 2013. Coexistence of structured populations with size-based prey selection. *Theor. Popul. Biol.* 89, 24–33. <https://doi.org/10.1016/j.tpb.2013.07.003>
- Hartvig, M., Andersen, K.H., Beyer, J.E., 2011. Food web framework for size-structured populations. *J. Theor. Biol.* 272, 113–122. <https://doi.org/10.1016/j.jtbi.2010.12.006>
- Hays, G., Hobson, V., Metcalfe, J.D., Righton, D., Sims, D.W., 2006. Flexible foraging movements of leatherback turtles across the North Atlantic Ocean. *Ecology* 87, 2647–2656.
- Hays, G.C., Bailey, H., Bograd, S.J., Bowen, W.D., Campagna, C., Carmichael, R.H., Casale, P., Chiaradia, A., Costa, D.P., Cuevas, E., Nico de Bruyn, P.J., Dias, M.P., Duarte, C.M., Dunn, D.C., Dutton, P.H., Esteban, N., Friedlaender, A., Goetz, K.T., Godley, B.J., Halpin, P.N., Hamann, M., Hammerschlag, N., Harcourt, R., Harrison, A.-L., Hazen, E.L., Heupel, M.R., Hoyt, E., Humphries, N.E., Kot, C.Y., Lea, J.S.E., Marsh, H., Maxwell, S.M., McMahon, C.R., Notarbartolo di Sciarra, G., Palacios, D.M., Phillips, R.A., Righton, D., Schofield, G., Seminoff, J.A., Simpfendorfer, C.A.,

- Sims, D.W., Takahashi, A., Tetley, M.J., Thums, M., Trathan, P.N., Villegas-Amtmann, S., Wells, R.S., Whiting, S.D., Wildermann, N.E., Sequeira, A.M.M., 2019. Translating Marine Animal Tracking Data into Conservation Policy and Management. *Trends Ecol. Evol.* 2491, 1–15. <https://doi.org/https://doi.org/10.1016/j.tree.2019.01.009>
- Hays, G.C., Ferreira, L.C., Sequeira, A.M.M., Meekan, M.G., Duarte, C.M., Bailey, H., Bailleul, F., Bowen, W.D., Caley, M.J., Costa, D.P., Eguíluz, V.M., Fossette, S., Friedlaender, A.S., Gales, N., Gleiss, A.C., Gunn, J., Harcourt, R., Hazen, E.L., Heithaus, M.R., Heupel, M., Holland, K., Horning, M., Jonsen, I., Kooyman, G.L., Lowe, C.G., Madsen, P.T., Marsh, H., Phillips, R.A., Righton, D., Ropert-Coudert, Y., Sato, K., Shaffer, S. A., Simpfendorfer, C. A., Sims, D.W., Skomal, G., Takahashi, A., Trathan, P.N., Wikelski, M., Womble, J.N., Thums, M., 2016. Key Questions in Marine Megafauna Movement Ecology. *Trends Ecol. Evol.* 31, 463–475. <https://doi.org/10.1016/j.tree.2016.02.015>
- Hays, G.C., Godley, B.J., Luschi, P., Santidrian, P., 2001. The implications of location accuracy for the interpretation of satellite-tracking data. *Anim. Behav.* 61, 1035–1040.
- Heath, M.R., Kunzlik, P.A., Gallego, A., Holmes, S.J., Wright, P.J., 2008. A model of meta-population dynamics for North Sea and West of Scotland cod-The dynamic consequences of natal fidelity. *Fish. Res.* 93, 92–116. <https://doi.org/10.1016/j.fishres.2008.02.014>
- Heath, M.R., Neat, F.C., Pinnegar, J.K., Reid, D.G., Sims, D.W., Wright, P.J., 2012. Review of climate change impacts on marine fish and shellfish around the UK and Ireland. *Aquat. Conserv. Mar. Freshw. Ecosyst.* 22, 337–367. <https://doi.org/10.1002/aqc.2244>
- Hebblewhite, M., Haydon, D.T., 2010. Distinguishing technology from biology: a critical review of the use of GPS telemetry data in ecology. *Philos. Trans. R. Soc. B Biol. Sci.* 365, 2303–2312. <https://doi.org/10.1098/rstb.2010.0087>
- Hedger, R.D., Rikardsen, A.H., Thorstad, E.B., 2017. Pop-up satellite archival tag effects on the diving behaviour, growth and survival of adult Atlantic salmon *Salmo salar* at sea. *J. Fish Biol.* 90, 294–310. <https://doi.org/10.1111/jfb.13174>
- Hein, A.M., Hou, C., Gillooly, J.F., 2012. Energetic and biomechanical constraints on animal migration distance. *Ecol. Lett.* 15, 104–110. <https://doi.org/10.1111/j.1461-0248.2011.01714.x>
- Heithaus, M.R., Dill, L.M., Marshall, G.J., Buhleier, B., 2002. Habitat use and foraging behaviour of tiger sharks (*Galeocerdo cuvier*) in a seagrass ecosystem. *Mar. Biol.* 140, 237–248. <https://doi.org/10.1007/s00227-001-0711-7>
- Hilborn, R., 2010. Pretty Good Yield and exploited fishes. *Mar. Policy* 34, 193–196. <https://doi.org/10.1016/j.marpol.2009.04.013>
- Hilborn, R., Litzinger, E., 2009. Causes of Decline and Potential for Recovery of Atlantic Cod Populations. *Open Fish Sci. J.* 2, 32–38. <https://doi.org/10.2174/1874401X00902010032>
- Hilborn, R., Ovando, D., 2014. Reflections on the success of traditional fisheries management. *ICES J. Mar. Sci.* 71, 1040–1046. <https://doi.org/10.1093/icesjms/fsu034>
- Hindell, M.A., McMahon, C.R., Bester, M.N., Boehme, L., Costa, D., Fedak, M.A., Guinet, C., Herraiz-Borreguero, L., Harcourt, R.G., Huckstadt, L., Kovacs, K.M., Lydersen, C., McIntyre, T., Muelbert, M., Patterson, T., Roquet, F., Williams, G., Charrassin, J.B., 2016. Circumpolar habitat use in the southern elephant seal: Implications for foraging success and population trajectories. *Ecosphere* 7, 1–27. <https://doi.org/10.1002/ecs2.1213>

- Hirt, M.R., Jetz, W., Rall, B.C., Brose, U., 2017. A general scaling law reveals why the largest animals are not the fastest. *Nat. Ecol. Evol.* 1, 1116–1122. <https://doi.org/10.1038/s41559-017-0241-4>
- Hobson, V.J., Righton, D., Metcalfe, J.D., Hays, G.C., 2009. Link between vertical and horizontal movement patterns of cod in the North Sea. *Aquat. Biol.* 5, 133–142. <https://doi.org/10.3354/ab00144>
- Hobson, V.J., Righton, D., Metcalfe, J.D., Hays, G.C., 2007. Vertical movements of North Sea cod. *Mar. Ecol. Prog. Ser.* 347, 101–110. <https://doi.org/10.3354/meps07047>
- Holland, K.N., Wetherbee, B.M., Lowe, C.G., Meyer, C.G., 1999. Movements of tiger sharks (*Galeocerdo cuvier*) in coastal Hawaiian waters. *Mar. Biol.* 134, 665–673.
- Holling, C.S., 1966. The Functional Response of Invertebrate Predators to Prey Density. *Mem. Entomol. Soc. Canada* 98, 5–86. [https://doi.org/DOI: 10.4039/entm9848fv](https://doi.org/DOI:10.4039/entm9848fv)
- Holmes, R.A., Gibson, R.N., 1983. A comparison of predatory behaviour in flatfish. *Anim. Behav.* 31, 1244–1255. [https://doi.org/https://doi.org/10.1016/S0003-3472\(83\)80031-1](https://doi.org/https://doi.org/10.1016/S0003-3472(83)80031-1)
- Hooten, M.B., Hobbs, N.T., 2015. A guide to Bayesian model selection for ecologists. *Ecol. Monogr.* 85, 3–28. <https://doi.org/10.1890/07-1861.1>
- Houle, J.E., Farnsworth, K.D., Rossberg, A.G., Reid, D.G., 2012. Assessing the sensitivity and specificity of fish community indicators to management action. *Can. J. Fish. Aquat. Sci.* 69, 1065–1079.
- Houle, J.E., Andersen, K.H., Farnsworth, K.D., Reid, D.G., 2013. Emerging asymmetric interactions between forage and predator fisheries impose management trade-offs. *J. Fish Biol.* 83, 890–904. <https://doi.org/10.1111/jfb.12163>
- Houle, J.E., de Castro, F., Cronin, M.A., Farnsworth, K.D., Gosch, M., Reid, D.G., 2016. Effects of seal predation on a modelled marine fish community and consequences for a commercial fishery. *J. Appl. Ecol.* 53, 54–63. <https://doi.org/10.1111/1365-2664.12548>
- Hua, E., Zhang, Z., Warwick, R.M., Deng, K., Lin, K., Wang, R., Yu, Z., 2013. Pattern of benthic biomass size spectra from shallow waters in the East China Seas. *Mar. Biol.* 160, 1723–1736. <https://doi.org/10.1007/s00227-013-2224-6>
- Hunter, E., Berry, F., Buckley, A., Stewart, C., Metcalfe, J.D., 2006. Seasonal migration of thornback rays and implications for closure management. *J. Appl. Ecol.* 43, 710–720. <https://doi.org/10.1111/j.1365-2664.2006.01194.x>
- Hunter, E., Metcalfe, J.D., Arnold, G.P., Reynolds, J.D., 2004a. Impacts of migratory behaviour on population structure in North Sea plaice. *J. Anim. Ecol.* 73, 377–385.
- Hunter, E., Metcalfe, J.D., Holford, B.H., Arnold, G.P., 2004. Geolocation of free-ranging fish on the European continental shelf as determined from environmental variables II. Reconstruction of plaice ground tracks. *Mar. Biol.* 144, 787–798. <https://doi.org/10.1007/s00227-003-1242-1>
- Hunter, E., Metcalfe, J.D., O'Brien, C.M., Arnold, G.P., Reynolds, J.D., 2004b. Vertical activity patterns of free-swimming adult plaice in the southern North Sea. *Mar. Ecol. Prog. Ser.* 279, 261–273. <https://doi.org/10.3354/meps279261>
- Hunter, E., Metcalfe, J.D., Reynolds, J.D., 2003. Migration route and spawning area fidelity by North Sea plaice. *Proc. R. Soc. B Biol. Sci.* 270, 2097–2103. <https://doi.org/10.1098/rspb.2003>

Hussey, N.E., Kessel, S.T., Aarestrup, K., Cooke, S.J., Cowley, P.D., Fisk, A.T., Harcourt, R.G., Holland, K.N., Iverson, S.J., Kocik, J.F., Flemming, J.E.M., Whoriskey, F.G., 2015. Aquatic animal telemetry: A panoramic window into the underwater world. *Science* (80). 348, 1255642. <https://doi.org/10.1126/science.1255642>

Hutchings, J. A, Bishop, T.D., McGregor-Shaw, C.R., 1999. Spawning behaviour of Atlantic cod, *Gadus morhua*: evidence of mate competition and mate choice in a broadcast spawner. *Can. J. Fish. Aquat. Sci.* 56, 97–104. <https://doi.org/10.1139/f98-216>

Hyder, K., Rossberg, A.G., Allen, J.I., Austen, M.C., Barciela, R.M., Bannister, H.J., Blackwell, P.G., Blanchard, J.L., Burrows, M.T., Defriez, E., Dorrington, T., Edwards, K.P., Garcia-Carreras, B., Heath, M.R., Hembury, D.J., Heymans, J.J., Holt, J., Houle, J.E., Jennings, S., Mackinson, S., Malcolm, S.J., McPike, R., Mee, L., Mills, D.K., Montgomery, C., Pearson, D., Pinnegar, J.K., Pollicino, M., Popova, E.E., Rae, L., Rogers, S.I., Speirs, D., Spence, M.A., Thorpe, R., Turner, R.K., van der Molen, J., Yool, A., Paterson, D.M., 2015. Making modelling count - increasing the contribution of shelf-seas community and ecosystem models to policy development and management. *Mar. Policy* 61, 291–302. <https://doi.org/https://doi.org/10.1016/j.marpol.2015.07.015>

ICES, 2018. ICES Advice on fishing opportunities, catch, and effort Greater Northern Sea, Celtic Seas, and Bay of Biscay and Iberian Coast ecoregions hke.27.3a46-8abd - Hake.

ICES, 2017a. ICES WGCSE REPORT 2017 - Report of the Working Group for the Celtic Seas Ecoregion (WGCSE).

ICES, 2017b. Report of the Benchmark Workshop on the Irish Sea Ecosystem (WKIrish3).

ICES, 2017c. ICES Advice on fishing opportunities, catch, and effort Celtic Seas Ecoregion (Division VIa - West of Scotland) - Atlantic cod. <https://doi.org/10.17895/ices.pub.3100>

ICES, 2017d. ICES Advice on fishing opportunities, catch, and effort Celtic Seas, Greater North Sea and Oceanic Northeast Atlantic ecoregions had.27.7. b–k - Haddock.

ICES, 2017e. Report of the Working Group on Celtic Seas Ecoregion (WGCSE), ICES CM 2017/ACOM:13. Copenhagen, Denmark.

ICES, 2016a. ICES Advice on fishing opportunities, catch, and effort Celtic Seas Ecoregion - Herring.

ICES, 2016b. Report of the Benchmark Workshop on sharing information on the Irish Sea ecosystem, stock assessments and fisheries issues, and scoping needs for assessment and management advice (WKIrish1), ICES CM 2015/BSG:01. Dublin, Ireland.

ICES, 2013a. Report of the Benchmark Workshop on Roundfish Stocks.

ICES, 2013b. Report of the Working Group on the Biology and Life History of Crabs (WGCRAB).

ICES, 2013c. ICES Advice Book 5.

Jacobsen, N.S., Burgess, M.G., Andersen, K.H., 2017. Efficiency of fisheries is increasing at the ecosystem level. *Fish Fish.* 18, 199–211. <https://doi.org/10.1111/faf.12171>

Jacobsen, N.S., Gislason, H., Andersen, K.H., 2013. The consequences of balanced harvesting of fish communities. *Proc. R. Soc. B Biol. Sci.* 281. <https://doi.org/10.1098/rspb.2013.2701>

- Jeffers, V.F., Godley, B.J., 2016. Satellite tracking in sea turtles: How do we find our way to the conservation dividends? *Biol. Conserv.* 199, 172–184. <https://doi.org/10.1016/j.biocon.2016.04.032>
- Jennings, S., Pinnegar, J.K., Polunin, N.V.C., Boon, T.W., 2001. Weak cross-species relationships between body size and trophic level belie powerful size-based trophic structuring in fish communities. *J. Anim. Ecol.* 70, 934–944. <https://doi.org/10.1046/j.0021-8790.2001.00552.x>
- Jepsen, N., Aarestrup, K., 1999. A comparison of the growth of radio-tagged and dye-marked pike. *J. Fish Biol.* 55, 880–883. <https://doi.org/10.1111/j.1095-8649.1999.tb00725.x>
- Jepsen, N., Aarestrup, K., Økland, F., Rasmussen, G., 1998. Survival of radiotagged Atlantic salmon (*Salmo salar* L.) and trout (*Salmo trutta* L.) smolts passing a reservoir during seaward migration. *Hydrobiologia* 371, 347. <https://doi.org/10.1023/A:1017047527478>
- Jepsen, N., Holthe, E., Økland, F., 2006. Observations of predation on salmon and trout smolts in a river mouth. *Fish. Manag. Ecol.* 13, 341–343. <https://doi.org/10.1111/j.1365-2400.2006.00509.x>
- Jepsen, N., Mikkelsen, J.S., Koed, A., 2008. Effects of tag and suture type on survival and growth of brown trout with surgically implanted telemetry tags in the wild. *J. Fish Biol.* 72, 594–602. <https://doi.org/10.1111/j.1095-8649.2007.01724.x>
- Jepsen, N., Thorstad, E.B., Havn, T., Lucas, M.C., 2015. The use of external electronic tags on fish: an evaluation of tag retention and tagging effects. *Anim. Biotelemetry* 3, 49. <https://doi.org/10.1186/s40317-015-0086-z>
- Jetz, W., Carbone, C., Fulford, J., Brown, J.H., 2004. The scale of animal space use. *Science* (80). 356, 266–268. <https://doi.org/10.1126/science.1102138>
- Joint Nature Conservation Committee (JNCC)., 2017. Offshores Marine Protected Areas in the Western Channel and Celtic Sea. <http://jncc.defra.gov.uk/page-6903>.
- Jonsen, I.D., 2016. Joint estimation over multiple individuals improves behavioural state inference from animal movement data. *Sci. Rep.* 6, 20625. <https://doi.org/10.1038/srep20625>
- Jonsen, I.D., Basson, M., Bestley, S., Bravington, M.V., Patterson, T.A., Pedersen, M.W., Thomson, R., Thygesen, U.H., Wotherspoon, S.J., 2013. State-space models for bio-loggers: A methodological road map. *Deep Sea Res. Part II* 88–89, 34–46. <https://doi.org/10.1016/j.dsr2.2012.07.008>
- Jonsen, I.D., Myers, R.A., James, M.C., 2007. Identifying leatherback turtle foraging behaviour from satellite telemetry using a switching state-space model. *Mar. Ecol. Prog. Ser.* 337, 255–264.
- Jorgensen, S.J., Gleiss, A.C., Kanive, P.E., Chapple, T.K., Anderson, S.D., Ezcurra, J.M., Brandt, W.T., Block, B.A., 2015. In the belly of the beast: Resolving stomach tag data to link temperature, acceleration and feeding in white sharks (*Carcharodon carcharias*). *Anim. Biotelemetry* 3, 1–10. <https://doi.org/10.1186/s40317-015-0071-6>
- Kahle, D., Wickham, H., 2013. ggmap: Spatial Visualization with ggplot2. *R J.* 5, 144–161.
- Kelly-Gerreyn, B.A., Martin, A.P., Bett, B.J., Anderson, T.R., Kaariainen, J.I., Main, C.E., Marcinko, C.J., Yool, A., 2014. Benthic biomass size spectra in shelf and deep-sea sediments. *Biogeosciences* 11, 6401–6416. <https://doi.org/10.5194/bg-11-6401-2014>
- Kelly, C.J., Codling, E.A., Rogan, E., 2006. The Irish Sea cod recovery plan: some lessons learned. *ICES J. Mar. Sci.* 63, 600–610. <https://doi.org/10.1016/j.icesjms.2005.12.001>

- Kerr, S., Dickie, L., 2001. *The Biomass Spectrum: A Predator-prey Theory of Aquatic Production*. Columbia University Press, New York.
- Kie, J.G., Matthiopoulos, J., Fieberg, J., Powell, R.A., Cagnacci, F., Mitchell, M.S., Gaillard, J.-M., Moorcroft, P.R., 2010. The home-range concept: are traditional estimators still relevant with modern telemetry technology? *Philos. Trans. R. Soc. B Biol. Sci.* 365, 2221–2231.
- Kitagawa, T., Boustany, A.M., Farwell, C.J., Williams, T.D., Castleton, M.R., Block, B.A., 2007. Horizontal and vertical movements of juvenile bluefin tuna (*Thunnus orientalis*) in relation to seasons and oceanographic conditions in the eastern Pacific Ocean. *Fish. Oceanogr.* 16, 409–421. <https://doi.org/10.1111/j.1365-2419.2007.00441.x>
- Kitchell, J.F., Stewart, D.J., 1977. Applications of a Bioenergetics Model to Yellow Perch (*Perca flavescens*) and Walleye (*Stizostedion vitreum vitreum*). *J. Fish. Res. Board Canada* 34, 1922–1935.
- Koed, A., Baktoft, H., Bak, B.D., 2006. Causes of mortality of Atlantic salmon (*Salmo salar*) and brown trout (*Salmo trutta*) smolts in a restored river and its estuary. *River Res. Appl.* 22, 69–78. <https://doi.org/10.1002/rra.894>
- Koed, A., Thorstad, E.B., 2001. Long-term effect of radio-tagging on the swimming performance of pikeperch. *J. Fish Biol.* 58, 1753–1756. <https://doi.org/10.1111/j.1095-8649.2001.tb02329.x>
- Köster, F.W., Möllmann, C., Hinrichsen, H.H., Wieland, K., Tomkiewicz, J., Kraus, G., Voss, R., Makarchouk, A., MacKenzie, B.R., St. John, M.A., Schnack, D., Rohlf, N., Linkowski, T., Beyer, J.E., 2005. Baltic cod recruitment - The impact of climate variability on key processes. *ICES J. Mar. Sci.* 62, 1408–1425. <https://doi.org/10.1016/j.icesjms.2005.05.004>
- Kranstauber, B., Cameron, A., Weinzerl, R., Fountain, T., Tilak, S., Wikelski, M., Kays, R., 2011. The Movebank data model for animal tracking. *Environ. Model. Softw.* 26, 834–835. <https://doi.org/10.1016/j.envsoft.2010.12.005>
- Kritzer, J.P., Sale, P.F., 2004. Metapopulation ecology in the sea: from Levin's' model to marine ecology and fisheries science. *Fish Fish.* 5, 131–140. <https://doi.org/10.1111/J.1467-2979.2004.00131>.
- Kurlansky, M., 1998. *Cod: a biography of the fish that changed the world*. Penguin Books, New York.
- Langerhans, B.R., Reznick, D.N., 2010. Ecology and Evolution of Swimming Performance in Fishes: Predicting Evolution with Biomechanics, in: *Fish Locomotion: An Eco-Ethological Perspective*. CRC Press, Oxford, pp. 200–248.
- Langrock, R., King, R., Matthiopoulos, J., Thomas, L., Fortin, D., Morales, J.M., 2012. Flexible and practical modeling of animal telemetry data: hidden Markov models and extensions. *Ecology* 93, 2336–2342.
- Law, R., Plank, M.J., James, A., Blanchard, J.L., 2009. Size-spectra dynamics from stochastic predation and growth of individuals. *Ecology* 90, 802–811.
- Law, R., Plank, M.J., Kolding, J., 2016. Balanced exploitation and coexistence of interacting, size-structured, fish species. *Fish Fish.* 17, 281–302. <https://doi.org/10.1111/faf.12098>
- Law, R., Plank, M.J., Kolding, J., 2012. On balanced exploitation of marine ecosystems: results from dynamic size spectra. *ICES J. Mar. Sci.* 69, 602–614.

- Lee, K.A., Huvneers, C., Macdonald, T., Harcourt, R.G., 2015. Size isn't everything: movements, home range, and habitat preferences of eastern blue groper (*Achoerodus viridis*) demonstrate the efficacy of a small marine reserve. *Aquat. Conserv. Mar. Freshw. Ecosyst.* 25, 174–186. <https://doi.org/10.1002/aqc.2431>
- Leis, J.M., 2006. Are Larvae of Demersal Fishes Plankton or Nekton? *Adv. Mar. Biol.* 51, 57–141.
- Leis, J.M., Carson-Ewart, B.M., 2003. Orientation of pelagic larvae of coral-reef fishes in the ocean. *Mar. Ecol. Prog. Ser.* 252, 239–253. <https://doi.org/10.3354/meps252239>
- Leis, J.M., Carson-Ewart, B.M., 2002. In situ settlement behaviour of damselfish (*Pomacentridae*) larvae. *J. Fish Biol.* 61, 325–346. <https://doi.org/10.1006/jfbi.2002.2030>
- Leis, J.M., Carson-Ewart, B.M., 2000. Behaviour of pelagic larvae of four coral-reef fish species in the ocean and an atoll lagoon. *Coral Reefs* 19, 247–257. <https://doi.org/10.1007/s003380000115>
- Leis, J.M., Carson-Ewart, B.M., 1998. Complex Behaviour of Coral-Reef Fish Larvae in Open Water and Near Shore Pelagic Environments. *Environ. Biol. Fishes.*
- Leis, J.M., Carson-Ewart, B.M., 1997. In situ swimming speeds of the late pelagic larvae of some Indo-Pacific coral-reef fishes. *Mar. Ecol. Prog. Ser.* 159, 165–174. <https://doi.org/10.3354/meps159165>
- Leis, J.M., Hay, A.C., Howarth, G.J., 2009a. Ontogeny of in situ behaviours relevant to dispersal and population connectivity in larvae of coral-reef fishes. *Mar. Ecol. Prog. Ser.* 379, 163–179. <https://doi.org/10.3354/meps07904>
- Leis, J.M., Hay, A.C., Trnski, T., 2006. In situ ontogeny of behaviour in pelagic larvae of three temperate, marine, demersal fishes. *Mar. Biol.* 148, 655–669. <https://doi.org/10.1007/s00227-005-0108-0>
- Leis, J.M., Piola, R.F., Hay, A.C., Wen, C., Kan, K.P., 2009b. Ontogeny of behaviour relevant to dispersal and connectivity in the larvae of two non-reef demersal, tropical fish species. *Mar. Freshw. Res.* 60, 211–223. <https://doi.org/10.1071/MF08186>
- Leos-Barajas, V., Gangloff, E.J., Adam, T., Langrock, R., van Beest, F.M., Nabe-Nielsen, J., Morales, J.M., 2017a. Multi-scale Modeling of Animal Movement and General Behaviour Data Using Hidden Markov Models with Hierarchical Structures. *J. Agric. Biol. Environ. Stat.* 22, 232–248. <https://doi.org/10.1007/s13253-017-0282-9>
- Leos-Barajas, V., Photopoulou, T., Langrock, R., Patterson, T.A., Watanabe, Y., Murgatroyd, M., Papastamatiou, Y.P., 2017b. Analysis of animal accelerometer data using hidden Markov models. *Methods Ecol. Evol.* 8, 161–173. <https://doi.org/10.1111/2041-210X.12657>
- Li, M., Bolker, B.M., 2017. Incorporating periodic variability in hidden Markov models for animal movement. *Mov. Ecol.* 5, 1–12. <https://doi.org/10.1186/s40462-016-0093-6>
- Lilly, G.R., Wieland, K., Rothschild, B.J., Sundby, S., Drinkwater, K.F., Brander, K., Ottersen, G., Carscadden, J.E., Stensen, G.B., Chouinard, G.A., Swain, D.P., Daan, N., Enberg, K., Hammill, M.O., Rosing-Asvid, A., Svedang, H., Vazques, A., 2008. Decline and Recovery of Atlantic Cod (*Gadus morhua*) Stocks throughout the North Atlantic, in: Kruse, G.H., Drinkwater, K.F., Ianelli, J.N., Link, J.S., Stram, D.L., Wespestad, V., D, W. (Eds.), *Resiliency of Gadoid Stocks to Fishing and Climate Change*. Alaska Sea grant College program, Fairbanks., pp. 39–66. <https://doi.org/10.4027/rgsfcc.2008.03>

- Lindberg, M.S., Walker, J., 2007. Satellite Telemetry in Avian Research and Management: Sample Size Considerations. *J. Wildl. Manage.* 71, 1002–1009. <https://doi.org/10.2193/2005-696>
- Lynch, M., 1991. Methods for the analysis of comparative data in evolutionary biology. *Evolution* (N. Y). 45, 1065–1080.
- Madon, B., Hingrat, Y., 2014. Deciphering behavioural changes in animal movement with a ‘multiple change point algorithm- classification tree’ framework. *Front. Ecol. Evol.* 2014, 2-30.
- Maljković, A., Côté, I.M., 2011. Effects of tourism-related provisioning on the trophic signatures and movement patterns of an apex predator, the Caribbean reef shark. *Biol. Conserv.* 144, 859–865. <https://doi.org/10.1016/j.biocon.2010.11.019>
- Marañón, E., Cermeño, P., López-Sandoval, D.C., Rodríguez-Ramos, T., Sobrino, C., Huete-Ortega, M., Blanco, J.M., Rodríguez, J., 2013. Unimodal size scaling of phytoplankton growth and the size dependence of nutrient uptake and use. *Ecol. Lett.* 16, 371–379. <https://doi.org/10.1111/ele.12052>
- Marine Management Organisation (MMO), 2017. Minimum Conservation Reference Sizes (MCRS) in UK waters. <https://www.gov.uk/government/publications/minimum-conservation-reference-sizes-mcrs>
- Marteinsdottir, G., Ruzzante, D., Nielsen, E.E., 2005. History of the North Atlantic cod stocks, ICES CM, 2005/AA19, pp. 17.
- Maury, O., 2010. An overview of APECOSM, a spatialized mass balanced “Apex Predators ECOSystem Model” to study physiologically structured tuna population dynamics in their ecosystem. *Prog. Oceanogr.* 84, 113–117. <https://doi.org/10.1016/j.pocean.2009.09.013>
- Maury, O., Faugeras, B., Shin, Y.-J., Poggiale, J.-C., Ben Ari, T., Marsac, F., 2007a. Modelling environmental effects on the size-structured energy flow through marine ecosystems. Part 1: The model. *Prog. Oceanogr.* 74, 479–499.
- Maury, O., Shin, Y.-J., Faugeras, B., Ben Ari, T., Marsac, F., 2007b. Modelling environmental effects on the size-structured energy flow through marine ecosystems. Part 2: Simulations. *Prog. Oceanogr.* 74, 500–514. <https://doi.org/10.1016/j.pocean.2007.05.001>
- Maxwell, S.M., Breed, G.A., Nickel, B.A., Makanga-Bahouna, J., Pemo-Makaya, E., Parnell, R.J., Formia, A., Ngouesso, S., Godley, B.J., Costa, D.P., Witt, M.J., Coyne, M.S., 2011. Using satellite tracking to optimize protection of long-lived marine species: Olive ridley sea turtle conservation in central Africa. *PLoS One* 6, e19905. <https://doi.org/10.1371/journal.pone.0019905>
- McCleave, J., Stred, K., 1975. Effect of Dummy Telemetry Transmitters on Stamina of Atlantic Salmon (*Salmo salar*) Smolts. *J. Fish. Res. Board Canada* 32, 559–563.
- McClintock, B.T., King, R., Thomas, L., Matthiopoulos, J., McConnell, B.J., Morales, J.M., 2012. A general discrete-time modelling framework for animal movement using multistate random walks. *Ecol. Monogr.* 82, 335–349. <https://doi.org/10.1890/11-0326.1>
- McClintock, B.T., Russell, D.J.F., Matthiopoulos, J., King, R., 2013. Combining individual animal movement and ancillary biotelemetry data to investigate population-level activity budgets. *Ecology* 94, 838–849. <https://doi.org/10.1890/12-0954.1>
- McGowan, J., Beger, M., Lewison, R.L., Harcourt, R., Campbell, H., Priest, M., Dwyer, R.G., Lin, H.Y., Lentini, P., Dudgeon, C., McMahan, C., Watts, M., Possingham, H.P., 2017. Integrating

- research using animal-borne telemetry with the needs of conservation management. *J. Appl. Ecol.* 54, 423–429. <https://doi.org/10.1111/1365-2664.12755>
- McKellar, A.E., Langrock, R., Walters, J.R., Kesler, D.C., 2015. Using mixed hidden Markov models to examine behavioural states in a cooperatively breeding bird. *Behav. Ecol.* 26, 148–157. <https://doi.org/10.1093/beheco/aru171>
- McKendrick, A.G., 1926. Applications of Mathematics to Medical Problems. *Proc. Edinburgh Math. Soc.* 44, 98–130. <https://doi.org/10.1017/S0013091500034428>
- McMahon, C.R., Harcourt, R., Bateson, P., Hindell, M.A., 2012. Animal welfare and decision making in wildlife research. *Biol. Conserv.* 153, 254–256. <https://doi.org/10.1016/j.biocon.2012.05.004>
- Meager, J.J., Skjaeraasen, J.E., Ferno, A., Karlsen, O., Lokkeborg, S., Michalsen, K., Utskot, S.O., 2009. Vertical dynamics and reproductive behaviour of farmed and wild Atlantic cod *Gadus morhua*. *Mar. Ecol. Prog. Ser.* 389, 233–243. <https://doi.org/10.3354/meps08156>
- Metcalf, J.D., Arnold, G., 1997. Tracking fish with electronic tags. *Nature* 387, 665–666. <https://doi.org/10.1038/42622>
- Metcalf, J.D., Hunter, E., Buckley, A.A., 2006. The migratory behaviour of North Sea plaice: Currents, clocks and clues. *Mar. Freshw. Behav. Physiol.* 39, 25–36.
- Michelot, T., Langrock, R., Bestley, S., Jonsen, I.D., Photopoulou, T., Patterson, T.A., 2017. Estimation and simulation of foraging trips in land-based marine predators. *Ecology* 98, 1932–1944. <https://doi.org/10.1002/ecy.1880>
- Michelot, T., Langrock, R., Patterson, T., 2016. moveHMM: An R package for the statistical modelling of animal movement data using hidden Markov models. *Methods Ecol. Evol.* 7, 1308–1315. <https://doi.org/10.1111/2041-210X.12578>
- Morales, J.M., Haydon, D.T., Frair, J., Holsinger, K.E., Fryxell, J.M., 2004b. Extracting more out of relocation data: building movement models as mixtures of random walks. *Ecology* 85, 2436–2445. <https://doi.org/10.1890/03-0269>
- Morris, W., Follmann, E., George, J., O'Hara, T., 2000. Surgical implantation of radio transmitters in Arctic broad whitefish in Alaska, in: *Biotelemetry 15: Proceeding of the 15th International Symposium on Biotelemetry*. Juneau, Alaska, USA, pp. 193–201.
- Moustakas, A., Silvert, W., Dimitromanolakis, A., 2006. A spatially explicit learning model of migratory fish and fishers for evaluating closed areas. *Ecol. Modell.* 192, 245–258. <https://doi.org/10.1016/j.ecolmodel.2005.07.007>
- Muller, U.K., Videler, J.J., 1996. Inertia as a 'safe harbour': do fish larvae increase length growth to escape viscous drag? *Rev. Fish Biol. Fish.* 6, 353–360.
- Myers, R.A., Worm, B., 2003. Rapid worldwide depletion of predatory fish communities. *Nature* 423, 280–283.
- Nachtigall, W., 2001. Some aspects of Reynolds number effects in animals. *Math. Methods Appl. Sci.* 24, 1401–1408.
- Nash, K.L., Cvitanovic, C., Fulton, E.A., Halpern, B.S., Milner-Gulland, E.J., Watson, R.A., Blanchard, J.L., 2017. Planetary boundaries for a blue planet. *Nat. Ecol. Evol.* 1, 1625–1634. <https://doi.org/10.1038/s41559-017-0319-z>

- Nash, K.L., Welsh, J.Q., Graham, N.A.J., Bellwood, D.R., 2015. Home-range allometry in coral reef fishes: comparison to other vertebrates, methodological issues and management implications. *Oecologia* 177, 73–83. <https://doi.org/10.1007/s00442-014-3152-y>
- Neat, F.C., Bendall, V., Berx, B., Wright, P.J., Cuaig, M., Townhill, B., Schon, P.J., Lee, J., Righton, D., 2014. Movement of Atlantic cod around the British Isles: Implications for finer scale stock management. *J. Appl. Ecol.* 51, 1564–1574. <https://doi.org/10.1111/1365-2664.12343>
- Neat, F.C., Wright, P.J., Zuur, A.F., Gibb, I.M., Gibb, F.M., Tulett, D., Righton, D.A., Turner, R.J., 2006. Residency and depth movements of a coastal group of Atlantic cod (*Gadus morhua* L.). *Mar. Biol.* 148, 643–654. <https://doi.org/10.1007/s00227-005-0110-6>
- Neuenfeldt, S., Köster, F.W., 2000. Trophodynamic control on recruitment success in Baltic cod: The influence of cannibalism. *ICES J. Mar. Sci.* 57, 300–309. <https://doi.org/10.1006/jmsc.2000.0647>
- Neutel, A.M., Heesterbeek, J.A.P., Van De Koppel, J., Hoenderboom, G., Vos, A., Kaldeway, C., Berendse, F., De Ruiter, P.C., 2007. Reconciling complexity with stability in naturally assembling food webs. *Nature* 449, 599–602. <https://doi.org/10.1038/nature06154>
- Nguyen, V.M., Brooks, J.L., Young, N., Lennox, R.J., Haddaway, N., Whoriskey, F.G., Harcourt, R., Cooke, S.J., 2017. To share or not to share in the emerging era of big data: perspectives from fish telemetry researchers on data sharing. *Can. J. Fish. Aquat. Sci.* 74, 1260–1274. <https://doi.org/10.1139/cjfas-2016-0261>
- Nichol, D.G., Chilton, E.A., 2006. Recuperation and behaviour of Pacific cod after barotrauma. *ICES J. Mar. Sci.* 63, 83–94. <https://doi.org/10.1016/j.icesjms.2005.05.021>
- Nielsen, A., Sibert, J.R., 2007. State–space model for light-based tracking of marine animals. *Can. J. Fish. Aquat. Sci.* 64, 1055–1068. <https://doi.org/10.1139/f07-064>
- Ogburn, M.B., Harrison, A.-L., Whoriskey, F.G., Cooke, S.J., Mills Flemming, J.E., Torres, L.G., 2017. Addressing Challenges in the Application of Animal Movement Ecology to Aquatic Conservation and Management. *Front. Mar. Sci.* 4, 70. <https://doi.org/10.3389/fmars.2017.00070>
- Paradis, E., Claude, J., Strimmer, K., 2004. APE: Analyses of phylogenetics and evolution in R language. *Bioinformatics* 20, 289–290. <https://doi.org/10.1093/bioinformatics/btg412>
- Parmesan, C., Yohe, G., 2003. A globally coherent fingerprint of climate change impacts across natural systems. *Nature* 421, 37–42. <https://doi.org/10.1038/nature01286>
- Parton, A., 2018. Bayesian inference for continuous-time step-and-turn movement models. University of Sheffield.
- Patterson, T.A., Basson, M., Bravington, M. V., Gunn, J.S., 2009. Classifying movement behaviour in relation to environmental conditions using hidden Markov models. *J. Anim. Ecol.* 78, 1113–1123. <https://doi.org/10.1111/j.1365-2656.2009.01583.x>
- Patterson, T.A., Parton, A., Langrock, R., Blackwell, P.G., Thomas, L., King, R., 2017. Statistical modelling of individual animal movement: an overview of key methods and a discussion of practical challenges. *ASTA Adv. Stat. Anal.* 101, 399–438. <https://doi.org/10.1007/s10182-017-0302-7>
- Patterson, T.A., Thomas, L., Wilcox, C., Ovaskainen, O., Matthiopoulos, J., 2008. State-space models of individual animal movement. *Trends Ecol. Evol.* 23, 87–94. <https://doi.org/10.1016/j.tree.2007.10.009>

- Pauly, D., Watson, R., Alder, J., 2005. Global trends in world fisheries: Impacts on marine ecosystems and food security. *Philos. Trans. R. Soc. B Biol. Sci.* 360, 5–12. <https://doi.org/10.1098/rstb.2004.1574>
- Pawar, S., Dell, A.I., Savage, V.M., 2012. Dimensionality of consumer search space drives trophic interaction strengths. *Nature* 486, 485–489. <https://doi.org/10.1038/nature11131>
- Pawson, M., 1993. Tagging identifies southern and western cod stocks. *Fish. News*.
- Peake, S., McKinley, R.S., Scruton, D.A., Moccia, R., 1997. Influence of Transmitter Attachment Procedures on Swimming Performance of Wild and Hatchery-Reared Atlantic Salmon Smolts. *Trans. Am. Fish. Soc.* 126, 707–714.
- Pebesma, E., 2018. Map overlay and spatial aggregation in *sp*, R Vignettes.
- Pedersen, M.W., Righton, D., Thygesen, U.H., Andersen, K.H., Madsen, H., 2008. Geolocation of North Sea cod (*Gadus morhua*) using hidden Markov models and behavioural switching. *Can. J. Fish. Aquat. Sci.* 65, 2367–2377. <https://doi.org/10.1139/F08-144>
- Peel, D., Good, N.M., 2011. A hidden Markov model approach for determining vessel activity from vessel monitoring system data. *Can. J. Fish. Aquat. Sci.* 68, 1252–1264. <https://doi.org/10.1139/f2011-055>
- Perry, R.W., Adams, N.S., Rondorf, D.W., 2001. Buoyancy compensation of juvenile chinook salmon implanted with two different size dummy transmitters. *Trans. Am. Fish. Soc.* 130, 46–52.
- Persson, L., Bystrom, P., Wahlstrom, E., 2000. Cannibalism and competition in Eurasian Perch: Population dynamics of an ontogenetic omnivore. *Ecology* 81, 1058–1071.
- Phillips, J.S., Patterson, T.A., Leroy, B., Pilling, G.M., Nicol, S.J., 2015. Objective classification of latent behavioural states in bio-logging data using multivariate-normal hidden Markov models. *Ecol. Appl.* 25, 1244–1258. <https://doi.org/10.1890/14-0862.1.sm>
- Pine, W.E., Pollock, K.H., Hightower, J.E., Kwak, T.J., Rice, J.A., 2003. A review of tagging methods for estimating fish population size and components of mortality. *Fish. Res.* 28, 10–23.
- Pinnegar, J.K., 2014. DAPSTOM - An Integrated Database and Portal for Fish Stomach Records.
- Pittman, S.J., Monaco, M.E., Friedlander, A.M., Legare, B., Nemeth, R.S., Kendall, M.S., Poti, M., Clark, R.D., Wedding, L.M., Caldow, C., 2014. Fish with chips: Tracking reef fish movements to evaluate size and connectivity of Caribbean marine protected areas. *PLoS One* 9, e96028.
- Plagányi, É., 2007. Models for an ecosystem approach to fisheries. FOA Fisheries Technical Paper No. 477. Rome.
- Plank, M.J., Law, R., 2012. Ecological drivers of stability and instability in marine ecosystems. *Theor. Ecol.* 5, 465–480. <https://doi.org/10.1007/s12080-011-0137-x>
- Pohle, J., Langrock, R., van Beest, F.M., Schmidt, N.M., 2017. Selecting the Number of States in Hidden Markov Models: Pragmatic Solutions Illustrated Using Animal Movement. *J. Agric. Biol. Environ. Stat.* 22, 270–293.
- Pope, J.G., Rice, J.C., Daan, N., Jennings, S., Gislason, H., 2006. Modelling an exploited marine fish community with 15 parameters - results from a simple size-based model. *ICES J. Mar. Sci.* 63, 1029–1044. <https://doi.org/10.1016/j.icesjms.2006.04.015>

- Pratt Jr., H.L., Casey, J.G., 1983. Age and Growth of the Shortfin Mako, *Isurus oxyrinchus*, Using Four Methods. *Can. J. Fish. Aquat. Sci.* 40, 1944–1957. <https://doi.org/10.1139/f83-224>
- Priede, I.G., 1984. A basking shark (*Cetorhinus maximus*) tracked by satellite together with simultaneous remote sensing. *Fish. Res.* 2, 201–216. [https://doi.org/10.1016/0165-7836\(84\)90003-1](https://doi.org/10.1016/0165-7836(84)90003-1)
- Prince, J., Hordyk, A., Valencia, S., Loneragan, N., Sainsbury, K., 2015. Revisiting the concept of Beverton–Holt life-history invariants with the aim of informing data-poor fisheries assessment. *ICES J. Mar. Sci.* 72, 194–203.
- R Core Team, 2016. A Language and Environment for Statistical Computing. R Foundation for Statistical Computing, Vienna.
- Rabosky, D.L., Santini, F., Eastman, J., Smith, S.A., Sidlauskas, B., Chang, J., Alfaro, M.E., 2013. Rates of speciation and morphological evolution are correlated across the largest vertebrate radiation. *Nat. Commun.* 4, 1958. <https://doi.org/10.1038/ncomms2958>
- Rall, B.C., Brose, U., Hartvig, M., Kalinkat, G., Schwarzmuller, F., Vucic-Pestic, O., Petchey, O.L., 2012. Universal temperature and body-mass scaling of feeding rates. *Philos. Trans. R. Soc. B Biol. Sci.* 367, 2923–2934. <https://doi.org/10.1098/rstb.2012.0242>
- Rambaut, A., 2009. FigTree version 1.4.3.
- Raymond, B., Lea, M.A., Patterson, T., Andrews-Goff, V., Sharples, R., Charrassin, J.B., Cottin, M., Emmerson, L., Gales, N., Gales, R., Goldsworthy, S.D., Harcourt, R., Kato, A., Kirkwood, R., Lawton, K., Ropert-Coudert, Y., Southwell, C., van den Hoff, J., Wienecke, B., Woehler, E.J., Wotherspoon, S., Hindell, M.A., 2015. Important marine habitat off east Antarctica revealed by two decades of multi-species predator tracking. *Ecography (Cop.)*. 38, 121–129. <https://doi.org/10.1111/ecog.01021>
- Reiss, H., Hoarau, G., Dickey-Collas, M., Wolff, W.J., 2009. Genetic population structure of marine fish: Mismatch between biological and fisheries management units. *Fish Fish.* 10, 361–395. <https://doi.org/10.1111/j.1467-2979.2008.00324.x>
- Revell, L.J., 2012. phytools: An R package for phylogenetic comparative biology (and other things). *Methods Ecol. Evol.* 3, 217–223. <https://doi.org/10.1111/j.2041-210X.2011.00169.x>
- Righton, D., Kjesbu, O.S., Metcalfe, J.D., 2006. A field and experimental evaluation of the effect of data storage tags on the growth of cod. *J. Fish Biol.* 68, 385–400. <https://doi.org/10.1111/j.1095-8649.2005.00899.x>
- Righton, D., Metcalfe, J.D., Connolly, P., 2001. Different behaviour of North and Irish Sea cod. *Nature* 411, 2001.
- Righton, D., Quayle, V.A., Hetherington, S., Burt, G., 2007. Movements and distribution of cod (*Gadus morhua*) in the southern North Sea and English Channel: Results from conventional and electronic tagging experiments. *J. Mar. Biol. Assoc. United Kingdom* 87, 599–613.
- Righton, D.A., Andersen, K.H., Neat, F., Thorsteinsson, V., Steingrund, P., Svedäng, H., Michalsen, K., Hinrichsen, H.-H., Bendall, V., Neuenfeldt, S., Wright, P.J., Jonsson, P., Huse, G., Van Der Kooij, J., Mosegaard, H., Hüseyin, K., Metcalfe, J.D., 2010. Thermal niche of Atlantic cod *Gadus morhua*: Limits, tolerance and optima. *Mar. Ecol. Prog. Ser.* 420, 1–13. <https://doi.org/10.3354/meps08889>

- Righton, D.A., Townhill, B., Van Der Kooij, J., 2009. Catch me if you can: archival tagging studies can help assess changes in the accessibility of Atlantic cod (*Gadus morhua*) to trawl gears. ICES CM 2009/J:08. ICES C. J:08.
- Rinaldo, A., Maritan, A., Cavender-Bares, K.K., Chisholm, S.W., 2002. Cross-scale ecological dynamics and microbial size spectra in marine ecosystems. *Proc. R. Soc. B Biol. Sci.* 269, 2051–2059. <https://doi.org/10.1098/rspb.2002.2102>
- Rip, J.M.K., Mccann, K.S., 2011. Cross-ecosystem differences in stability and the principle of energy flux. *Ecol. Lett.* 14, 733–740. <https://doi.org/10.1111/j.1461-0248.2011.01636.x>
- Robertson, M.J., Scruton, D.A., Brown, J.A., 2003. Effects of surgically implanted transmitters on swimming performance, food consumption and growth of wild Atlantic salmon *parr.* *J. Fish Biol.* 62, 673–678. <https://doi.org/10.1046/j.1095-8649.2003.00055.x>
- Robichaud, D., Rose, G.A., 2004. Migratory behaviour and range in Atlantic cod: Inference from a century of tagging. *Fish Fish.* 5, 185–214. <https://doi.org/10.1111/j.1467-2679.2004.00141.x>
- Robichaud, D., Rose, G.A., 2001. Multiyear homing of Atlantic cod to a spawning ground. *Can. J. Fish. Aquat. Sci.* 58, 2325–2329. <https://doi.org/10.1139/cjfas-58-12-2325>
- Rodriguez, J., Tintore, J., Allen, J.T., Blanco, J.M., Gomis, D., Reul, A., Rulz, J., Rodriguez, V., Echevarria, F., Jimenez-Gomez, F., 2001. Mesoscale vertical motion and the size structure of phytoplakton in the ocean. *Nature* 410, 360–362.
- Rogers, A., Blanchard, J.L., Mumby, P.J., 2014. Vulnerability of coral reef fisheries to a loss of structural complexity. *Curr. Biol.* 24, 1000–1005. <https://doi.org/10.1016/j.cub.2014.03.026>
- Rose, G.A., 2004. Reconciling overfishing and climate change with stock dynamics of Atlantic cod (*Gadus morhua*) over 500 years. *Can. J. Fish. Aquat. Sci.* 61, 1553–1557. <https://doi.org/10.1139/f04-173>
- Rose, G.A., Kulka, D.W., 1999. Hyperaggregation of fish and fisheries: how catch-per-unit-effort increased as the northern cod (*Gadus morhua*) declined. *Can. J. Fish. Aquat. Sci.* 56, 118–127.
- Rudis, B., Ross, N., Garnier, S., 2018. The viridis color palettes.
- Rutterford, L.A., Simpson, S.D., Jennings, S., Johnson, M.P., Blanchard, J.L., Schön, P.J., Sims, D.W., Tinker, J., Genner, M.J., 2015. Future fish distributions constrained by depth in warming seas. *Nat. Clim. Chang.* 5, 569–573. <https://doi.org/10.1038/nclimate2607>
- Rutz, C., Hays, G.C., 2009. New frontiers in biologging science. *Biol. Lett.* 5, 289–292. <https://doi.org/10.1098/rsbl.2009.0089>
- San Martin, E., Harris, R.P., Irigoien, X., 2006. Latitudinal variation in plankton size spectra in the Atlantic Ocean. *Deep. Res. Part II Top. Stud. Oceanogr.* 53, 1560–1572.
- Savage, V.M., Gillooly, J.F., Brown, J.H., West, G.B., Charnov, E.L., 2004. Effects of body size and temperature on population growth. *Am. Nat.* 163, 429–441.
- Savenkoff, C., Castonguay, M., Vézina, A.F., Despatie, S.-P., Chabot, D., Morissette, L., Hammill, M.O., 2004. Inverse modelling of trophic flows through an entire ecosystem: the northern Gulf of St. Lawrence in the mid-1980s. *Can. J. Fish. Aquat. Sci.* 61, 2194–2214. <https://doi.org/10.1139/f04-154>
- Schaefer, M.B., 1957. A study of the dynamics of fishery for yellowfin tuna in the Eastern Tropical Pacific Ocean. *Bull. Inter-American Trop. Tuna Comm.* 2, 247–285.

- Schaefer, M.B., 1954. Some aspects of the dynamics of populations important to the management of the commercial marine fisheries. *Bull. Inter-American Trop. Tuna Comm.* 1, 27–56.
- Scott, F., Blanchard, J.L., Andersen, K.H., 2014. *mizer*: An R package for multispecies, trait-based and community size spectrum ecological modelling. *Methods Ecol. Evol.* 5, 1121–1125. <https://doi.org/10.1111/2041-210X.12256>
- Scott, R., Hodgson, D.J., Witt, M.J., Coyne, M.S., Adnyana, W., Blumenthal, J.M., Broderick, A.C., Canbolat, A.F., Catry, P., Ciccione, S., Delcroix, E., Hitipeuw, C., Luschi, P., Pet-Soede, L., Pendoley, K., Richardson, P.B., Rees, A.F., Godley, B.J., 2012. Global analysis of satellite tracking data shows that adult green turtles are significantly aggregated in Marine Protected Areas. *Glob. Ecol. Biogeogr.* 21, 1053–1061. <https://doi.org/10.1111/j.1466-8238.2011.00757.x>
- Seaman, E.D., Powell, R.A., 1996. An Evaluation of the Accuracy of Kernel Density Estimators for Home Range Analysis. *Ecology* 77, 2075–2085. <https://doi.org/10.2307/2265701>
- Serpetti, N., Baudron, A.R., Burrows, M.T., Payne, B.L., Helaouët, P., Fernandes, P.G., Heymans, J.J., 2017. Impact of ocean warming on sustainable fisheries management informs the Ecosystem Approach to Fisheries. *Sci. Rep.* 7, 1–15. <https://doi.org/10.1038/s41598-017-13220-7>
- Sheldon, R., Parsons, T., 1967. A Continuous Size Spectrum for Particulate Matter in the Sea. *J. Fish. Board Canada* 24, 909–915. <https://doi.org/10.1139/f67-081>
- Sheldon, R.W., Prakash, A., Sutcliffe, W.H., 1972. The Size Distribution of Particles in the Ocean. *Limnol. Oceanogr.* 17, 327–340. <https://doi.org/10.4319/lo.1972.17.3.0327>
- Shepard, E.L.C., Ahmed, M.Z., Southall, E.J., Witt, M.J., Metcalfe, J.D., Sims, D.W., 2006. Diel and tidal rhythms in diving behaviour of pelagic sharks identified by signal processing of archival tagging data. *Mar. Ecol. Prog. Ser.* 328, 205–213. <https://doi.org/10.3354/meps328205>
- Siceloff, L., Howell, W.H., 2013. Fine-scale temporal and spatial distributions of Atlantic cod (*Gadus morhua*) on a western Gulf of Maine spawning ground. *Fish. Res.* 141, 31–43.
- Silverman, B., 1986. Density estimation for statistics and data analysis. Chapman and Hall, London, UK.
- Sims, D.W., Witt, M.J., Richardson, A.J., Southall, E.J., Metcalfe, J.D., 2006. Encounter success of free-ranging marine predator movements across a dynamic prey landscape. *Proc. R. Soc. B* 273, 1195–1201. <https://doi.org/10.1098/rspb.2005.3444>
- Sippel, T., Holdsworth, J., Dennis, T., Montgomery, J., 2011. Investigating Behaviour and Population Dynamics of Striped Marlin (*Kajikia audax*) from the Southwest Pacific Ocean with Satellite Tags 6.
- Sippel, T., Paige Eveson, J., Galuardi, B., Lam, C., Hoyle, S., Maunder, M., Kleiber, P., Carvalho, F., Tsonos, V., Teo, S.L.H., Aires-da-Silva, A., Nicol, S., 2015. Using movement data from electronic tags in fisheries stock assessment: A review of models, technology and experimental design. *Fish. Res.* 163, 152–160. <https://doi.org/10.1016/j.fishres.2014.04.006>
- Sippel, T.J., Davie, P.S., Holdsworth, J.C., Block, B.A., 2007. Striped marlin (*Tetrapturus audax*) movements and habitat utilization during a summer and autumn in the Southwest Pacific Ocean. *Fish. Oceanogr.* 16, 459–472. <https://doi.org/10.1111/j.1365-2419.2007.00446.x>

- Skjæraasen, J.E., Meager, J.J., Karlsen, Ø., Hutchings, J.A., Fernö, A., 2011. Extreme spawning-site fidelity in Atlantic cod. *ICES J. Mar. Sci.* 68, 1472–1477. <https://doi.org/10.1093/icesjms/fsr055>
- Skomal, G.B., Zeeman, S.I., Chisholm, J.H., Summers, E.L., Walsh, H.J., McMahon, K.W., Thorrold, S.R., 2009. Transequatorial Migrations by Basking Sharks in the Western Atlantic Ocean. *Curr. Biol.* 19, 1019–1022. <https://doi.org/10.1016/j.cub.2009.04.019>
- Smith, C., Reay, P., 1991. Cannibalism in teleost fish. *Rev. Fish Biol. Fish.* 1, 41–64. <https://doi.org/10.1007/BF00042661>
- Spence, M.A., Heath, M.R., Blanchard, J.L., Rossberg, A.G., Mackinson, S., Heymans, J.J., Speirs, D.C., Thorpe, R.B., Blackwell, P.G., 2018. A general framework for combining ecosystem models. *Fish Fish.* 19, 1031–1042. <https://doi.org/10.1111/faf.12310>
- Sprules, W.G., Barth, L.E., Giacomini, H., 2016. Surfing the biomass size spectrum: some remarks on history, theory, and application. *Can. J. Fish. Aquat. Sci.* 73, 477–495. <https://doi.org/10.1139/cjfas-2015-0115>
- Strøm, J.F., Thorstad, E.B., Chafe, G., Sørbye, S.H., Righton, D., Rikardsen, A.H., Carr, J., 2016. Ocean migration of pop-up satellite tagged Atlantic salmon from the Miramich River in Canada. *ICES J. Mar. Sci.* <https://doi.org/10.1093/icesjms/fsw220>
- Swain, D.P., Sinclair, A.F., 2000. Pelagic fishes and the cod recruitment dilemma in the Northwest Atlantic. *Can. J. Fish. Aquat. Sci.* 57, 1321–1325. <https://doi.org/10.1139/cjfas-57-7-1321>
- Tamburello, N., Côté, I.M., Dulvy, N.K., 2015. Energy and the Scaling of Animal Space Use. *Am. Nat.* 186, 196–211. <https://doi.org/10.1086/682070>
- Teo, S.L.H., Boustany, A., Blackwell, S., Walli, A., Weng, K.C., Block, B.A., 2004. Validation of geolocation estimates based on light level and sea surface temperature from electronic tags. *Mar. Ecol. Prog. Ser.* 238, 81–98. <https://doi.org/10.3354/meps283081>
- Thompson, B.C., Porak, W., Allen, M.S., 2014. Effects of Surgically Implanting Radio Transmitters in Juvenile Largemouth Bass. *Trans. Am. Fish. Soc.* 143, 346–352.
- Thoreau, X., Baras, E., 1997. Evaluation of surgery procedures for implanting telemetry transmitters into the body cavity of tilapia *Oreochromis aureus*. *Aquat. Living Resour.* 10, 207–211.
- Thorpe, R.B., Quesne, W.J.F. Le, Luxford, F., Collie, J.S., Jennings, S., 2015. Evaluation and management implications of uncertainty in a multispecies size-structured model of population and community responses to fishing. *Methods Ecol. Evol.* 6, 49–58. <https://doi.org/10.1111/2041-210X.12292>
- Thorstad, E.B., Økland, F., Finstad, B., 2000. Effects of telemetry transmitters on swimming performance of adult Atlantic salmon. *J. Fish Biol.* 57, 531–535. <https://doi.org/10.1111/j.1095-8649.2000.tb02192.x>
- Thorstad, E.B., Rikardsen, A.H., Alp, A., Økland, F., 2013. The Use of Electronic Tags in Fish Research – An Overview of Fish Telemetry Methods. *Turkish J. Fish. Aquat. Sci.* 13, 881–896. <https://doi.org/10.4194/1303-2712-v13>
- Thums, M., Meekan, M., Stevens, J., Wilson, S., Polovina, J., 2012. Evidence for behavioural thermoregulation by the world's largest fish. *J. R. Society Interface* 10, 20120477.

- Towner, A. V., Leos-Barajas, V., Langrock, R., Schick, R.S., Smale, M.J., Kaschke, T., Jewell, O.J.D., Papastamatiou, Y.P., Hopkins, W., 2016. Sex-specific and individual preferences for hunting strategies in white sharks. *Funct. Ecol.* 30, 1397–1407. <https://doi.org/10.1111/1365-2435.12613>
- Trzcinski, M.K., Mohn, R., Bowen, W.D., 2006. Continued Decline of an Atlantic Cod Population: How Important Is Gray Seal Predation? *Ecol. Appl.* 16, 2276–2292.
- Ulrich, C., Vermard, Y., Dolder, P.J., Brunel, T., Jardim, E., Holmes, S.J., Kempf, A., Mortensen, L.O., Poos, J.J., Rindorf, A., 2017. Achieving maximum sustainable yield in mixed fisheries: A management approach for the North Sea demersal fisheries. *ICES J. Mar. Sci.* 74, 566–575. <https://doi.org/10.1093/icesjms/fsw126>
- Ursin, E., 1973. On the prey size preferences of cod and dab. *Meddelelser fra Danmarks Fisk. Havundersogelser* 7, 85–98.
- van de Kerk, M., Onorato, D.P., Criffield, M.A., Bolker, B.M., Augustine, B.C., Mckinley, S.A., Oli, M.K., 2015. Hidden semi-Markov models reveal multiphasic movement of the endangered Florida panther. *J. Anim. Ecol.* 84, 576–585. <https://doi.org/10.1111/1365-2656.12290>
- van der Kooij, J., Righton, D., Strand, E., Michalsen, K., Thorsteinsson, V., Svedäng, H., Neat, F.C., Neuenfeldt, S., 2007. Life under pressure: Insights from electronic data-storage tags into cod swimbladder function. *ICES J. Mar. Sci.* 64, 1293–1301. <https://doi.org/10.1093/icesjms/fsm119>
- van Moorter, B., Visscher, D.R., Jerde, C.L., Frair, J.L., Merrill, E.H., 2010. Identifying Movement States From Location Data Using Cluster Analysis. *J. Wildl. Manage.* 74, 588–594.
- Vehtari, A., Gelman, A., Gabry, J., 2016. Practical Bayesian model evaluation using leave-one-out cross-validation and WAIC. *Stat. Comput.* 1–20. <https://doi.org/10.1007/s11222-016-9696-4>
- Vélez-Zuazo, X., Agnarsson, I., 2011. Shark tales: A molecular species-level phylogeny of sharks (*Selachimorpha*, *Chondrichthyes*). *Mol. Phylogenet. Evol.* 58, 207–217.
- Vermard, Y., Rivot, E., Mahévas, S., Marchal, P., Gascuel, D., 2010. Identifying fishing trip behaviour and estimating fishing effort from VMS data using Bayesian Hidden Markov Models. *Ecol. Modell.* 221, 1757–1769. <https://doi.org/10.1016/j.ecolmodel.2010.04.005>
- Videler, J.J., Wardle, C.S., 1991. Fish swimming stride by stride: speed limits and endurance. *Rev. Fish Biol. Fish.* 1, 23–40. <https://doi.org/10.1007/BF00042660>
- Vigliola, L., Meekan, M.G., 2002. Size at hatching and planktonic growth determine post-settlement survivorship of a coral reef fish. *Oecologia* 131, 89–93. <https://doi.org/10.1007/s00442-001-0866-4>
- Voesenek, C.J., Muijres, F.T., Leeuwen, J.L. Van, 2018. Biomechanics of swimming in developing larval fish. *J. Exp. Biol.* 221, jeb149583. <https://doi.org/10.1242/jeb.149583>
- von Foerster, H., 1959. Some remarks on changing populations, in: Frederick, S. (Ed.), *The Kinetics of Cellular Proliferation*. New York, NY: Grune & Stratton, pp. 982–407.
- Wakefield, E.D., Phillips, R.A., Trathan, P.N., Arata, J., Gales, R., Huin, N., Robertson, G., Waugh, S.M., Weimerskirch, H., Wakefield, E.D., Phillips, R.A., Trathan, P.N., Arata, J., Gales, R., Huin, N., Robertson, G., Waugh, S.M., Weimerskirch, H., Matthiopoulos, J., 2011. Habitat preference, accessibility, and competition limit the global distribution of breeding Black-browed Albatrosses. *Ecol. Monogr.* 81, 141–167.

- Wand, M., Jones, M., 1995. Kernel smoothing. Chapman and Hall/CRC.
- Ware, D.M., 1978. Bioenergetics of pelagic fish: theoretical change in swimming speed and ration with body size. *J. Fish. Res. Board Canada* 35, 220–228. <https://doi.org/10.1139/f78-036>
- Ware, D.M., 1972. Predation by Rainbow Trout (*Salmo gairdneri*): The Influence of Hunger, Prey Density, and Prey Size. *J. Fish. Res. Board Canada* 29, 1193–1201. <https://doi.org/10.1139/f72-175>
- Wargo-Rub, A.M., Jepsen, N., Liedtke, T.L., Moser, M.L., Weber III, S., 2014. Surgical insertion of transmitters and telemetry methods in fisheries research. *Am. J. Vet. Res.* 75, 402–416. <https://doi.org/10.2460/ajvr.75.4.402>
- Watanabe, Y.Y., Goldman, K.J., Caselle, J.E., Chapman, D.D., Papastamatiou, Y.P., 2015. Comparative analyses of animal-tracking data reveal ecological significance of endothermy in fishes. *Proc. Natl. Acad. Sci. U. S. A.* 112, 6104–6109. <https://doi.org/10.1073/pnas.1500316112>
- Webb, P., Weihs, D., 1986. Functional locomotor morphology of early life history stages of fishes. *Trans. Am. Fish. Soc.* 115, 115–127.
- Weimer, E.J., Duehr, J.P., Brown, M.L., 2006. Comparison of Two External Transmitter Types on Two Sizes of Bluegills and Yellow Perch. *North Am. J. Fish. Manag.* 26, 670–675. <https://doi.org/10.1577/M05-149.1>
- Werner, E.E., Gilliam, J.F., 1984. The ontogenetic niche and species interactions in size-structured populations. *Annu. Rev. Ecol. Syst.* 15, 393–425.
- West, G. B., Brown, J. H. & Enquist, B.J., 1997. General Model for the Origin of Allometric Scaling Laws in Biology. *Science* (80). 276, 122–126. <https://doi.org/10.1126/science.276.5309.122>
- Wickham, H., 2009. ggplot2: Elegant Graphics for Data Analysis.
- Winberg, G., 1956. Rate of metabolism and food requirements of fishes. *J. Fish. Res. Board Canada* 194, 1–253.
- Winter, J., 1996. Advances in underwater biotelemetry, in: Murphy, B., Willis, D. (Eds.), *Fisheries Techniques*. American Fisheries Society, Bethesda, Maryland., pp. 555–590.
- Womble, J.N., Gende, S.M., 2013. Post-Breeding Season Migrations of a Top Predator, the Harbor Seal (*Phoca vitulina richardii*), from a Marine Protected Area in Alaska. *PLoS One* 8, e55386.
- Woodworth-Jefcoats, P.A., Polovina, J.J., Dunne, J.P., Blanchard, J.L., 2013. Ecosystem size structure response to 21st century climate projection: Large fish abundance decreases in the central North Pacific and increases in the California Current. *Glob. Chang. Biol.* 19, 724–733.
- Worm, B., 2016. Averting a global fisheries disaster. *Proc. Natl. Acad. Sci.* 113, 4895–4897. <https://doi.org/10.1073/pnas.1604008113>
- Worm, B., Hilborn, R., Baum, J.K., Branch, T. a, Collie, J.S., Costello, C., Fogarty, M.J., Fulton, E. a, Hutchings, J. a, Jennings, S., Jensen, O.P., Lotze, H.K., Mace, P.M., McClanahan, T.R., Minto, C., Palumbi, S.R., Parma, A.M., Ricard, D., Rosenberg, A. a, Watson, R., Zeller, D., 2009. Rebuilding global fisheries. *Science* (80). 325, 578–85. <https://doi.org/10.1126/science.1173146>
- Worton, B.J., 1989. Kernel Methods for Estimating the Utilization Distribution in Home-Range Studies. *Ecology* 70, 164–168.

- Worton, B.J., 1987. A review of models of home range for animal movement. *Ecol. Modell.* 38, 277–298. [https://doi.org/10.1016/0304-3800\(87\)90101-3](https://doi.org/10.1016/0304-3800(87)90101-3)
- Zemeckis, D.R., Hoffman, W.S., Dean, M.J., Armstrong, M.P., Cadrin, S.X., 2014. Spawning site fidelity by Atlantic cod (*Gadus morhua*) in the Gulf of Maine: implications for population structure and rebuilding. *ICES J. Mar. Sci.* 71, 1356–1365.
- Zhang, C., Chen, Y., Ren, Y., 2016. An evaluation of implementing long-term MSY in ecosystem-based fisheries management: Incorporating trophic interaction, bycatch and uncertainty. *Fish. Res.* 174, 179–189. <https://doi.org/10.1016/j.fishres.2015.10.007>
- Zhou, S., Yin, S., Thorson, J.T., Smith, A.D.M., Fuller, M., Walters, C.J., 2012. Linking fishing mortality reference points to life history traits: an empirical study. *Can. J. Fish. Aquat. Sci.* 69, 1292–1301. <https://doi.org/10.1139/f2012-060>
- Zucchini, W., MacDonald, I.L., Langrock, R., 2016. Hidden Markov models for time series: an introduction using R (second edition). Chapman and Hall/CRC.

Appendices

Appendix documents for Chapters 2-5.

Appendix 2

Appendix 2.1.

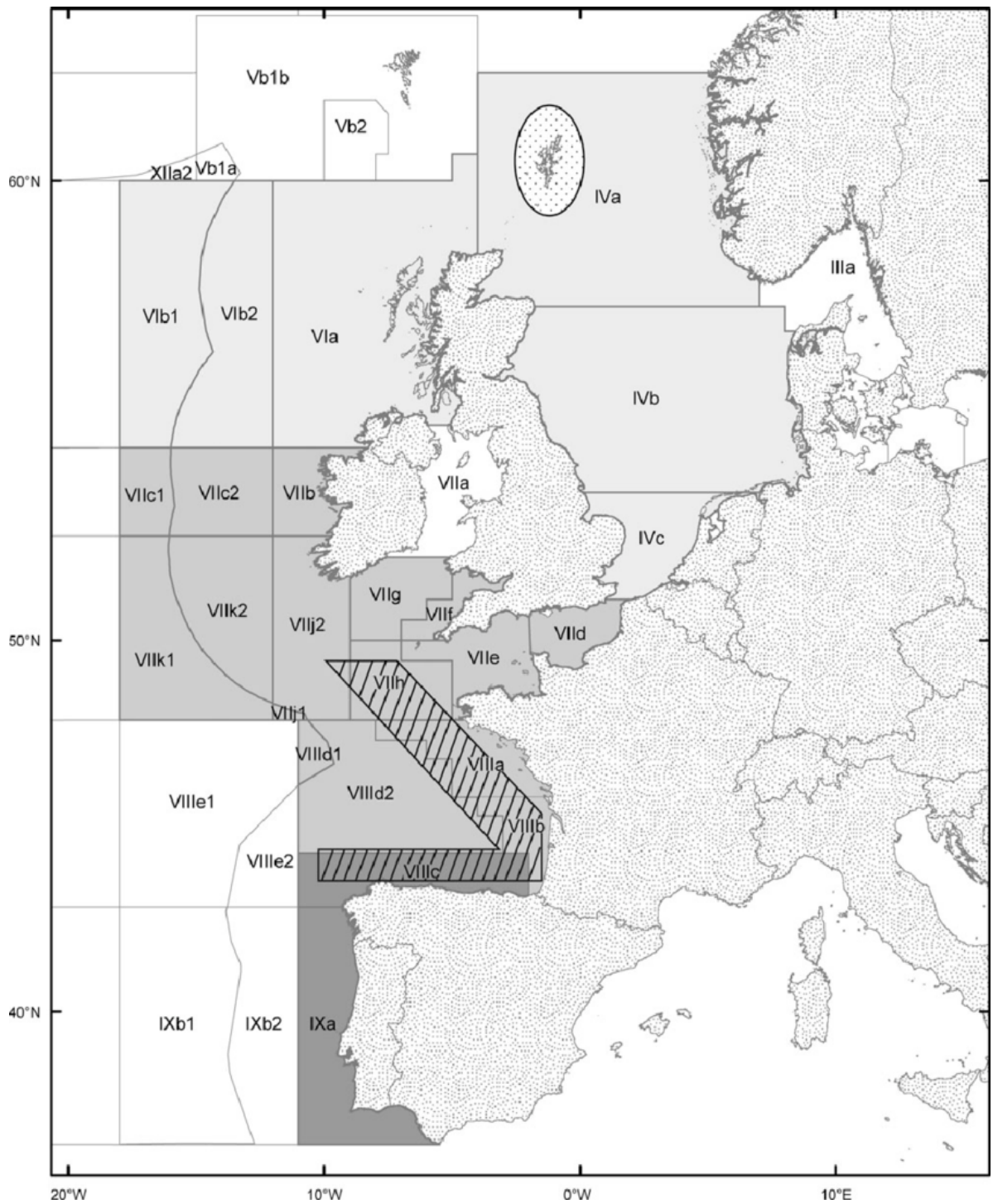


Figure. Spatial occurrence of ICES Divisions in the waters surrounding the British Isles. ICES Divisions of interest are VIIa, VIIg, VIIh and VIIi. Map taken from www.ices.dk.

Appendix 2.2.

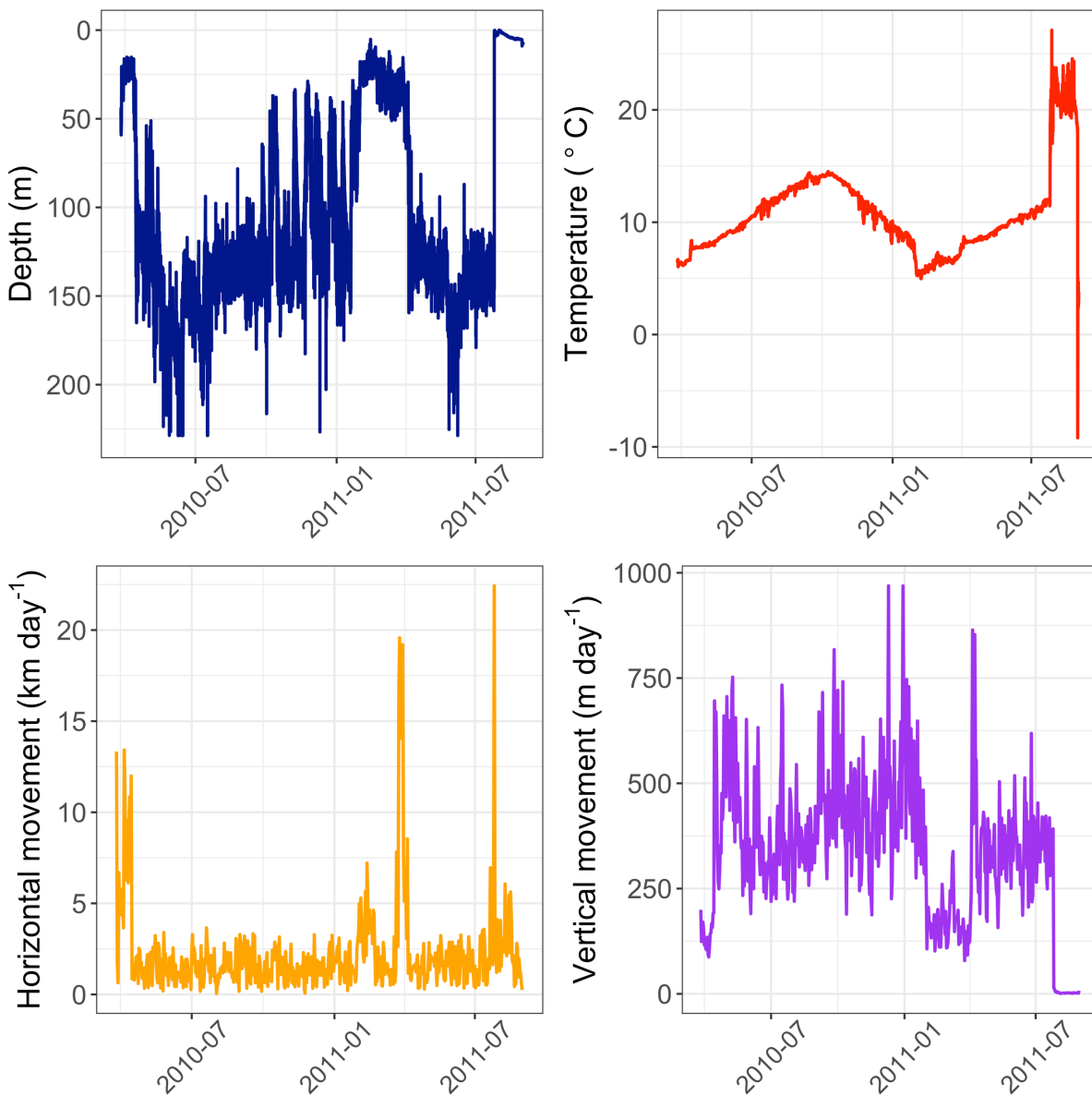


Figure. Observed depth (m), temperature (°C) and movement rates (horizontal (km day⁻¹) and vertical (m day⁻¹) movement) of cod IRE_5596 through time. The cod in question was released in the Irish Sea on the 26th March 2010 and was recaptured on the 15th June 2011, spending 447 days at liberty.

Appendix 2.3.

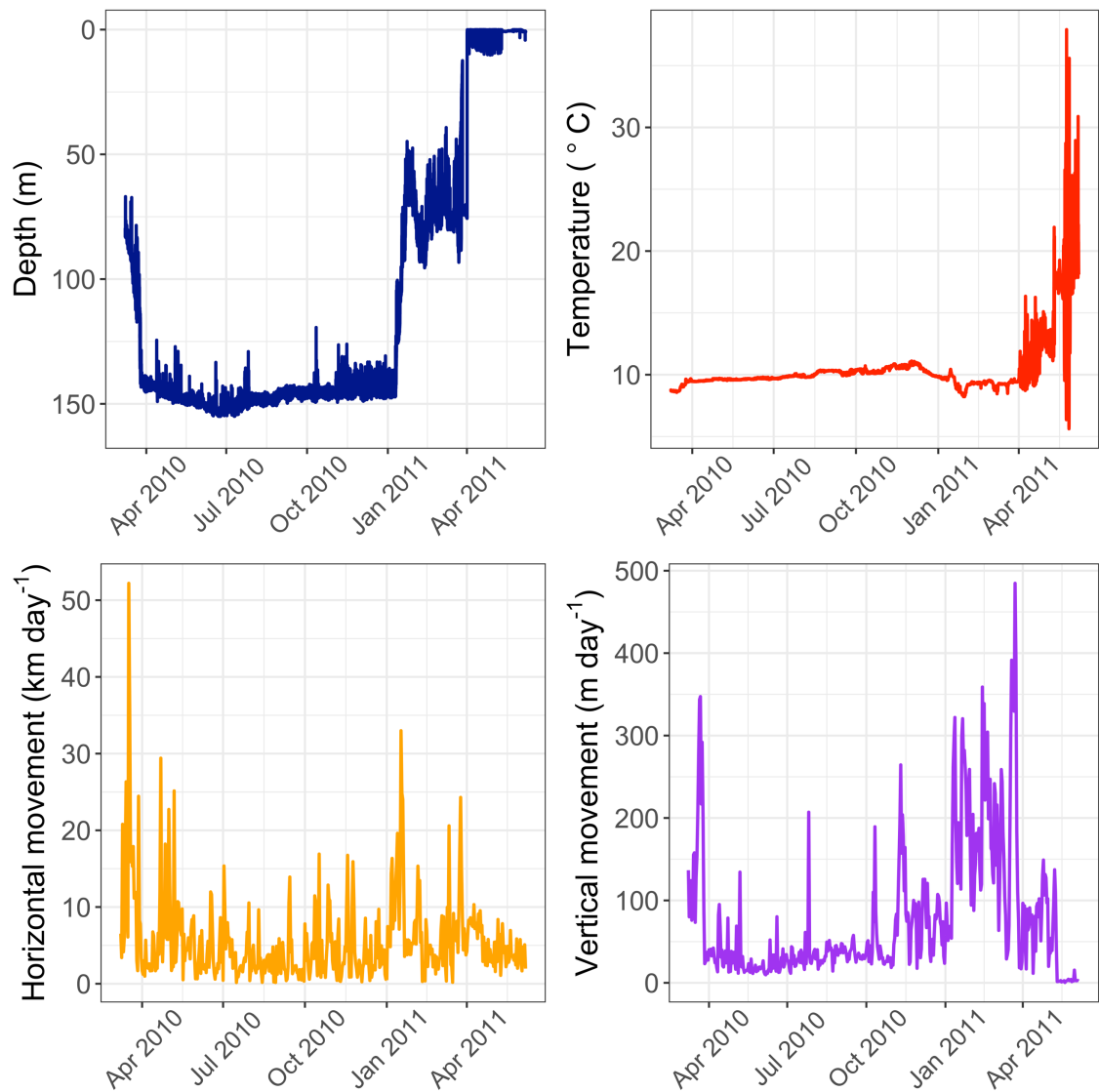


Figure. Observed depth (m), temperature (°C) and movement rates (horizontal (km day⁻¹) and vertical (m day⁻¹) movement) of cod CEL_5613 through time. The cod was released in the Celtic Sea on the 8th March 2010 and was recaptured on the 9th January 2011, spending 308 days at liberty.

Appendix 2.4.

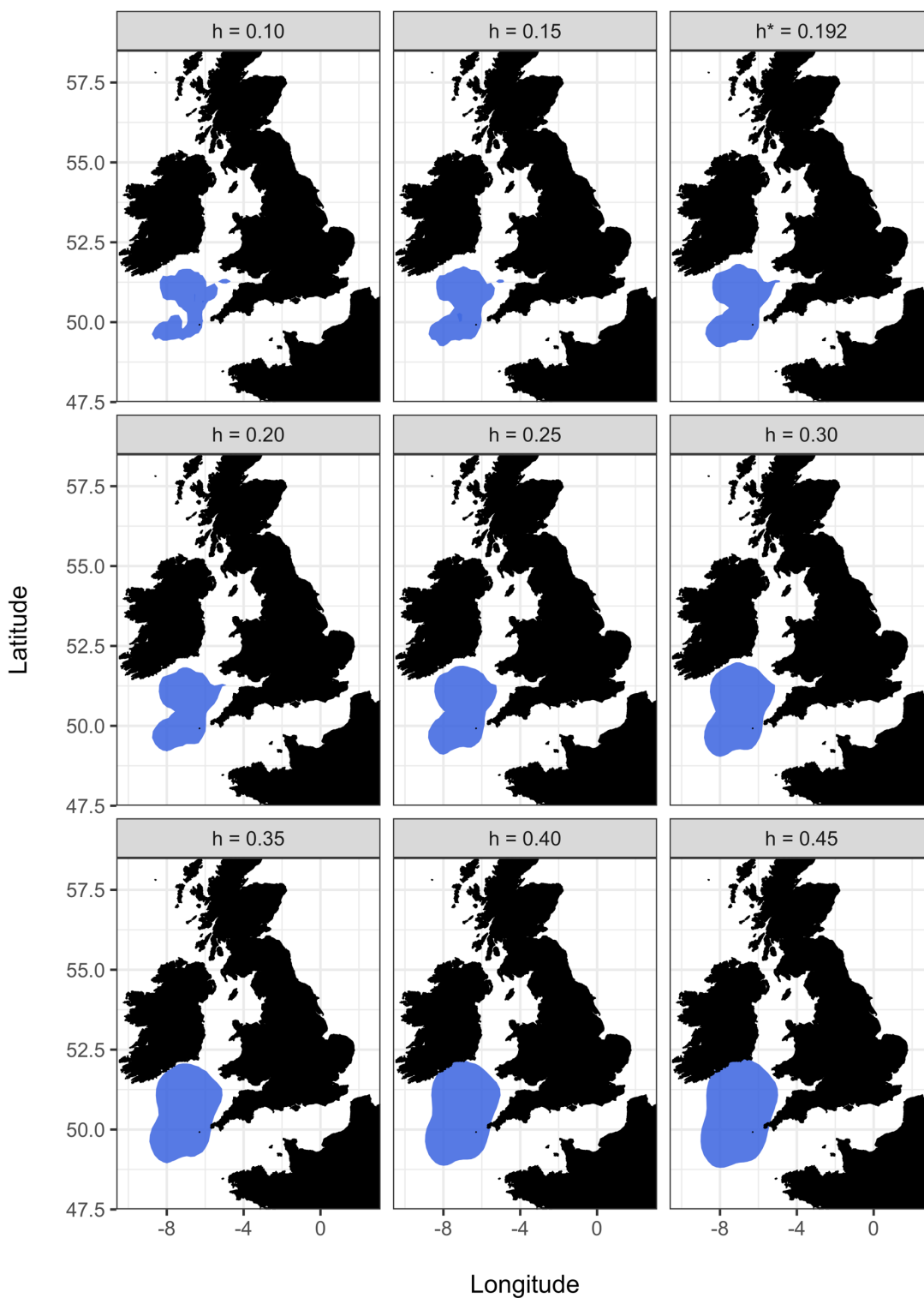


Figure. Composite utilisation distributions calculated under a range of h values for Atlantic cod in the Celtic Sea. h^* indicates the h value calculated using the 'reference bandwidth' approach.

Appendix 2.5.

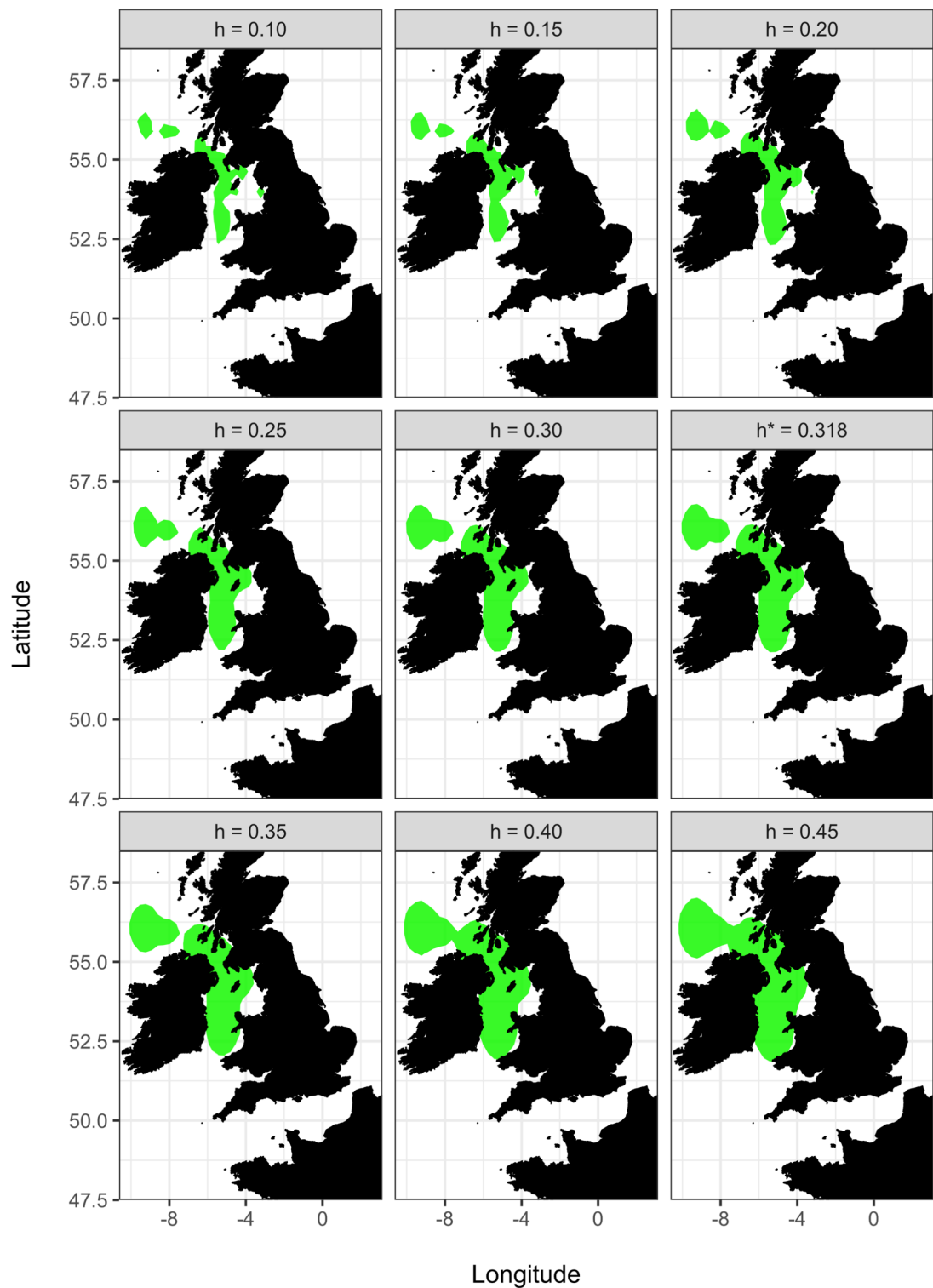


Figure. Composite utilisation distributions calculated under a range of h values for Atlantic cod in the Irish Sea. h^* indicates the h value calculated using the 'reference bandwidth' approach.

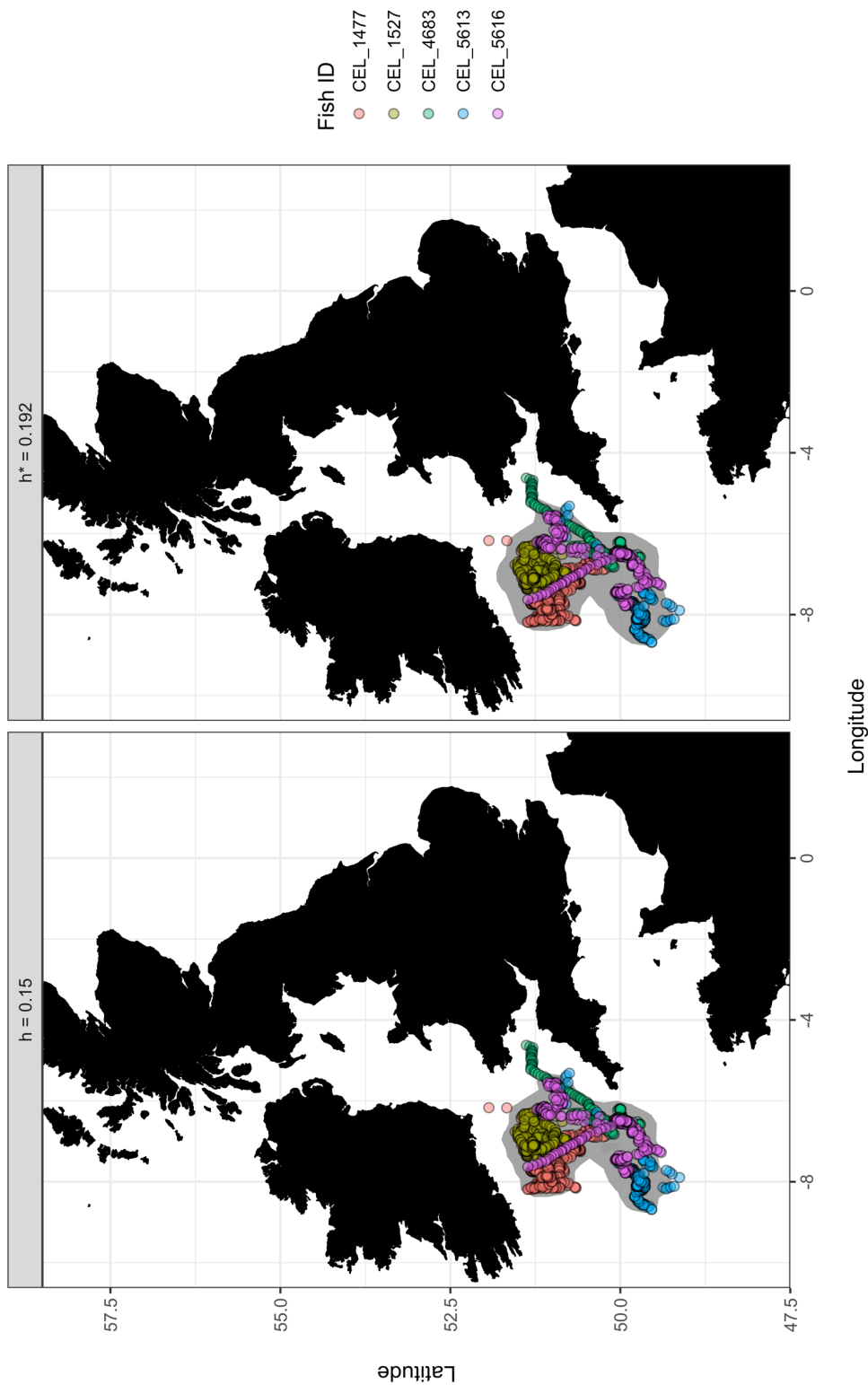


Figure. Composite utilisations distributions (UD) calculated for Atlantic cod in the Celtic Sea under the chosen h value ($h = 0.15$; left) and under the 'reference bandwidth' approach ($h^* = 0.192$; right)

Appendix 2.7.

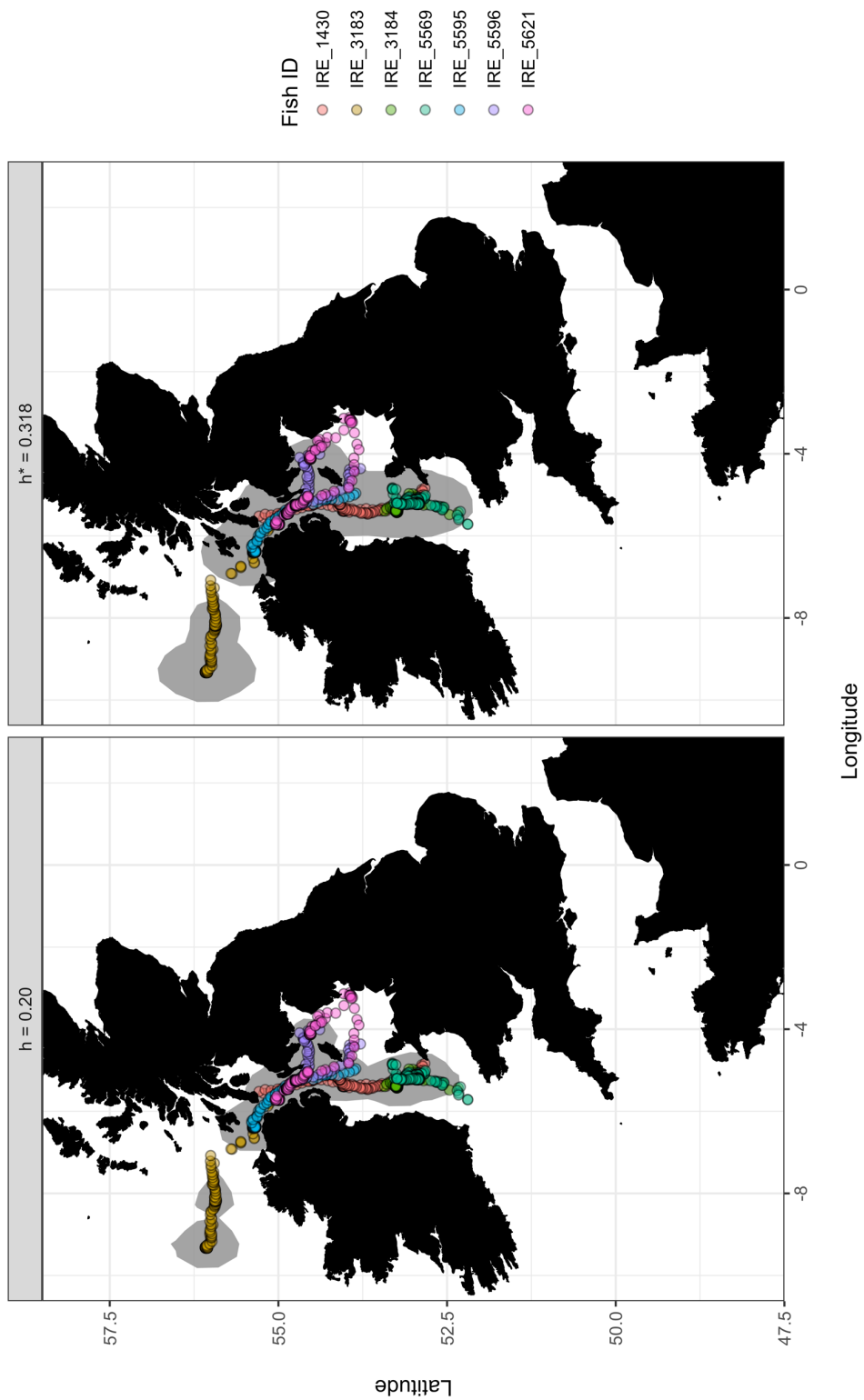


Figure. Composite utilizations distributions (UD) calculated for Atlantic cod in the Irish Sea under the chosen h value ($h = 0.20$; left) and under the 'reference bandwidth' approach ($h^* = 0.318$; right)

Appendix 2.8.

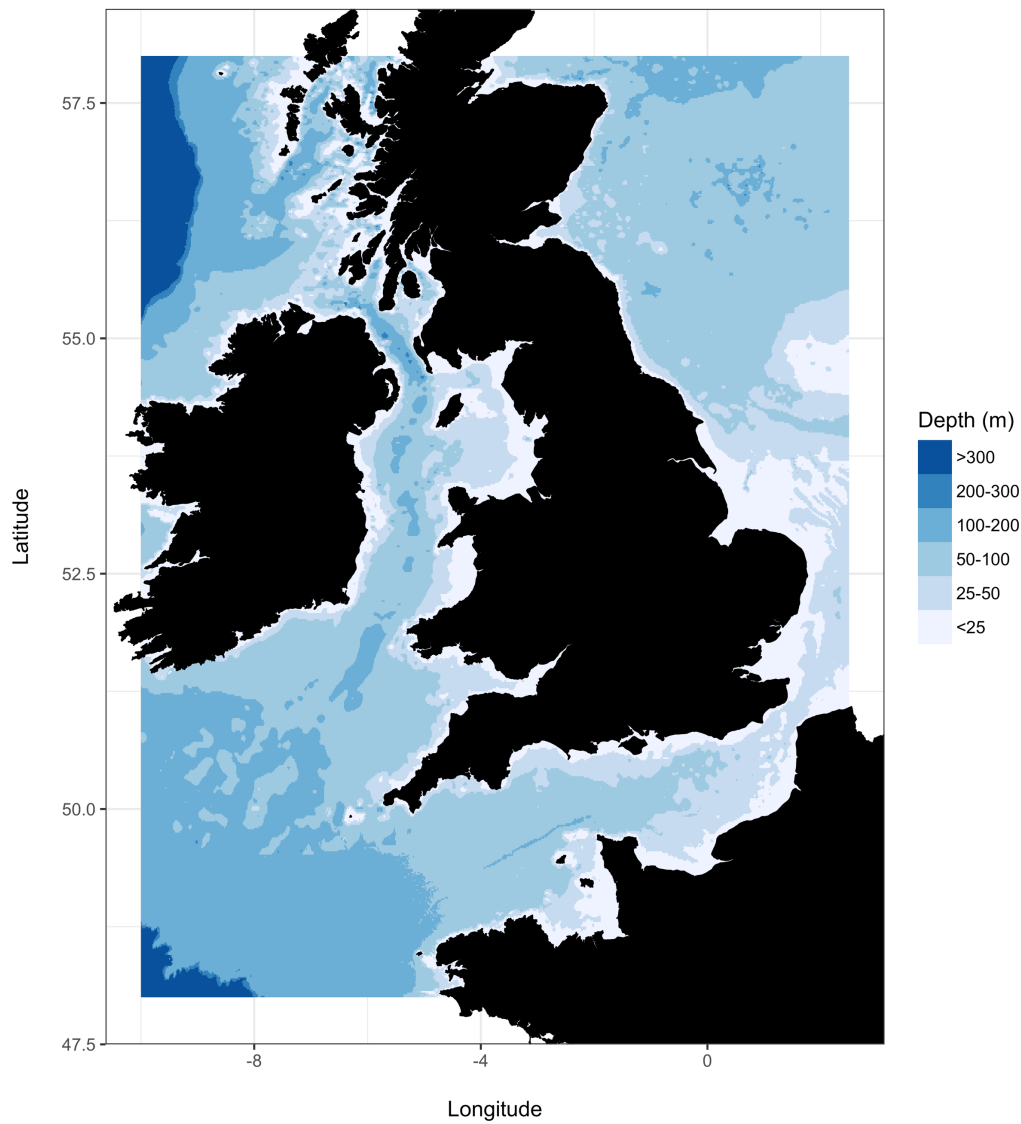


Figure. Bathymetric data in the waters surrounding the British Isles. Depth (m) has been discretised into six groups to add visual interpretation. Bathymetric data was sourced from the General Bathymetric Chart of the Oceans online repository (GEBCO, 2017), which is a global topographic dataset with a one-minute (1') spatial resolution.

Appendix 2.9.

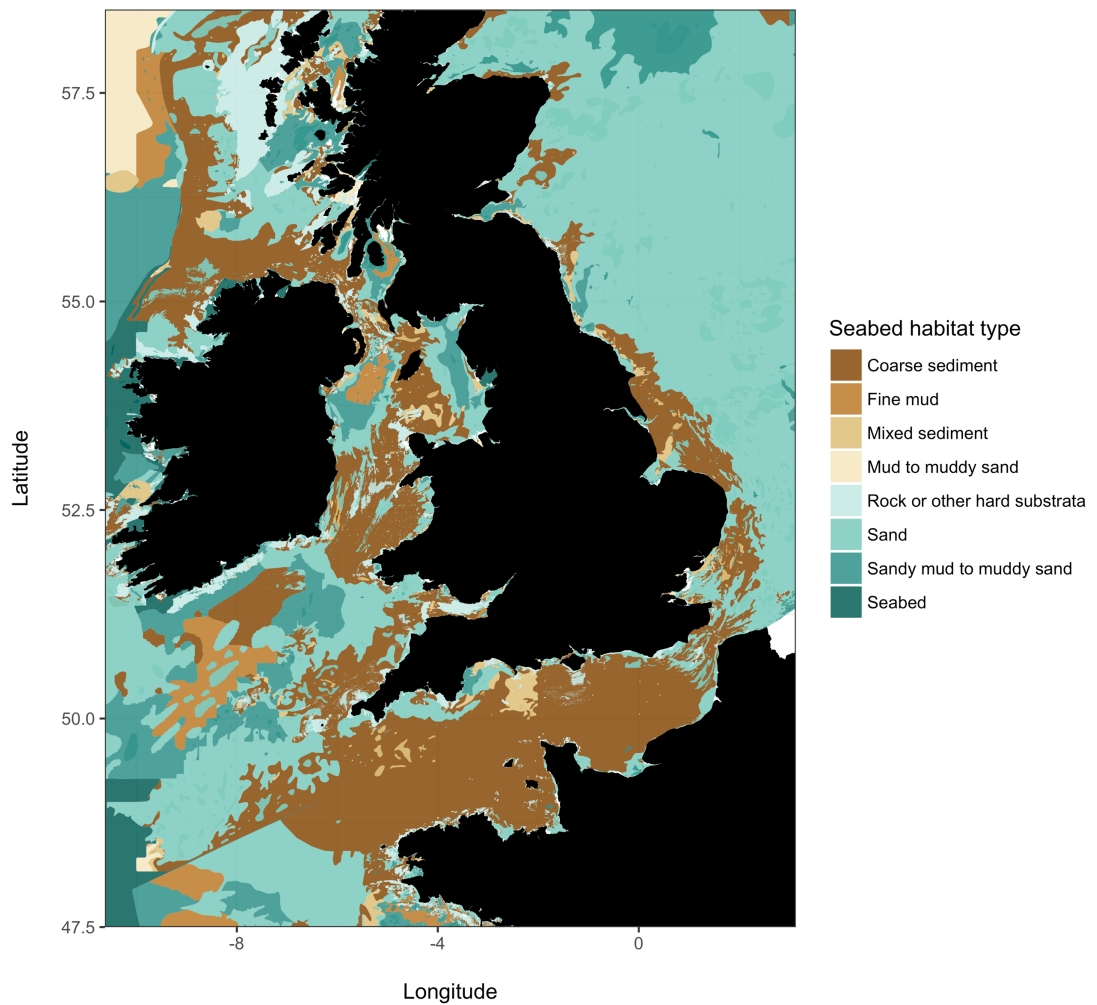


Figure. Seabed habitat types in the waters surrounding the British Isles. Habitat data is sourced from EMODnet's (The European Marine Observation and Data Network) Seabed Habitats online data portal (EMODnet, 2016).

Appendix 2.10.

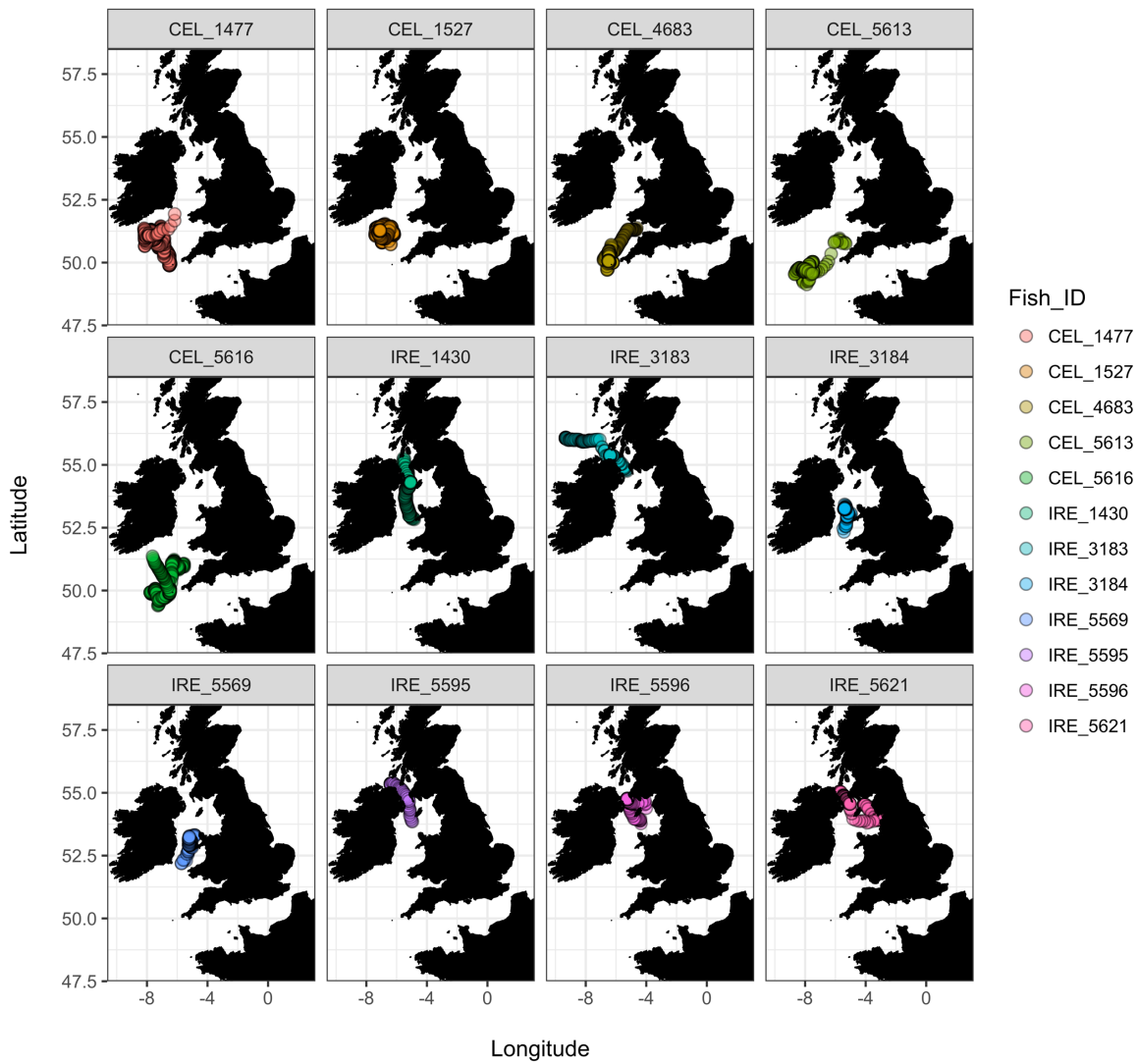


Figure. Estimated geographic positions of individual cod during their time at liberty in the Irish (n = 7) and Celtic (n = 5) Sea.

Appendix 2.11.

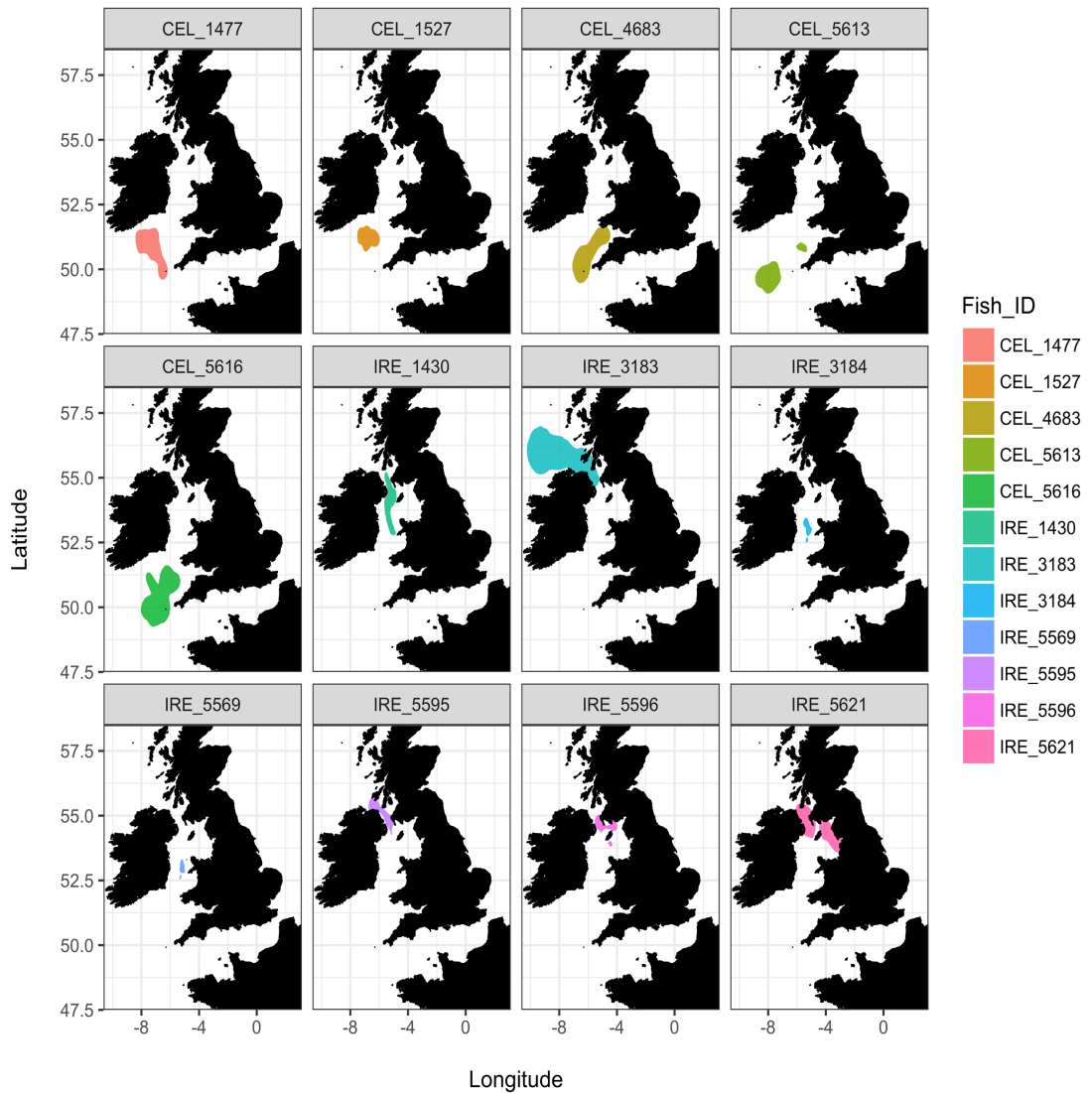


Figure. Estimated individual home ranges of cod tagged in the Irish (n = 7) and Celtic (n = 5) Sea.

Appendix 2.12.

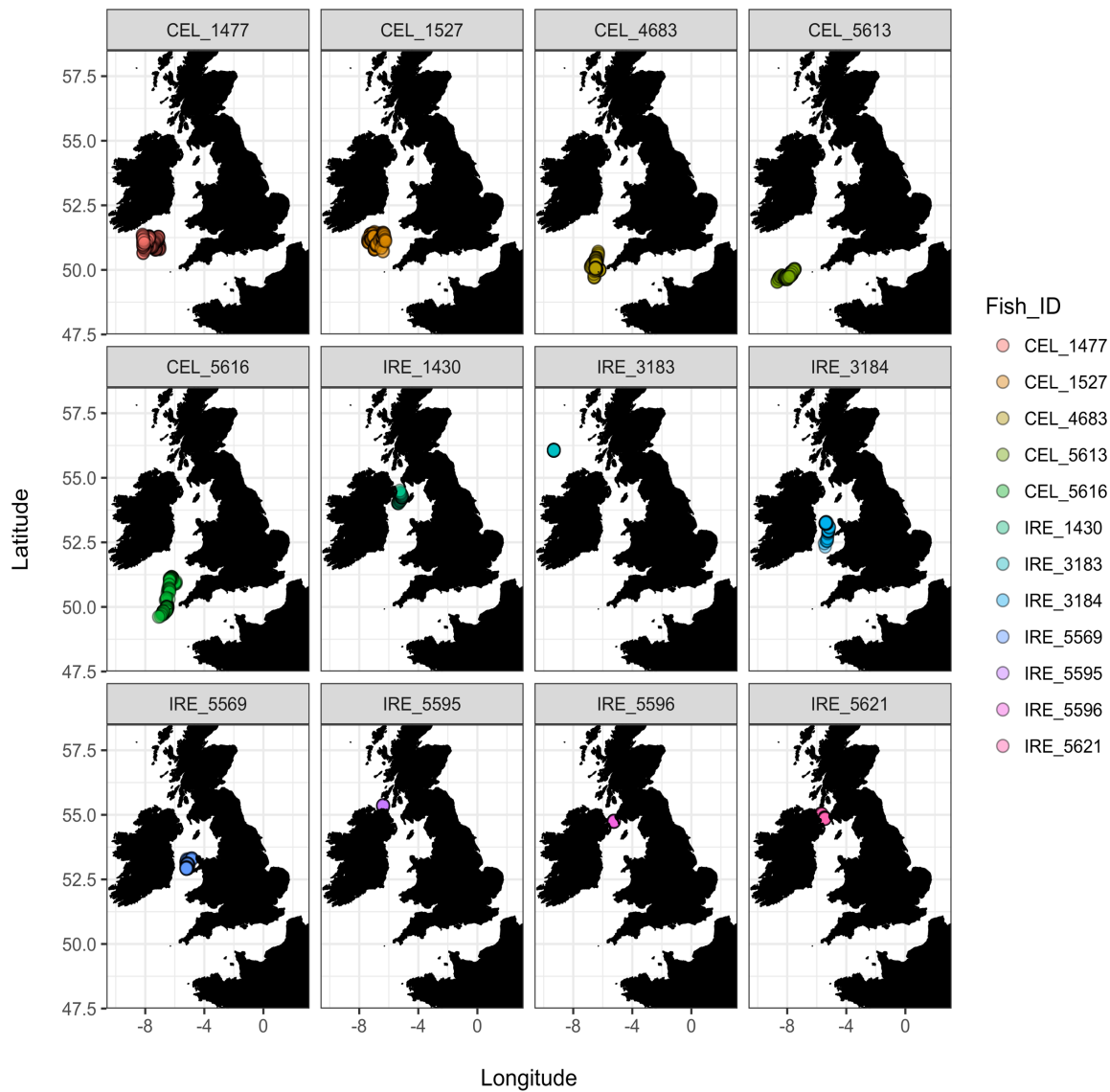


Figure. Estimated geographic positions of individual cod during the foraging period (1st June – 31st October) in the Irish (n = 7) and Celtic (n = 5) Sea.

Appendix 2.13.

Table. Statistics summarising the movement (horizontal and vertical movement), fish depth, sea depth and temperature experienced of individual cod in the Irish (n = 7) and Celtic sea (n = 5). All values are averages (\pm 1 standard deviation) calculated at the daily level for the duration of the foraging period (1st June – 31st October).

Fish ID	Area	Horizontal distance travelled (km)	Vertical distance travelled (m)	Fish depth (m)	Sea depth (m)	Temperature (°C)
IRE_1430	Irish Sea	1.3 (\pm 0.8)	161.5 (\pm 38.1)	64.4 (\pm 3.6)	117.2 (\pm 7.9)	12.2 (\pm 1.9)
IRE_3183	Irish Sea	1.5 (\pm 0.8)	601.1 (\pm 158.4)	153.0 (\pm 22.6)	762.6 (\pm 14.7)	12.7 (\pm 1.7)
IRE_3184	Irish Sea	3.3 (\pm 4.6)	344.4 (\pm 127.2)	107.8 (\pm 14.9)	140.7 (\pm 15.5)	12.7 (\pm 1.0)
IRE_5569	Irish Sea	3.1 (\pm 3.1)	186.4 (\pm 102.4)	76.1 (\pm 28.0)	122.7 (\pm 21.1)	14.0 (\pm 1.3)
IRE_5595	Irish Sea	1.6 (\pm 0.9)	619.7 (\pm 188.0)	165.1 (\pm 48.2)	200.5 (\pm 59.2)	12.5 (\pm 1.7)
IRE_5596	Irish Sea	1.5 (\pm 0.8)	396.9 (\pm 120.2)	137.4 (\pm 24.0)	230.2 (\pm 22.0)	12.3 (\pm 1.7)
IRE_5621	Irish Sea	1.6 (\pm 1.4)	441.7 (\pm 210.6)	141.6 (\pm 29.1)	188.6 (\pm 41.4)	12.1 (\pm 1.5)
CEL_1477	Celtic Sea	2.9 (\pm 2.0)	56.9 (\pm 44.3)	100.6 (\pm 1.4)	99.5 (\pm 3.9)	10.0 (\pm 0.4)
CEL_1527	Celtic Sea	3.9 (\pm 3.8)	86.5 (\pm 56.8)	98.5 (\pm 14.1)	98.6 (\pm 9.7)	10.4 (\pm 0.3)
CEL_4683	Celtic Sea	5.0 (\pm 4.7)	61.7 (\pm 26.6)	101.4 (\pm 1.9)	106.0 (\pm 19.9)	11.2 (\pm 0.4)
CEL_5613	Celtic Sea	3.8 (\pm 3.3)	34.6 (\pm 23.7)	148.2 (\pm 2.6)	150.9 (\pm 12.4)	10.0 (\pm 0.3)
CEL_5616	Celtic Sea	5.5 (\pm 6.3)	66.8 (\pm 24.8)	115.4 (\pm 6.7)	118.9 (\pm 24.2)	9.7 (\pm 0.4)

Appendix 2.14.

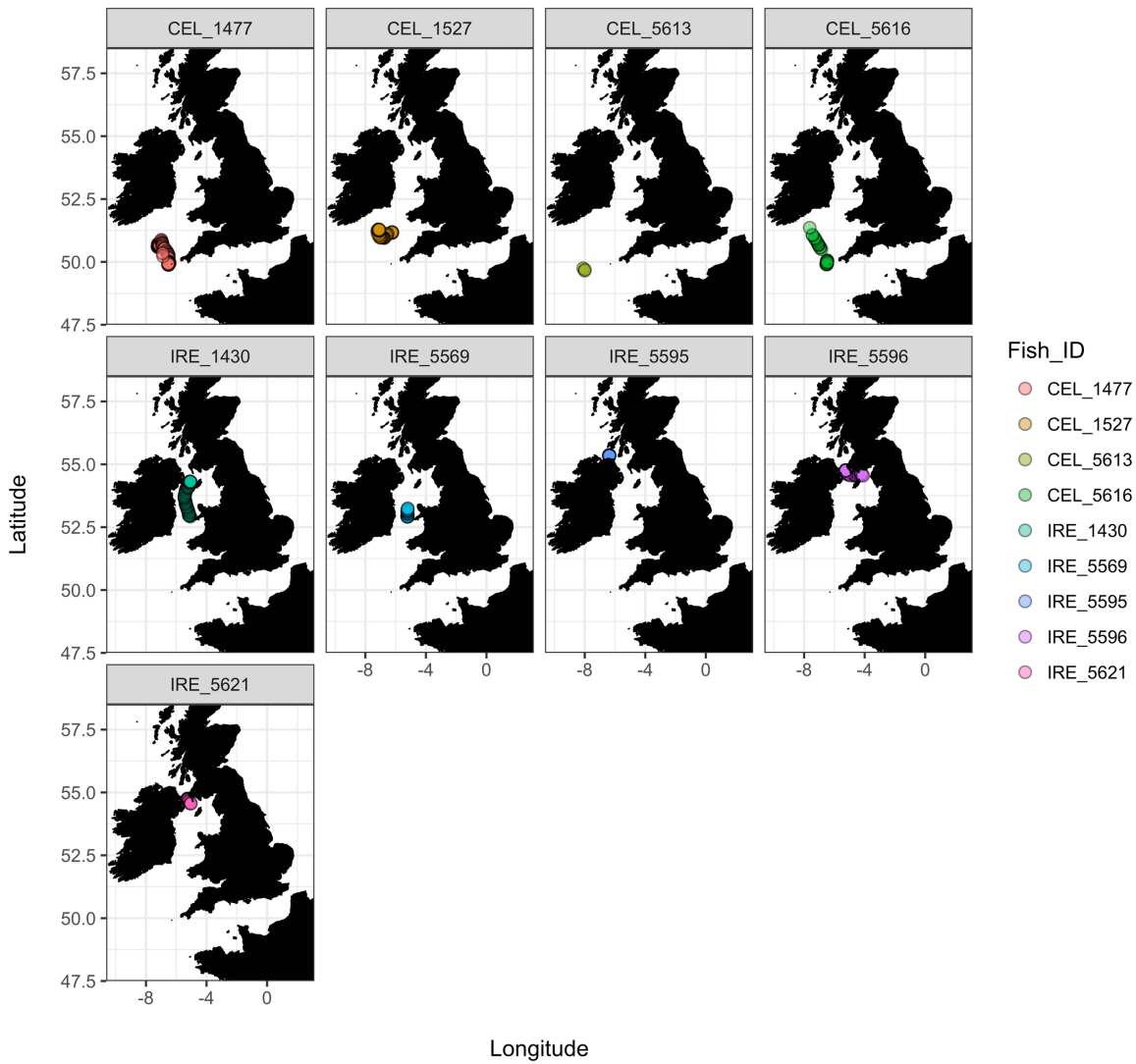
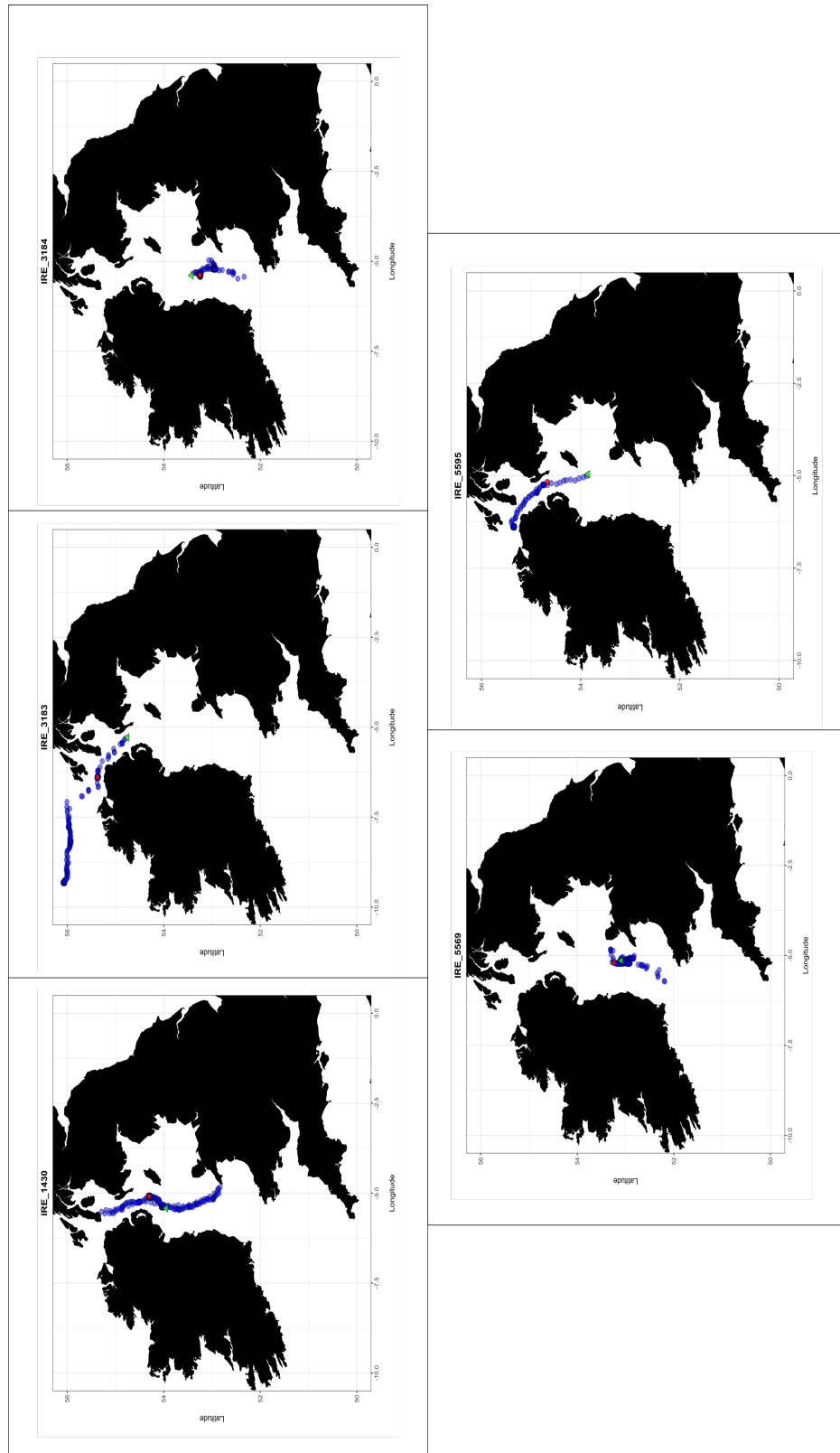


Figure. Estimated geographic positions of individual cod during the spawning period (1st January – 30th April) in the Irish (n = 5) and Celtic (n = 4) Sea.

Appendix 2.15.

Table. Statistics summarising the movement (horizontal and vertical movement), fish depth, sea depth and temperature experienced of individual cod in the Irish (n = 5) and Celtic sea (n = 4). All values are averages (\pm 1 standard deviation) calculated at the daily level for the duration of the spawning period (1st January – 30th April).

Fish ID	Area	Horizontal distance travelled (km)	Vertical distance travelled (m)	Fish depth (m)	Sea depth (m)	Temperature (°C)
IRE_1430	Irish Sea	1.7 (\pm 1.0)	225.3 (\pm 97.7)	59.8 (\pm 15.1)	116.8 (\pm 14.7)	8.6 (\pm 0.7)
IRE_5569	Irish Sea	1.8 (\pm 1.0)	343.4 (\pm 178.9)	37.4 (\pm 21.7)	132.2 (\pm 10.7)	6.8 (\pm 1.5)
IRE_5595	Irish Sea	1.6 (\pm 0.7)	451.6 (\pm 100.0)	91.6 (\pm 16.5)	194.6 (\pm 59.6)	8.4 (\pm 0.7)
IRE_5596	Irish Sea	1.9 (\pm 1.1)	314.5 (\pm 170.9)	69.5 (\pm 43.4)	161.0 (\pm 86.3)	7.5 (\pm 1.3)
IRE_5621	Irish Sea	1.9 (\pm 0.9)	374.8 (\pm 147.5)	104.9 (\pm 31.8)	183.6 (\pm 20.3)	8.6 (\pm 0.9)
CEL_1477	Celtic Sea	2.0 (\pm 1.3)	233.5 (\pm 124.4)	94.8 (\pm 15.5)	141.4 (\pm 42.4)	9.1 (\pm 0.4)
CEL_1527	Celtic Sea	2.0 (\pm 1.3)	214.2 (\pm 95.6)	89.8 (\pm 9.4)	101.0 (\pm 8.9)	9.0 (\pm 0.7)
CEL_5613	Celtic Sea	3.4 (\pm 2.5)	55.9 (\pm 3.9)	144.5 (\pm 3.0)	154.3 (\pm 15.5)	9.7 (\pm 0.1)
CEL_5616	Celtic Sea	2.2 (\pm 1.4)	237.8 (\pm 138.6)	102.4 (\pm 18.9)	151.8 (\pm 42.6)	9.2 (\pm 0.5)



Appendix 2.16.

Figure. Estimated geographical positions of individual cod tagged in the central/western Irish Sea ($n = 5$). Release (green triangle) and recapture (red circle) locations are shown.

Appendix 2.17.

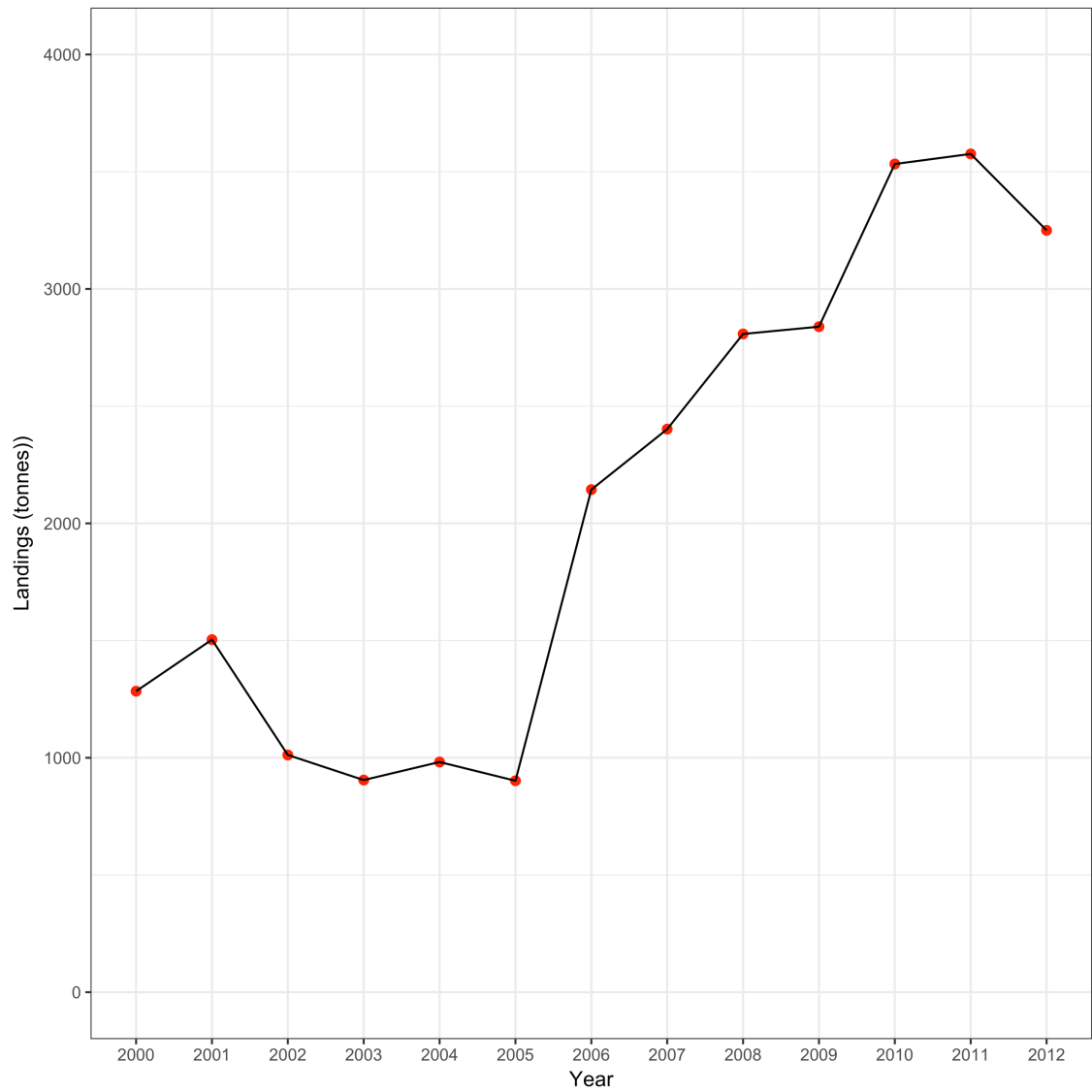


Figure. Landings (tonnes) of brown crab (*Cancer pagurus*) in the Celtic Sea from 2000 to 2012. All values are extracted from Table 5 (page 13) in ICES WGCRAB REPORT 2013 (Report of the Working Group on the Biology and Life History of Crabs).

Appendix 3

Appendix 3.1.

Table. Summary of movement paths by sub-stock.

Species	Sub-stock	n*	Movement path duration (days)		
			Minimum	Mean	Maximum
Atlantic cod (<i>Gadus morhua</i>)	Southern North Sea	23	40	97	295
	English Channel	23	41	145	364
European plaice (<i>Pleuronectes platessa</i>)	Southern North Sea	24	42	205	399
	German Bight	10	56	183	356
	Central North Sea	27	49	131	368

*n, number of individual fish.

Appendix 3.2.

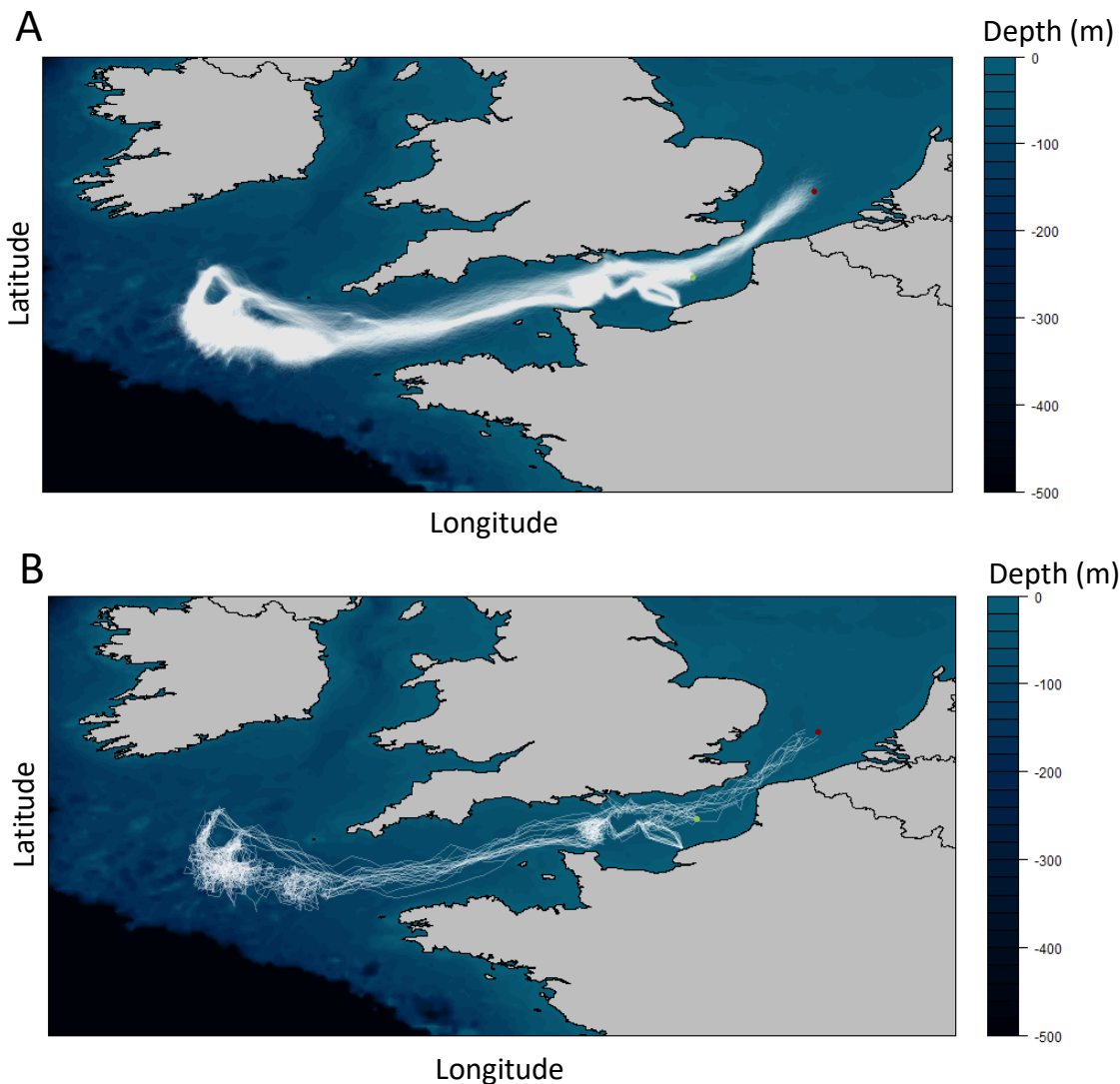


Figure. Uncertainty associated with the geolocation of a single Atlantic cod (cod 1186) tagged with a data storage tag (DST) in the English Channel. Pictured are one thousand possible sample paths (A) and the top ten most probable sample paths (B). The ten most probable paths are calculated in a two-step process. First, each track is given a p value based on the cumulative probability associated with each daily location conditional on the observed depth (m) and whether or not a tidal signal has been detected. Second, the top ten ‘most probable’ paths are selected, where selection is based on the minimisation of that p value. For further methodological details see Pedersen et al. (2018). Cod 1186 is also illustrated in a behavioural context in Figure 3.6. Release and recapture locations are shown in green and red, respectively. Seabed depth is sourced from the General Bathymetric Chart of the Oceans online repository (GEBCO, 2017).

Appendix 3.3.

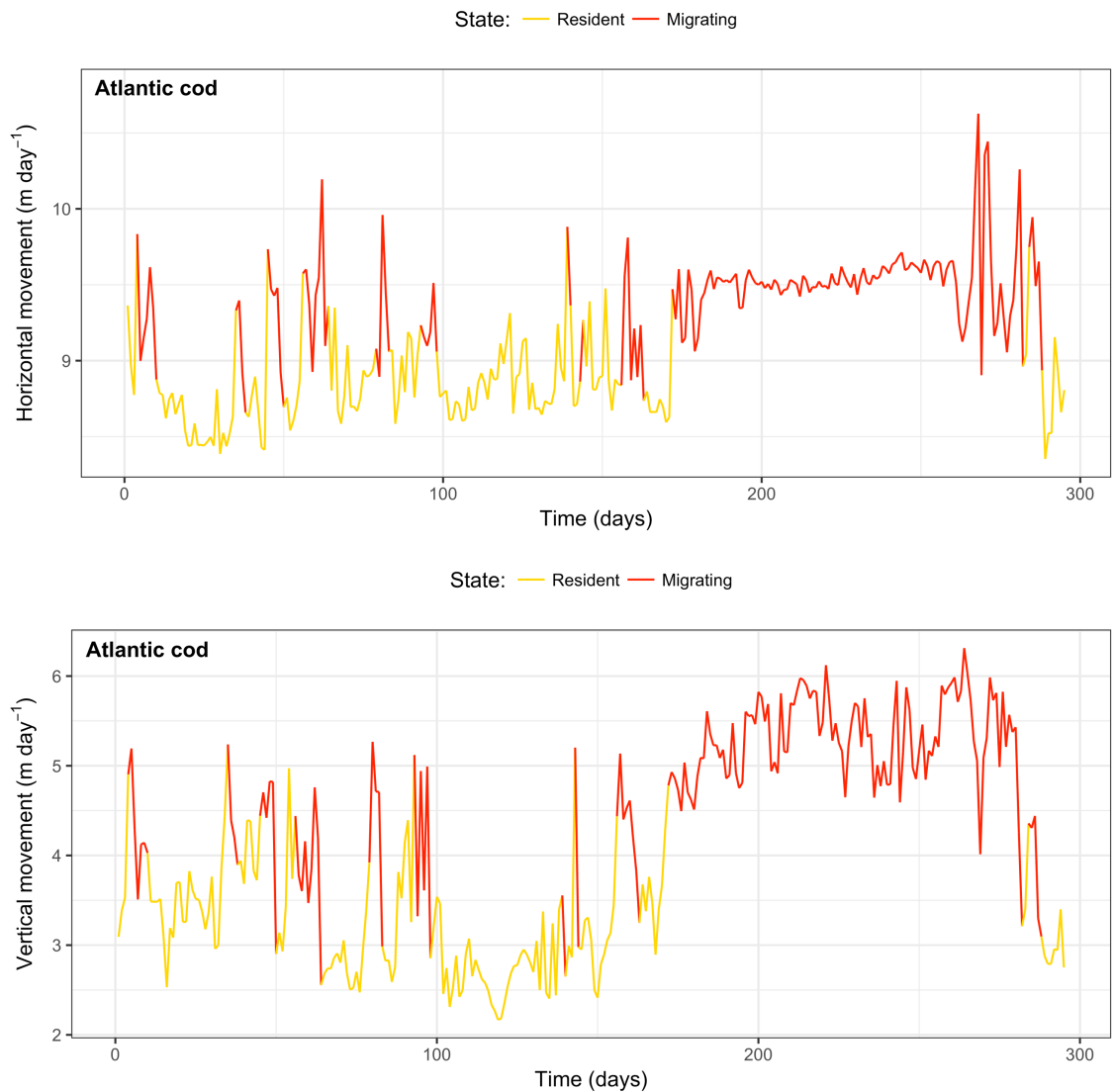


Figure. HMM output for an individual movement path (number of days = 295). Shown are the time-varying changes in state as the model switches between a resident (gold) and a migrating (red) state. The fish in question is an Atlantic cod in the Southern North Sea sub-stock, tagged on the 17th April 2001 and recaptured on the 5th February 2002. All horizontal and vertical observations have been log (natural log) transformed.

Appendix 3.4.

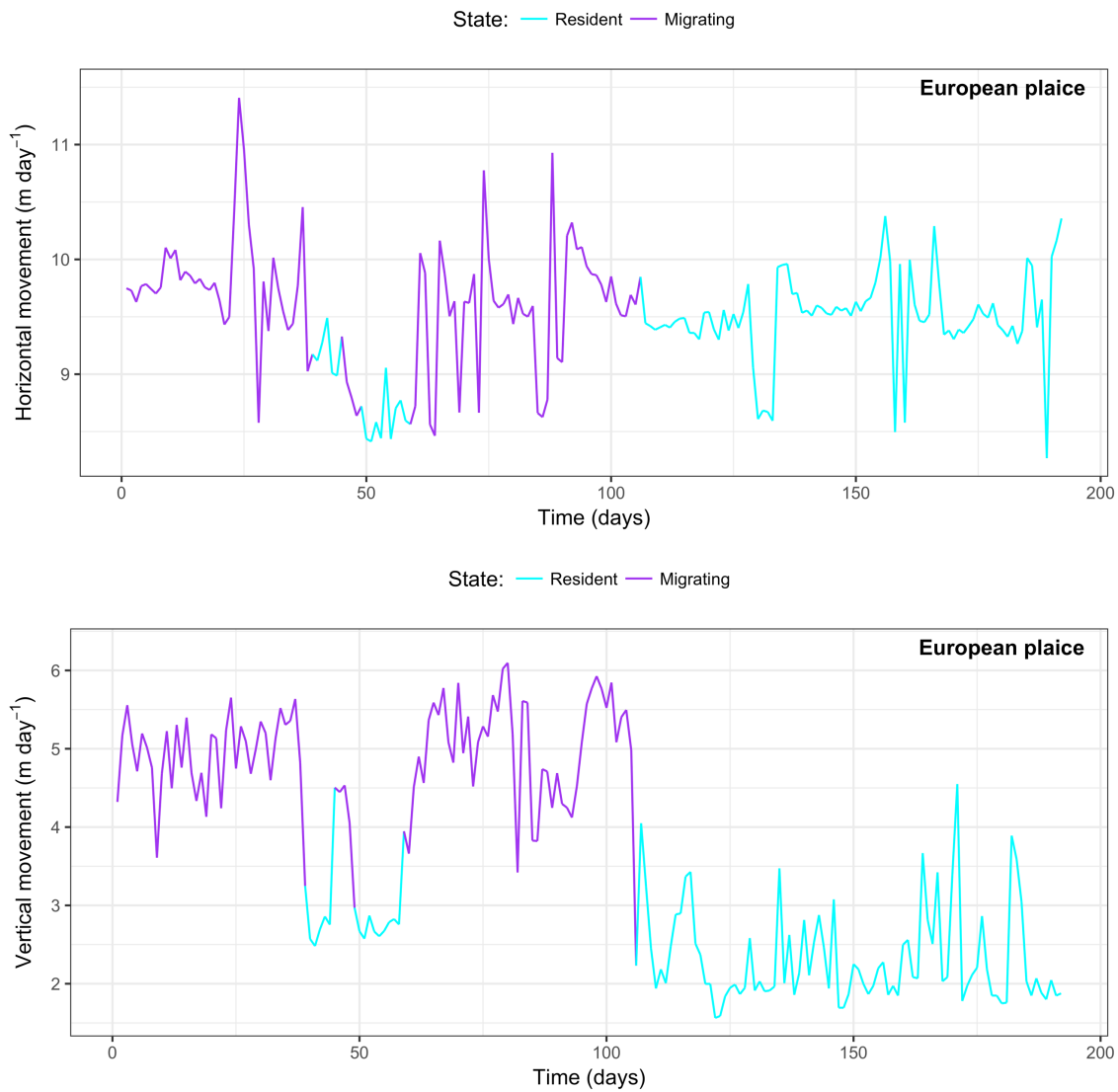
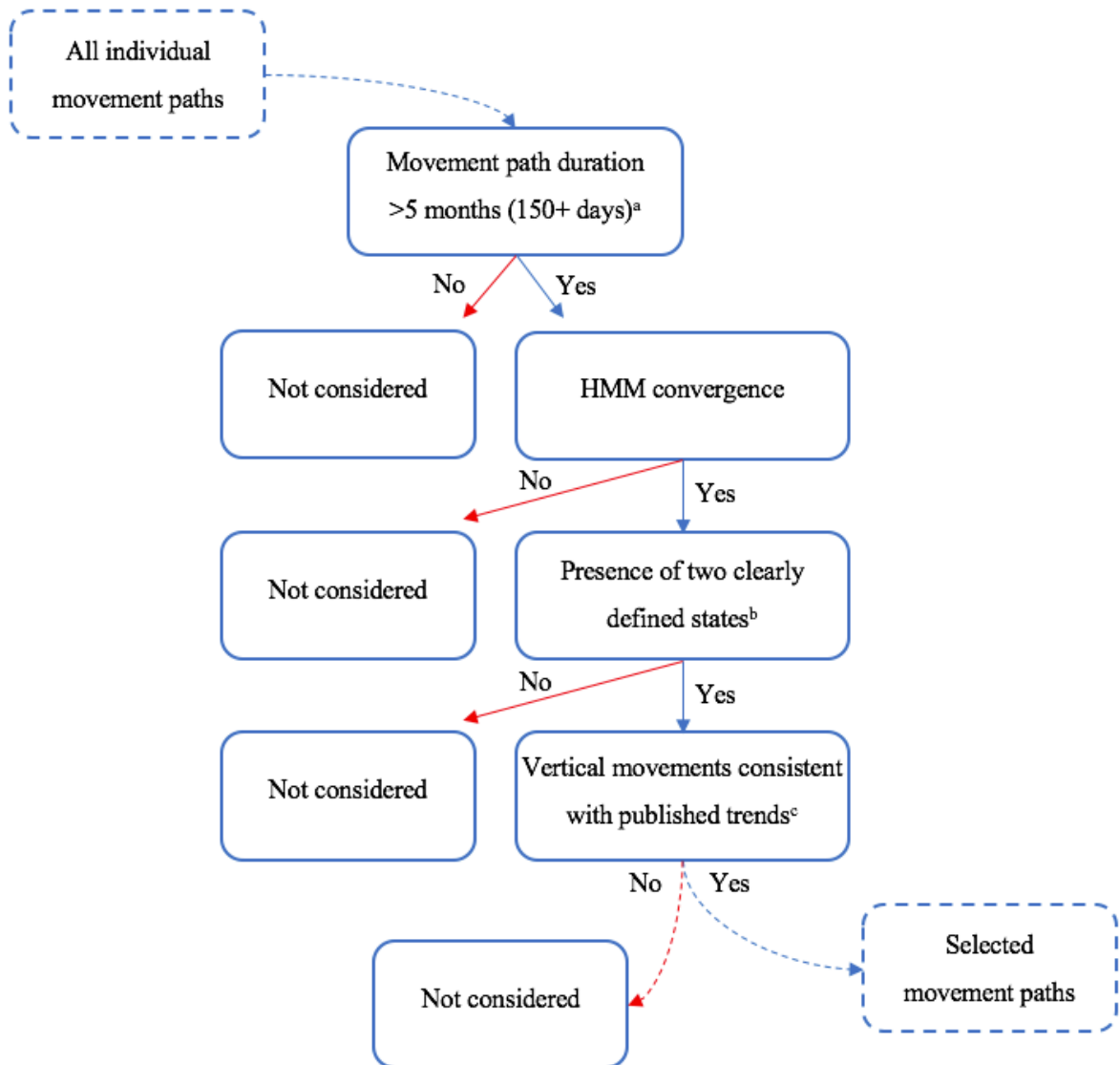


Figure. HMM output for an individual movement path (number of days = 192). Shown are the time-varying changes in state as the model switches between a resident (cyan) and a migrating (purple) state. The fish in question is a European plaice in the Southern North Sea sub-stock, tagged on the 18th December 1997 and recaptured on the 27th June 1998. All horizontal and vertical observations have been log (natural log) transformed.

Appendix 3.5.



^a So as to encompass any underlying seasonal shift in movement behaviour (Metcalf et al. 2006; Righton et al., 2010).

^b One more active and one less active state (Metcalf et al. 2006; Righton et al., 2010).

^c For vertical movement types we refer to Hobson et al. (2009, 2007 - Atlantic cod) and Hunter et al. (2004a, 2004b; European plaice).

Figure. Criteria used to select individual movement paths based on published movement types. Selection is species-specific.

Appendix 3.6.

Table. Summary of selected movement paths by sub-stock.

Species	Sub-stock	n*	Average duration of movement path (days)
Atlantic cod (<i>Gadus morhua</i>)	Southern North Sea	4	160
	English Channel	7	174
European plaice (<i>Pleuronectes platessa</i>)	Southern North Sea	10	241
	German Bight	7	201
	Central North Sea	6	171

*n, number of individual fish.

Appendix 3.7.

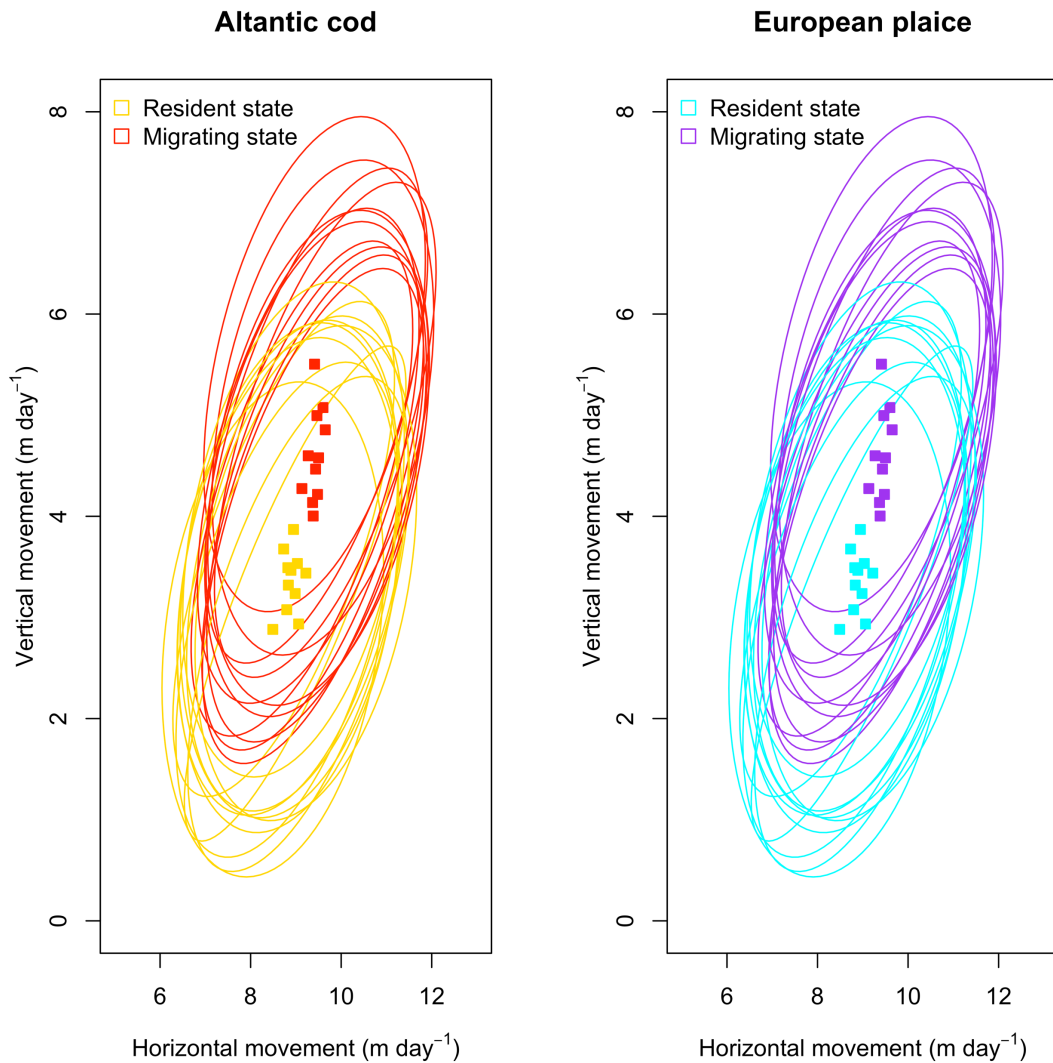


Figure. Prior state-distributions by state in Atlantic cod ($n=11$) and European plaice ($n=23$). Points and lines are movement path specific, points show the mean bivariate movement rate per state and ellipses show the highest density region sampled from each state covariance matrix. Plotted are all movement paths that were selected and synthesized into movement parameter priors following initial HMM runs. All horizontal and vertical observations have been log (natural log) transformed.

Appendix 3.8.

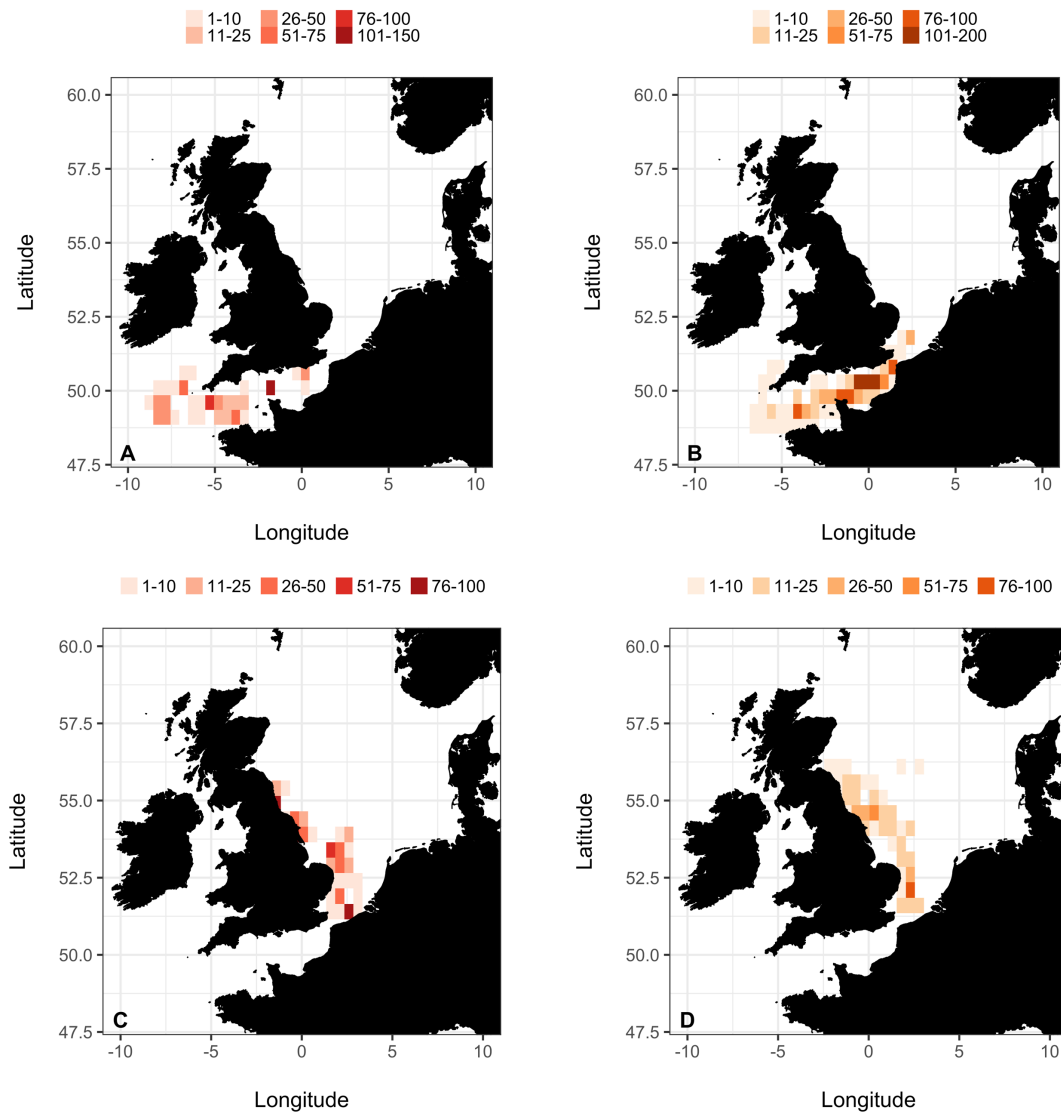


Figure. Spatial utilisation distributions by state and sub-stock (English Channel: A and B; Southern North Sea: C and D) in Atlantic cod. Plots are split into periods of resident dominant (A and C) and migrating dominant (B and D), where dominance is defined by a mean probability of observing a given state at a given time that exceeds 0.5. Resident dominance runs from June to October. Migrating dominance runs from November to May. All grid cells (5km²) are illustrated in a colour gradient so as to illustrate the sum total number of days spent in a certain state in a given grid cell within a specified time period.

Appendix 3.9.

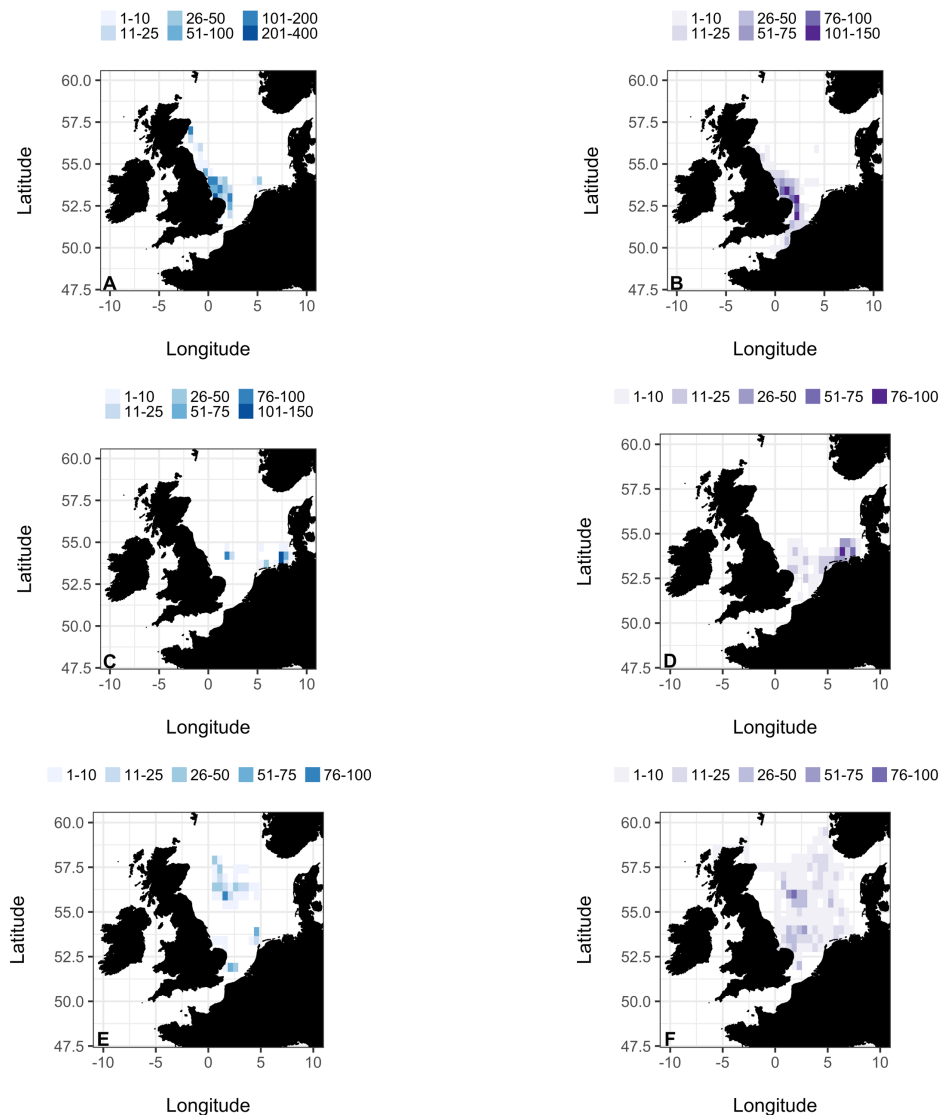


Figure. Spatial utilisation distributions by state and sub-stock (Southern North Sea: A and B; German Bight: C and D; Central North Sea: E and F) in European plaice. Plots are split into periods of resident dominant (A, C, E) and migrating dominant (B, D, F), where dominance is defined by a mean probability of observing a given state at a given time that exceeds 0.5. Resident dominance runs from April to September. Migrating dominance runs from October to March. All grid cells (5km²) are illustrated in a colour gradient so as to illustrate the sum total number of days spent in a certain state in a given grid cell within a specified time period.

Appendix 3.10.

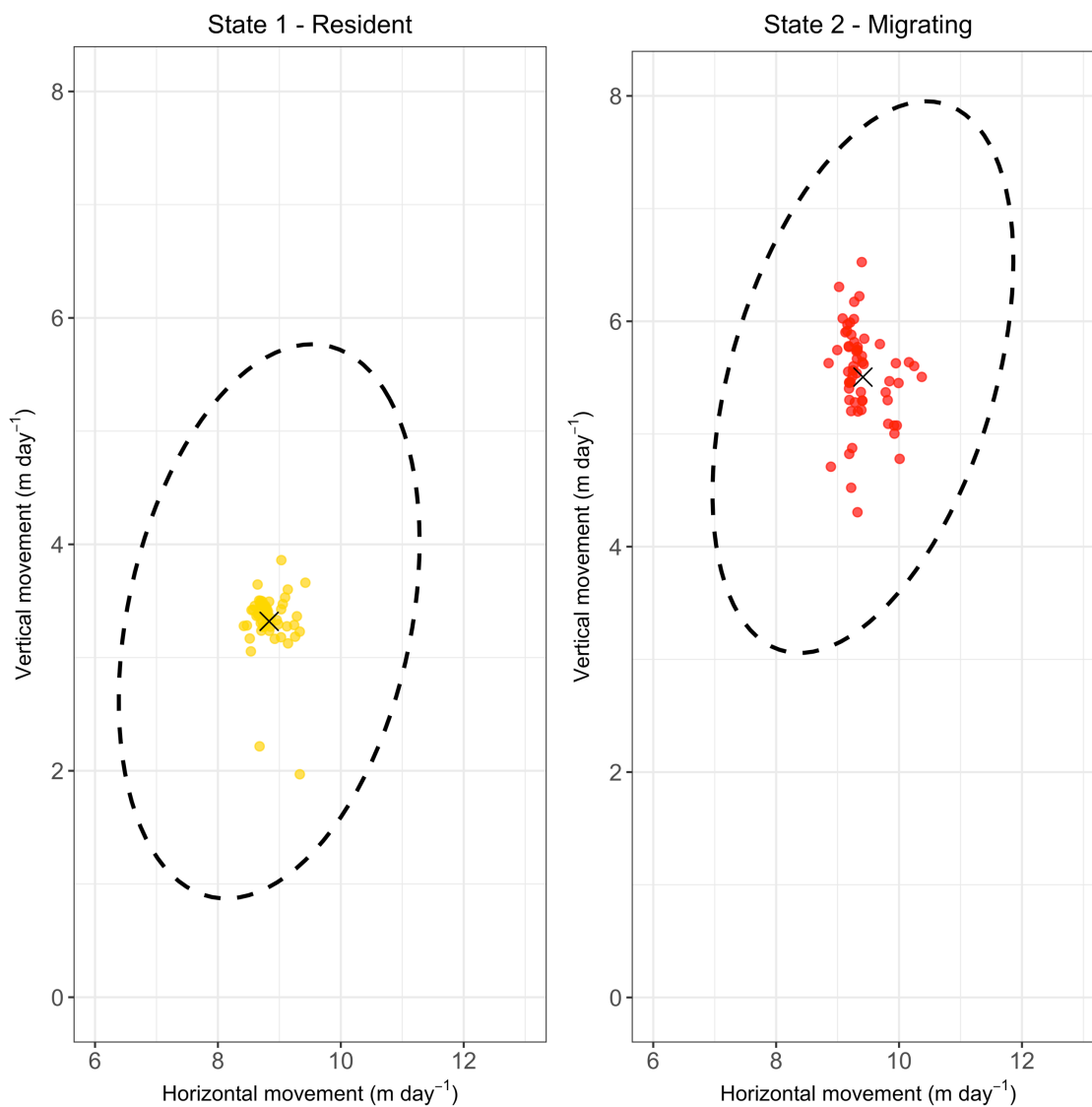


Figure. Observed vs. fitted values for a single Atlantic cod (movement path duration = 114 days). Observed points (coloured) are plotted alongside the estimated sample (all 46 fish) mean of each state (black cross). Dashed ellipses are calculated from the estimated sample covariance and centred on the estimated mean of each state. Horizontal and vertical observations have been log (natural log) transformed.

Appendix 3.11.

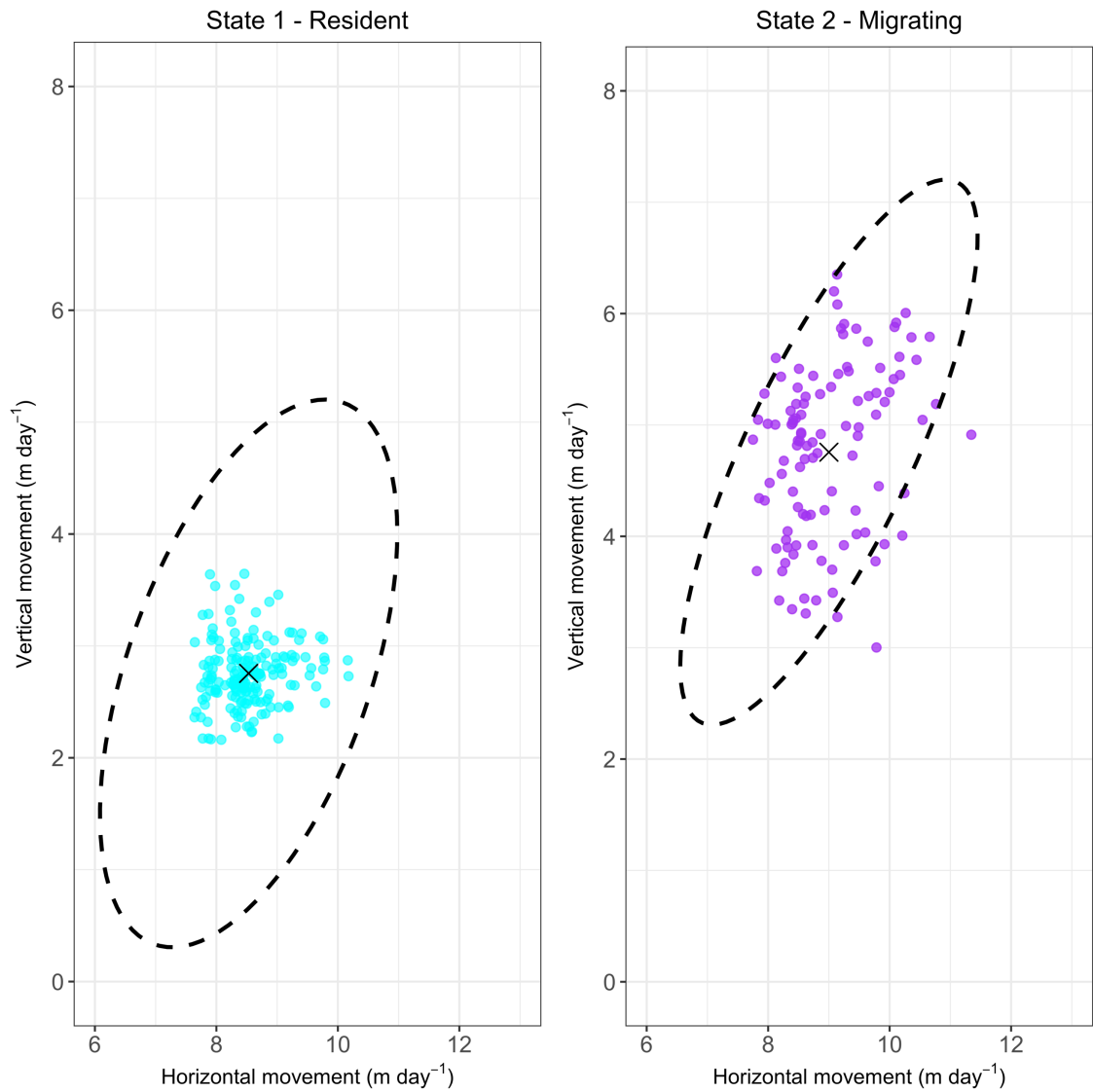


Figure. Observed vs. fitted values for a single European plaice (movement path duration = 289 days). Observed points (coloured) are plotted alongside the estimated sample (all 61 fish) mean of each state (black cross). Dashed ellipses are calculated from the estimated sample covariance and centred on the estimated mean of each state. Horizontal and vertical observations have been log (natural log) transformed.

Appendix 4

Appendix 4.1.

Table. Taxa independent vs. species average model fit.

Data	Model	Model equation	n	Log(intercept)	Slope
All	Taxa independent	$M_{real} \sim \text{body mass [1]}$	583	7.14 (l=7.09, u=7.2)	0.30 (l=0.3, u=0.31)
	Species average	$M_{real} \sim \text{body mass} + (1 \text{phylo}) [1]$	18	7.06 (l=6.36, u=7.73)	0.31 (l=0.27, u=0.36)
Larvae	Taxa independent	$M_{real} \sim \text{body mass [3]}$	155	6.94 (l=6.56, u=7.33)	0.27 (l=0.17, u=0.37)
	Species average	$M_{real} \sim \text{body mass} + (1 \text{phylo}) [3]$	9	7.09 (l=4.00, u=10.14)	0.32 (l=-0.26, u=0.93)
Adult	Taxa independent	$M_{real} \sim \text{body mass [3]}$	428	8.09 (l=7.91, u=8.27)	0.19 (l=0.16, u=0.21)
	Species average	$M_{real} \sim \text{body mass} + (1 \text{phylo}) [3]$	9	8.05 (l=6.01, u=10.86)	0.21 (l=-0.01, u=0.39)

l, lower 95% credible interval. u, upper 95% credible interval. n, number of data points considered. In species average models, M_{real} and body mass values are species specific averages. phylo, patterns of phylogenetic relatedness among species. The investigation each model is specific to is identified within [...].

Appendix 4.2.

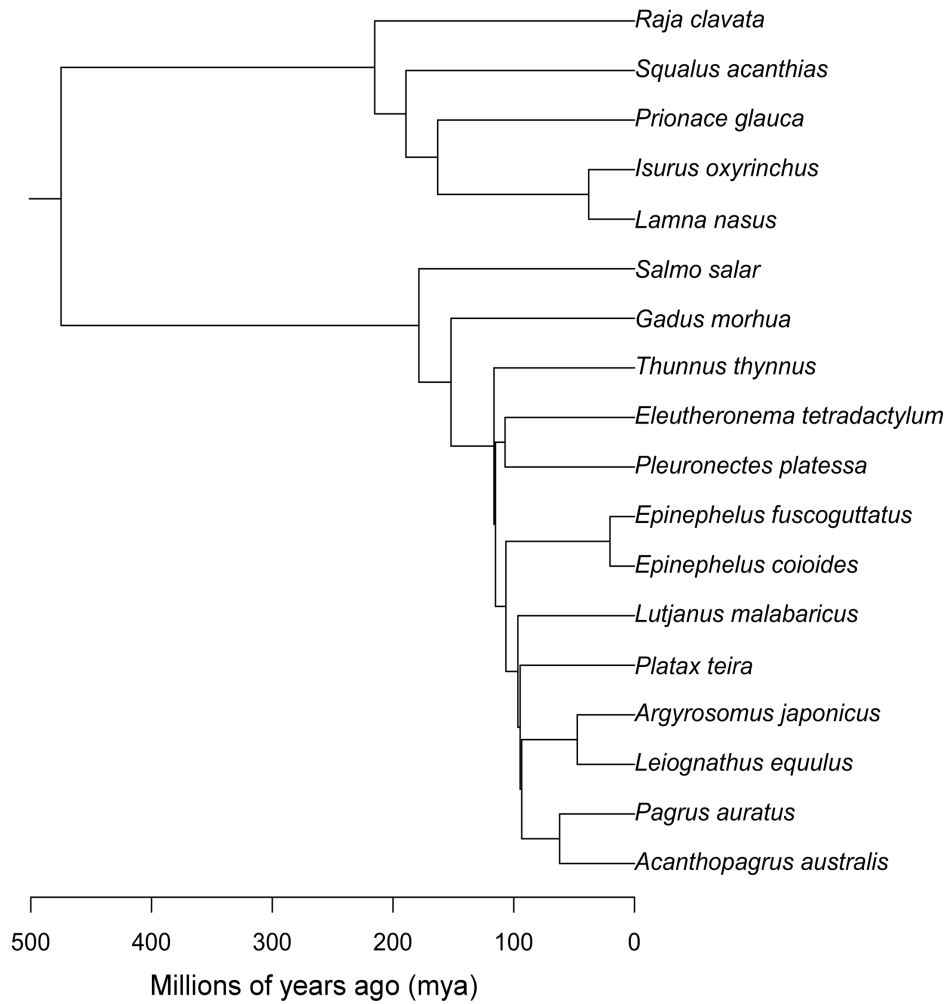


Figure. Dendrogram used in phylogenetic regressions in Chapter 4. Latin names of each species are used.

Appendix 4.3.

Table. Estimated species-level effects within the random intercept model fitted to all fish movement data in Chapter 4.

Species	Log(intercept)*	Common slope	Life stage
Atlantic cod (<i>Gadus morhua</i>)	0.03	0.16	Adult
European plaice (<i>Pleuronectes platessa</i>)	0.31	0.16	Adult
Atlantic salmon (<i>Salmo salar</i>)	0.84	0.16	Adult
Atlantic Bluefin tuna (<i>Thunnus thynnus</i>)	0.13	0.16	Adult
Porbeagle shark (<i>Lamna nasus</i>)	0.53	0.16	Adult
Blue shark (<i>Prionace glauca</i>)	0.30	0.16	Adult
Shortfin mako shark (<i>Isurus oxyrinchus</i>)	0.62	0.16	Adult
Spiny dogfish (<i>Squalus acanthias</i>)	0.37	0.16	Adult
Thornback Ray (<i>Raja clavata</i>)	0.05	0.16	Adult
Orange-spotted grouper (<i>Epinephelus coioides</i>)	-0.98	0.16	Larvae
Brown-marbled grouper (<i>Epinephelus fuscoguttatus</i>)	-1.07	0.16	Larvae
Four-finger threadfin (<i>Eleutheronema tetradactylum</i>)	-1.43	0.16	Larvae
Common ponyfish (<i>Leiognathus equulus</i>)	-1.71	0.16	Larvae
Saddletail snapper (<i>Lutjanus malabaricus</i>)	-1.32	0.16	Larvae
Longfin batfish (<i>Platax teira</i>)	-1.39	0.16	Larvae
Australasian snapper (<i>Pagrus auratus</i>)	-2.35	0.16	Larvae
Surf bream (<i>Acanthopagrus australis</i>)	-1.49	0.16	Larvae
Mulloway (<i>Argyrosomus japonicus</i>)	-2.20	0.16	Larvae

*Estimated log(intercepts) are reported as deviates from the population estimate of 8.06.

Appendix 4.4.

Table. Estimated species-level effects within the random intercept and slope model fitted to all fish movement data in Chapter 4.

Species	Log(intercept)*	Slope†	Life stage
Atlantic cod (<i>Gadus morhua</i>)	0.14	-0.01	Adult
European plaice (<i>Pleuronectes platessa</i>)	1.49	-0.20	Adult
Atlantic salmon (<i>Salmo salar</i>)	0.85	0.01	Adult
Atlantic Bluefin tuna (<i>Thunnus thynnus</i>)	-1.86	0.22	Adult
Porbeagle shark (<i>Lamna nasus</i>)	1.78	-0.09	Adult
Blue shark (<i>Prionace glauca</i>)	0.57	0.00	Adult
Shortfin mako shark (<i>Isurus oxyrinchus</i>)	1.37	-0.06	Adult
Spiny dogfish (<i>Squalus acanthias</i>)	0.54	-0.01	Adult
Thornback Ray (<i>Raja clavata</i>)	0.28	-0.03	Adult
Orange-spotted grouper (<i>Epinephelus coioides</i>)	-1.62	-0.02	Larvae
Brown-marbled grouper (<i>Epinephelus fuscoguttatus</i>)	-1.71	-0.01	Larvae
Four-finger threadfin (<i>Eleutheronema tetradactylum</i>)	-1.94	0.05	Larvae
Common ponyfish (<i>Leiognathus equulus</i>)	-2.09	0.08	Larvae
Saddletail snapper (<i>Lutjanus malabaricus</i>)	-1.84	0.03	Larvae
Longfin batfish (<i>Platax teira</i>)	-2.06	0.00	Larvae
Australasian snapper (<i>Pagrus auratus</i>)	-2.90	0.04	Larvae
Surf bream (<i>Acanthopagrus australis</i>)	-2.17	0.01	Larvae
Mulloway (<i>Argyrosomus japonicus</i>)	-2.91	-0.01	Larvae

*Estimated log(intercepts) are reported as deviates from the population estimate of 8.51. †Estimated slopes are reported as deviates from the population estimate of 0.10.

Appendix 4.5.

Table. Estimated species-level effects within the random intercept and slope model fitted to all adult fish movement data in Chapter 4.

Species	Log(intercept)*	Slope†	Thermoregulation strategy	Habitat	Phylogenetic class
Atlantic cod (<i>Gadus morhua</i>)	-0.82	0.05	Ectothermic	Demersal	Actinopterygii
European plaice (<i>Pleuronectes platessa</i>)	0.99	-0.21	Ectothermic	Demersal	Actinopterygii
Atlantic salmon (<i>Salmo salar</i>)	1.15	-0.07	Ectothermic	Pelagic	Actinopterygii
Atlantic Bluefin tuna (<i>Thunnus thynnus</i>)	-3.24	0.33	Endothermic	Pelagic	Actinopterygii
Porbeagle shark (<i>Lamna nasus</i>)	2.07	-0.14	Endothermic	Pelagic	Chondrichthyes
Blue shark (<i>Prionace glauca</i>)	-0.10	0.03	Ectothermic	Pelagic	Chondrichthyes
Shortfin mako shark (<i>Isurus oxyrinchus</i>)	0.91	-0.04	Endothermic	Pelagic	Chondrichthyes
Spiny dogfish (<i>Squalus acanthias</i>)	-0.15	0.02	Ectothermic	Demersal	Chondrichthyes
Thornback Ray (<i>Raja clavata</i>)	-0.67	0.03	Ectothermic	Demersal	Chondrichthyes

*Estimated intercepts are reported as differences from the population estimate of 9.58. †Estimated slopes are reported as differences from the population estimate of 0.02.

Appendix 5

Appendix 5.1.

Table. Main parameter values employed in the trait-based size spectrum literature compared to those used in Chapter 5. The parameters that we allow to vary (q , λ and γ) are not listed. Parameter names and units are listed in Table 5.2.

f_0	α	h	n	k_s	p	β	σ	μ_0	κ_r	r_0	ε	Reference
0.6	0.6	85	0.75	10	0.75	100	1.0	0.84	0.005	4	-	Hartvig et al., 2011
-	0.6	40	2/3	4	0.75	100	1.3	3.0	0.005	4	-	Andersen and Rice, 2010
-	0.6	20	0.75	2.4	0.75	100	1.3	2.0	0.005	4	-	Jacobsen et al., 2013
varied	0.6	85	0.75	10	0.75	100	1.0	0.84	0.005	4	-	Hartvig and Andersen, 2013
0.5	0.6	30	2/3	4	0.75	100	1.3	0.6	0.005	4	-	Andersen and Pedersen, 2010
-	0.6	varied	0.75	0.8*h	0.75	100	1.3	-	0.005	4	0.1	Jacobsen et al., 2017
-	0.6	85	0.75	10	0.75	100	2	0.84	0.005	4	0.1	Houle et al., 2013
	0.6	20	0.75	2.4	0.75	100	1.3	2	0.005	4	0.1	Houle et al., 2012
0.5	0.6	30	2/3	4	0.75	100	1.3	0.6	0.005	4	0.1	Parameters used in Chapter 5

varied, parameter is estimated or allowed to vary based on the aims of study. -, parameter value not listed or not used.

Appendix 5.2.

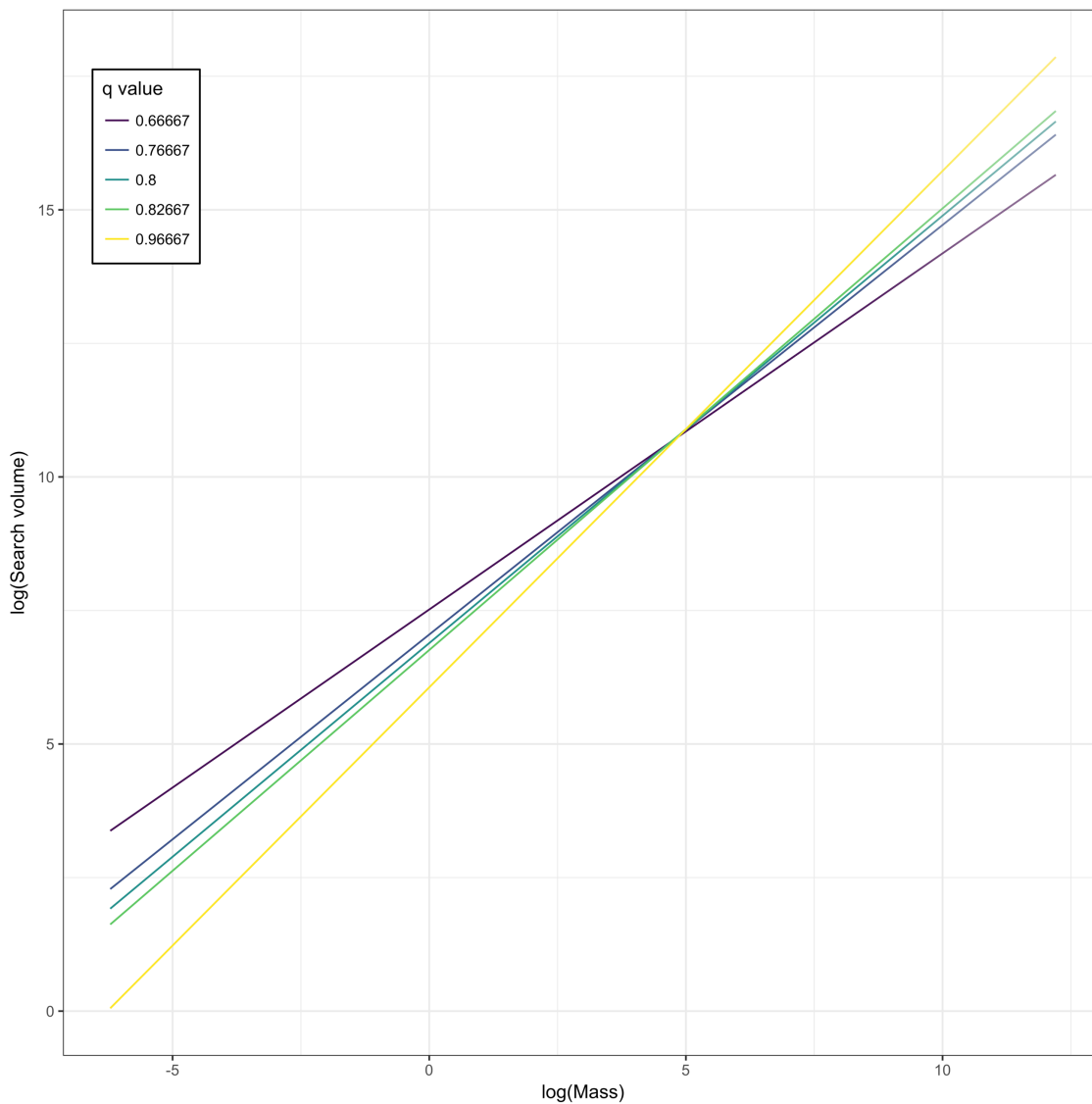


Figure. Relationship between search volume (V ; year⁻¹) and body mass (grams) at q values of empirical interest. Search volume and mass have log (natural log) transformed to aid visual interpretation.

Appendix 5.3.

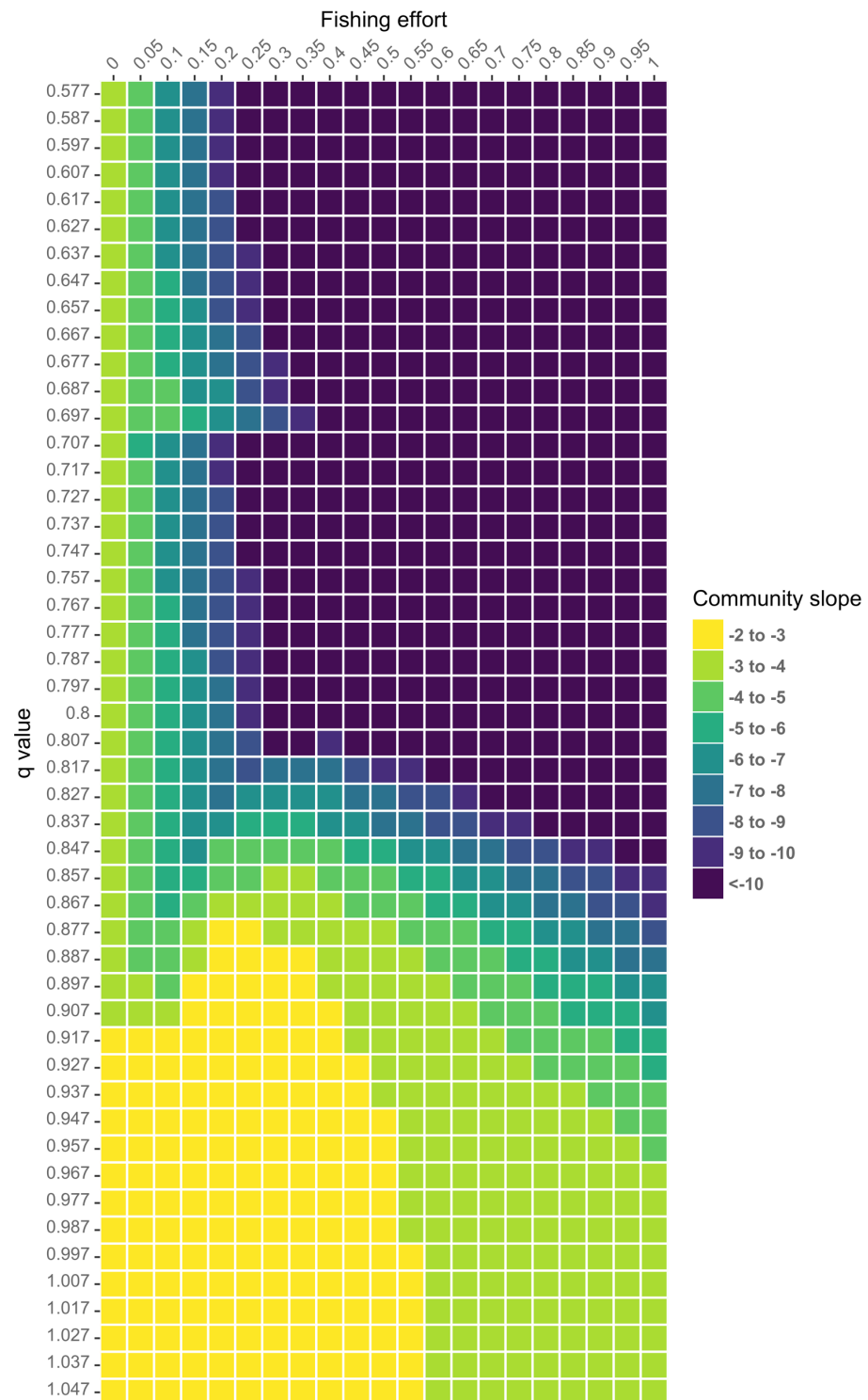


Figure. Community slope as a function of a varying q (rounded to 3 decimal places) and a varying f . All slope estimates have been discretised to aid visual interpretation. All φ values are fixed at 0.5. A lower threshold of -10 has been imposed because values beyond this point are indicative of a truncated size spectrum where abundance at large size class has been completely lost.

Appendix 5.4.

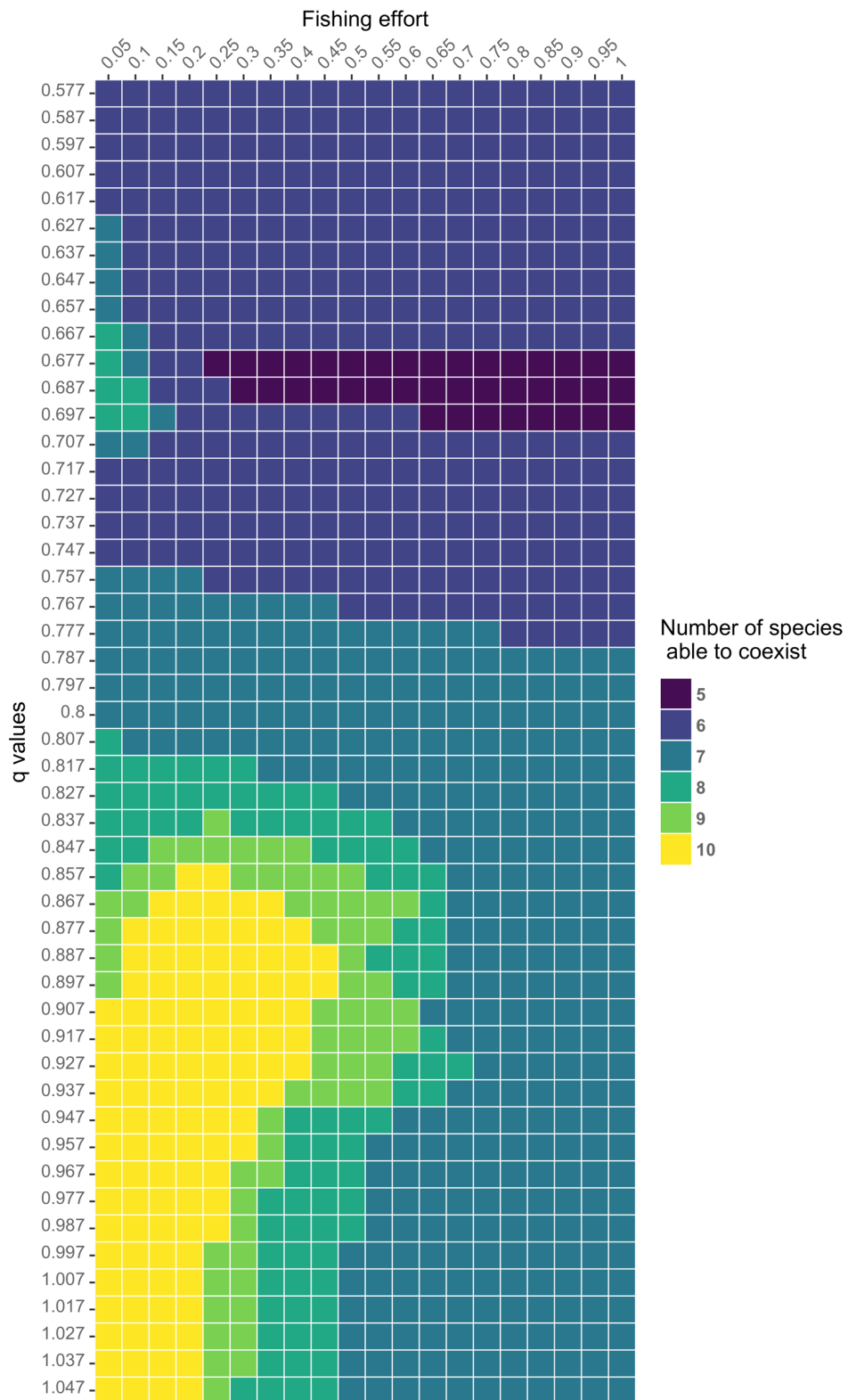


Figure. Species coexistence as a function of a varying q (rounded to 3 decimal places) and a varying f . All φ values are fixed at 0.5.

Appendix 5.5.

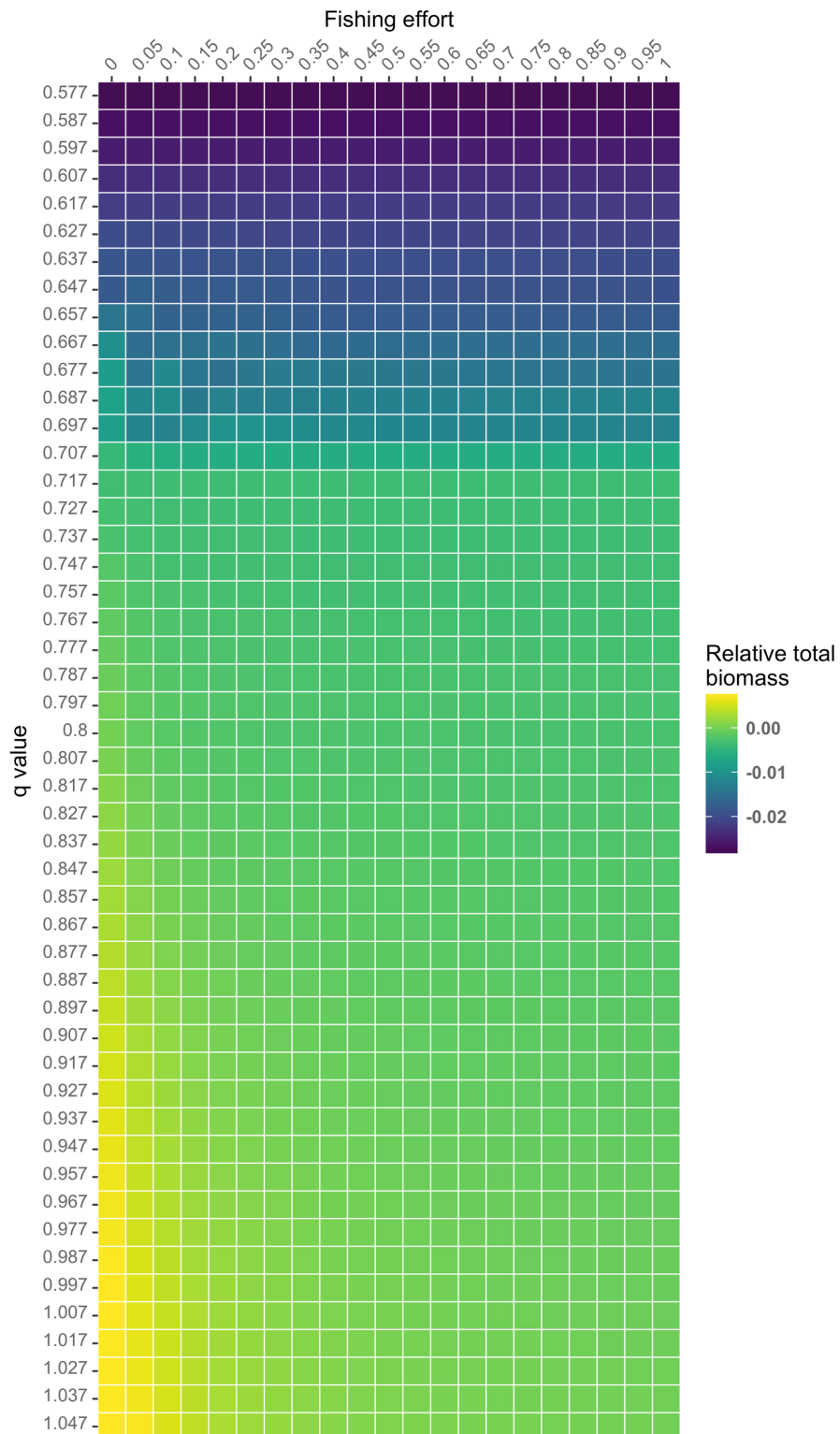


Figure. Relative total biomass as a function of a varying q (rounded to 3 decimal places) and a varying f . All values are relative to the null model ($q = 0.8$ and $f = 0$). All φ values are fixed at 0.5.

Appendix 5.6.

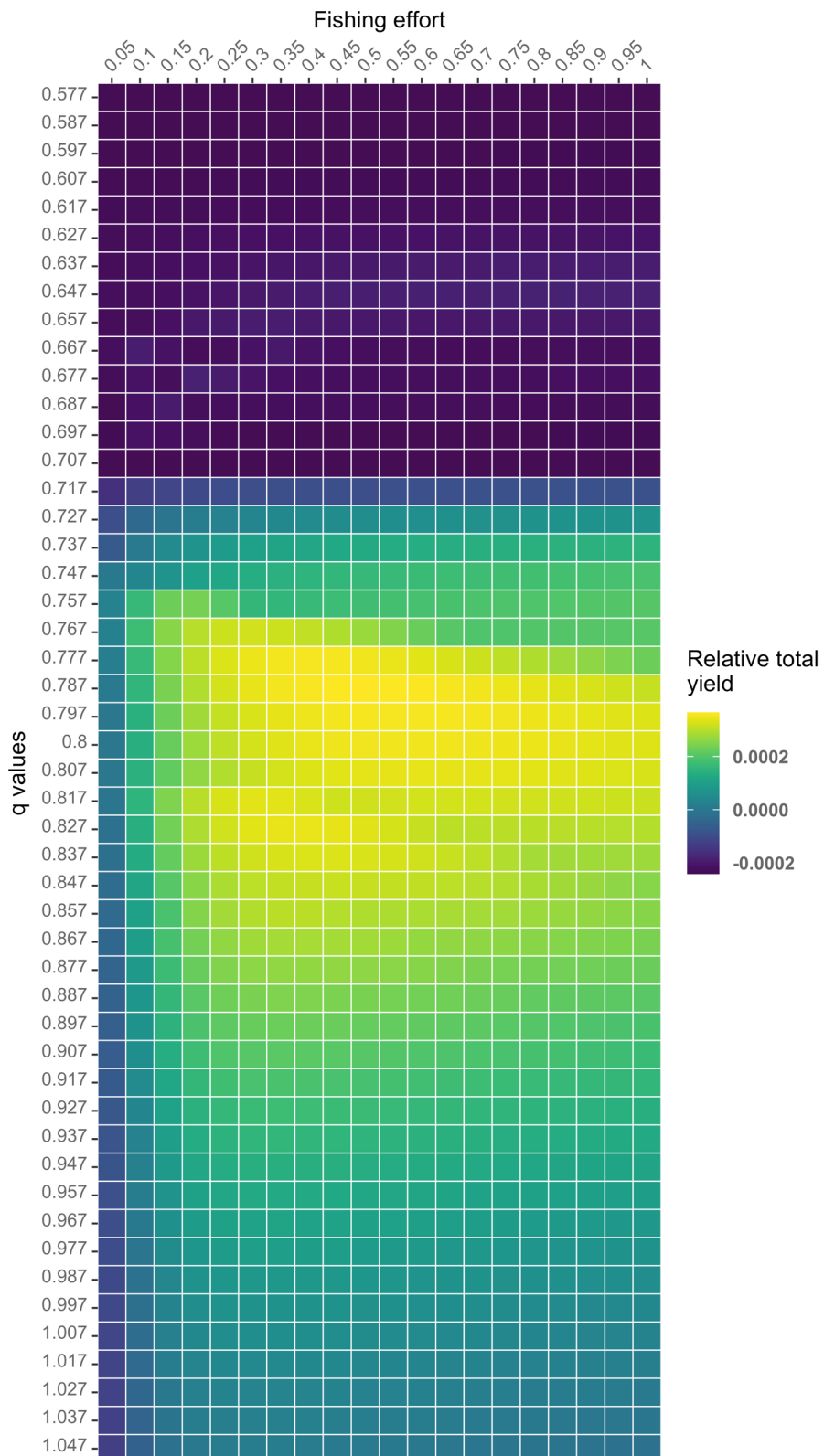


Figure. Relative total yield as a function of a varying q (rounded to 3 decimal places) and a varying f . All values are relative to the null model ($q = 0.8$ and $f = 0.5$). All φ values are fixed at 0.5.

Appendix 5.7.

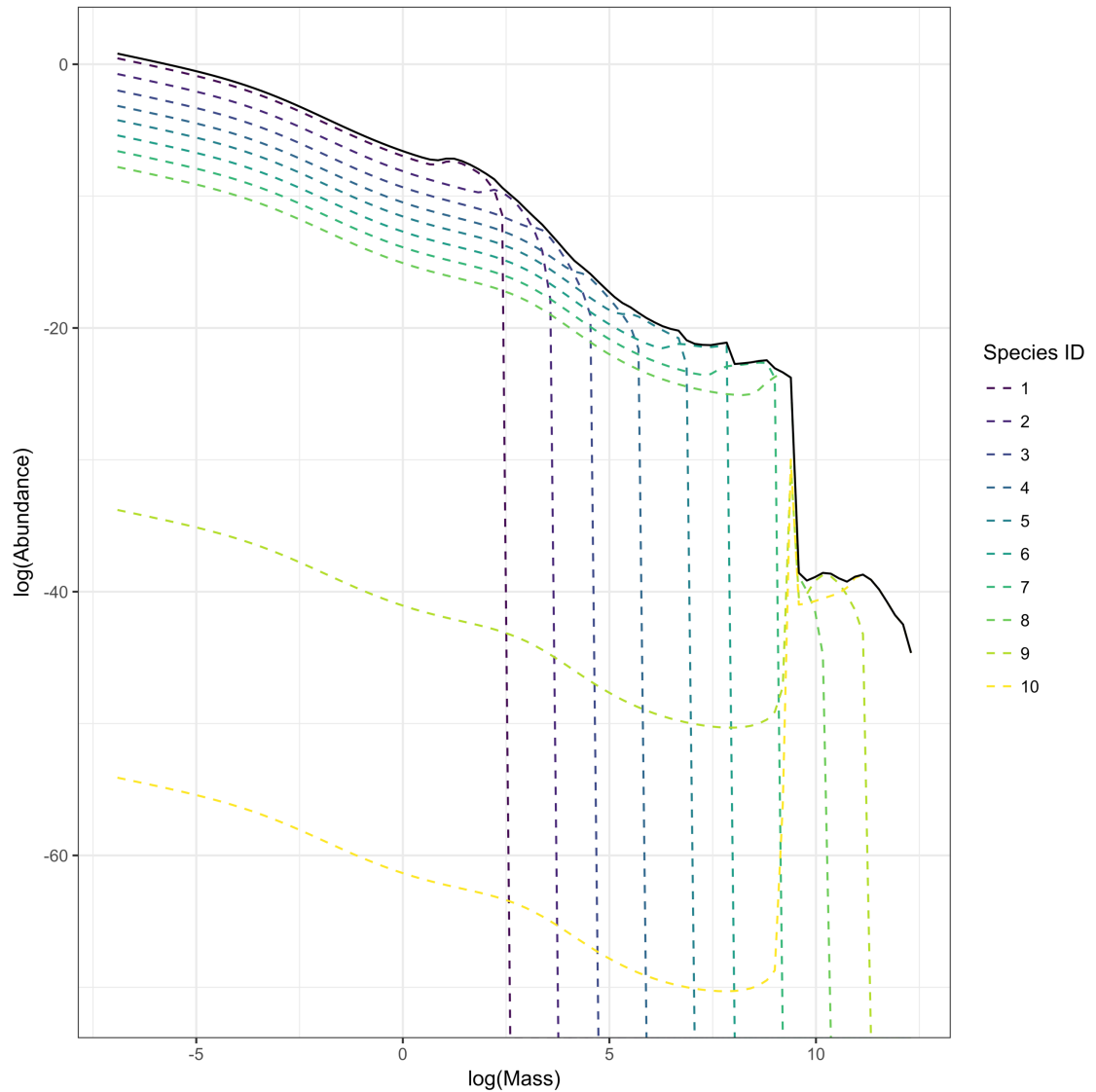


Figure. Abundance at size of each species when the community is projected under a q value of 0.8 and a fishing effort of 0. The community's abundance at size is also illustrated (black line) and represents the sum total of each species' abundance at size. Abundance and mass were log (natural log) transformed to aid visual interpretation. All φ values are fixed at 1.0.

Appendix 5.8.

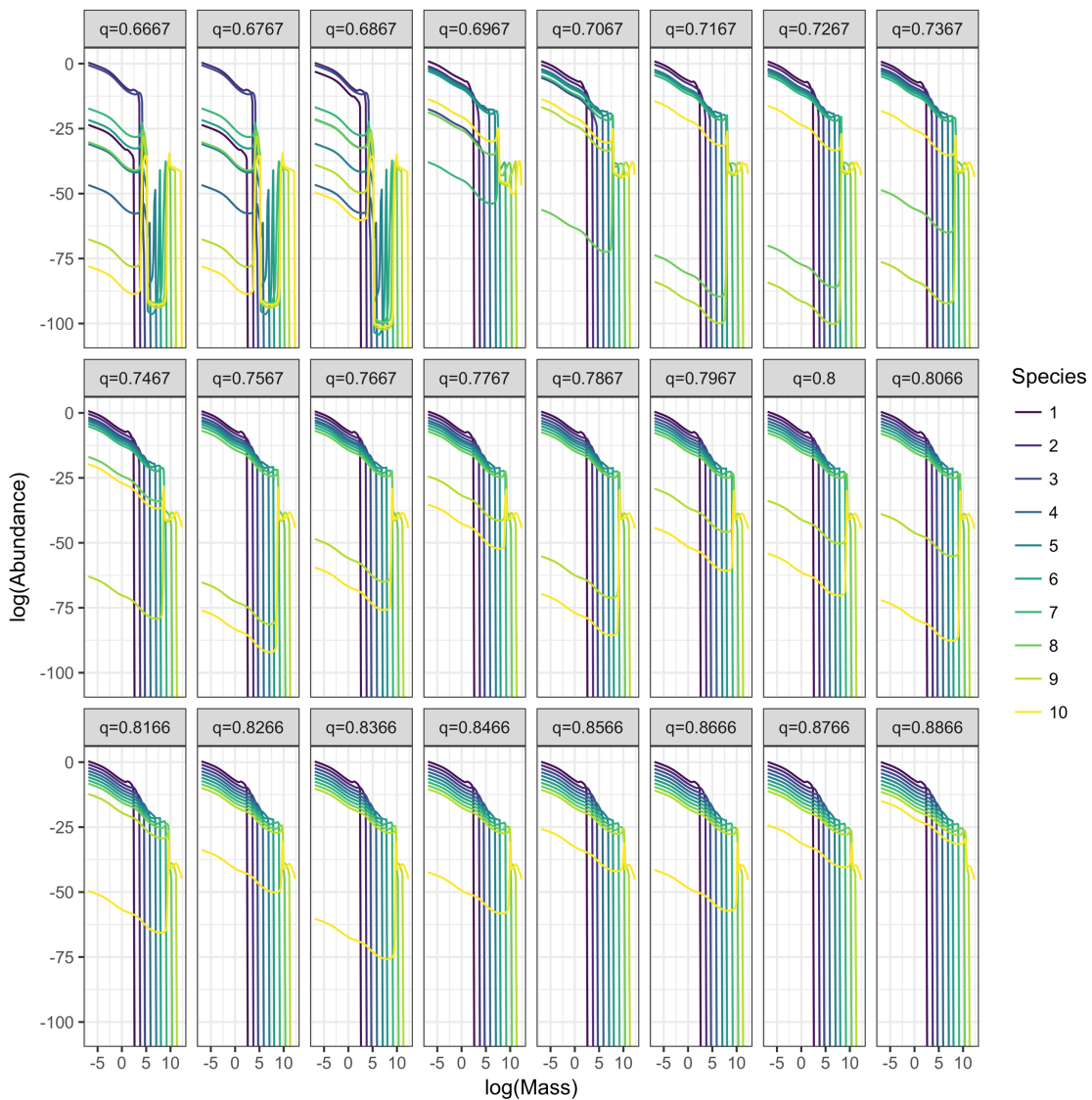


Figure. Abundance at size of each species when the community is projected under a range of q values and a fixed fishing effort of 0. Abundance and mass have been log (natural log) transformed to aid visual interpretation. All φ values are fixed at 1.0.

Appendix 5.9.

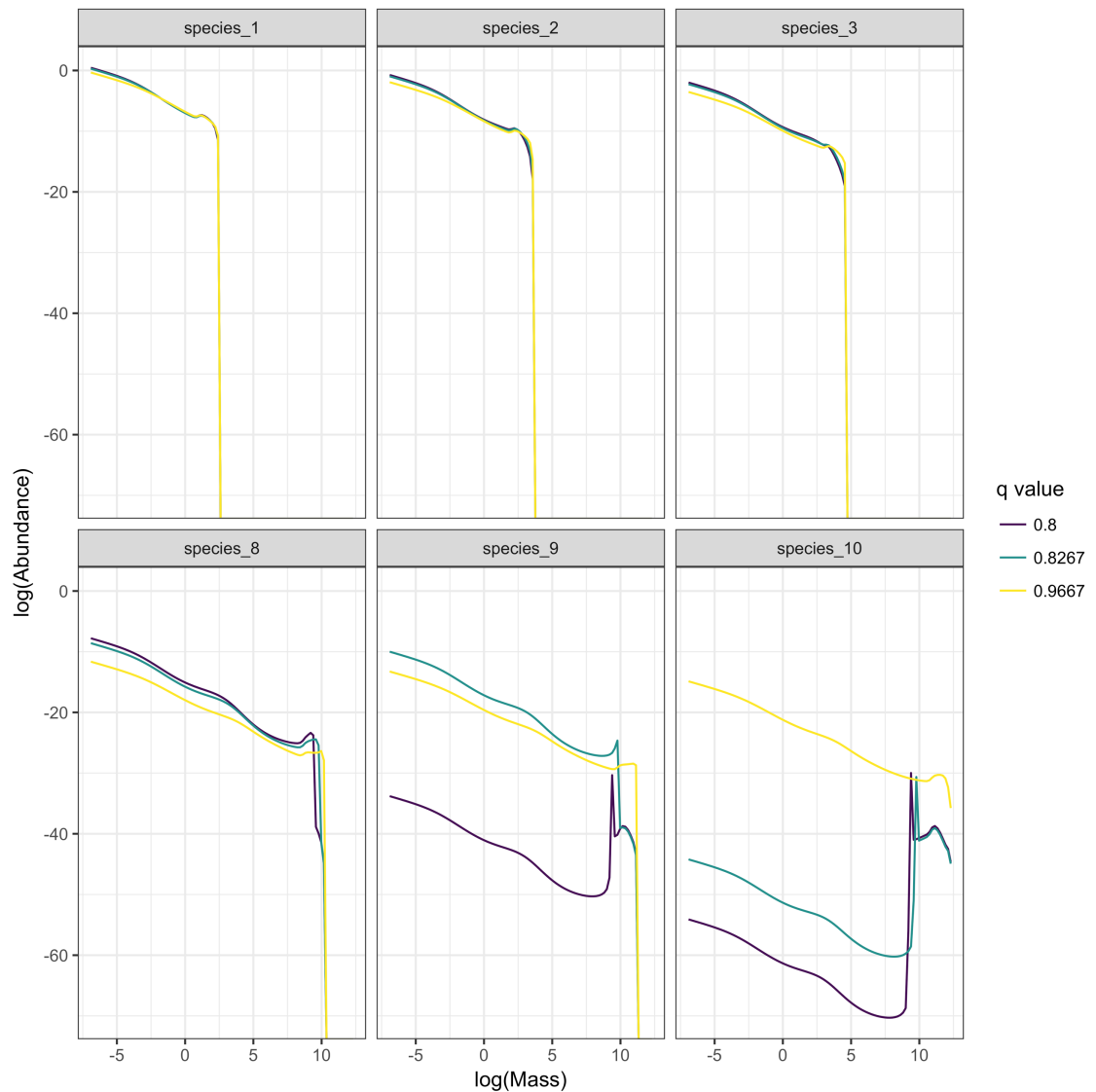


Figure. Species specific abundance at size when the community is projected under a select number of empirically derived q values and a fixed fishing effort of 0. Only the three smallest (species 1 – 3) and the three largest species (species 8 -10) are illustrated. Abundance and mass were log (natural log) transformed to aid visual interpretation. All φ values are fixed at 1.0.

Appendix 5.10.

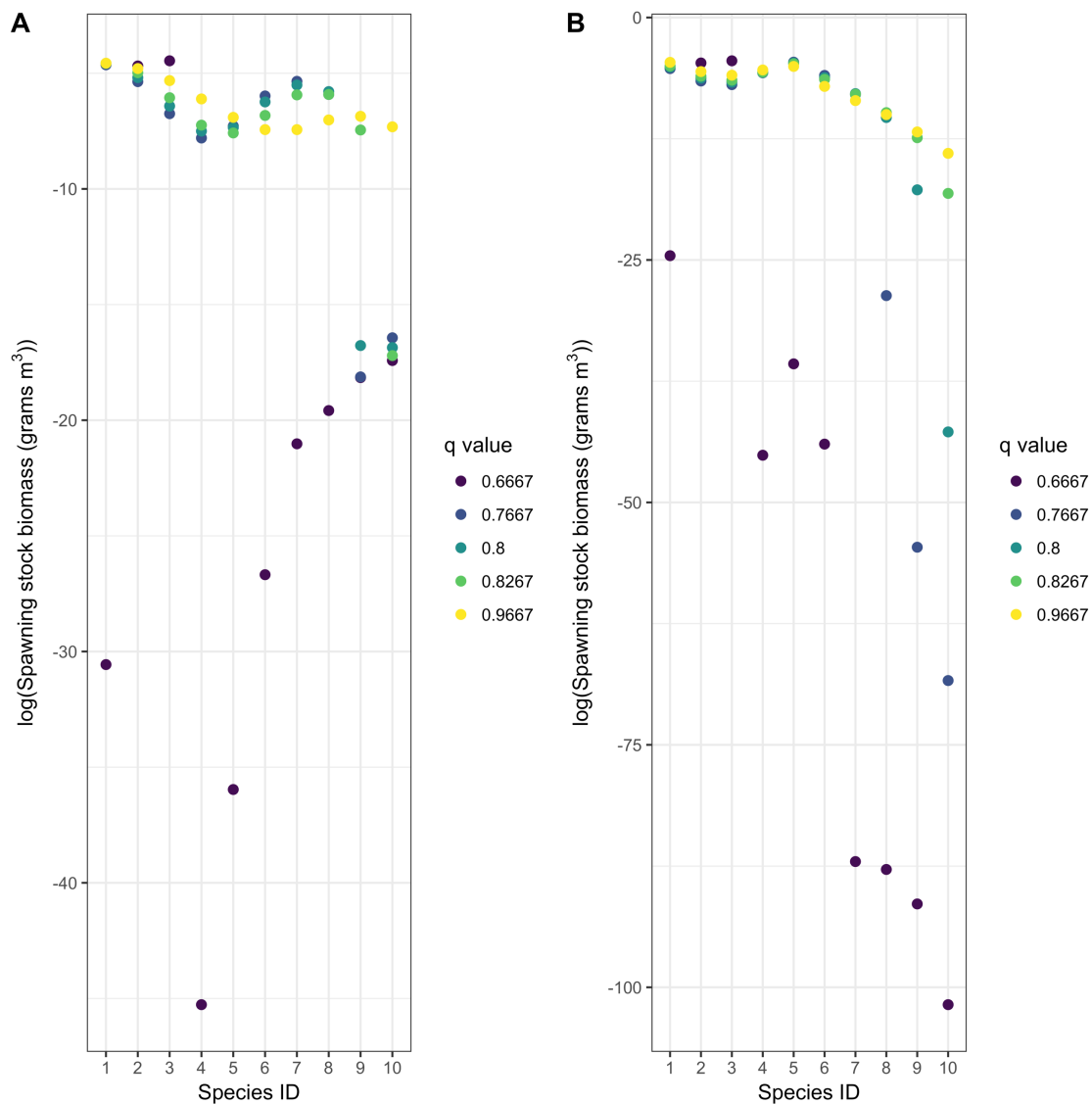


Figure. Spawning stock biomass (SSB) of each species when the community is projected under empirically derived q values and fixed fishing efforts of 0 (A) and 0.25 (B). SSB is calculated using the *getSSB* wrapper function in the *mizer* package (Scott et al., 2014) and represents the total mass of all mature individuals. Each SSB was calculated as an averaged value taken from the last 500 model iterations. SSB has been log (natural log) transformed to aid visual interpretation. All φ values are fixed at 1.0.

THE END